Figures

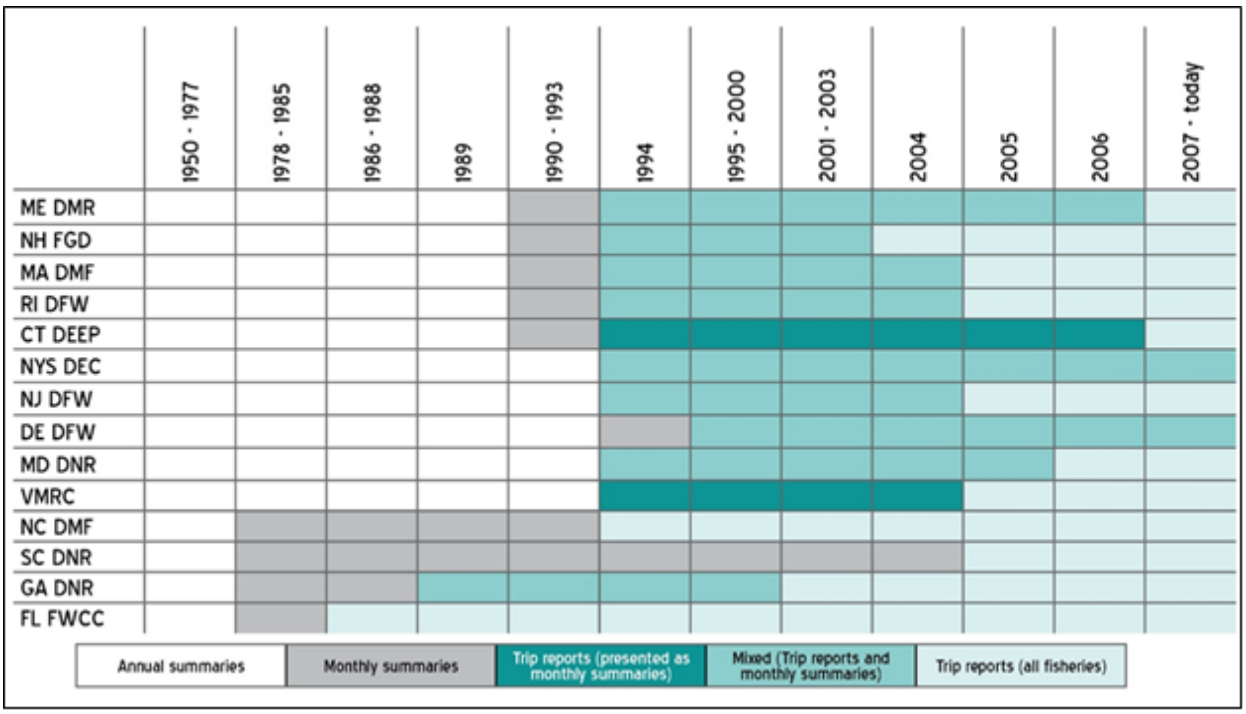

Figure B4.1. ACCSP data sources and collection methods.

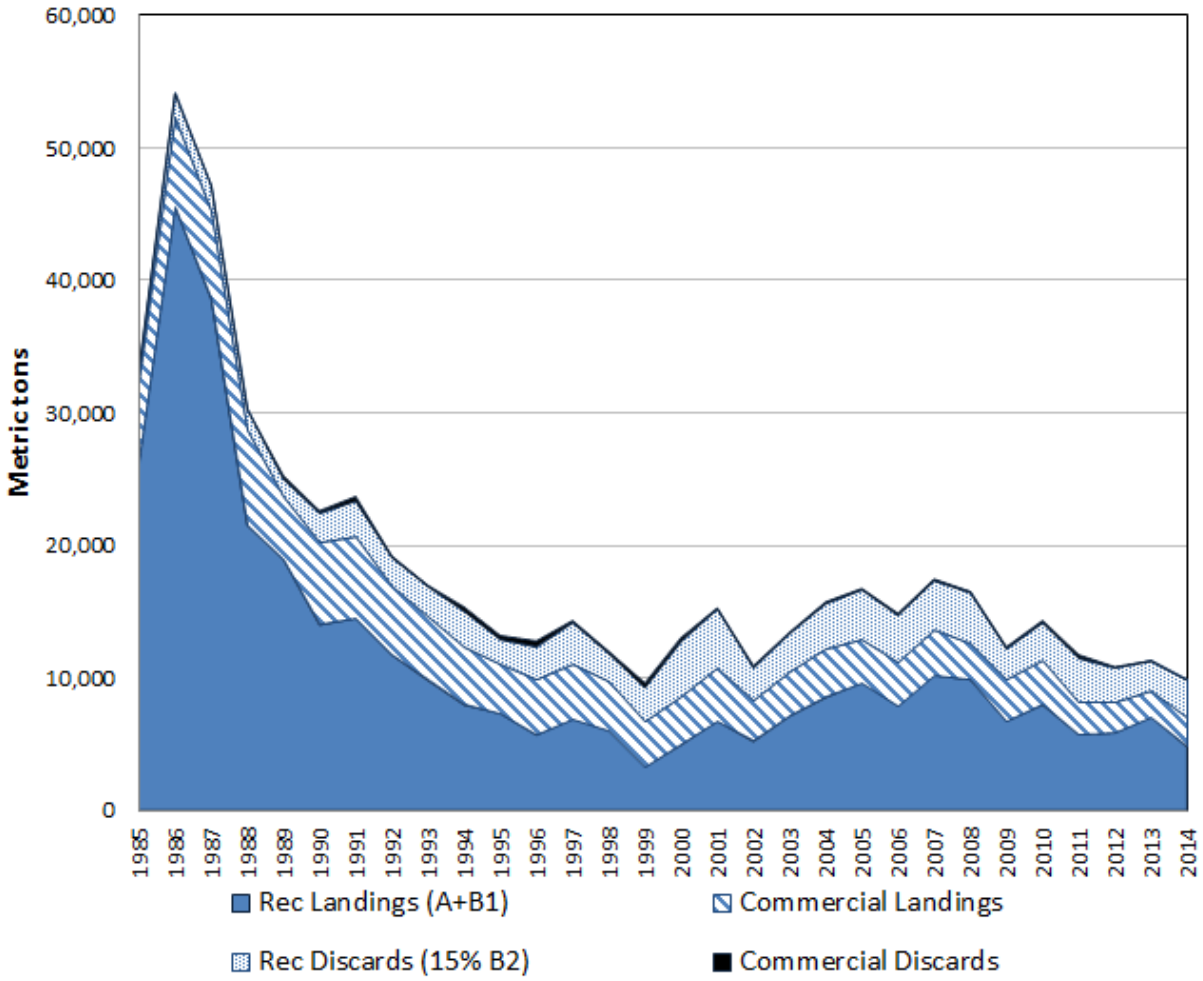

Figure B4.2. Bluefish landings by fleet and disposition.

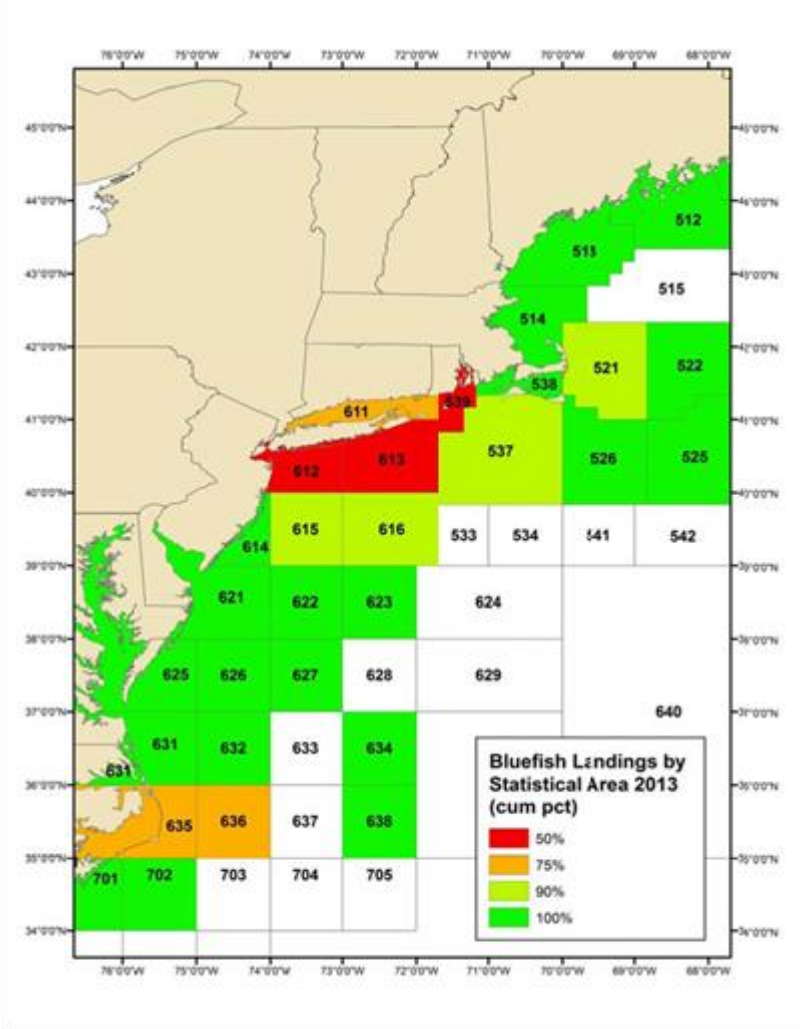

Figure B4.3. Bluefish landings by NMFS statistical areas. Shading reflects the cumulative percentage of landings with red and orange being the primary areas where the commercial landings are taken.

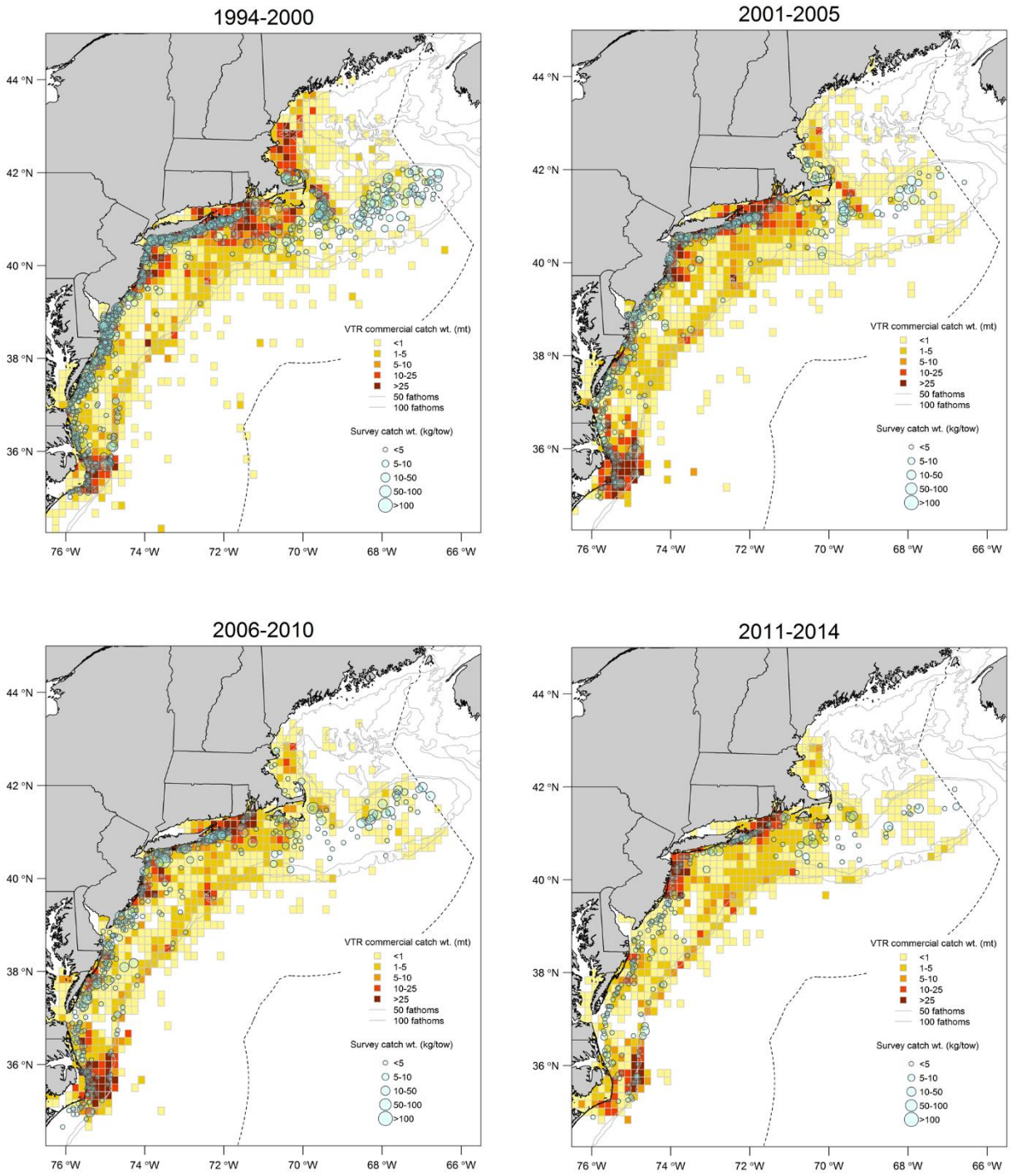

Figure B4.4. Spatial distribution of bluefish commercial catch by time period as reported through Vessel Trip Reports (VTR). Source: NEFSC.

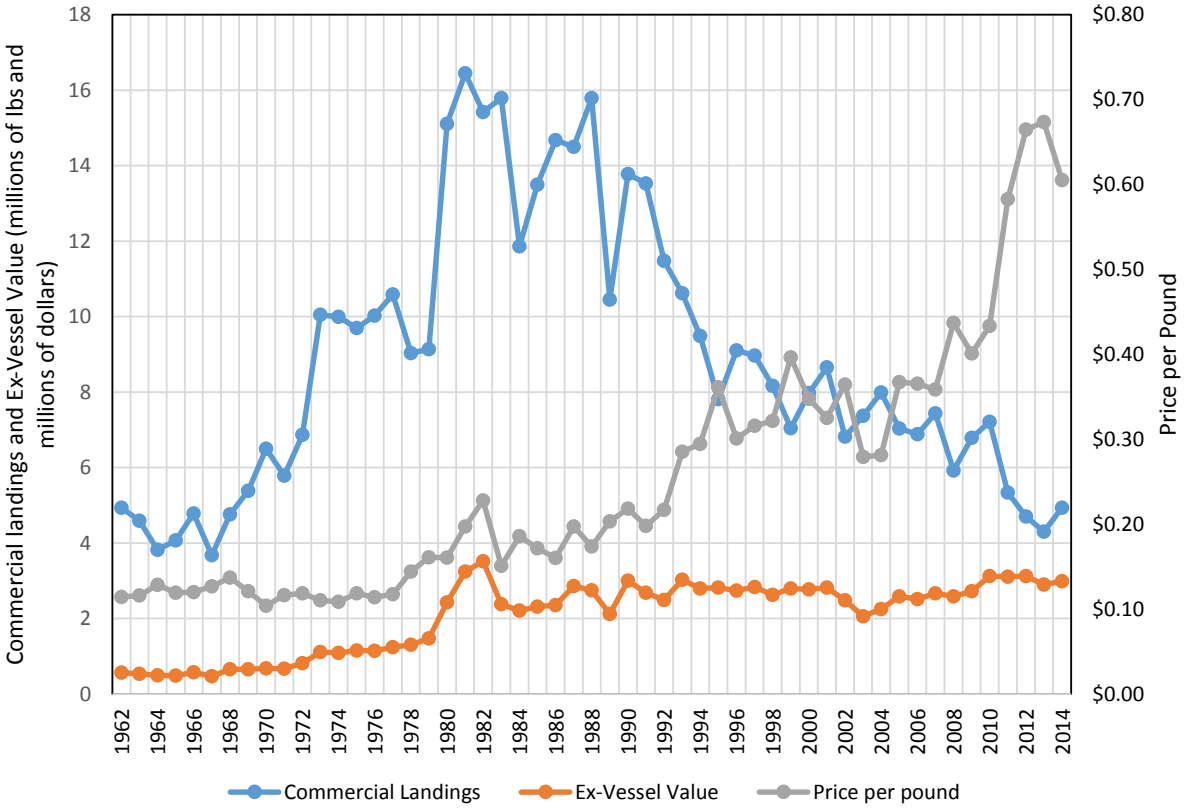

Figure B4.5. Landings, ex-vessel value, and price for bluefish, 1960 - 2014. Source: ACCSP Data Warehouse. Prices are not adjusted for inflation.

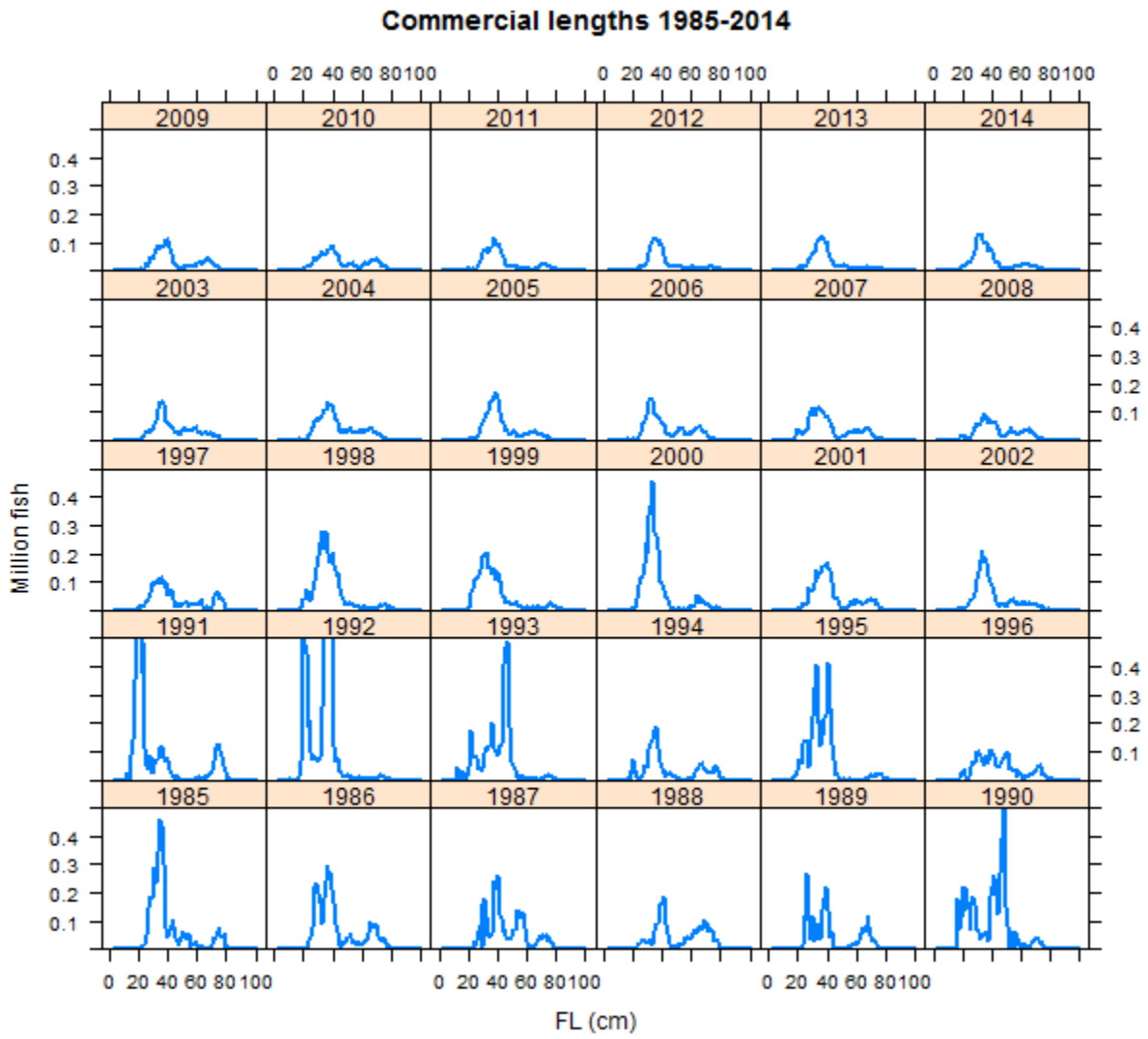

Figure B4.6. Length frequency distributions of commercial bluefish landings from Maine to Florida.

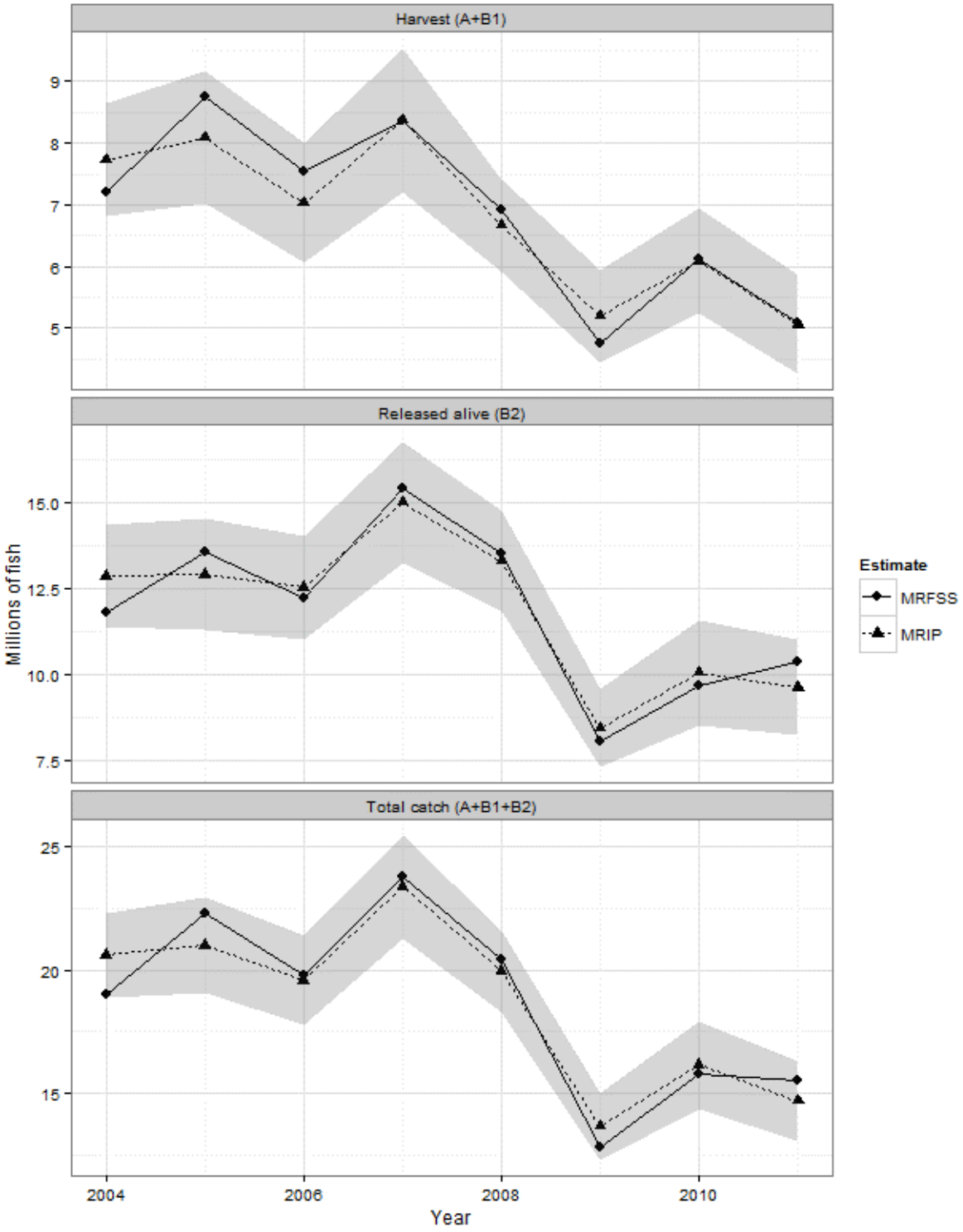

Figure B4.7. Comparison of MRFSS and MRIP estimates of bluefish catch for 2004 - 2011. Shaded bands indicate 95% confidence intervals calculated from MRIP PSEs.

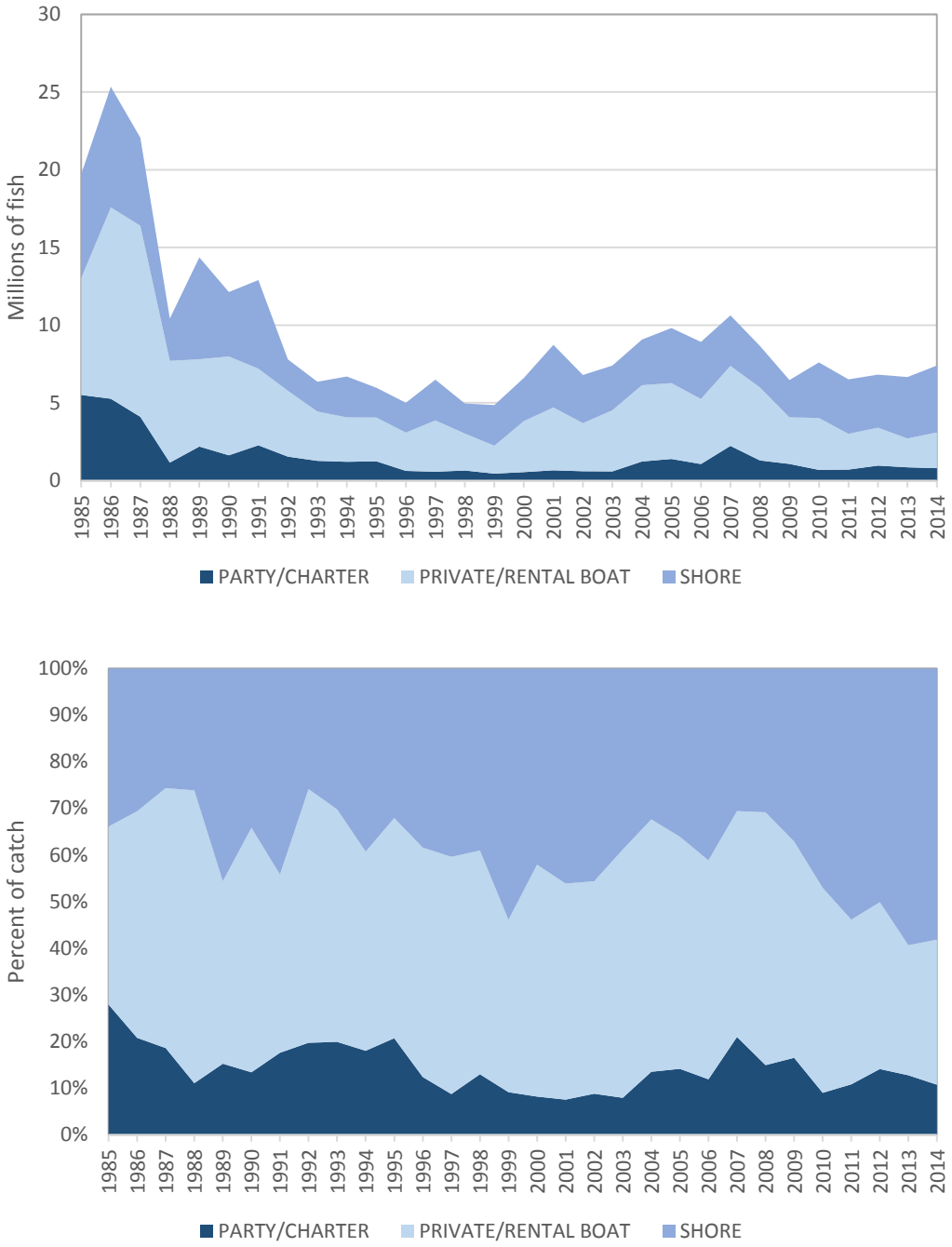

Figure B4.8. Bluefish recreational removals by mode for the Atlantic coast, shown in numbers of fish (top) and percent of catch (bottom.).

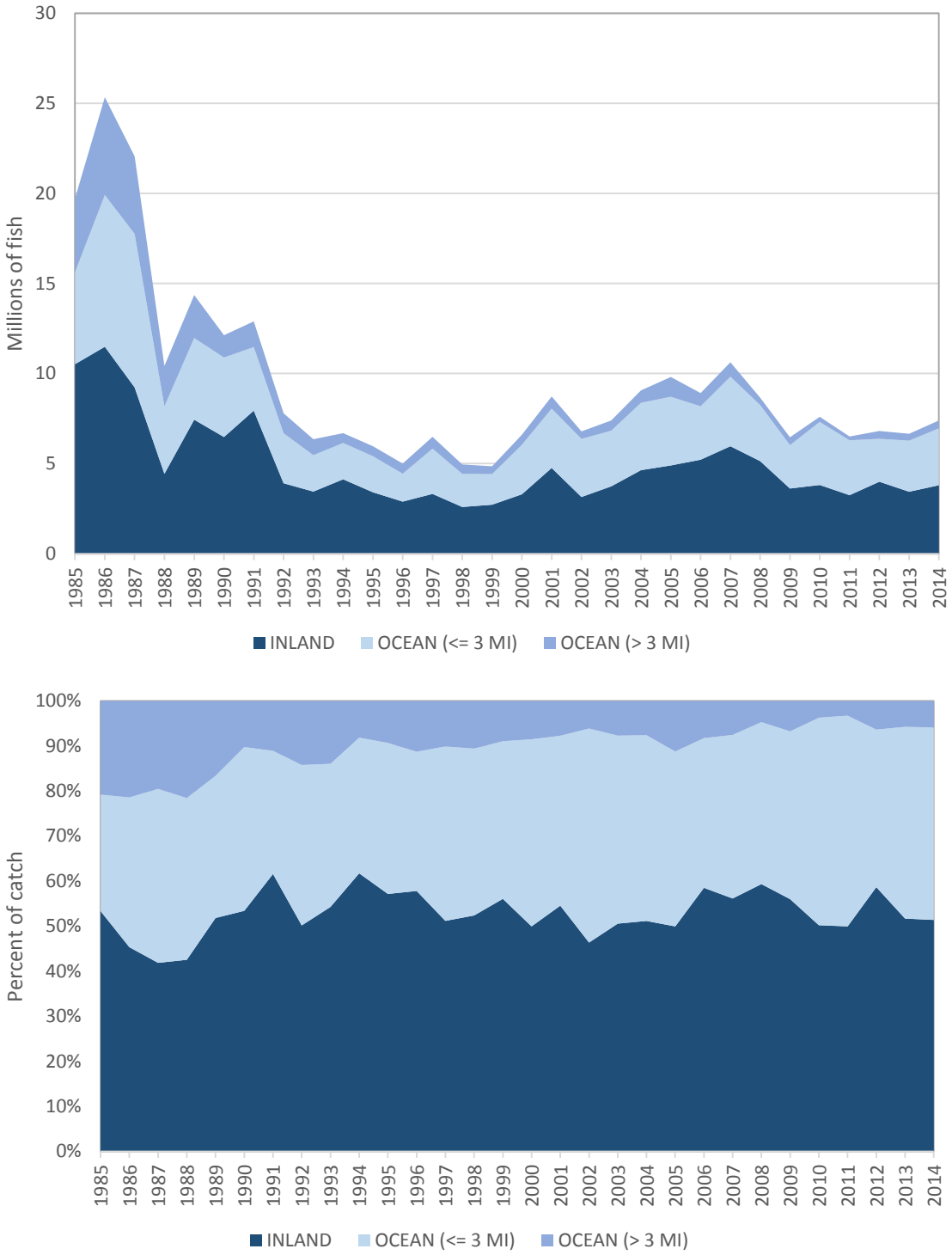

Figure B4.9. Bluefish recreational removals by area fished for the Atlantic coast, shown in numbers of fish (top) and percent of catch (bottom).

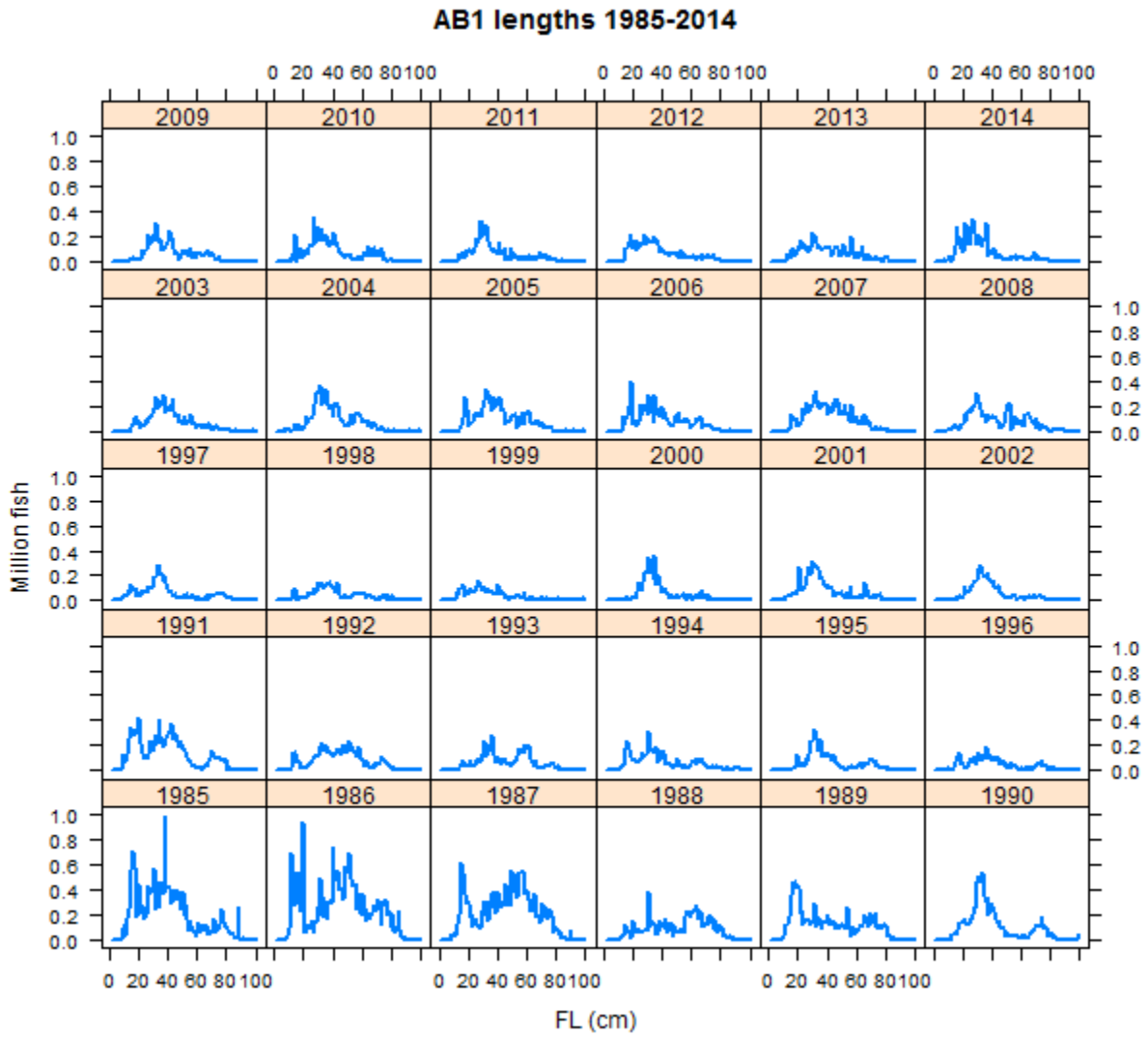

Figure B4.10A. Length frequency distributions of recreational landings for the Atlantic coast.

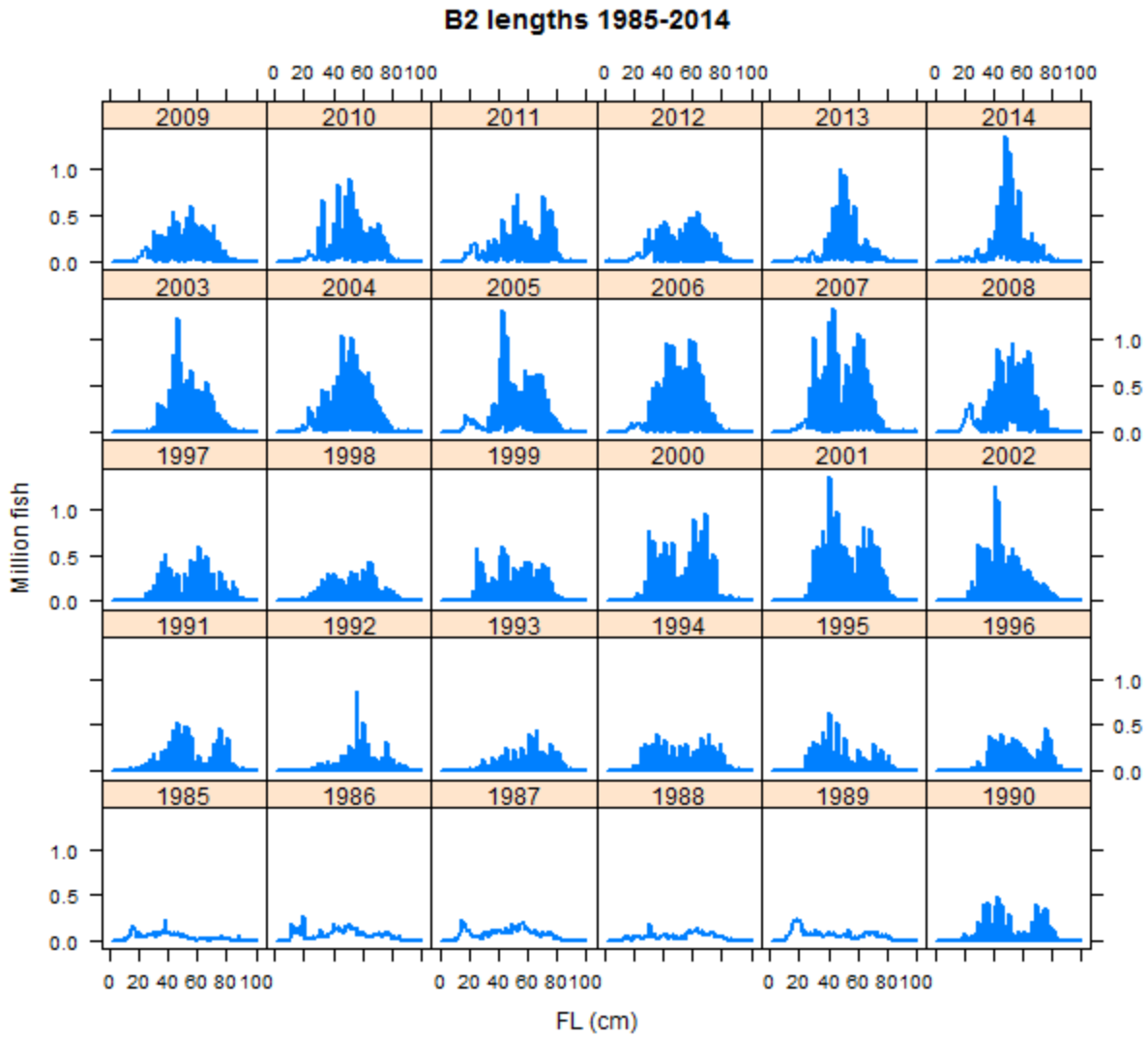

Figure B4.10B. Length frequency distributions of recreational discards for the Atlantic coast.

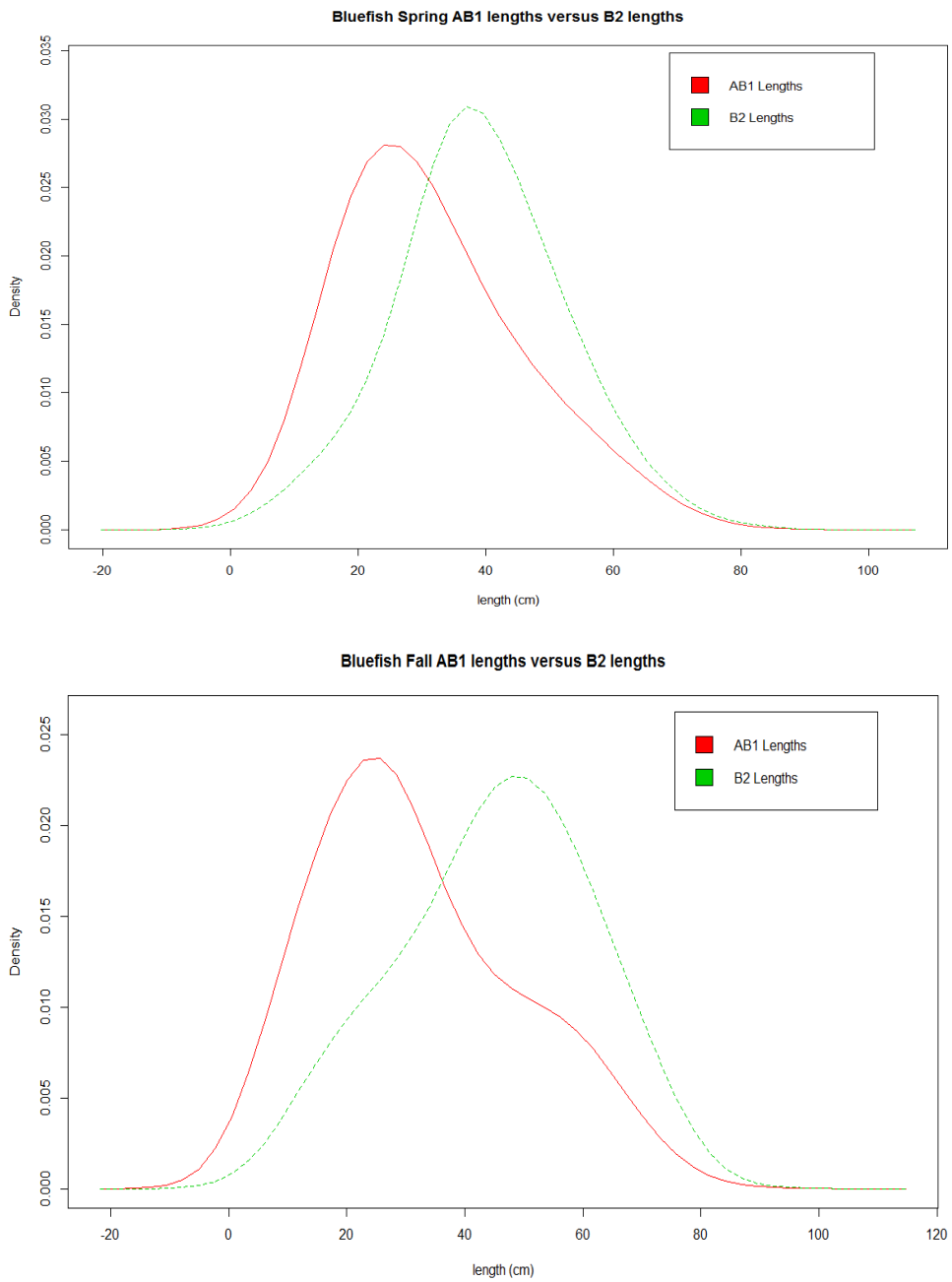

Figure B4.11. Density plots of the length frequency distributions of recreational landings (A+B1) versus discards (B2) for bluefish in the spring (top) and fall (bottom).

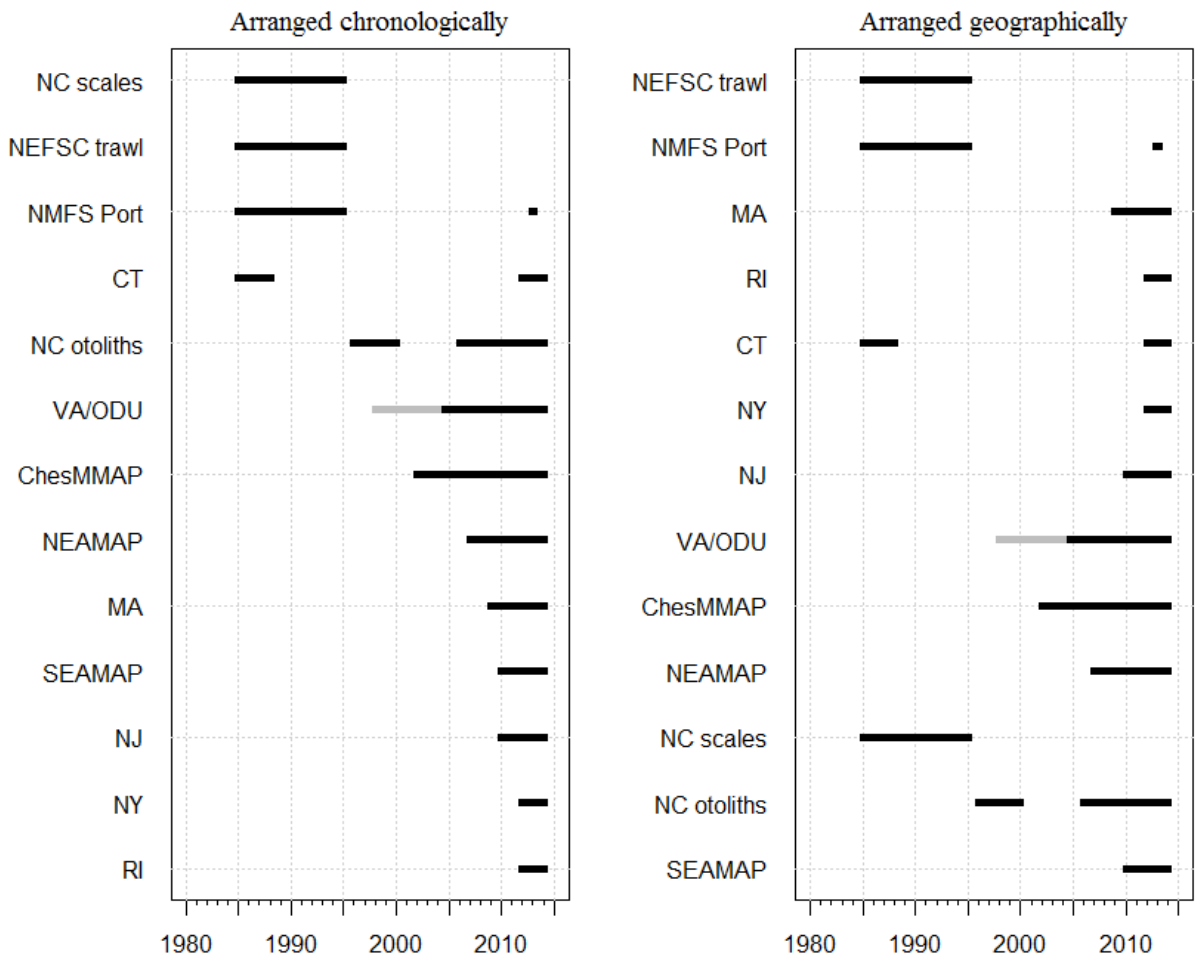

Figure B5.1. Depiction of available bluefish age data arranged chronologically (left) and geographically (right). Samples from 1985-1995 are scales, all others are otoliths. NMFS Port samples in 2013 came from RI, NY, and NJ (state of origin not retrievable prior to 2013); NEAMAP samples came from states between MA/RI and NC, inclusive; SEAMAP samples came from states between NC and FL, inclusive. Grey bar at VA/ODU represents years where age data were shared across some years.

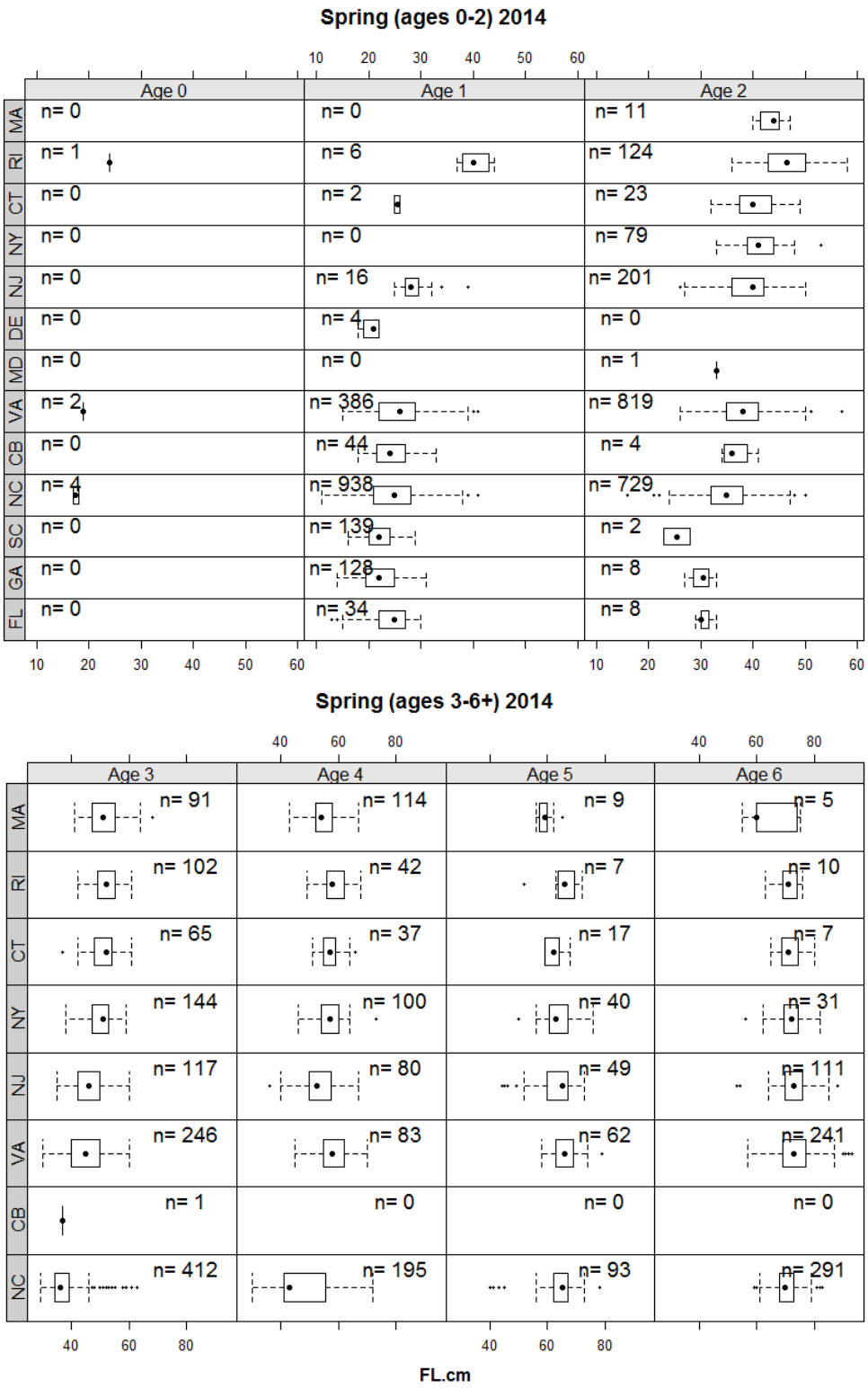

Figure B5.2A. Boxplots of size at age by state in spring 2014.

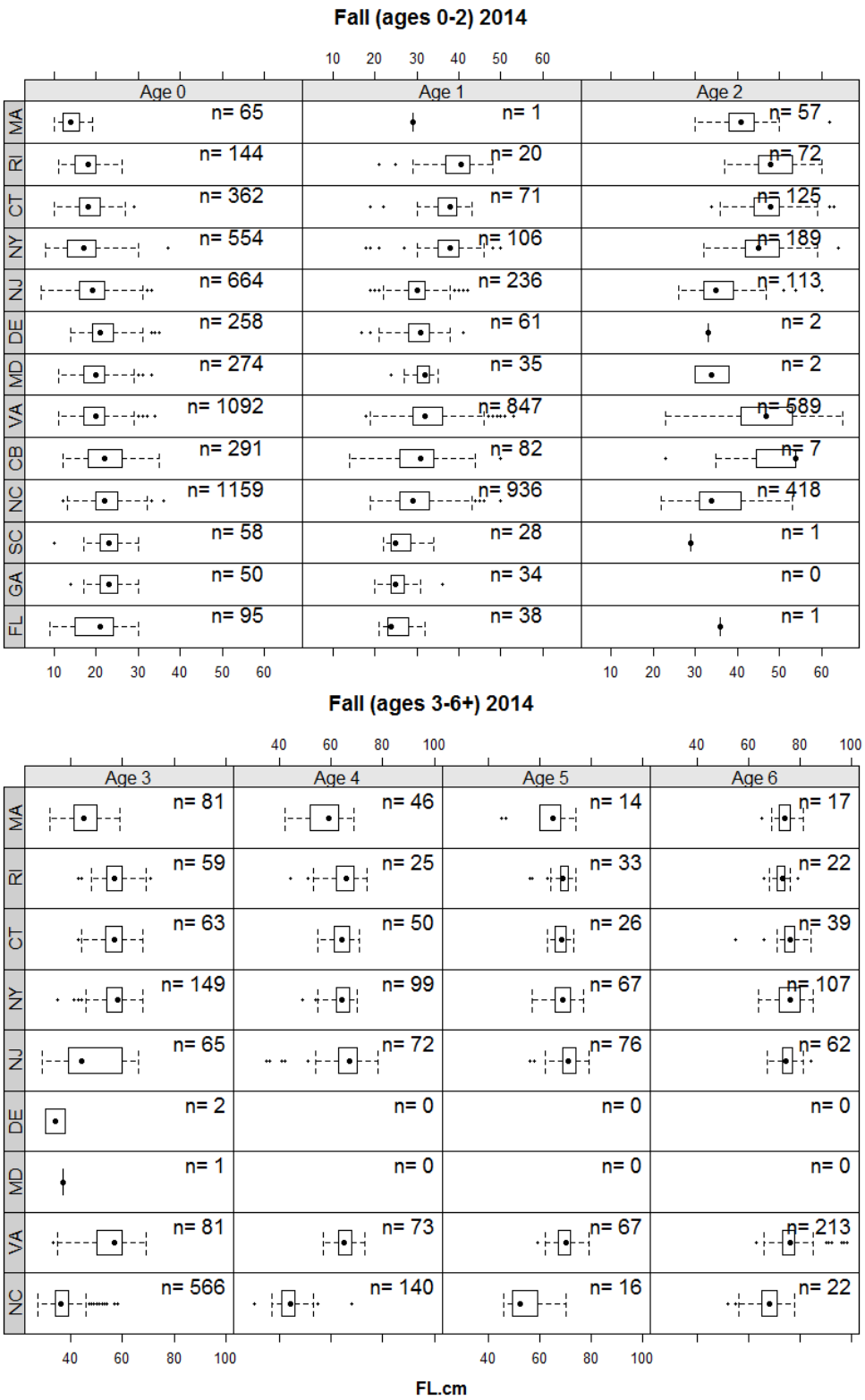

Figure B5.2B. Boxplots of size at age by state in fall 2014.

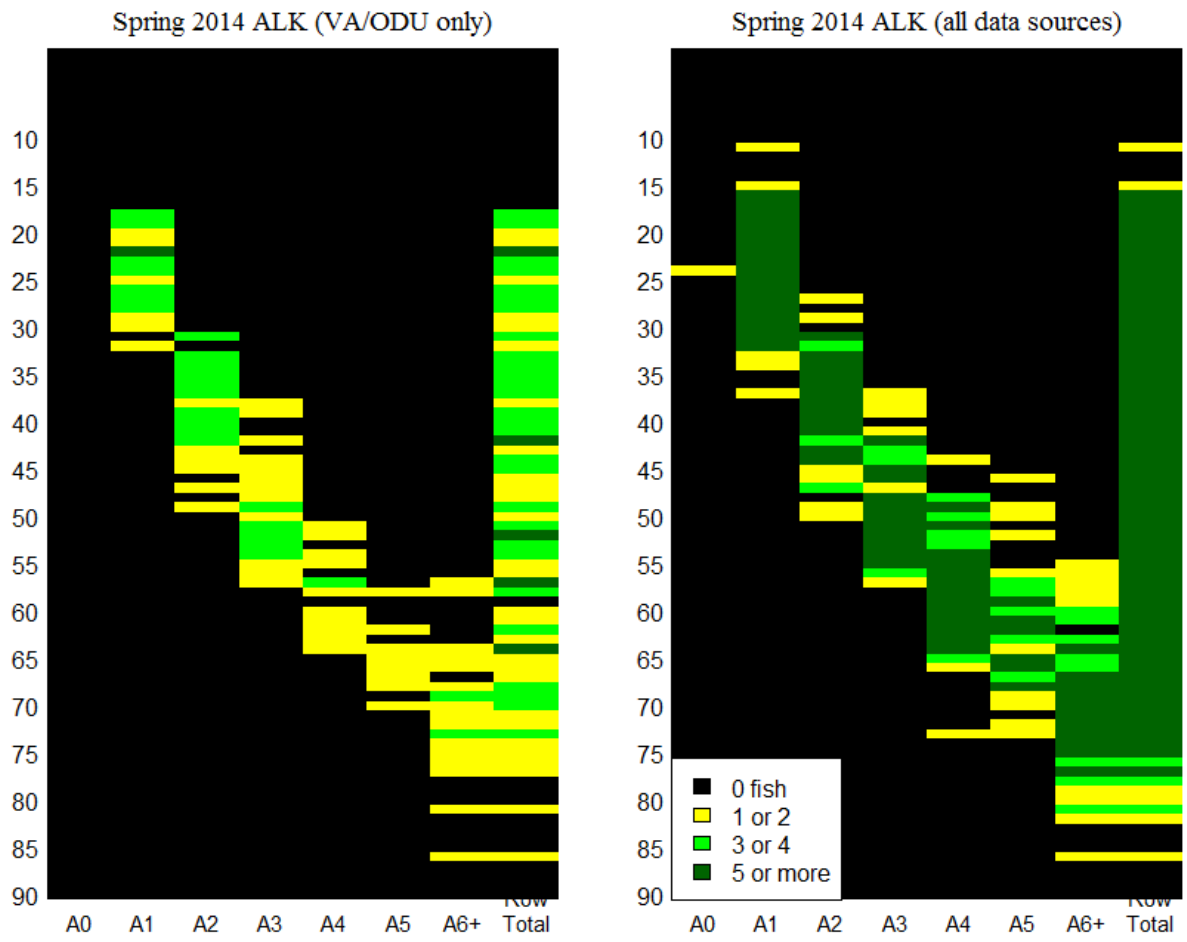

Figure B5.3. Comparison of age-length keys derived from VA/ODU versus all data sources ALK for spring 2014. Column on far right of each plot depicts the row total. Y-axis is FL (cm).

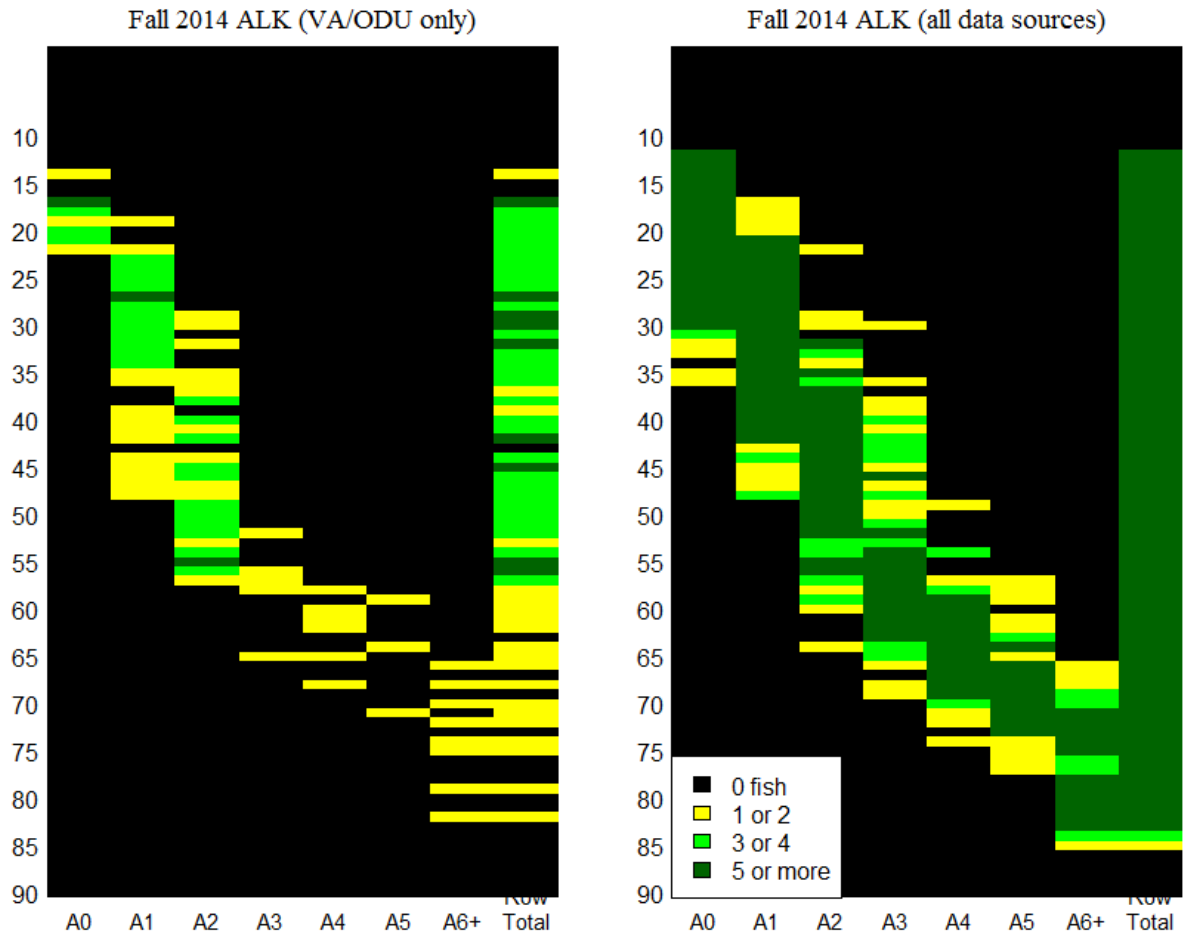

Figure B5.4. Comparison of age-length keys derived from VA/ODU versus all data sources ALK for fall 2014. Column on far right of each plot depicts the row total. Y-axis is FL (cm).

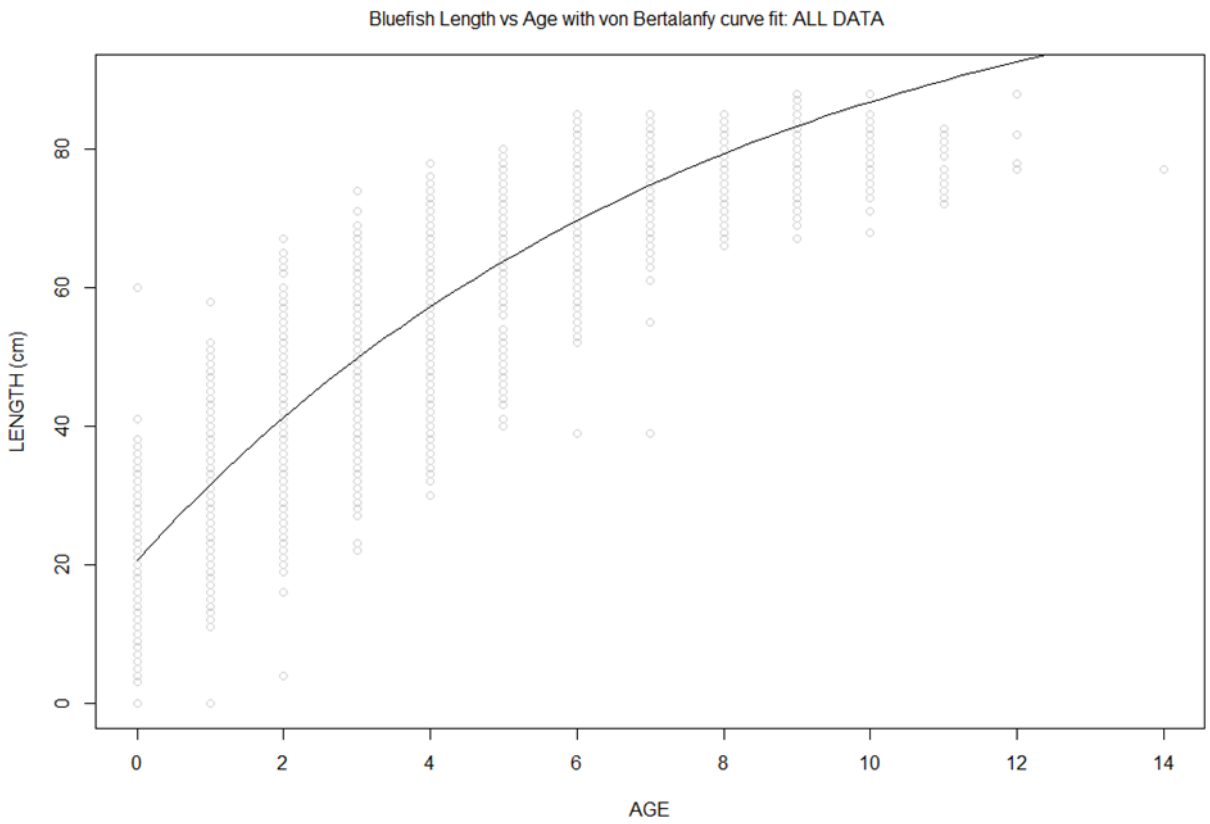

Figure B5.5. Von Bertalanffy growth curve fit to all bluefish data.

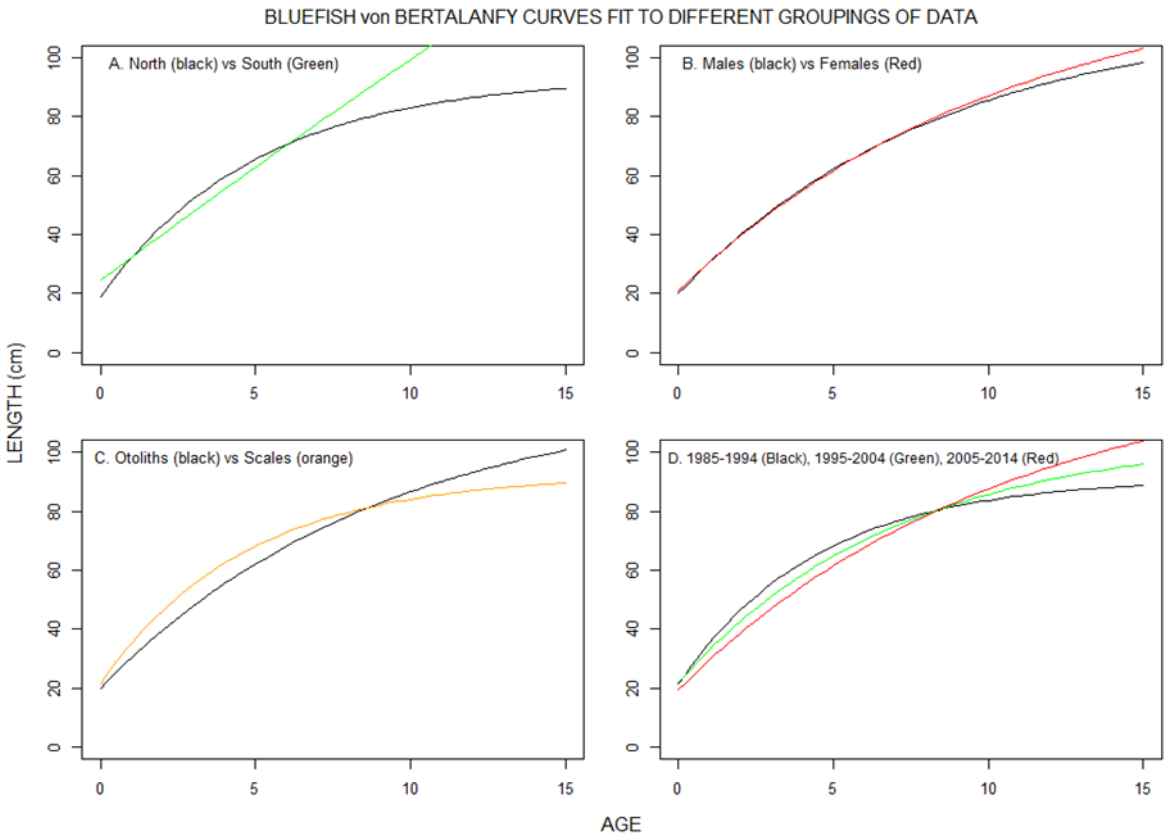

Figure B5.6. Von Bertalanfy growth curves fit to different groupings of data. (A) Northern and Southern fish, (B) Male and Females, (C) Otolith Ages and Scale Ages, and (D) Three time blocks.

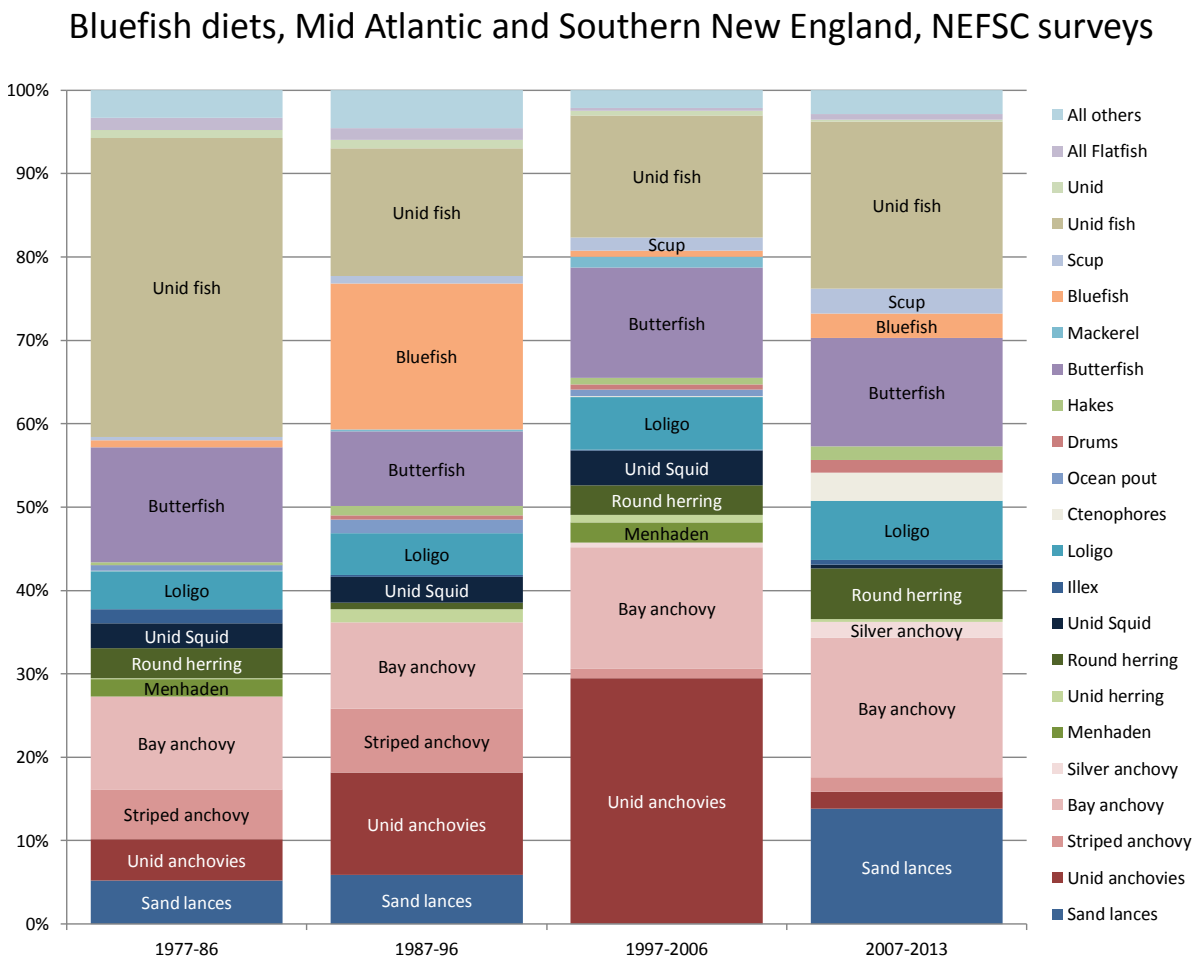

Figure B5.7. Bluefish historic diet composition: prey proportion by weight in 10-year intervals.

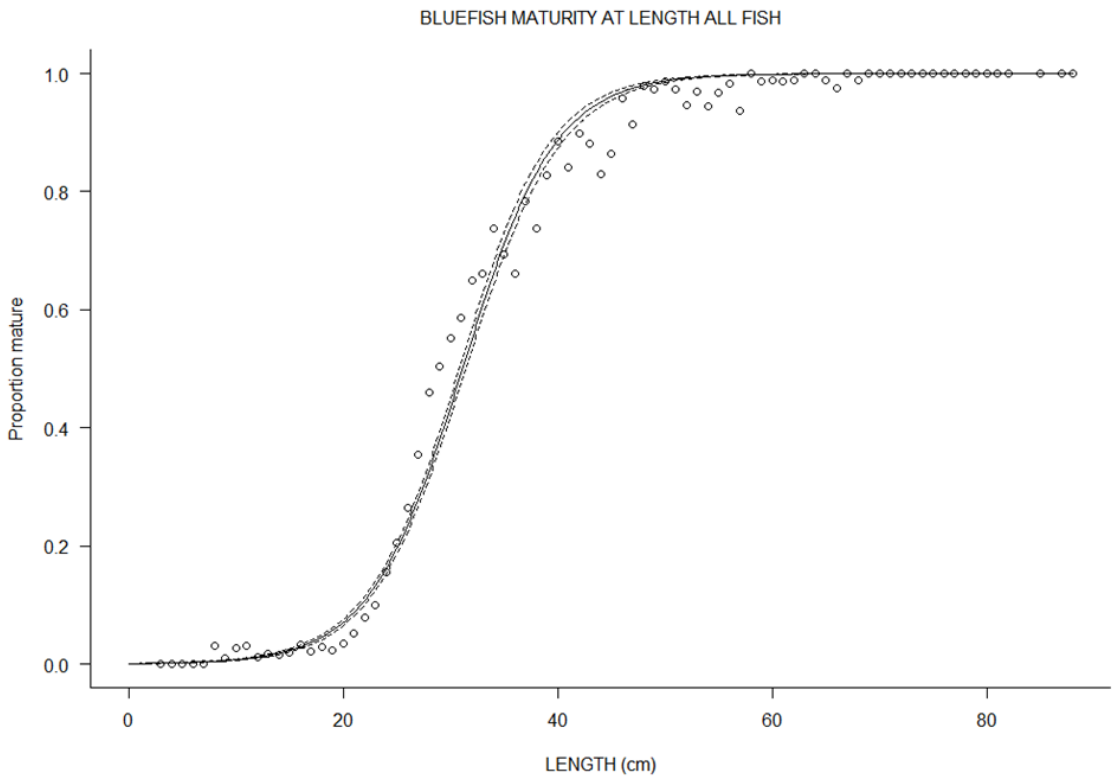

Figure B5.8. Bluefish maturity at length for all fish in the study. (L50 = 29.9 cm, L95 = 44.3 cm).

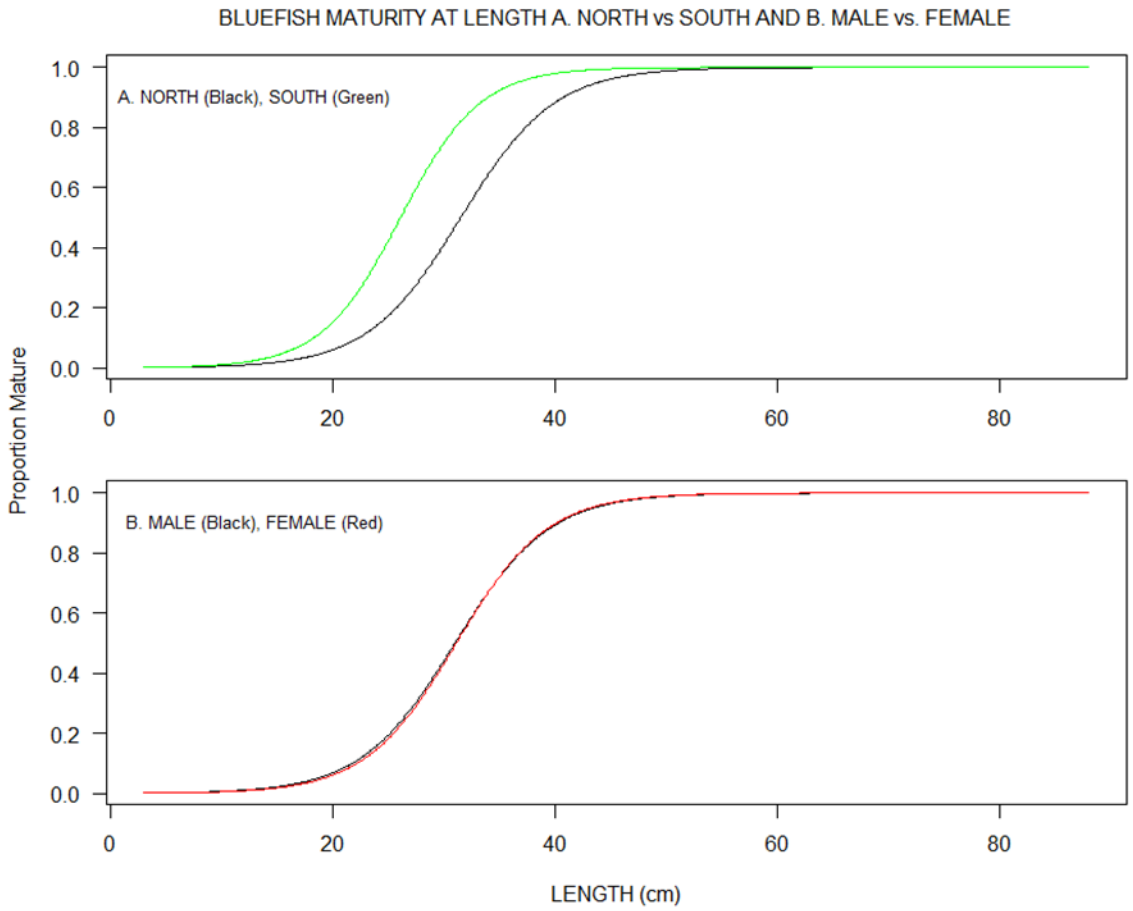

Figure B5.9. Bluefish maturity at length by region (A) and sex (B).

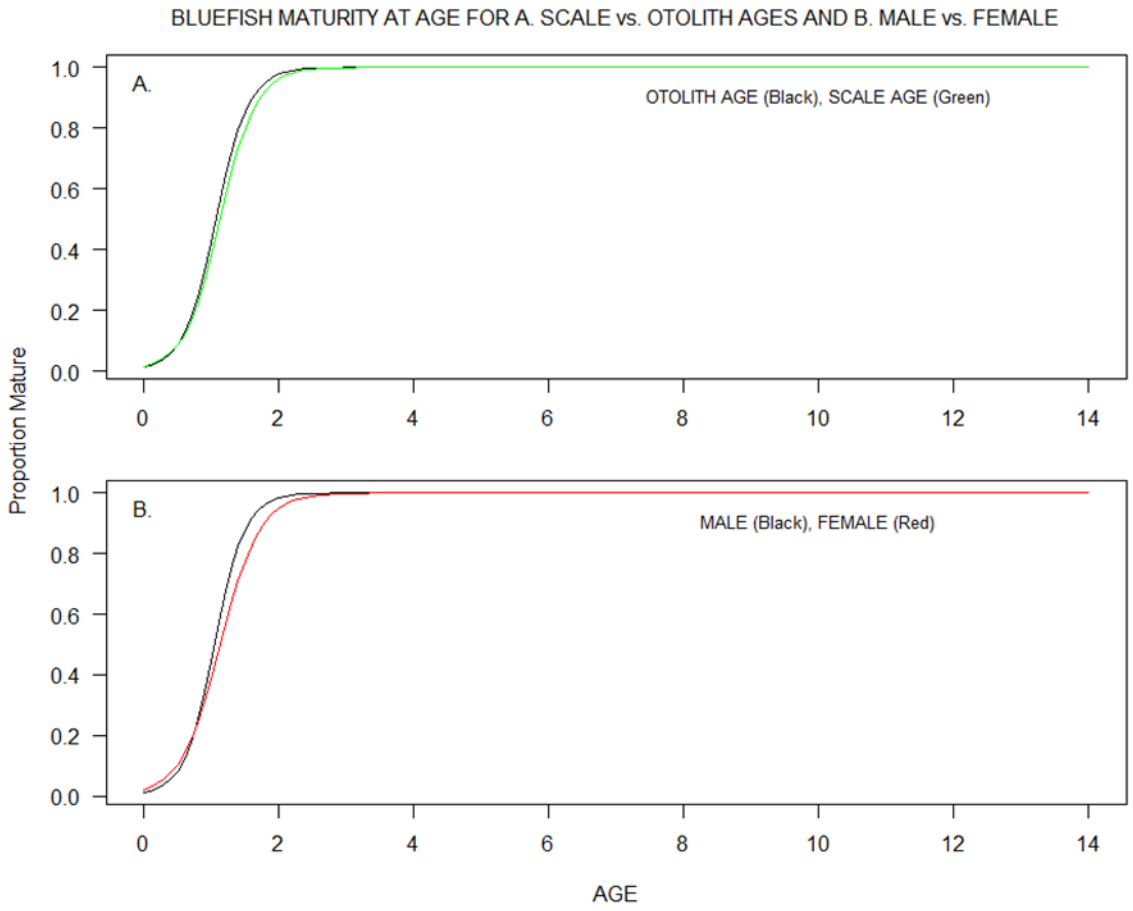

Figure B5.10. Bluefish maturity at age by ageing structure (A) and sex (B).

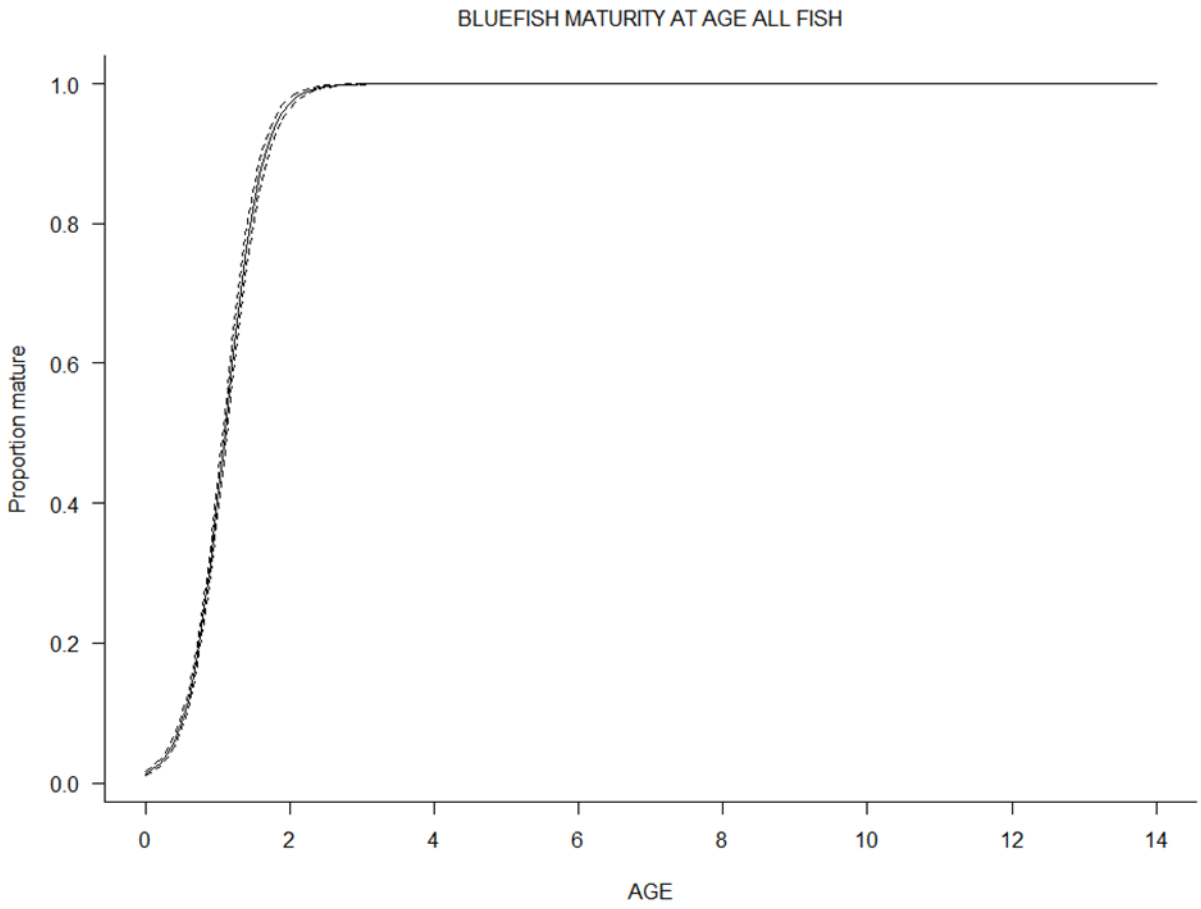

Figure B5.11. Bluefish maturity at age for all fish in the study. (A50 = 1.1 years, A95 = 1.84 years)

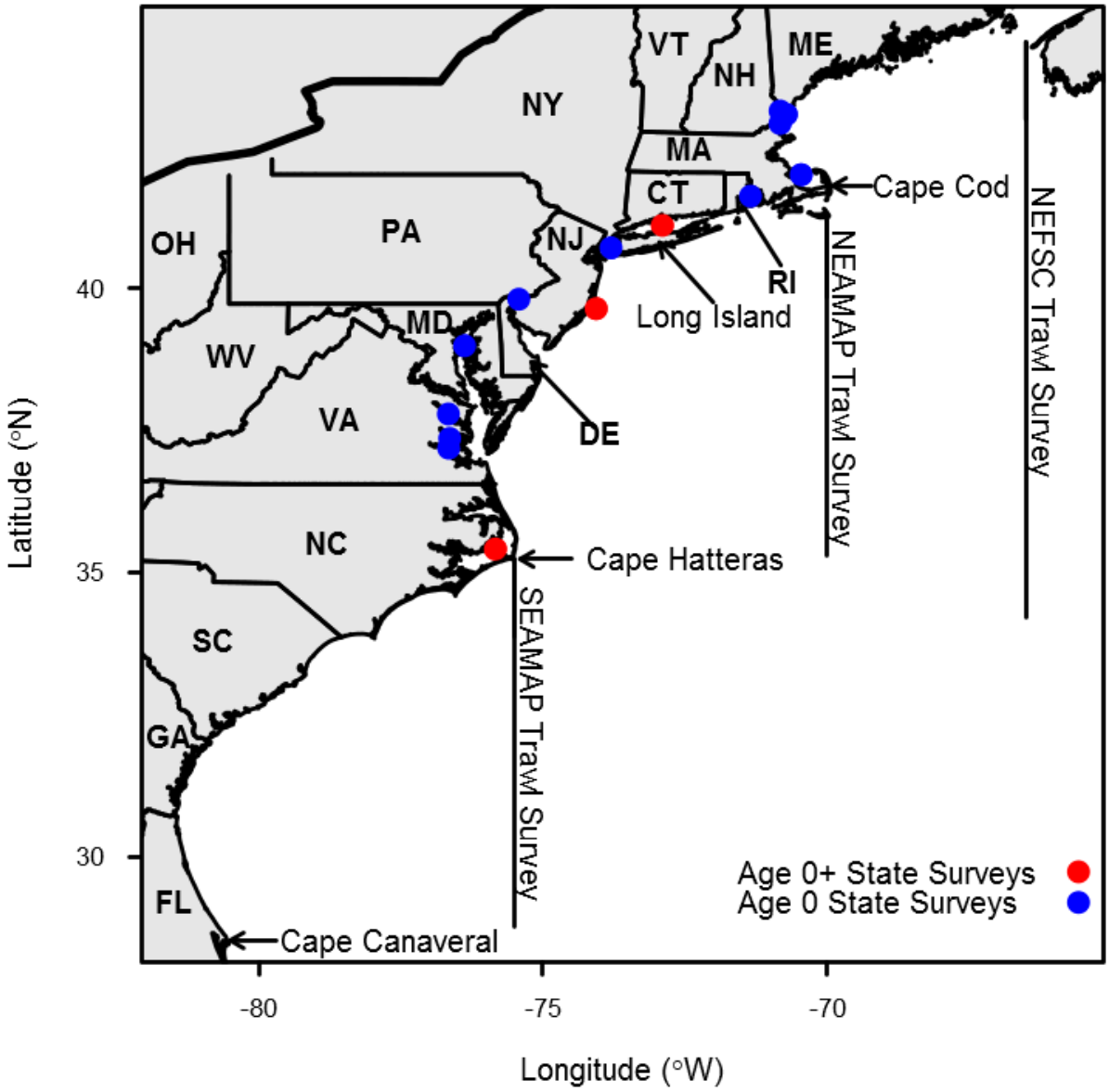

Figure B6.1. Map of available regional and state specific surveys. Regional surveys include SEAMAP Fall Trawl Survey Age-0 Index, NEAMAP Trawl Survey, and NEFSC Fall Trawl Surveys (R/V Albatross and R/V Bigelow). Vertical lines associated with regional surveys represent their latitudinal extent. State surveys include New Hampshire Juvenile Finfish Survey, Massachusetts Inshore Bottom Trawl Survey (not included in final base run), Rhode Island Seine Survey, Connecticut Long Island Sound Trawl Survey, New York Western Long Island Sound Seine Survey, New Jersey Delaware River Seine Survey, New Jersey Ocean Trawl Survey, Maryland Juvenile Striped Bass Survey, VIMS Juvenile Striped Bass Survey, and North Carolina PSIGNS.

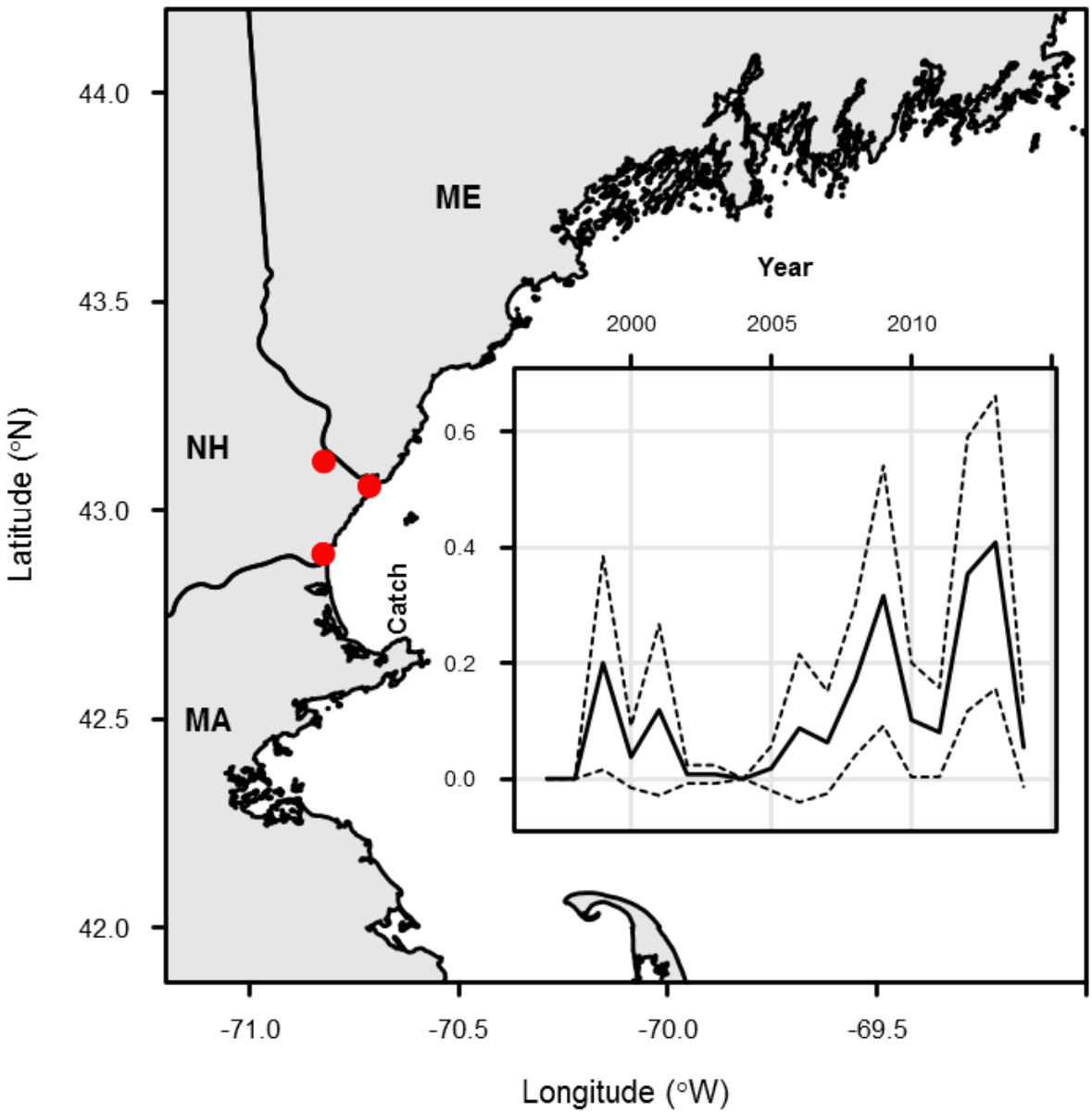

Figure B6.2. Map of the New Hampshire Juvenile Finfish Seine Survey area and resulting index of abundance (inset). Red dot indicates the center point in each of the three river systems surveyed.

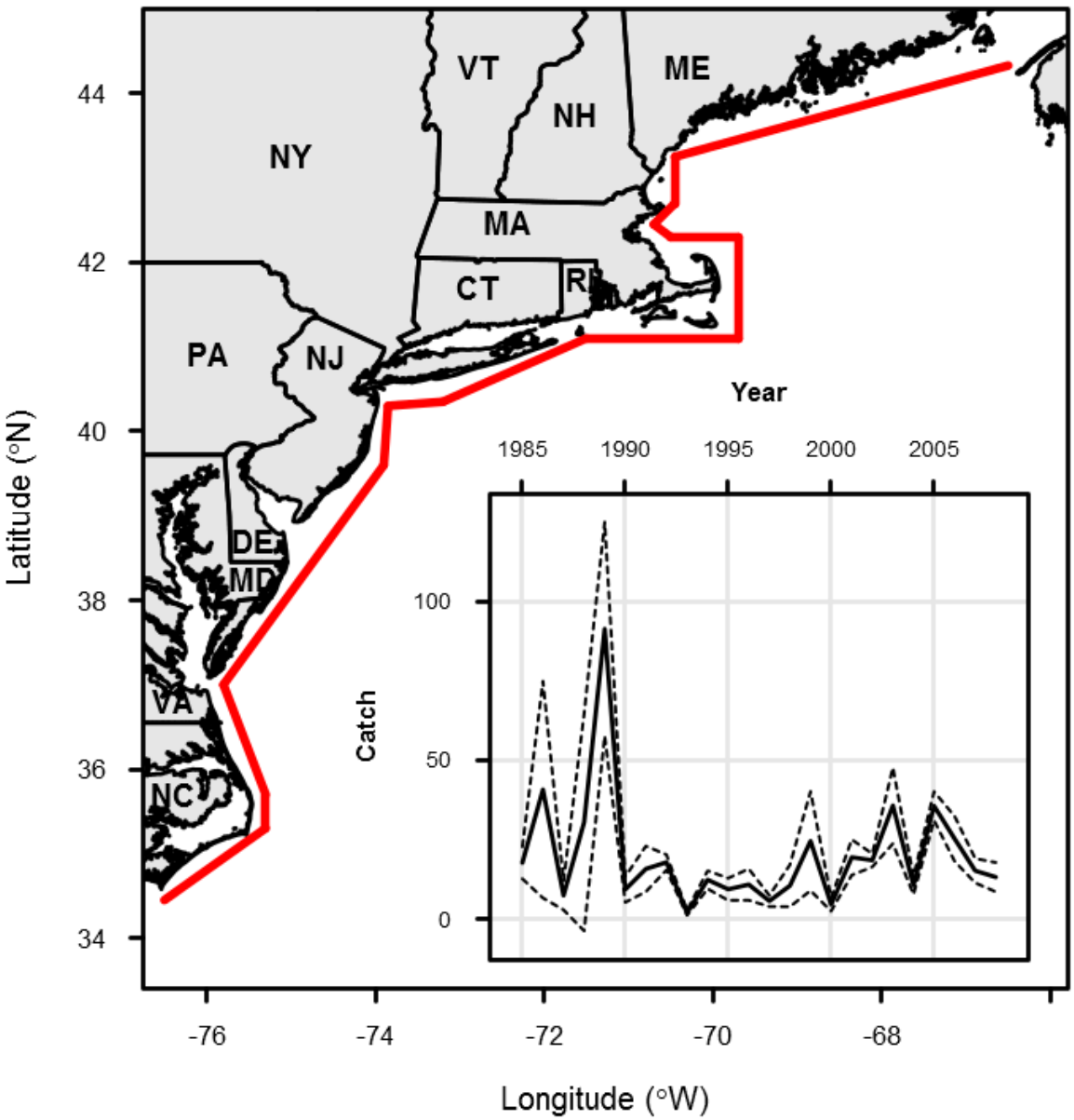

Figure B6.3A. Map of the NEFSC Fall Bottom Trawl Survey area and resultant index from the R/V Albatross years (inset). Red line represents extent of the survey area.

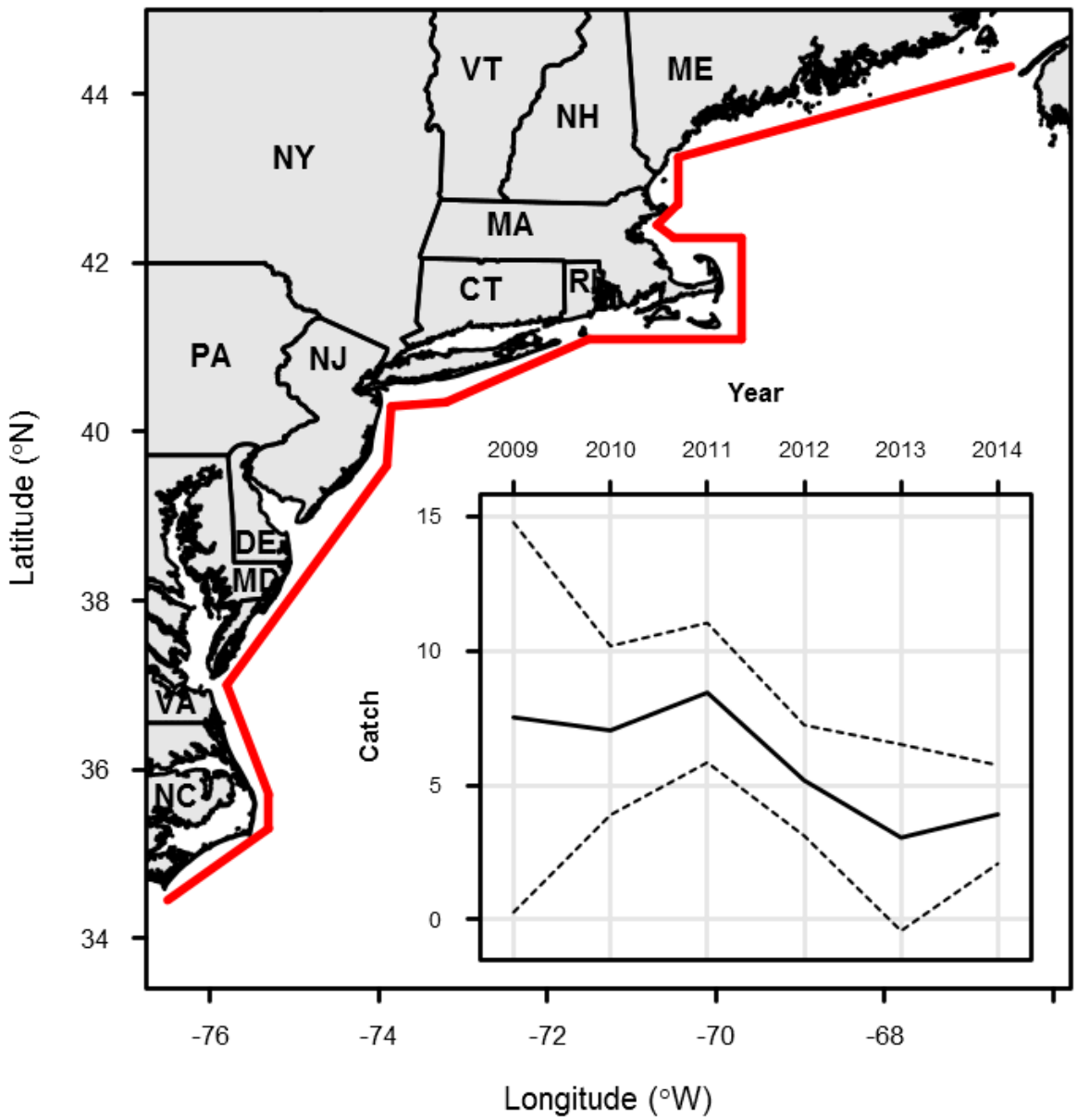

Figure B6.3B. Map of the NEFSC Fall Bottom Trawl Survey area and resultant index from the R/V Bigelow years (inset). Red line represents extent of the survey area.

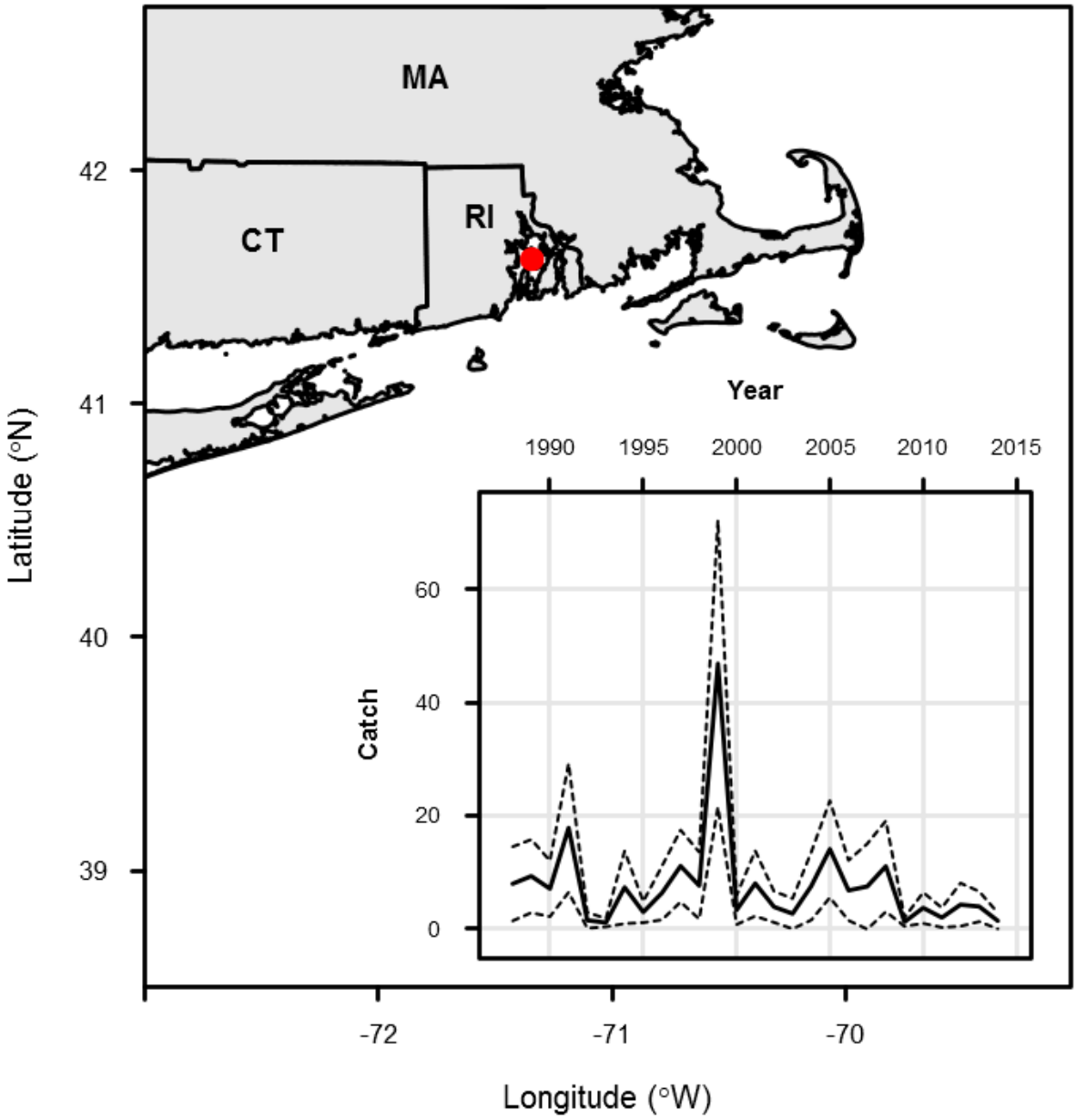

Figure B6.4. Map of the Rhode Island Narragansett Bay Juvenile Finfish Beach Seine Survey and resultant index of abundance (inset). Red dot indicates center point of survey area.

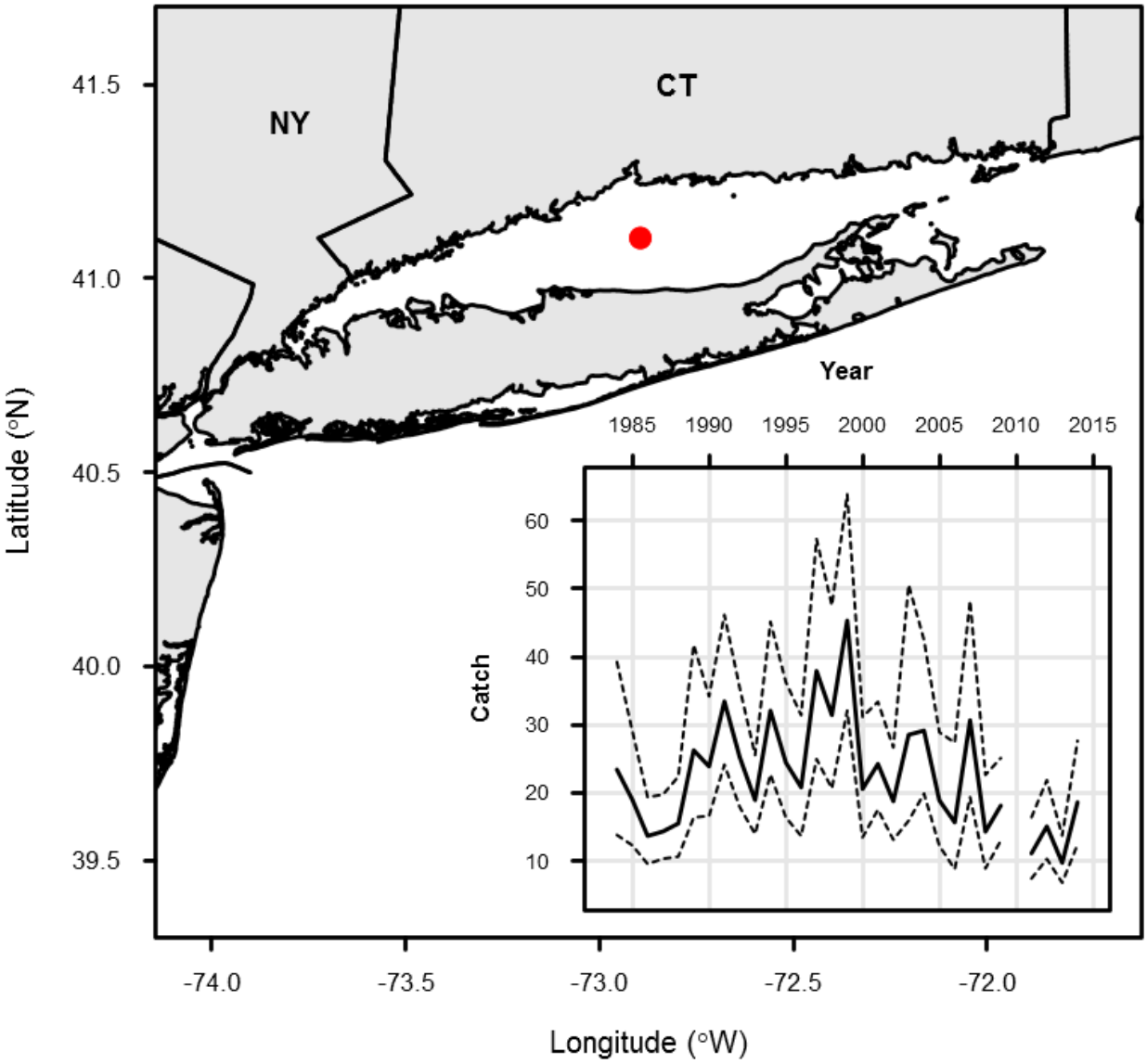

Figure B6.5. Map of the Connecticut Long Island Sound Bottom Trawl Survey and resultant index of abundance (inset). Red dot indicates center point of survey area.

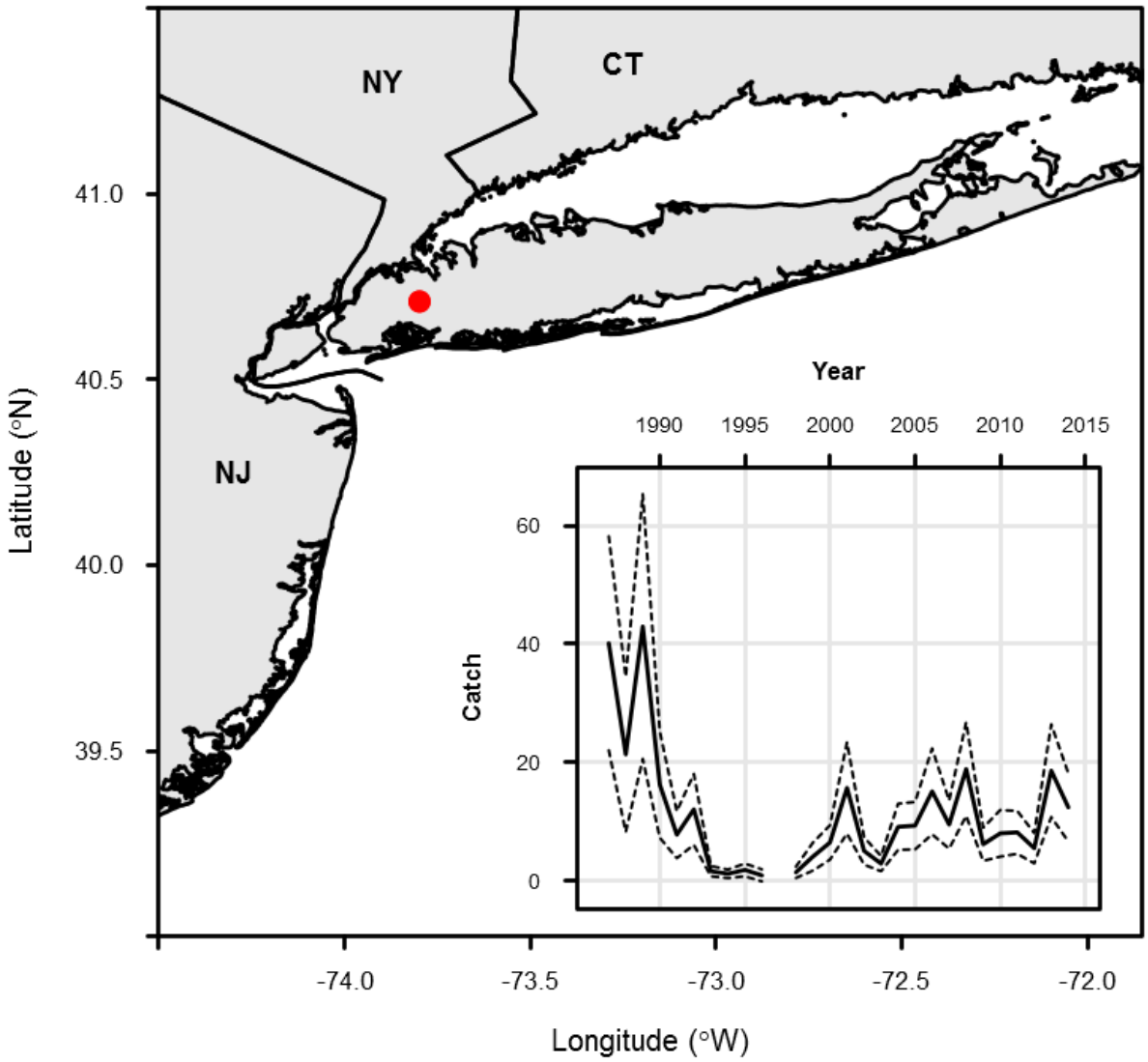

Figure B6.6. Map of the New York Western Long Island Sound Beach Seine Survey and resultant index of abundance (inset). Red dot indicates center point of survey area.

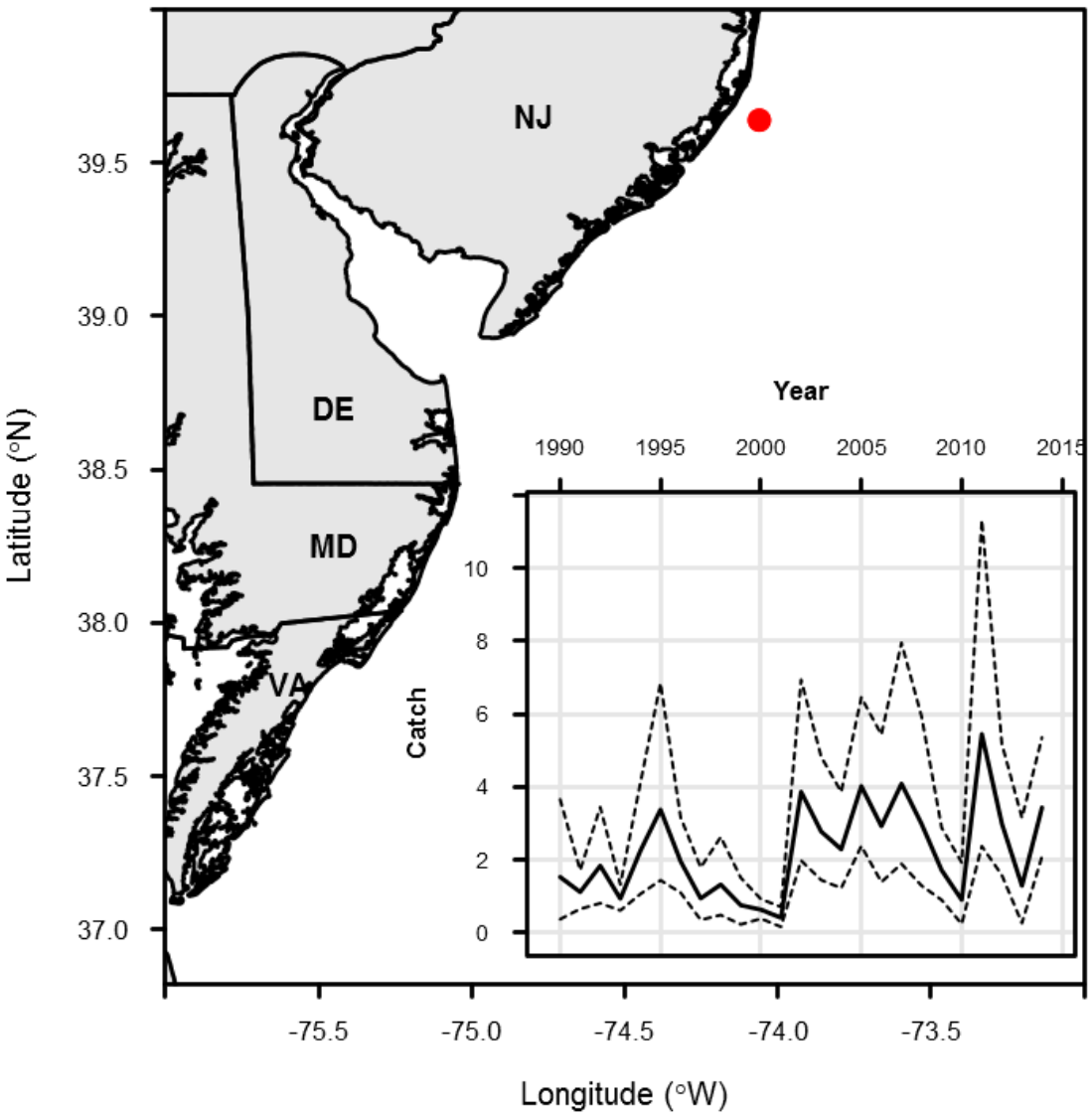

Figure B6.7. Map of the New Jersey Ocean Bottom Trawl Survey and resultant index of abundance (inset). Red dot indicates center point of survey area.

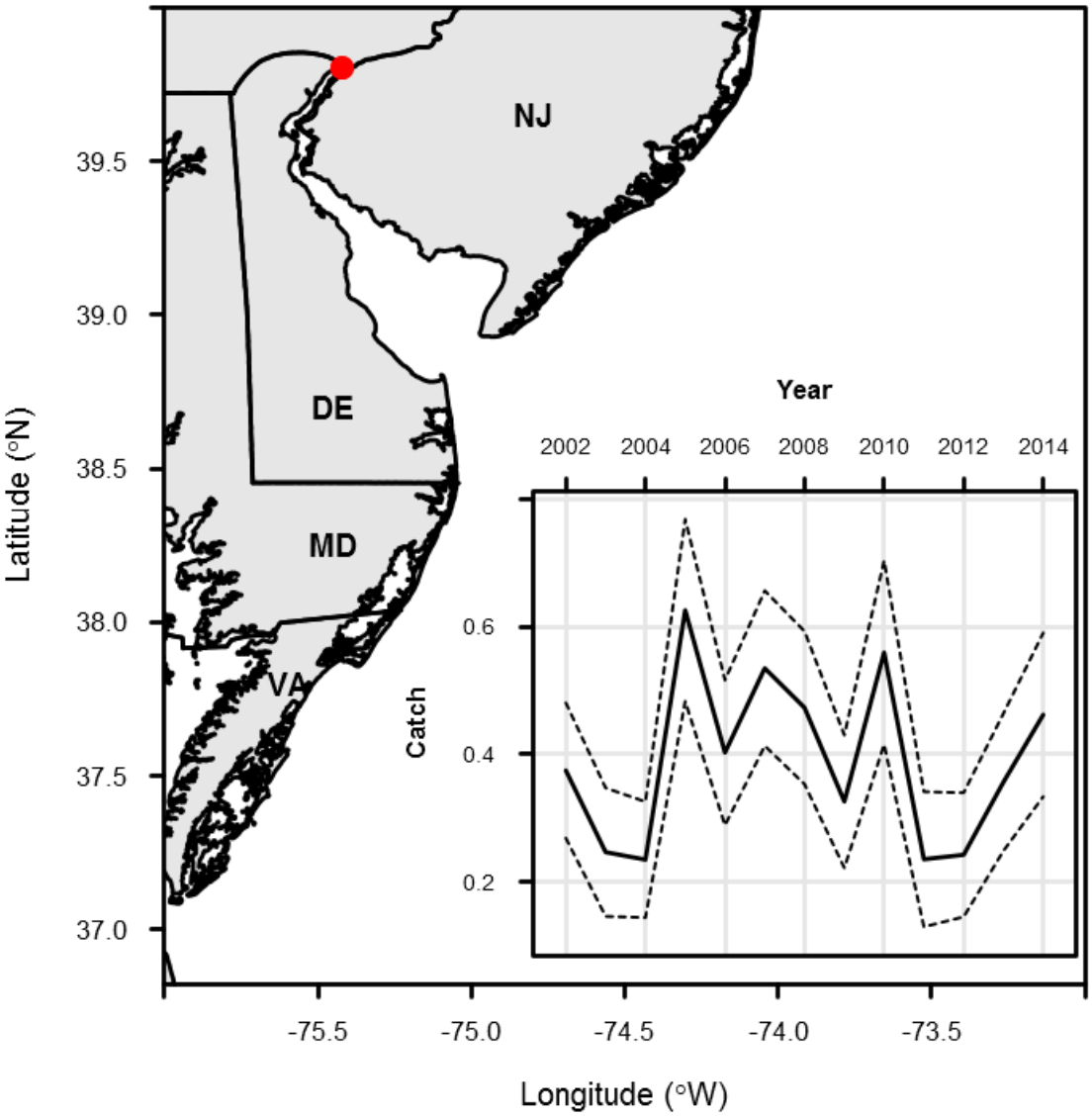

Figure B6.8. Map of the New Jersey Delaware River Seine Survey and resultant index of abundance (inset). Red dot indicates center point of survey area.

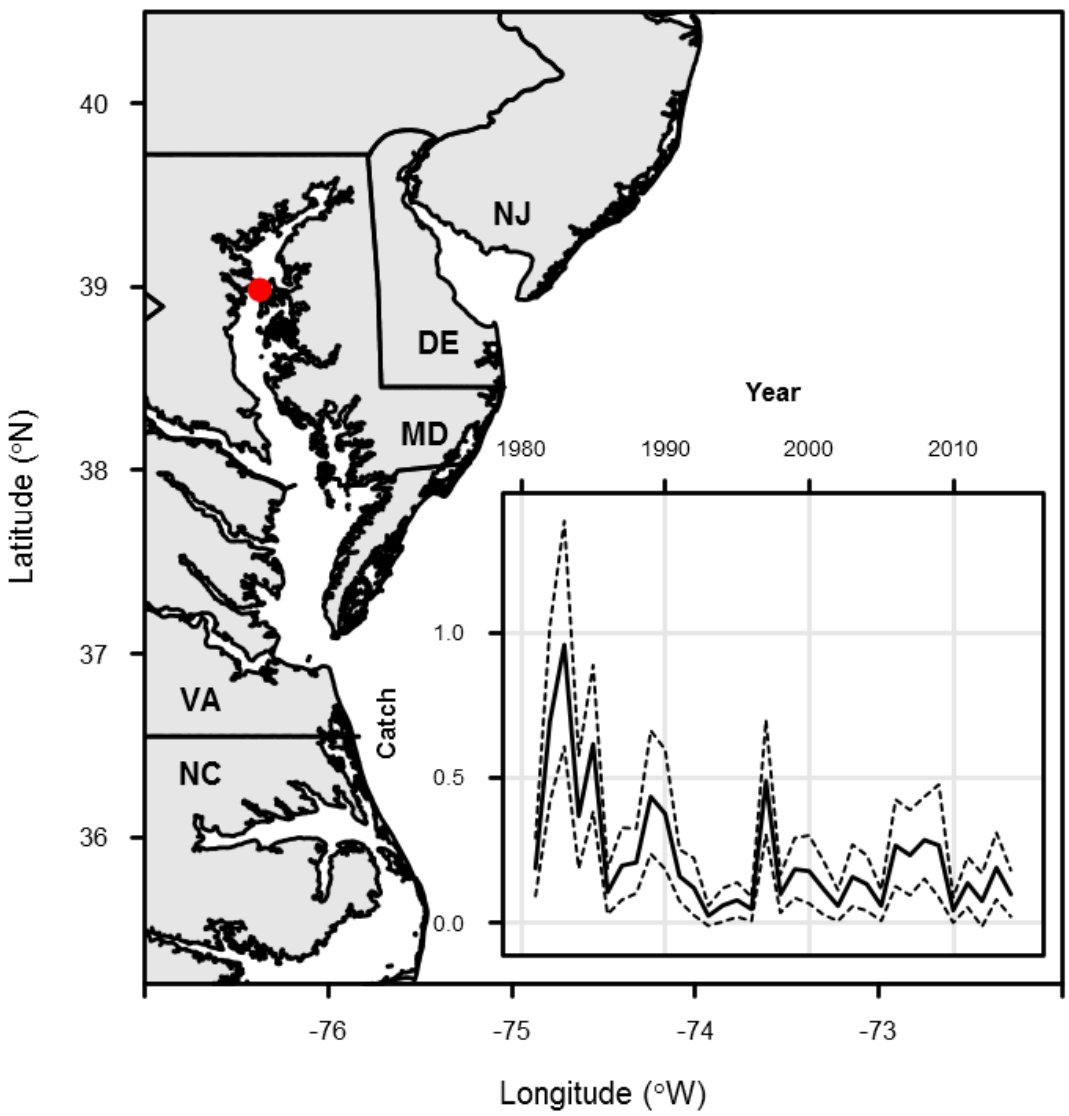

Figure B6.9. Map of the Maryland Juvenile Striped Bass Seine Survey and resultant index of abundance (inset). Red dot indicates center point of survey area.

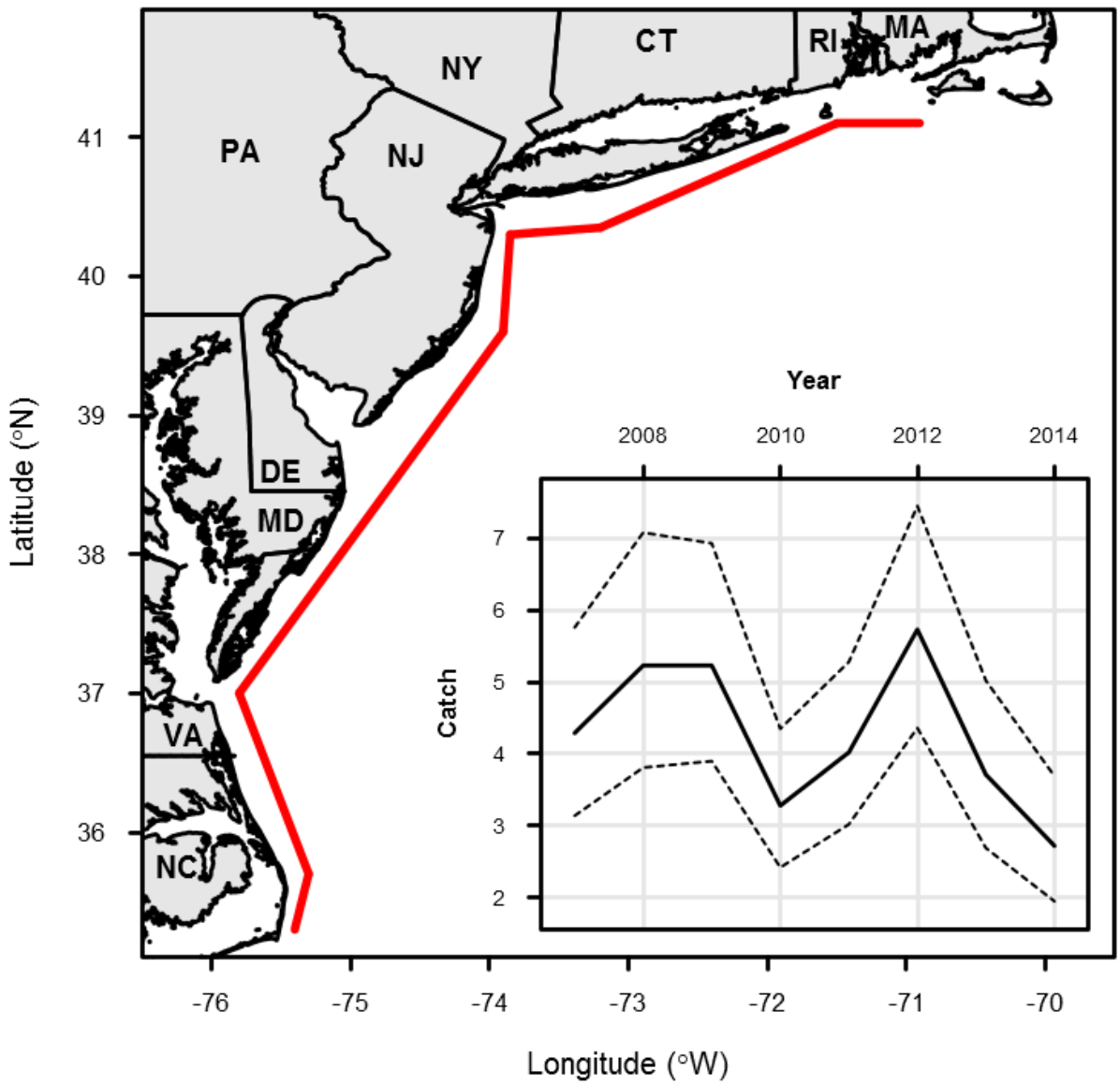

Figure B6.10. Map of the NEAMAP Fall Bottom Trawl survey area and resultant index (inset). Red line represents extent of the survey area.

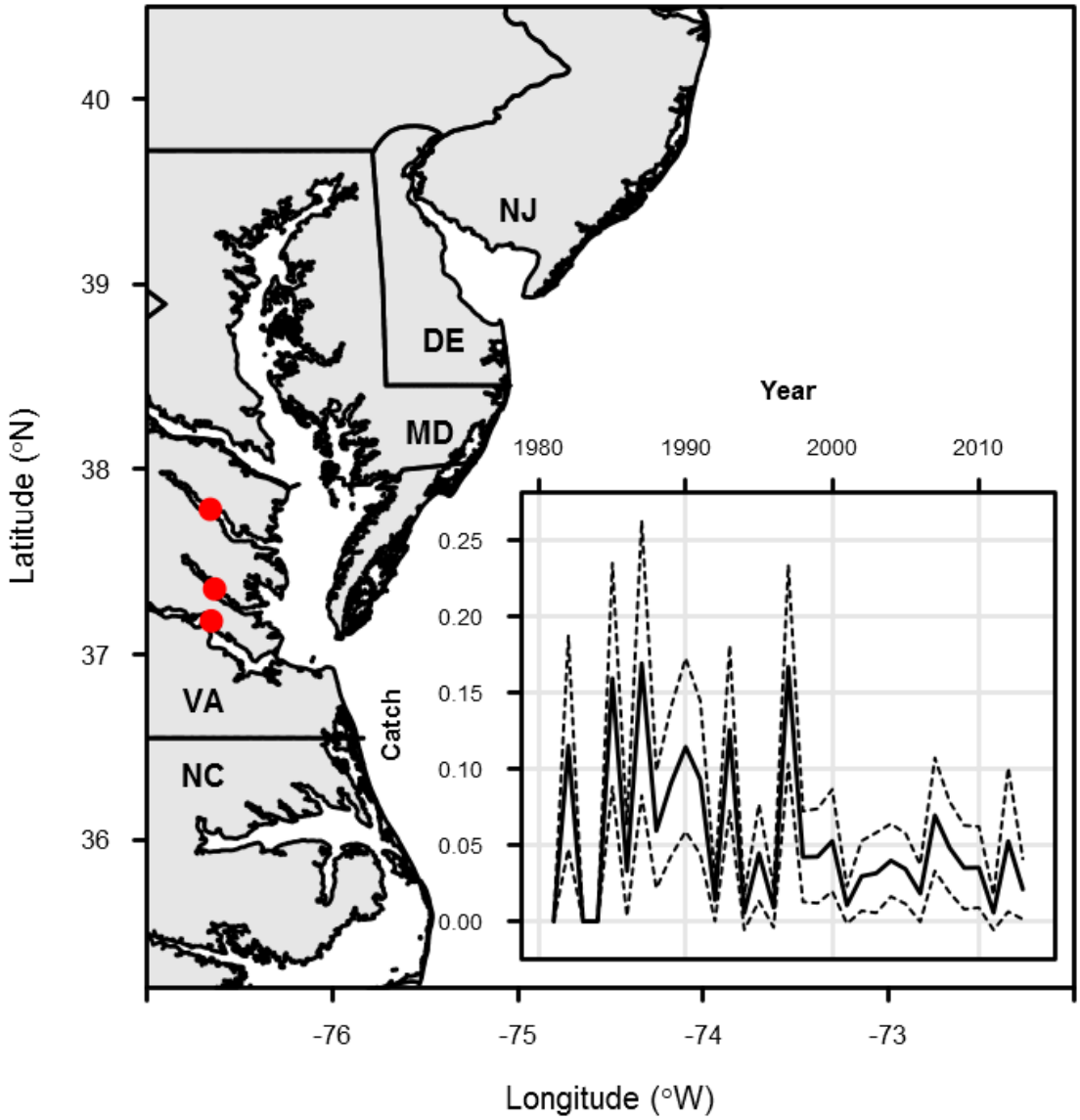

Figure B6.11. Map of the VIMS Juvenile Striped Bass Seine Survey area and resulting index of abundance (inset). Red dot indicates the center point in each of the three river systems surveyed.

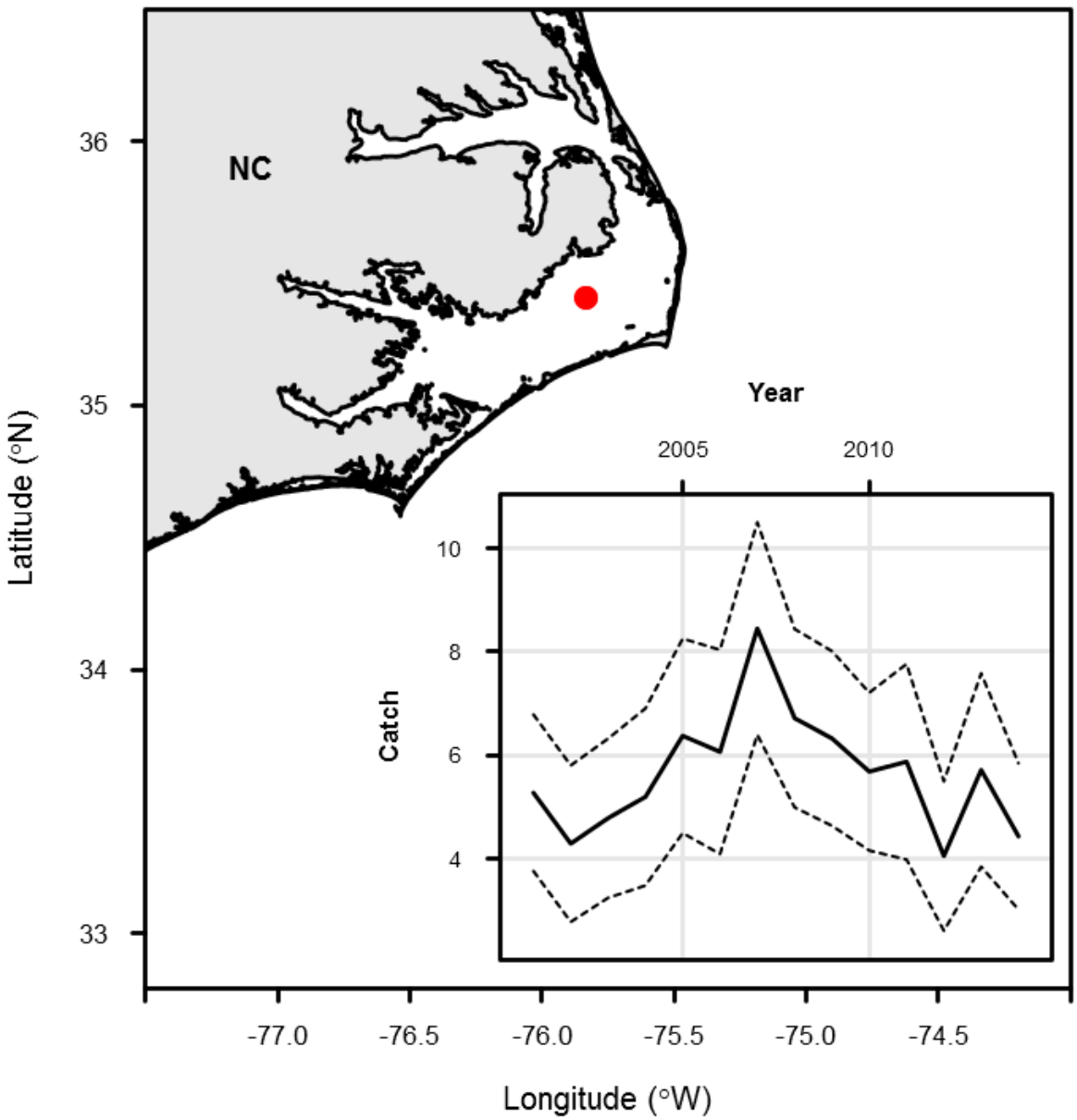

Figure B6.12. Map of the North Carolina Pamlico Sound Independent Gillnet Survey and resultant index of abundance (inset). Red dot indicates center point of survey area.

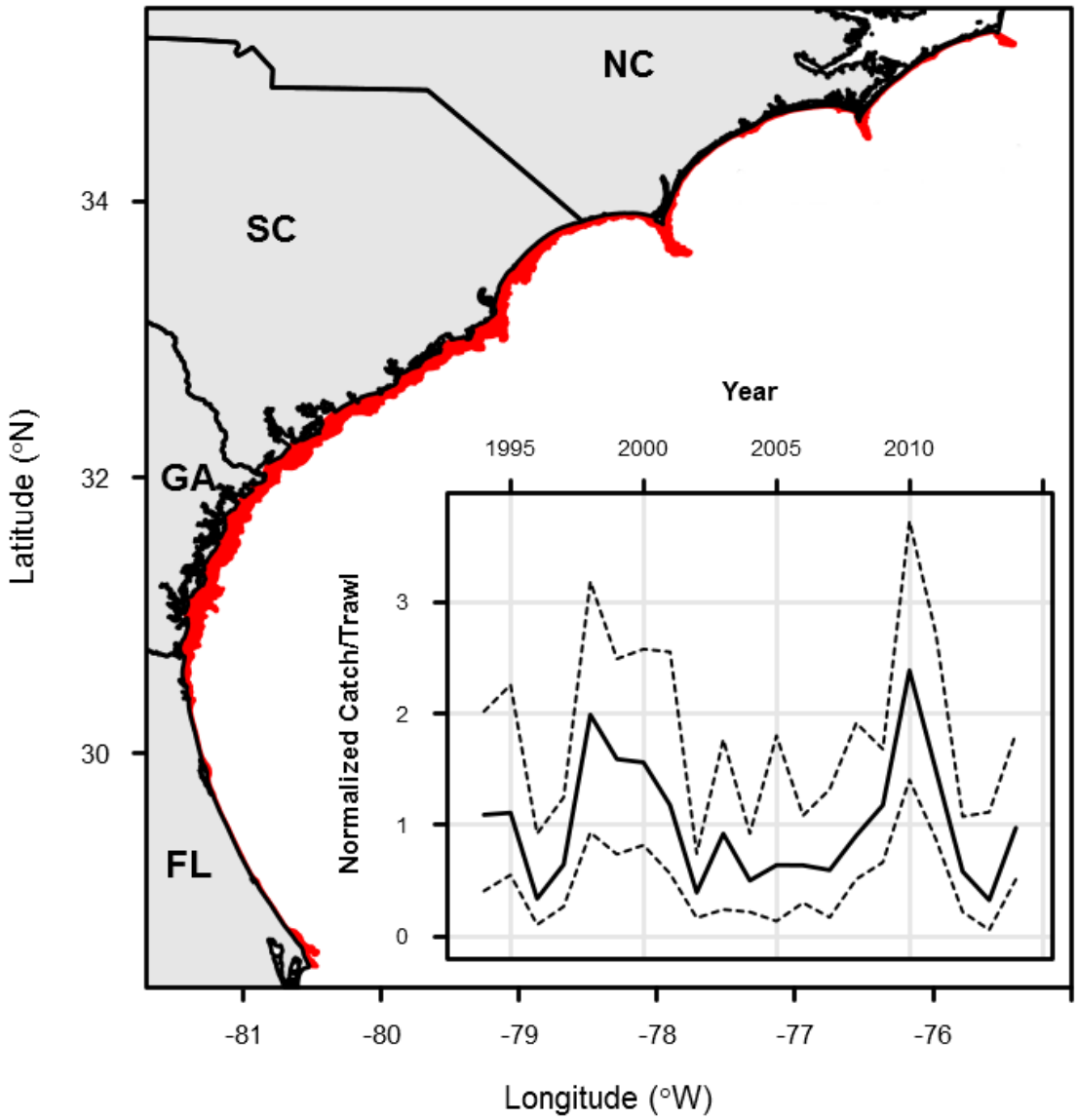

Figure B6.13. Map of the SEAMAP-SA Fall Bottom Trawl survey area and resultant index (inset). Red area represents total survey area.

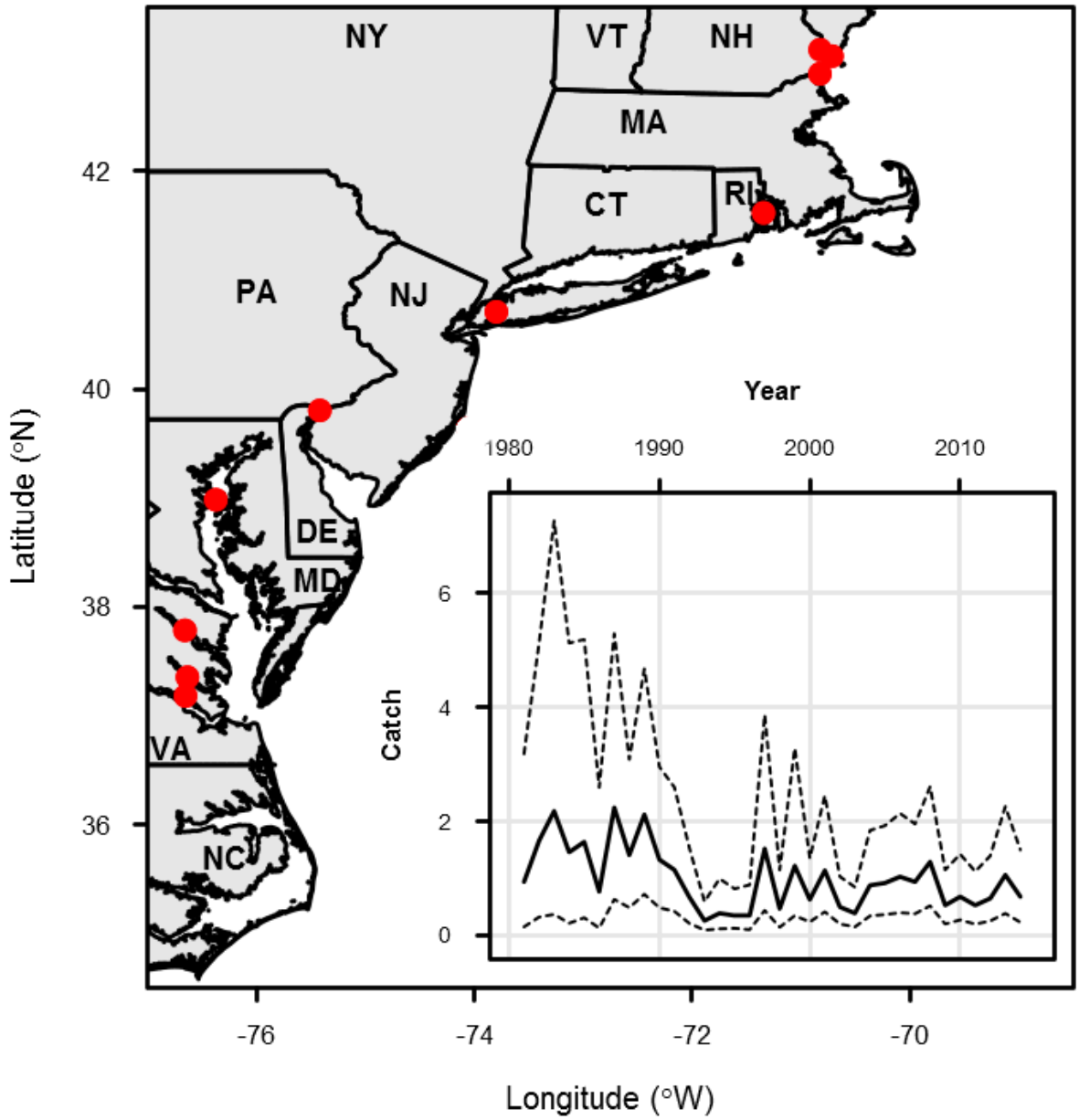

Figure B6.14. Map of all state seine surveys included in the composite young-of-year index with resultant index (inset).

Age 0

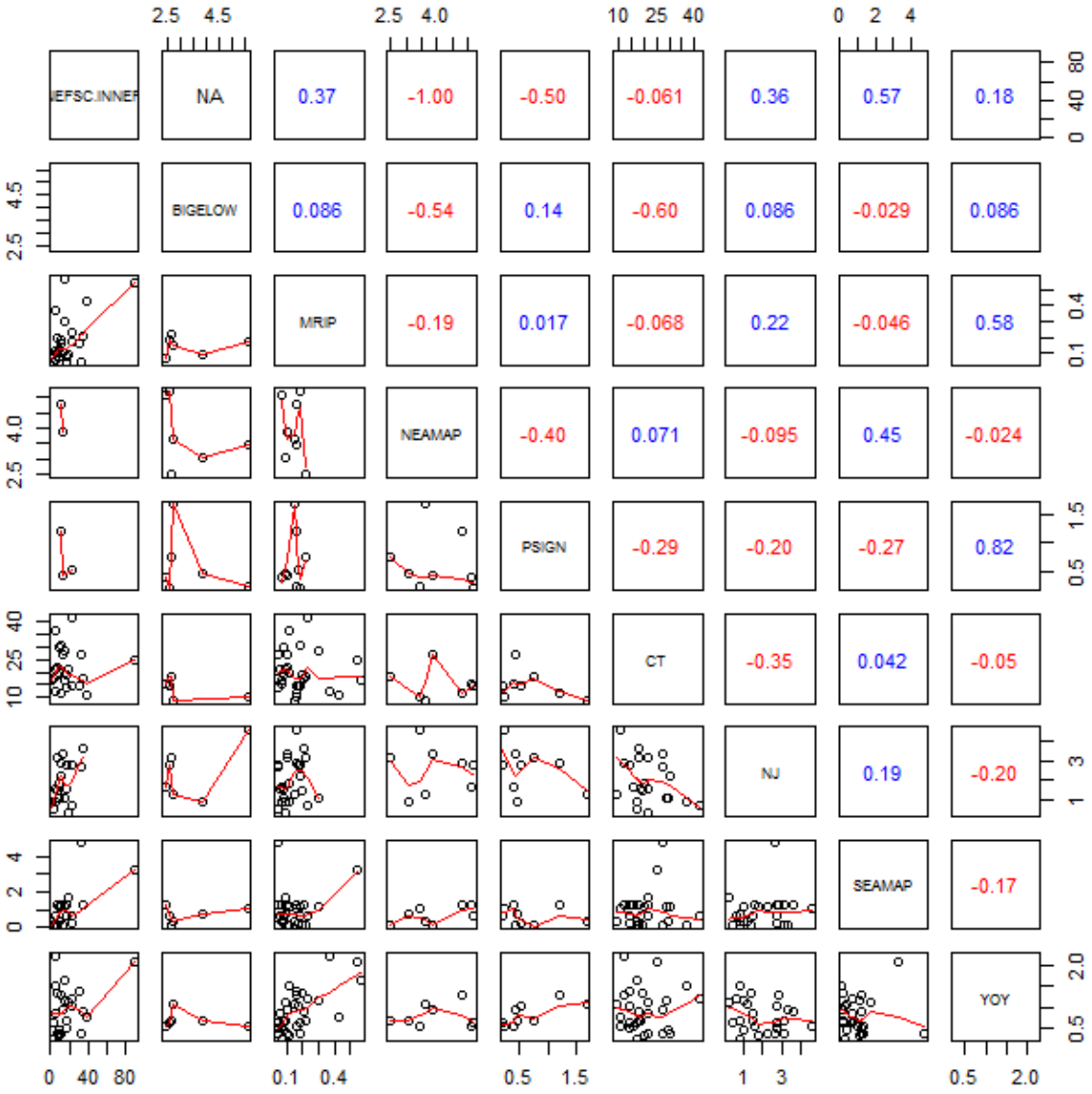

Figure B6.15. Correlation matrices of age specific indices. A locally-weighted polynomial regression smoother (lowess) trend line (red) is added to each pairwise comparison. Spearman correlation coefficients are indicated in the upper half of the matrix (red for negative correlations, blue for positive)

Age 1

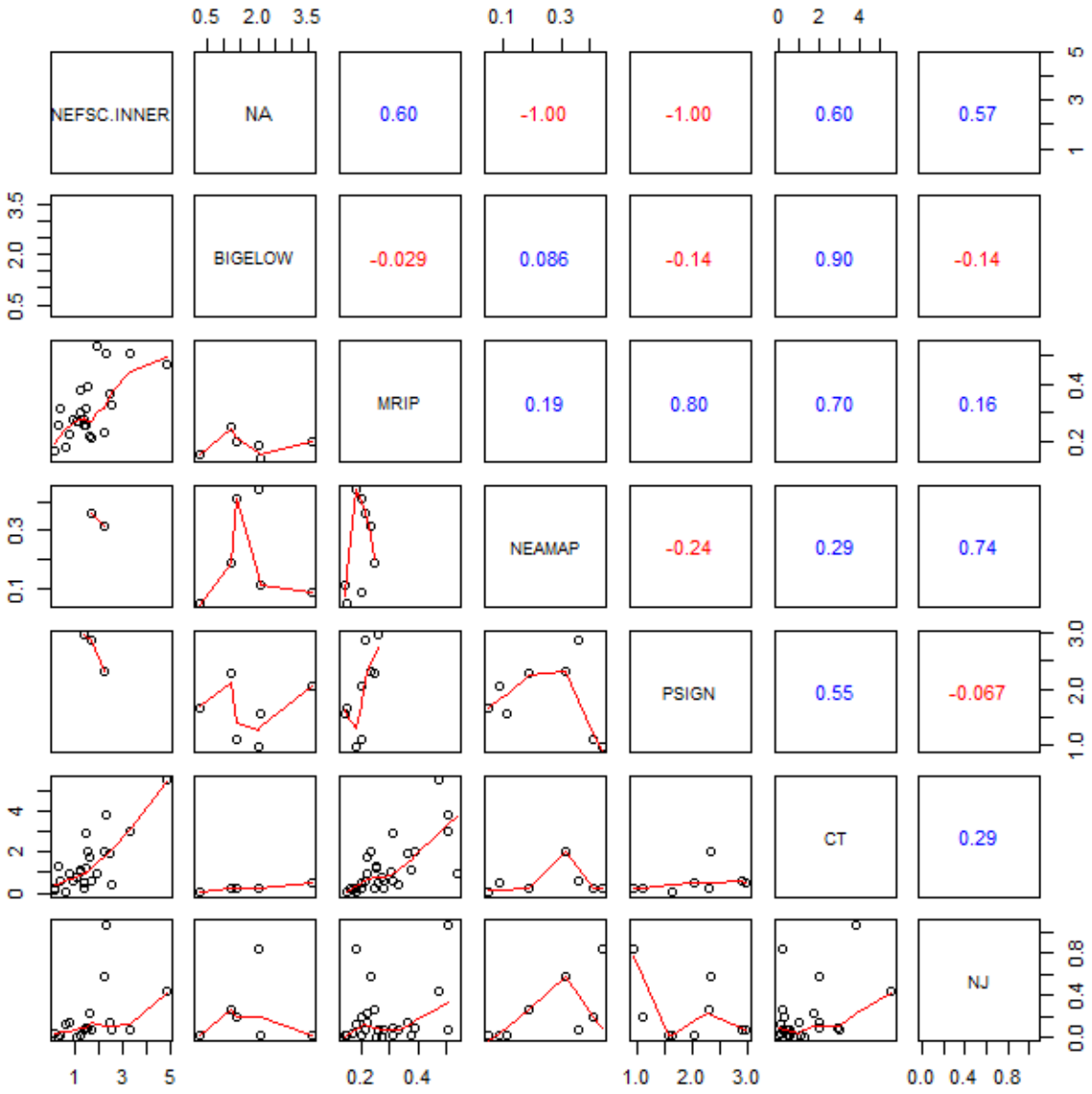

Figure B6.15 (cont.)

Age 2

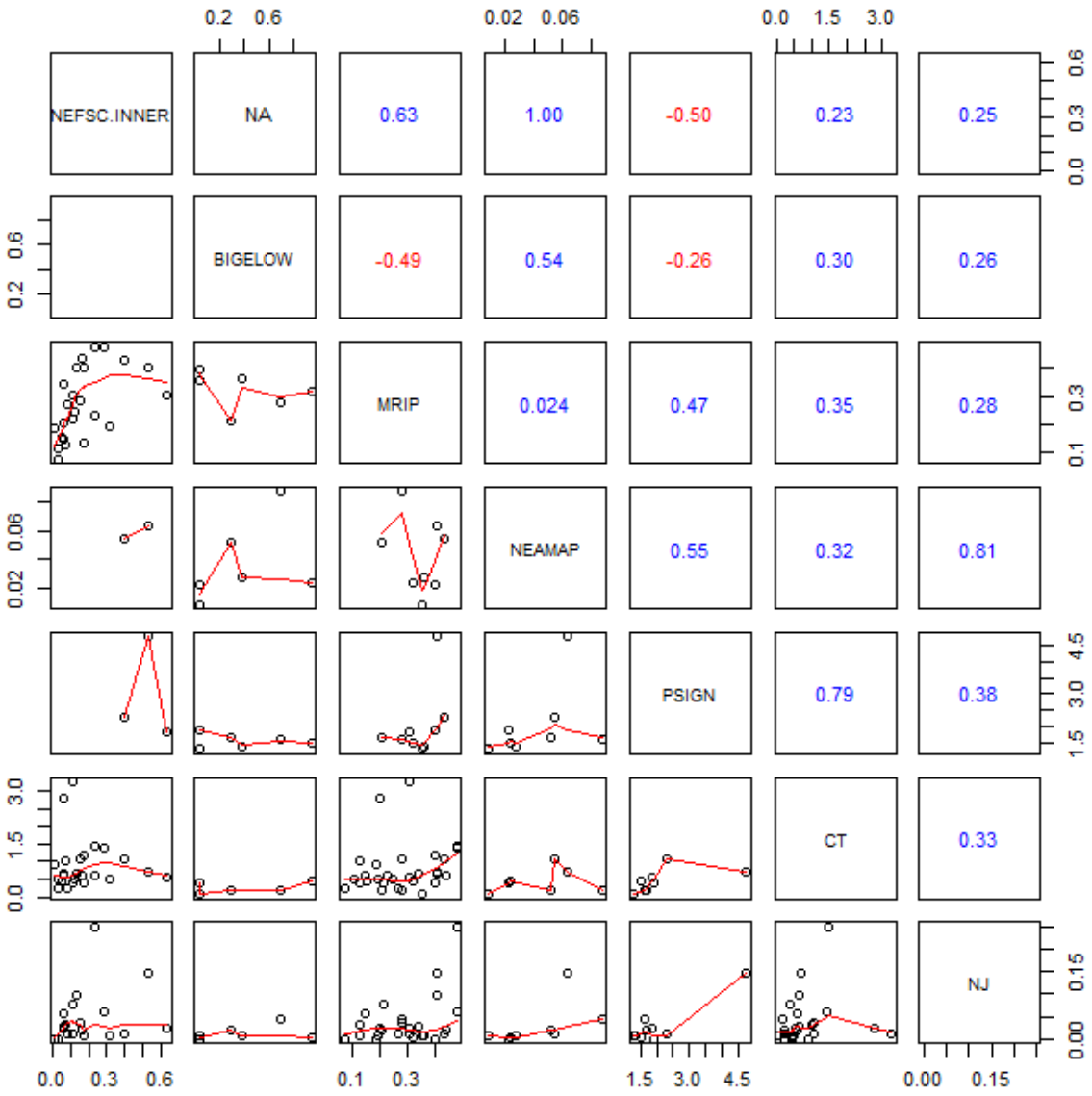

Figure B6.15 (cont.)

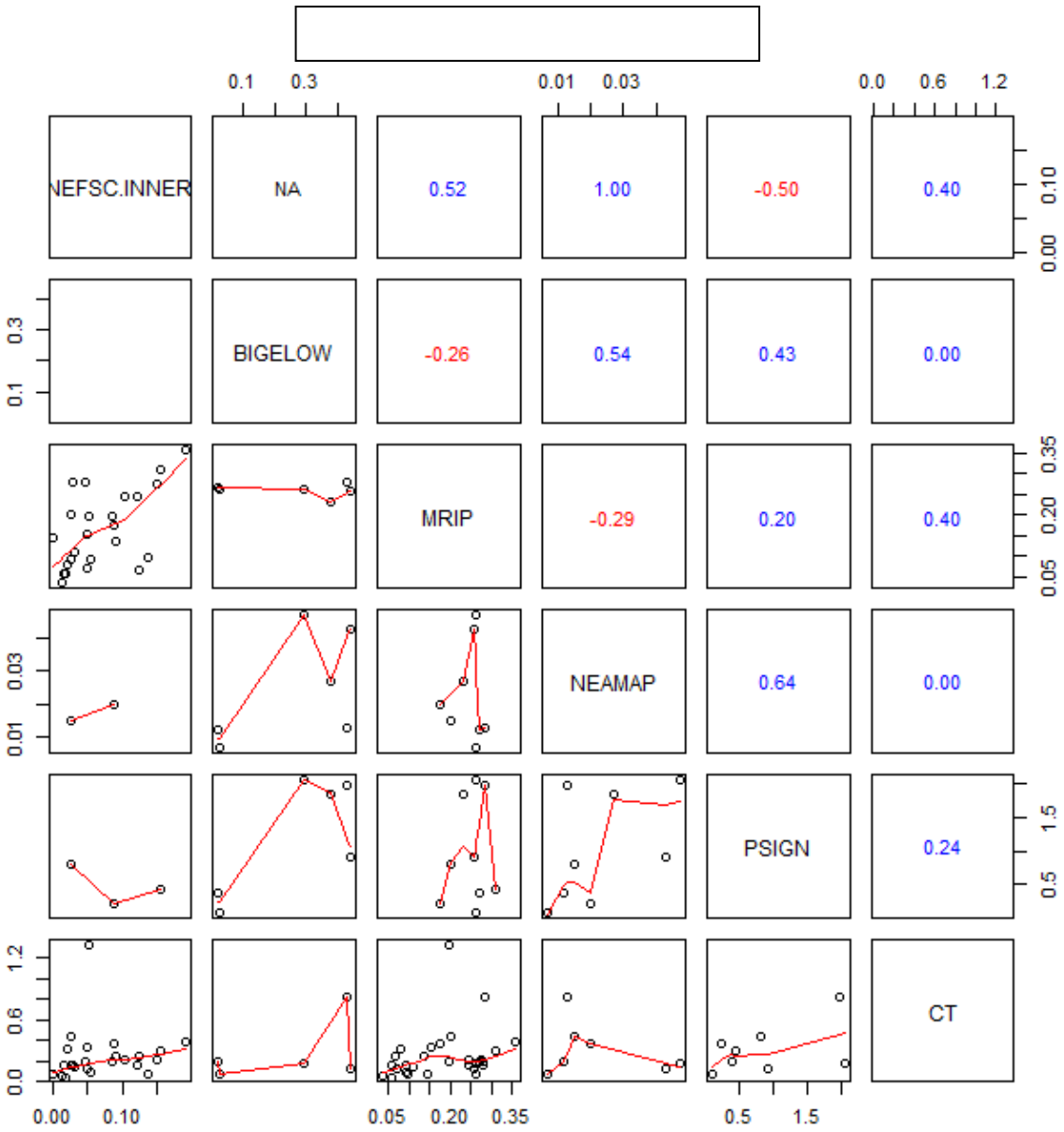

Figure B6.15 (cont.)

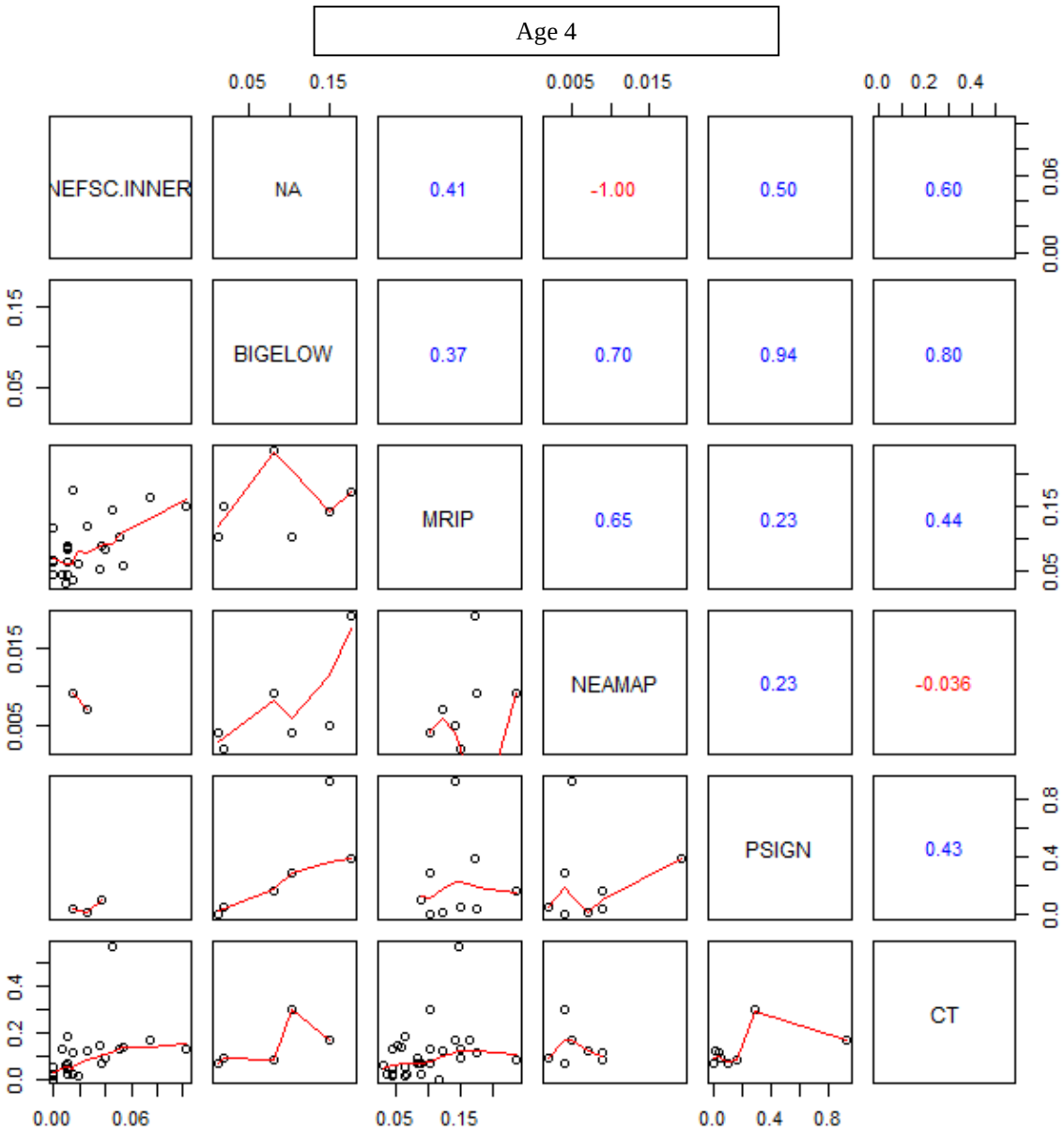

Figure B6.15 (cont.)

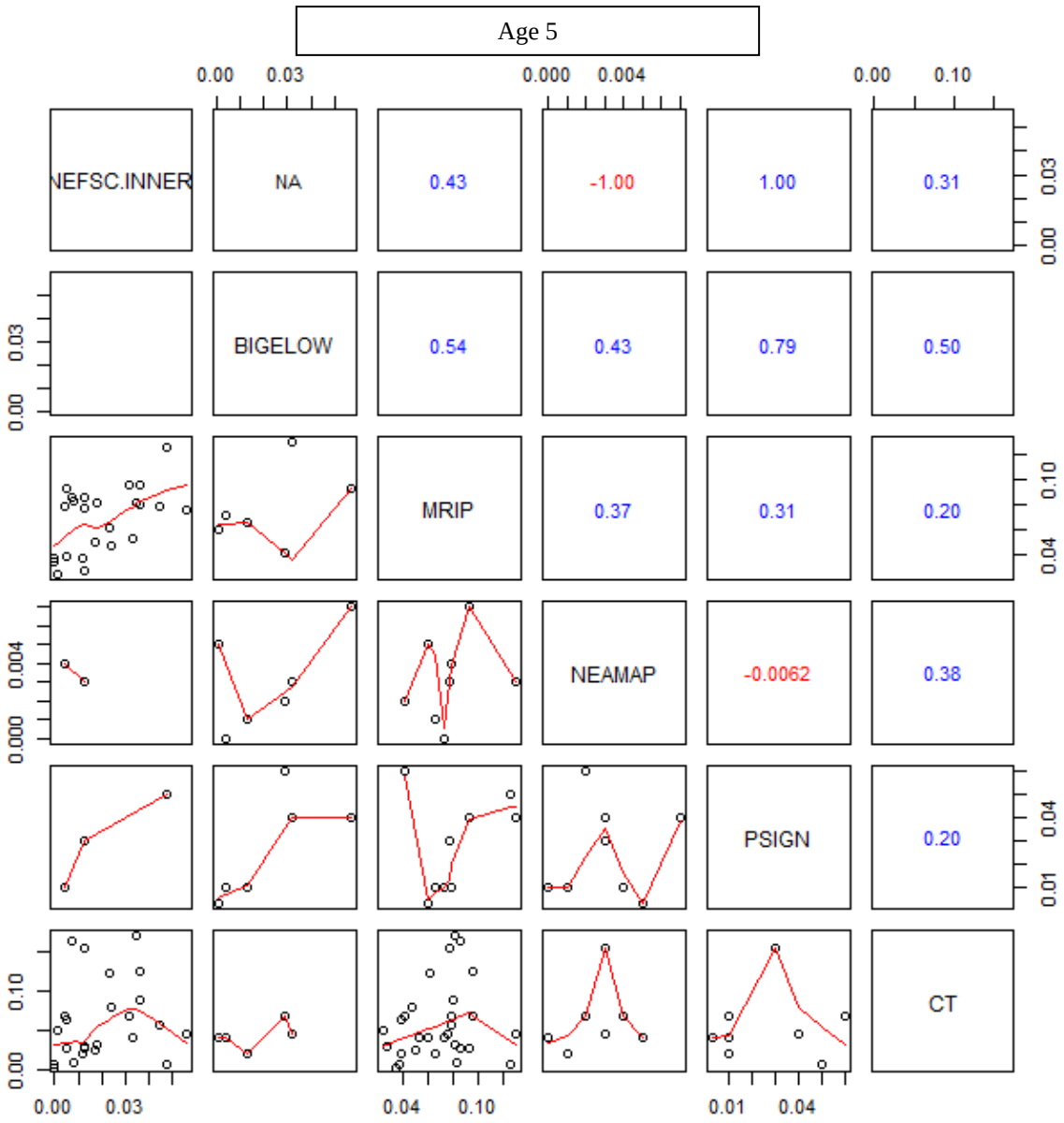

Figure B6.15 (cont.)

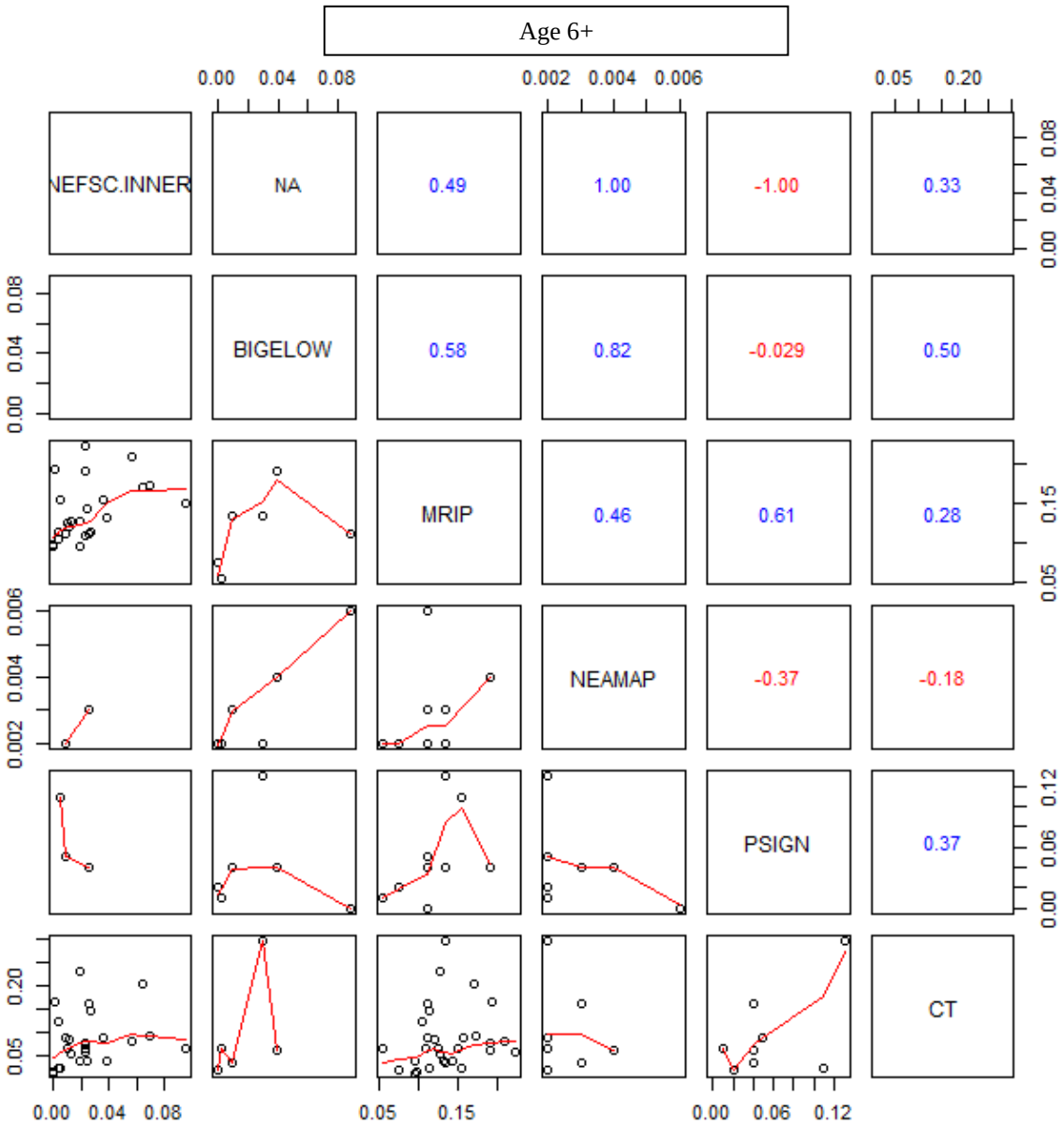

Figure B6.15 (cont.)

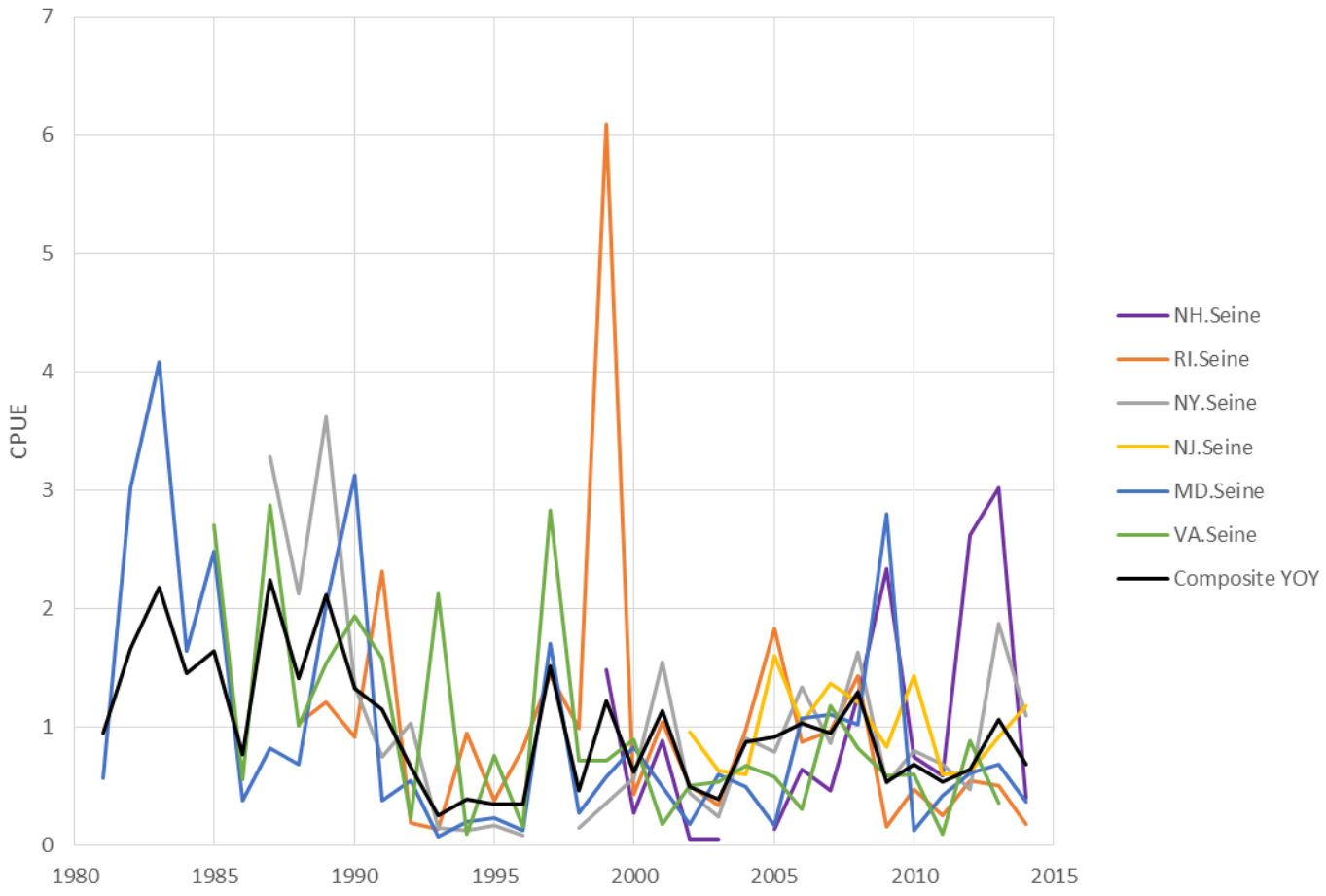

Figure B6.16. Composite young-of-year index plotted with component state indices. All indices are scaled to their mean.

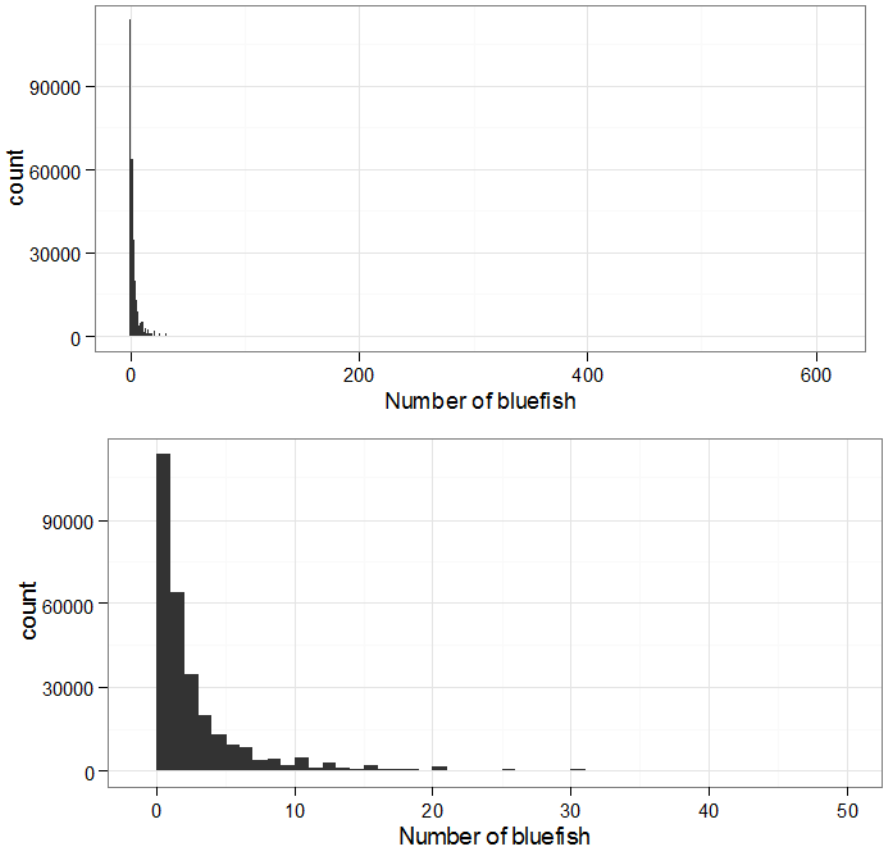

Figure B6.17. Distribution of observed catch-per-trip of bluefish. Lower figure has been truncated to trips with less than 50 bluefish per trip to improve readability.

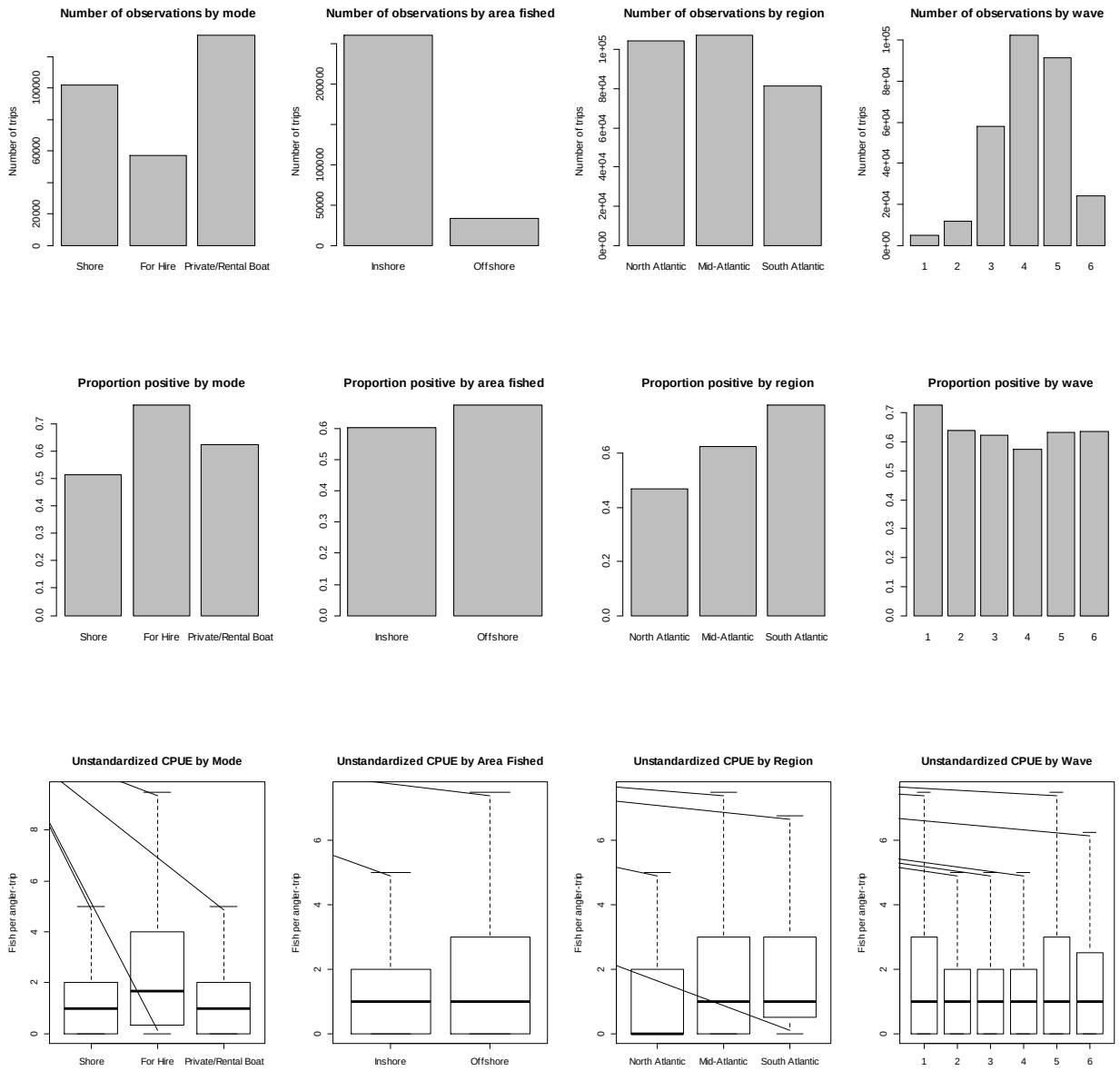

Figure B6.18. Number of observations (top), proportion positive trips (middle), and unstandardized CPUE (bottom) by factor for MRIP intercept data.

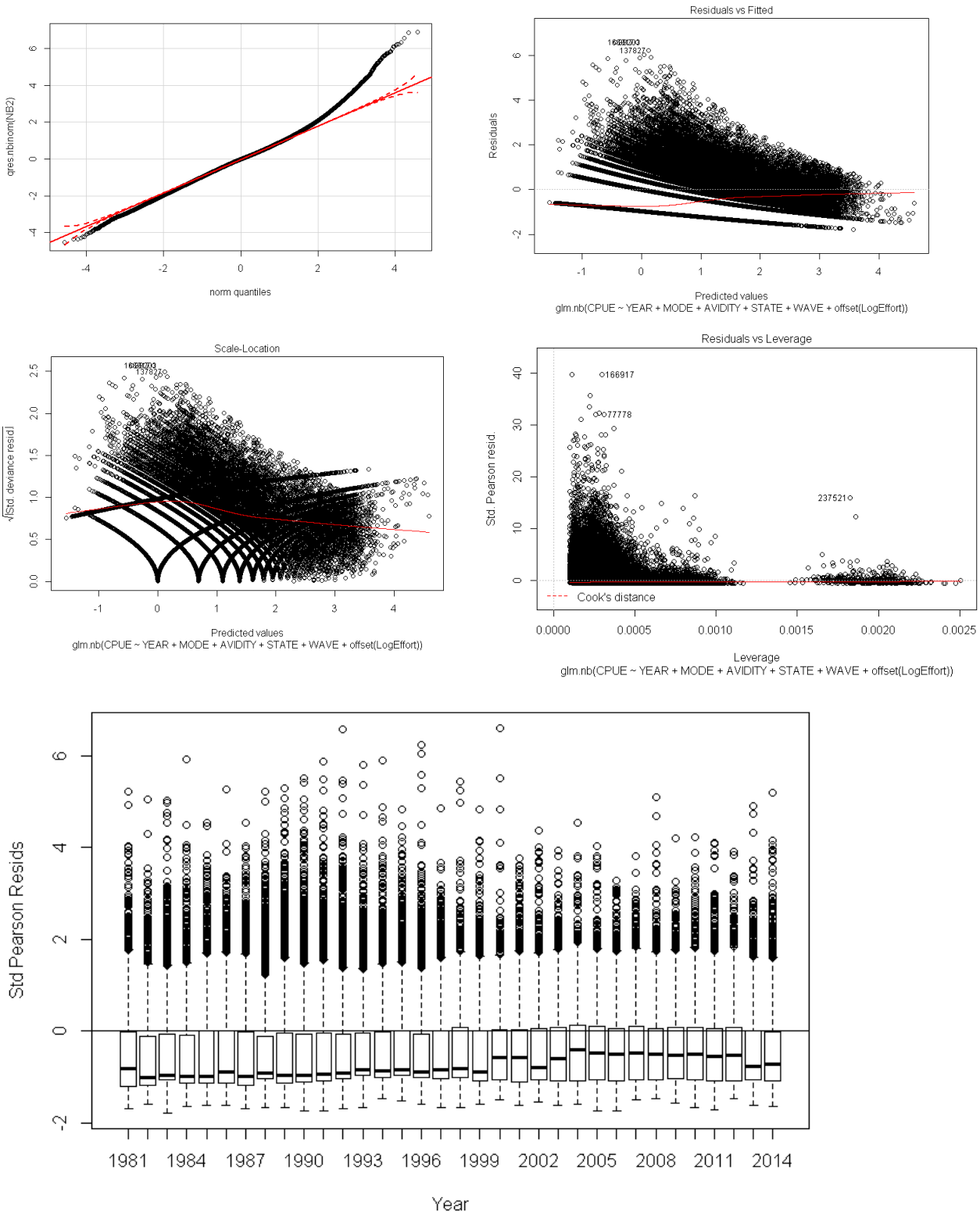

Figure B6.19.Diagnostic plots for GLM standardization of MRIP CPUE.

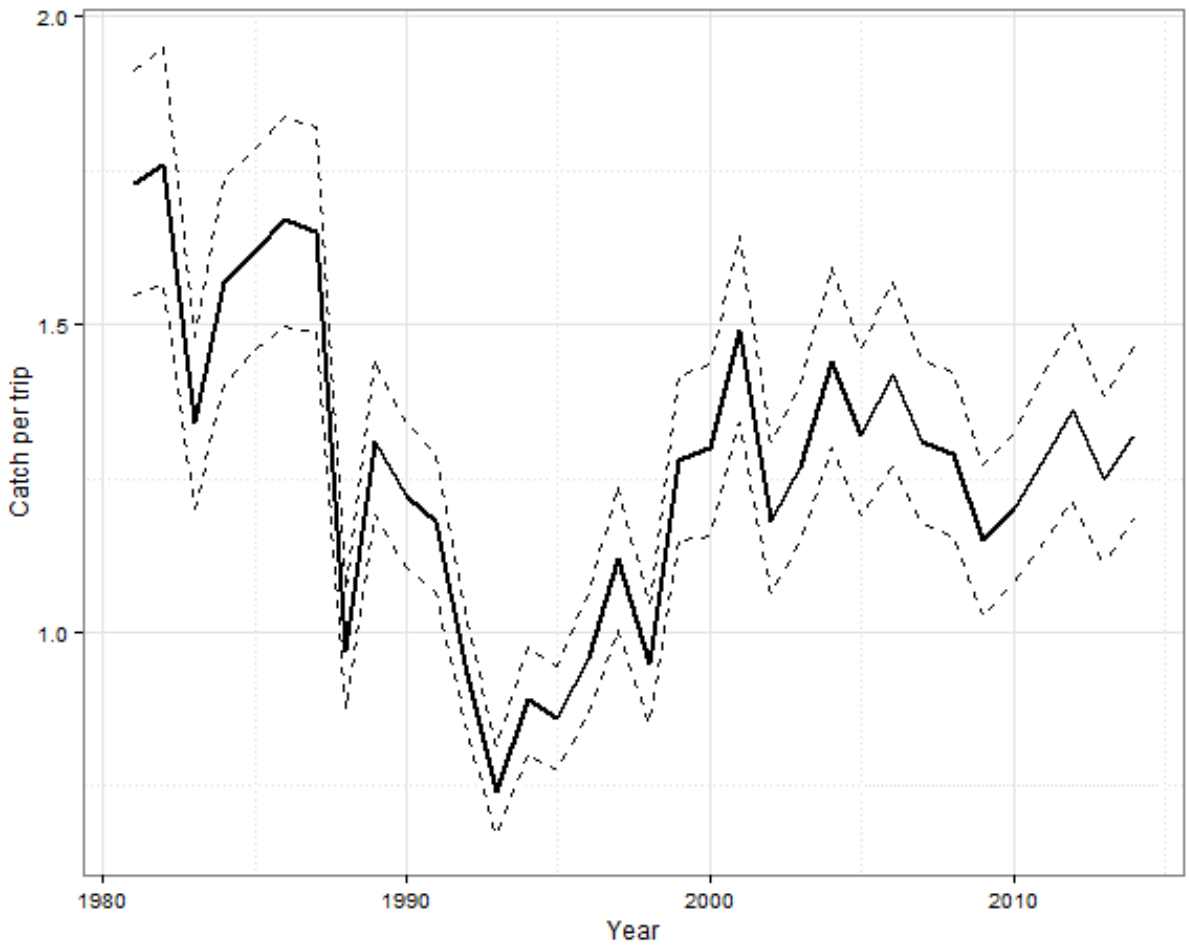

Figure B6.20.Standardized MRIP CPUE with 95% confidence intervals.

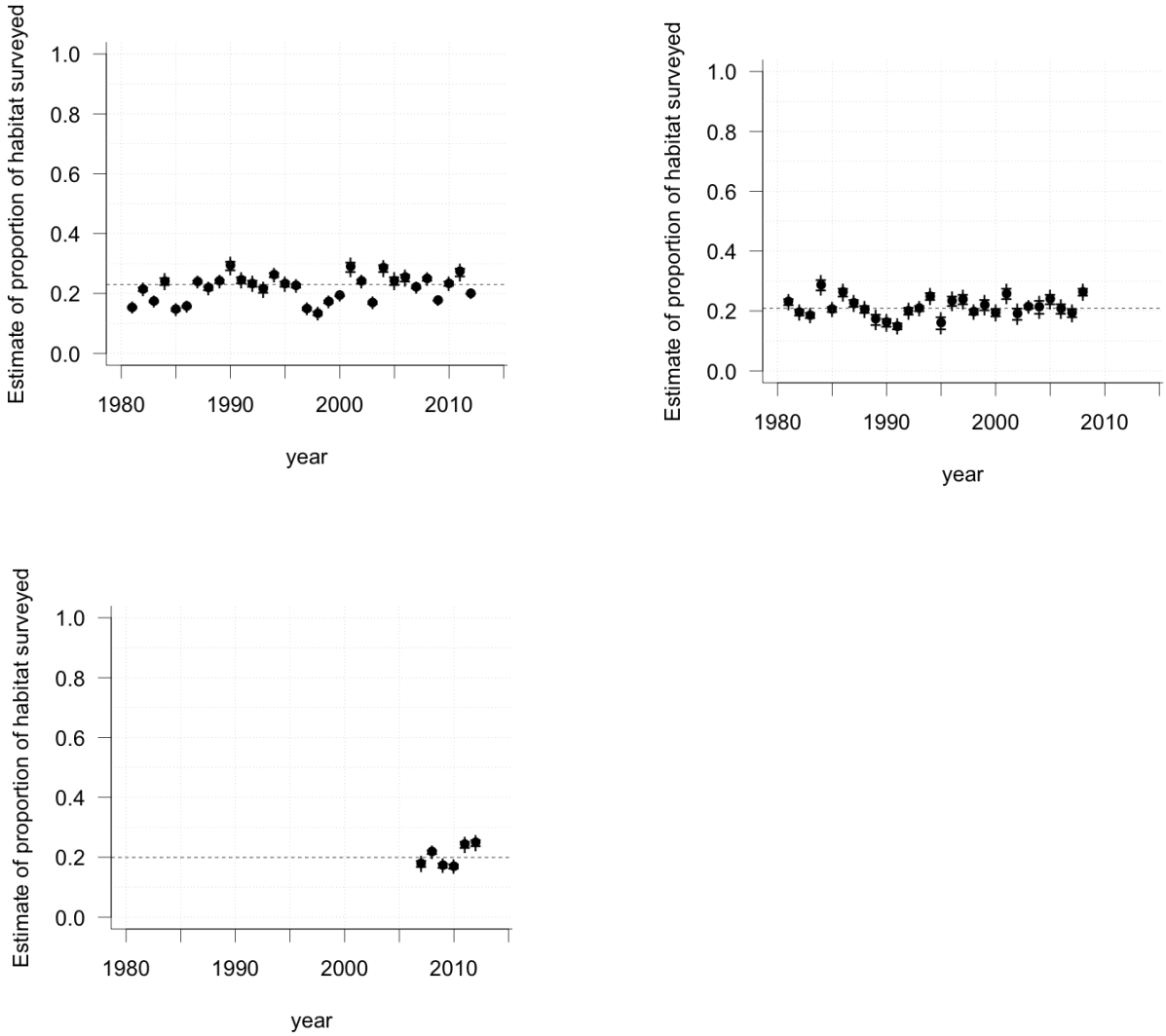

Figure B6.21 Estimates of the proportion of thermal habitat suitability surveyed for bluefish estimated using the niche model coupled to the debiased bottom temperature hindcast for NEFSC "offshore" inshore strata (top left), NEFSC "inshore" inshore strata and NEAMAP survey strata during the fall.

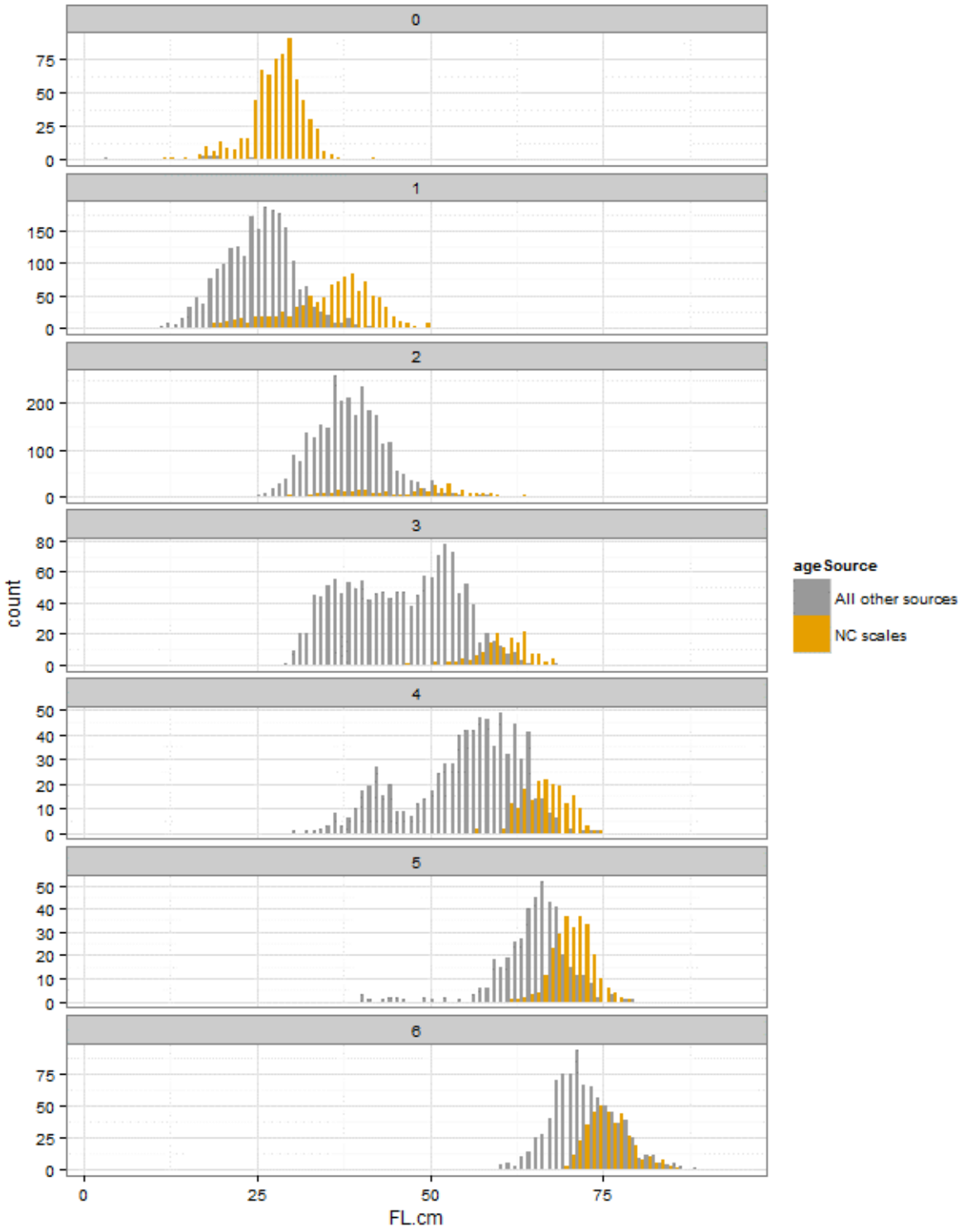

Figure B6.22. Length frequency of spring age data by age and source.

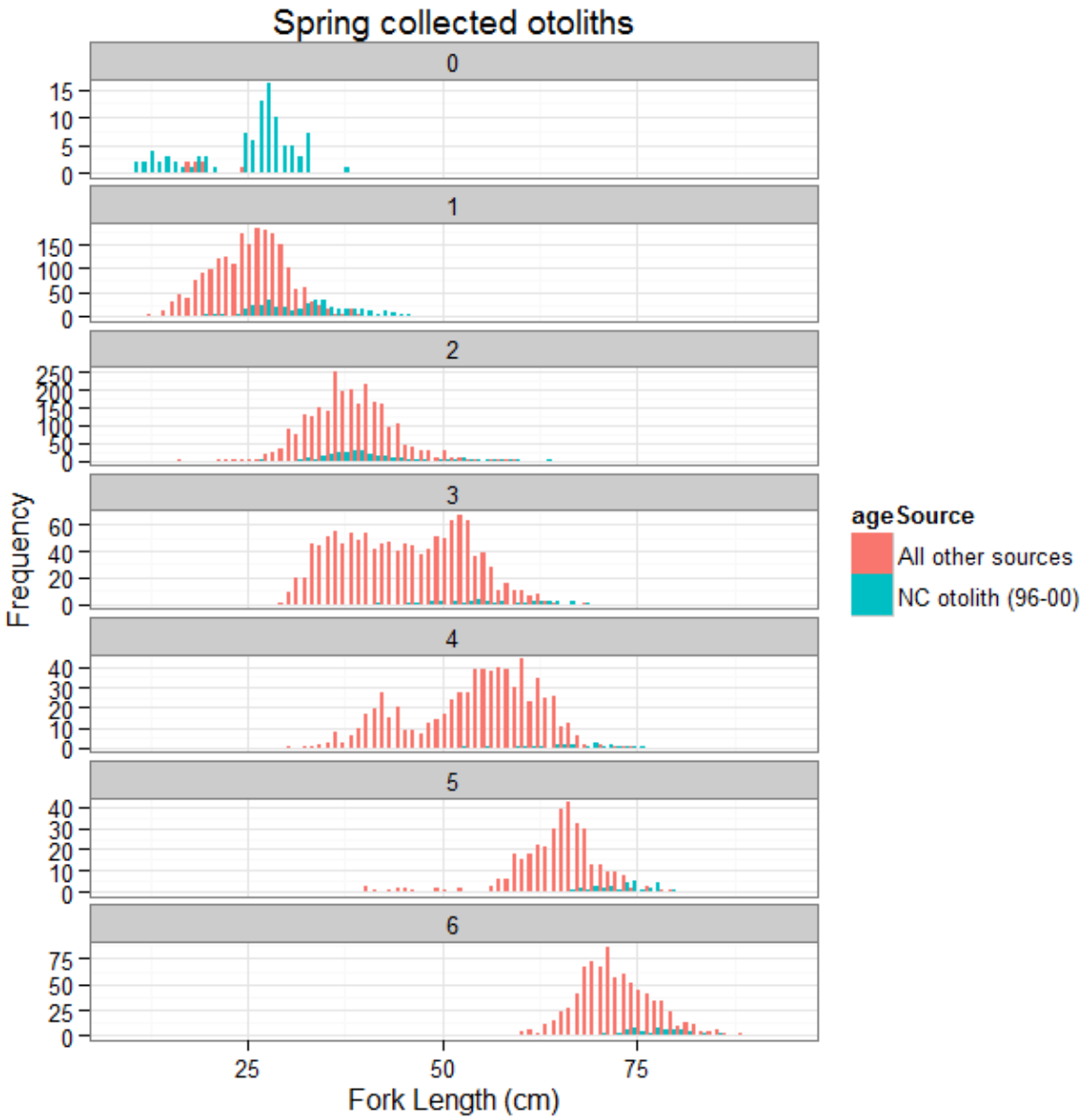

Figure B6.23. Length frequency of spring collected otolith data by age and source.

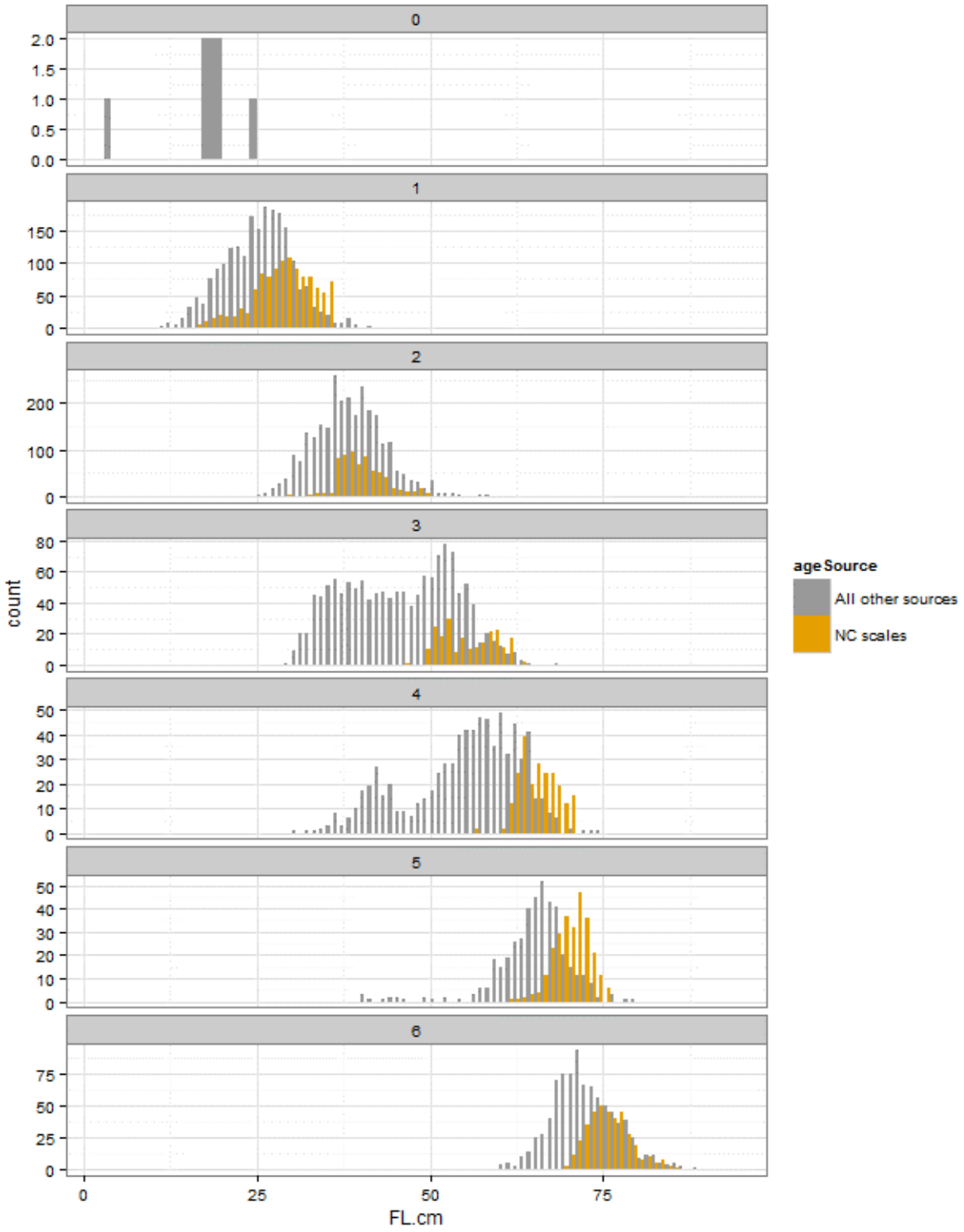

Figure B6.24. Length frequency of spring collected fish by age and source, with NC scales corrected for the birthday issue.

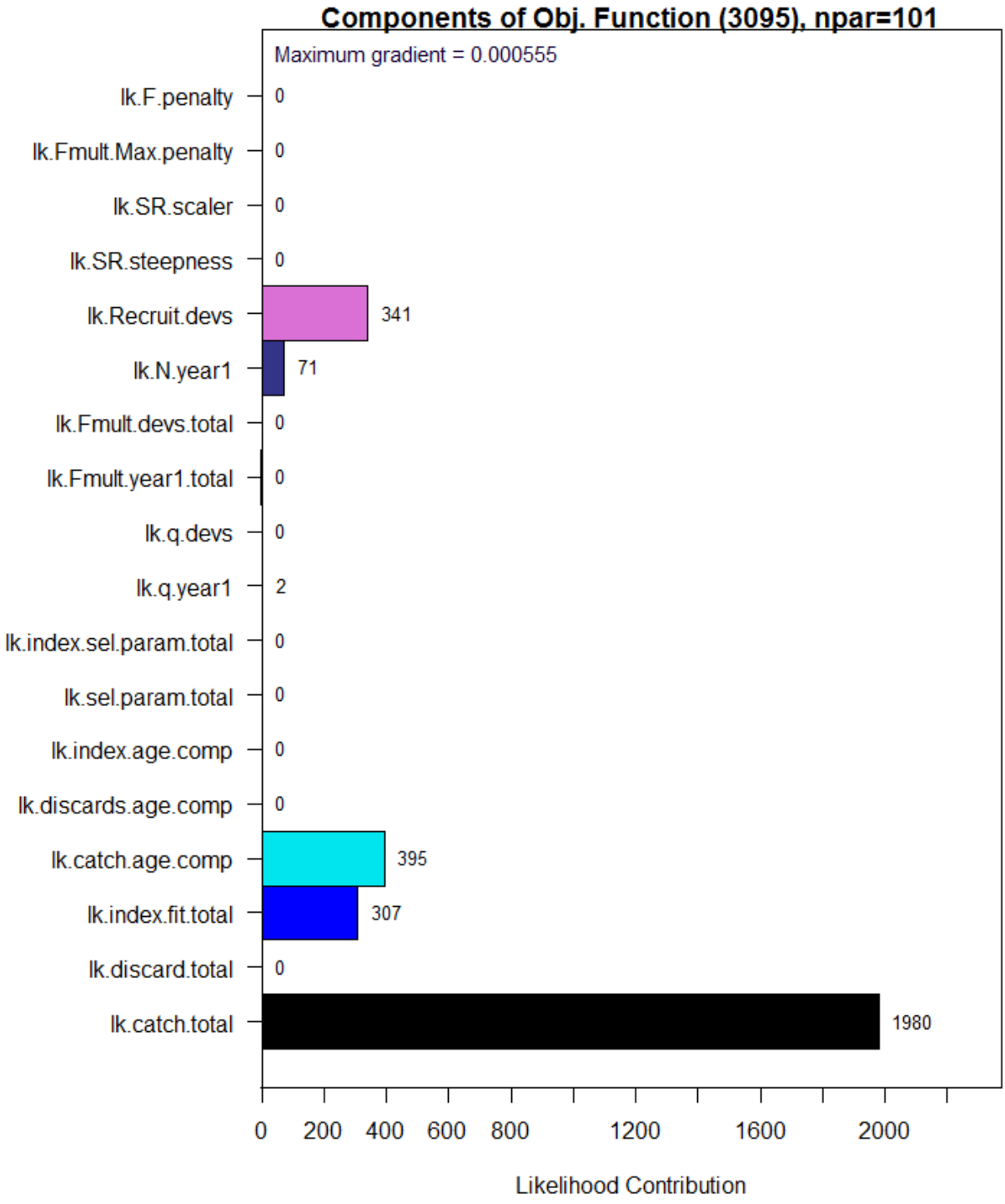

Figure B7.1. Likelihood components from the bluefish continuity model run (B001) showing the relative contribution of each component to the objective function.

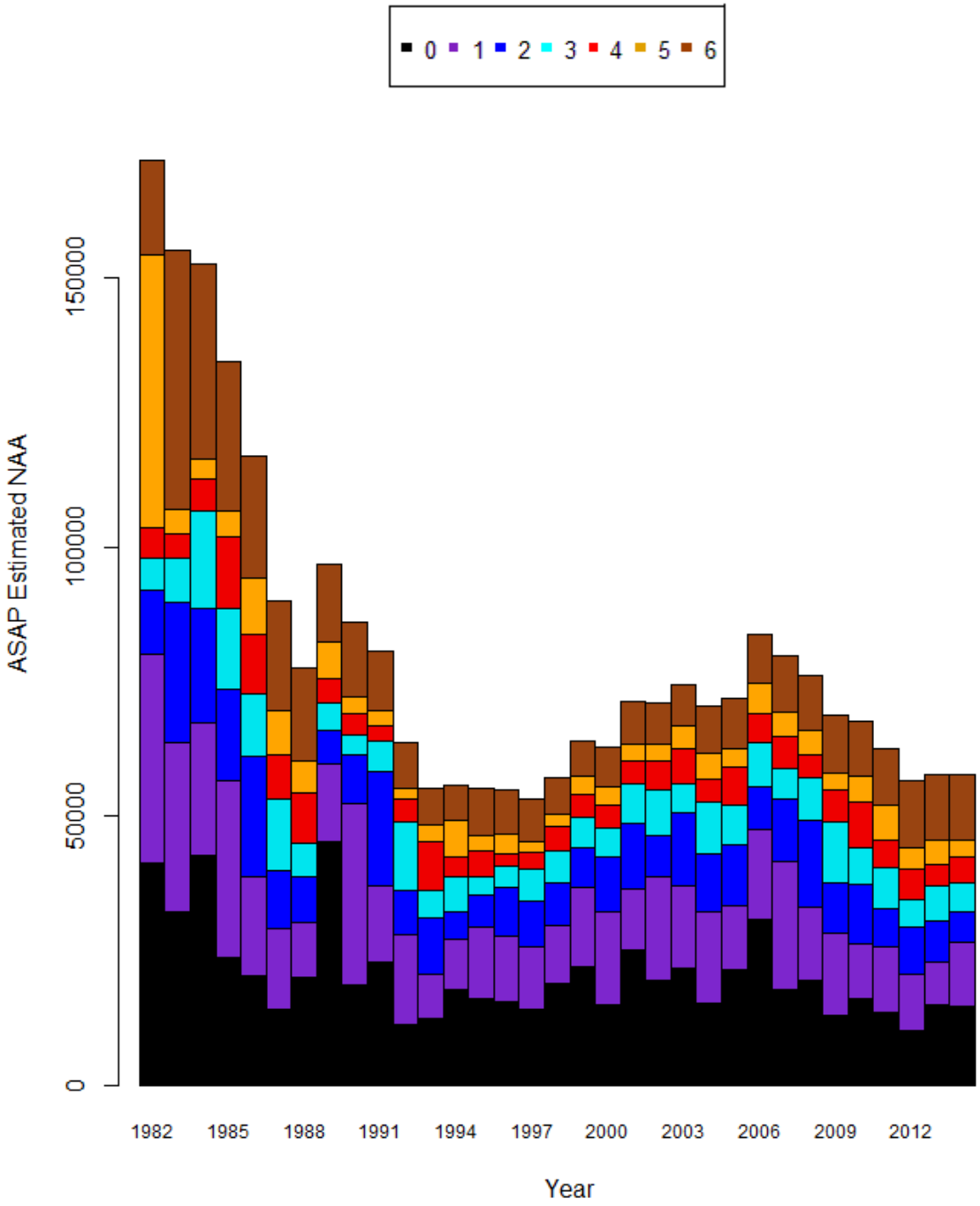

Figure B7.2. Bluefish numbers at age from 1982-2014 estimated from the continuity model run (B001).

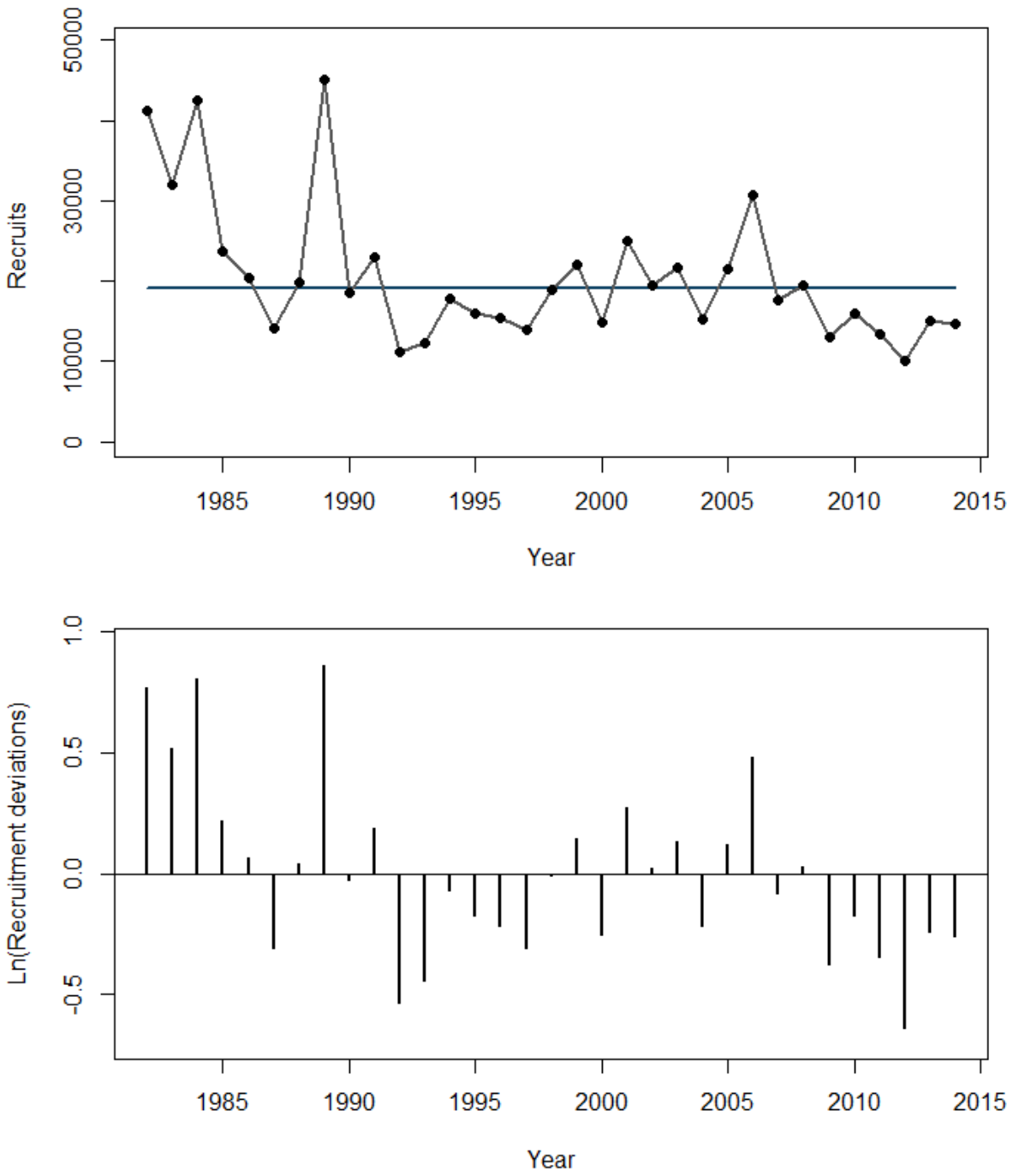

Figure B7.3. Bluefish recruitment, average recruitment over the time series (horizontal line), and recruitment deviations from the continuity model run (B001).

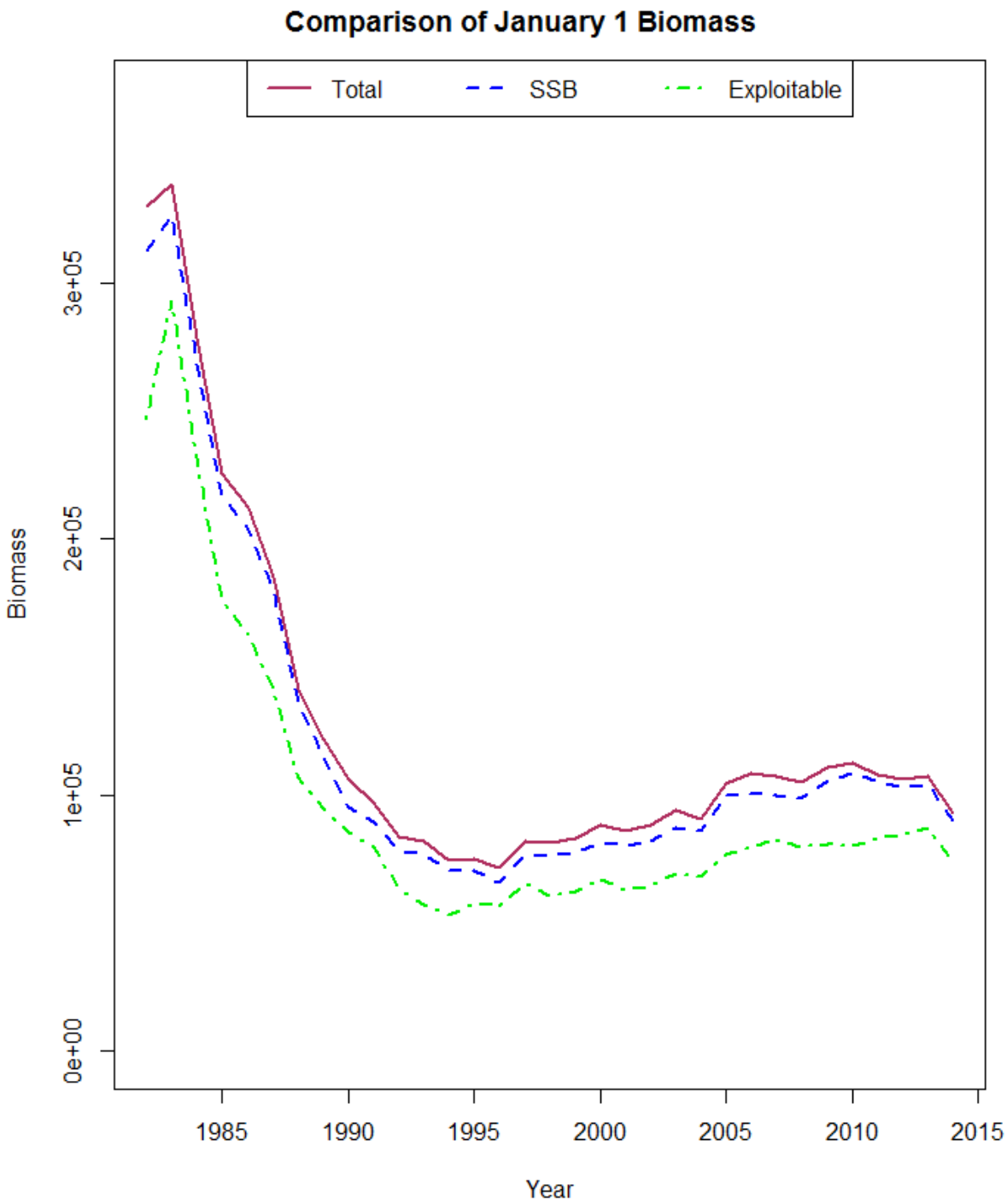

Figure B7.4. A comparison of bluefish total biomass (Jan-1), spawning stock biomass, and exploitable biomass estimated from the continuity model run (B001).

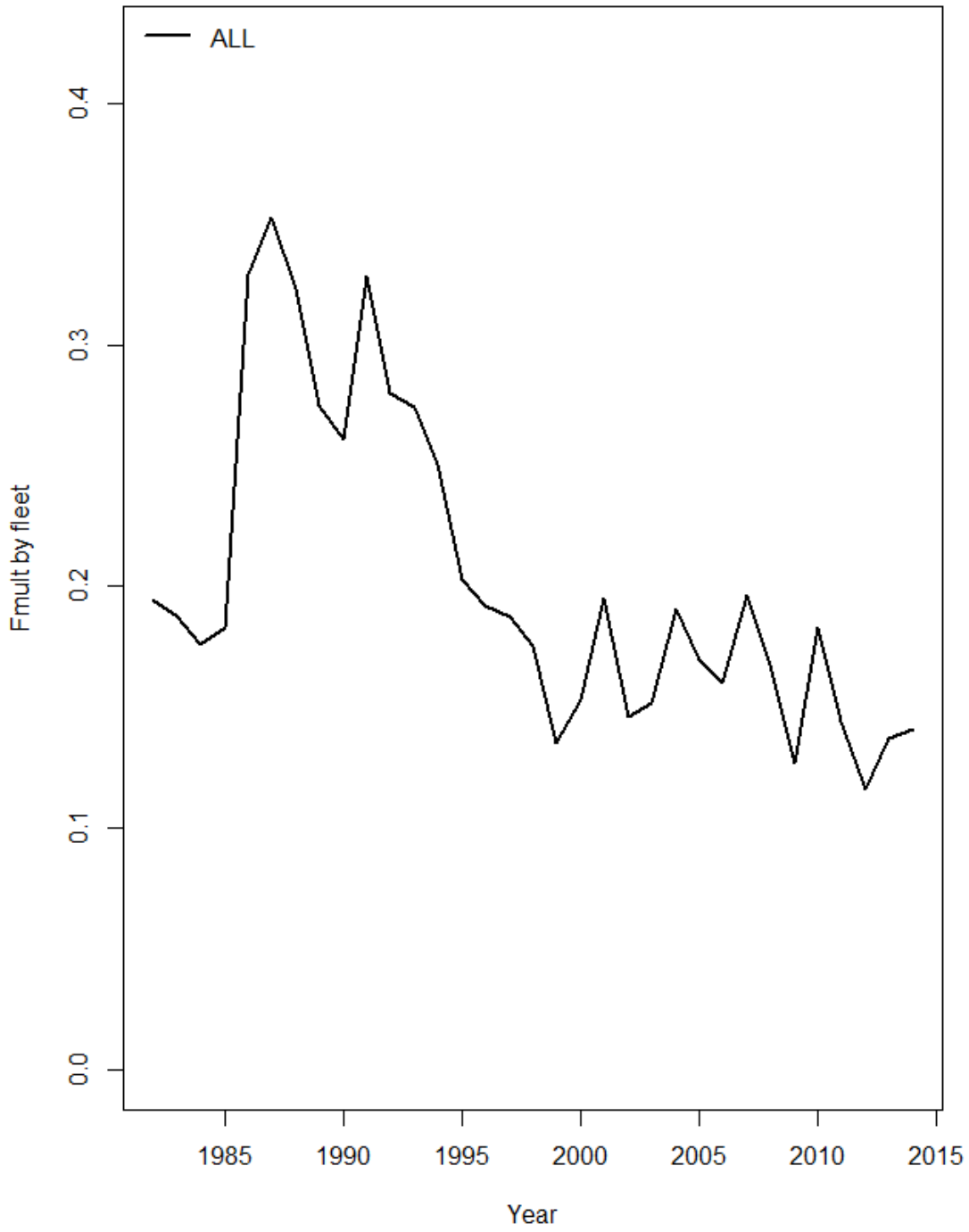

Figure B7.5. Estimates of fishing mortality for bluefish from 1982 to 2014 from model B001, the continuity run.

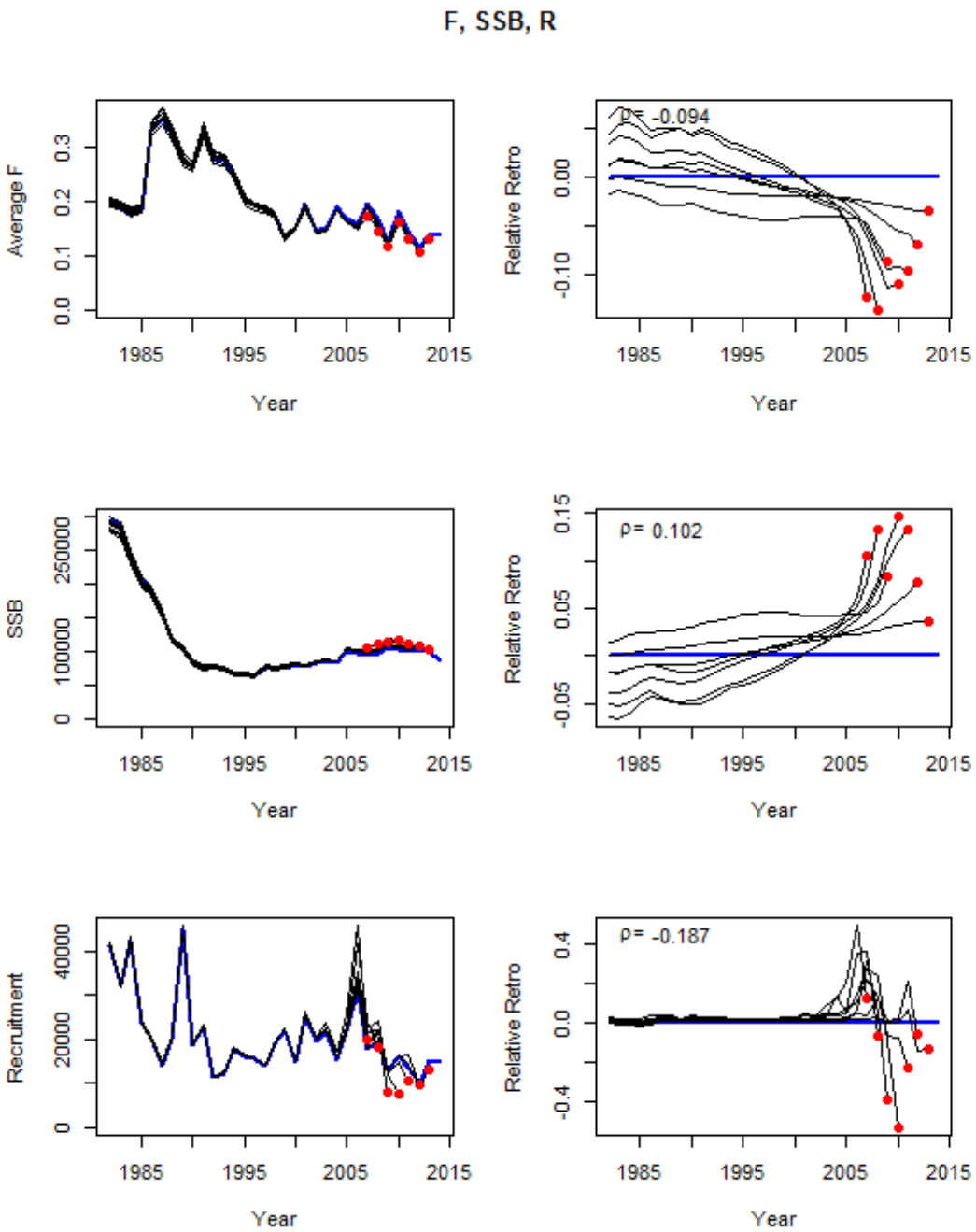

Figure B7.6. Retrospective bias for F, SSB, and Recruitment estimated from the bluefish model continuity run (B001).

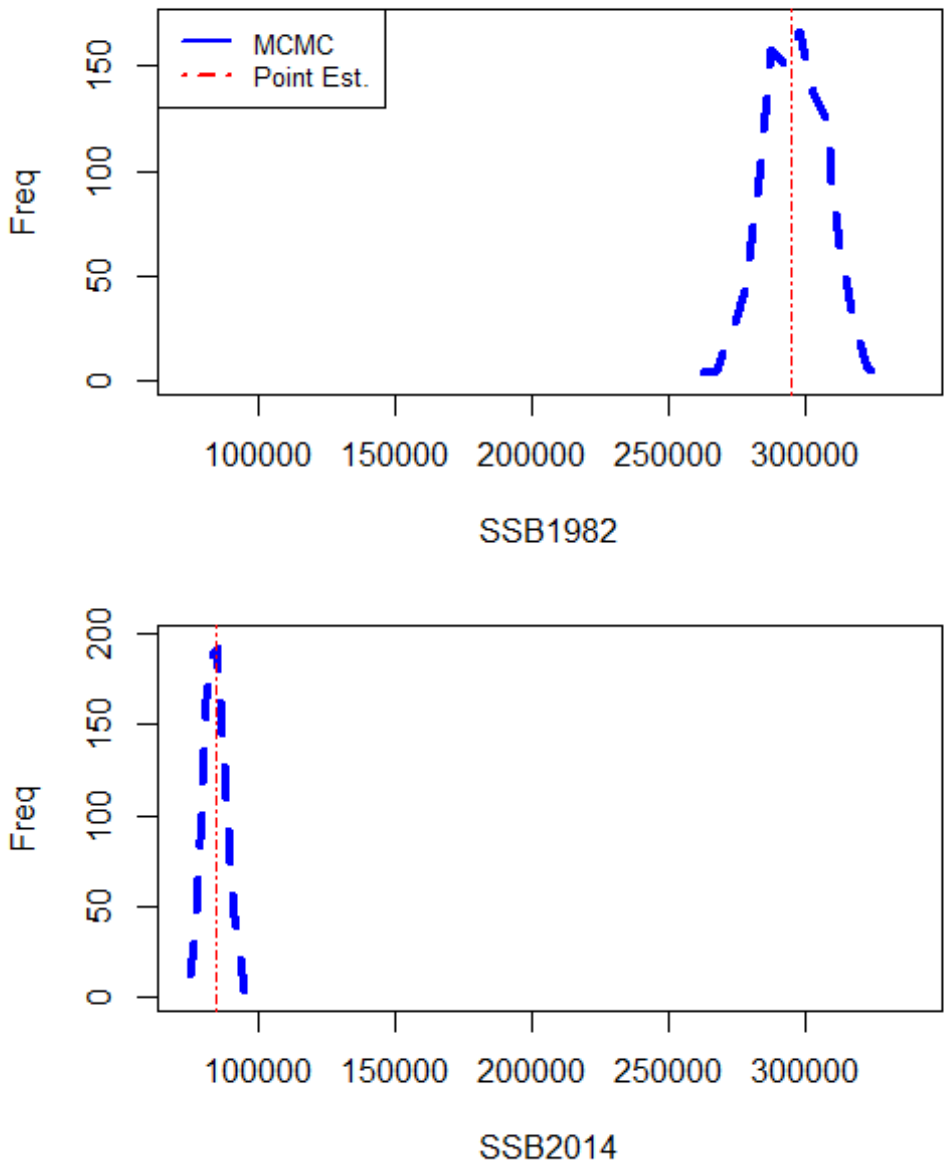

Figure B7.7. MCMC distribution of bluefish spawning stock biomass in 1982 and 2014 from 1000 iterations (thinning factor of 1000) of the continuity model (B001).

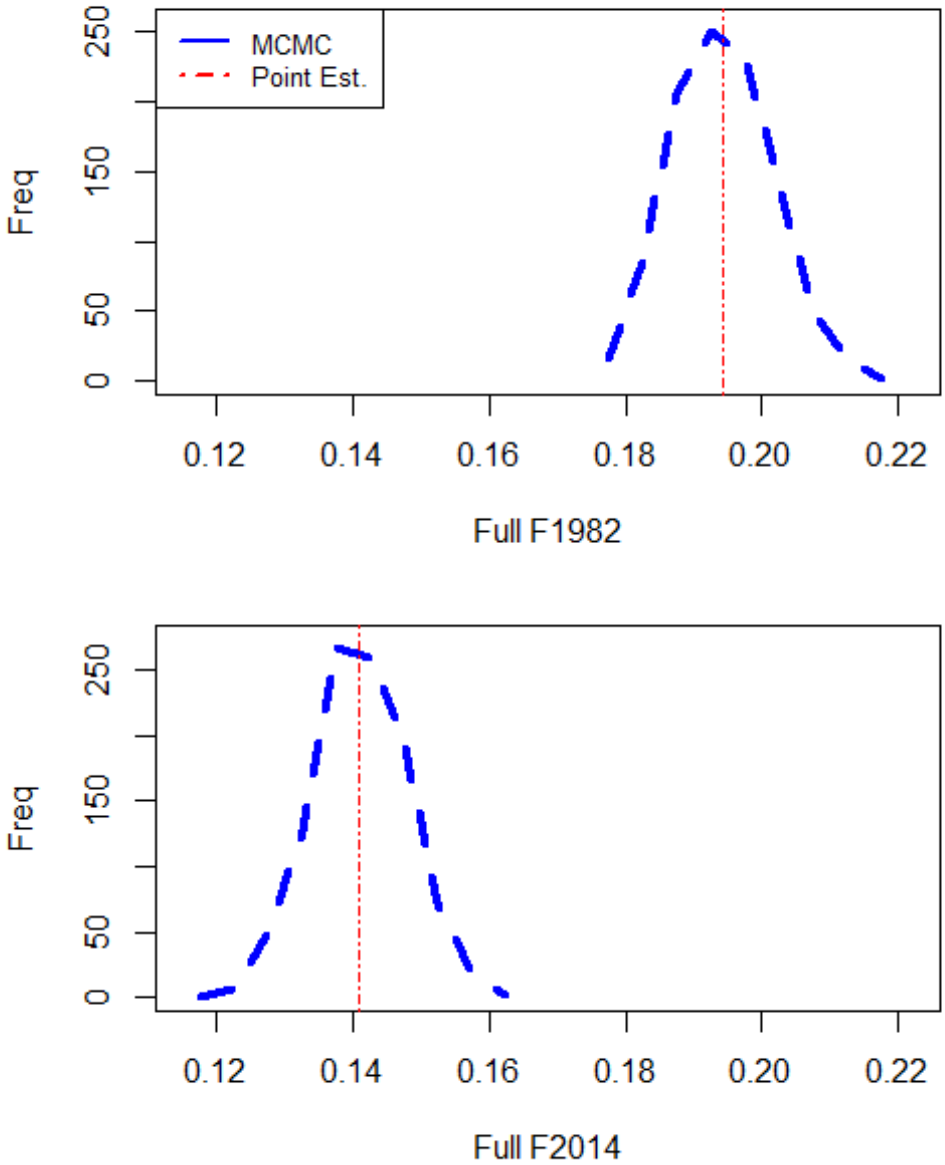

Figure B7.8. MCMC distribution of bluefish fishing mortality in 1982 and 2014 from 1000 iterations (thinning factor of 1000) of the continuity model (B001).

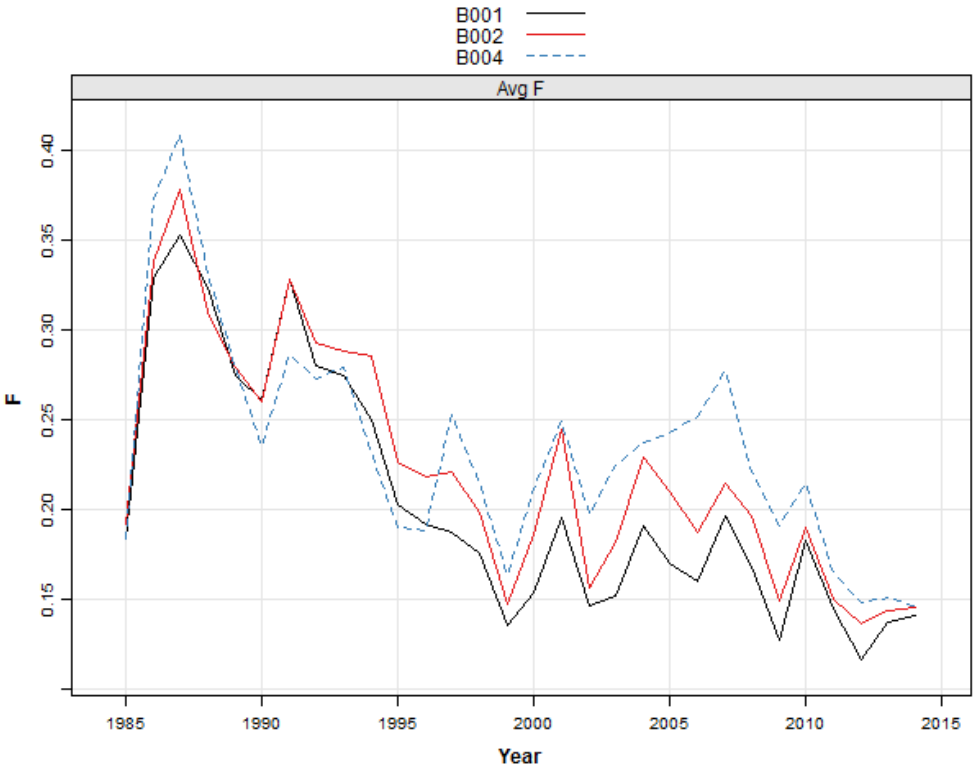

Figure B7.9. A comparison of bluefish fishing mortality estimates between the continuity run (B001: 1982-2014), the cropped continuity run (B002: 1985-2014), and the base model run (B004: 1985-2014).

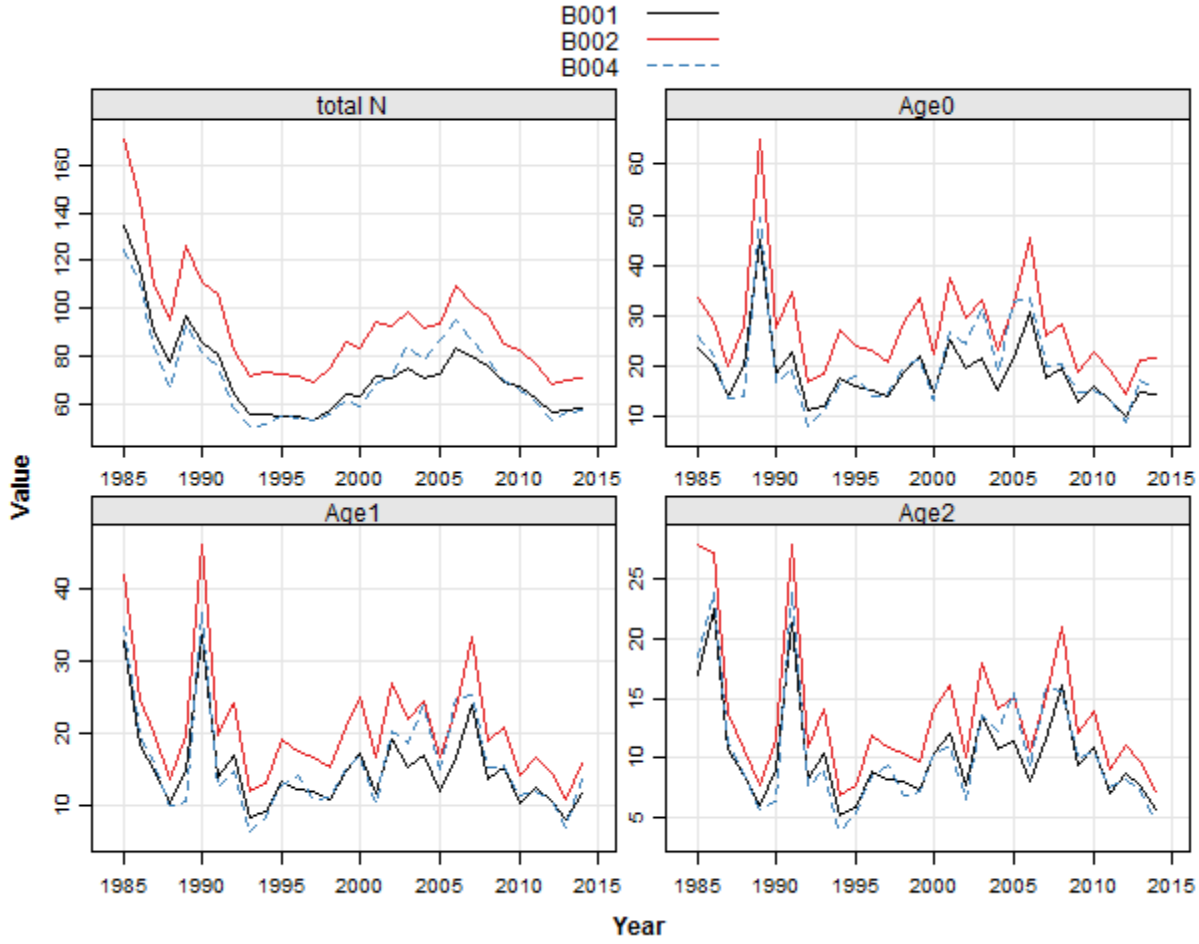

Figure B7.10. A comparison of bluefish total stock numbers and numbers at age for age 0 – age 2. Consistently lower estimates for numbers at age 0 to age 2 for model B004 are driving the differences in total stock numbers and recruitment from model B002.

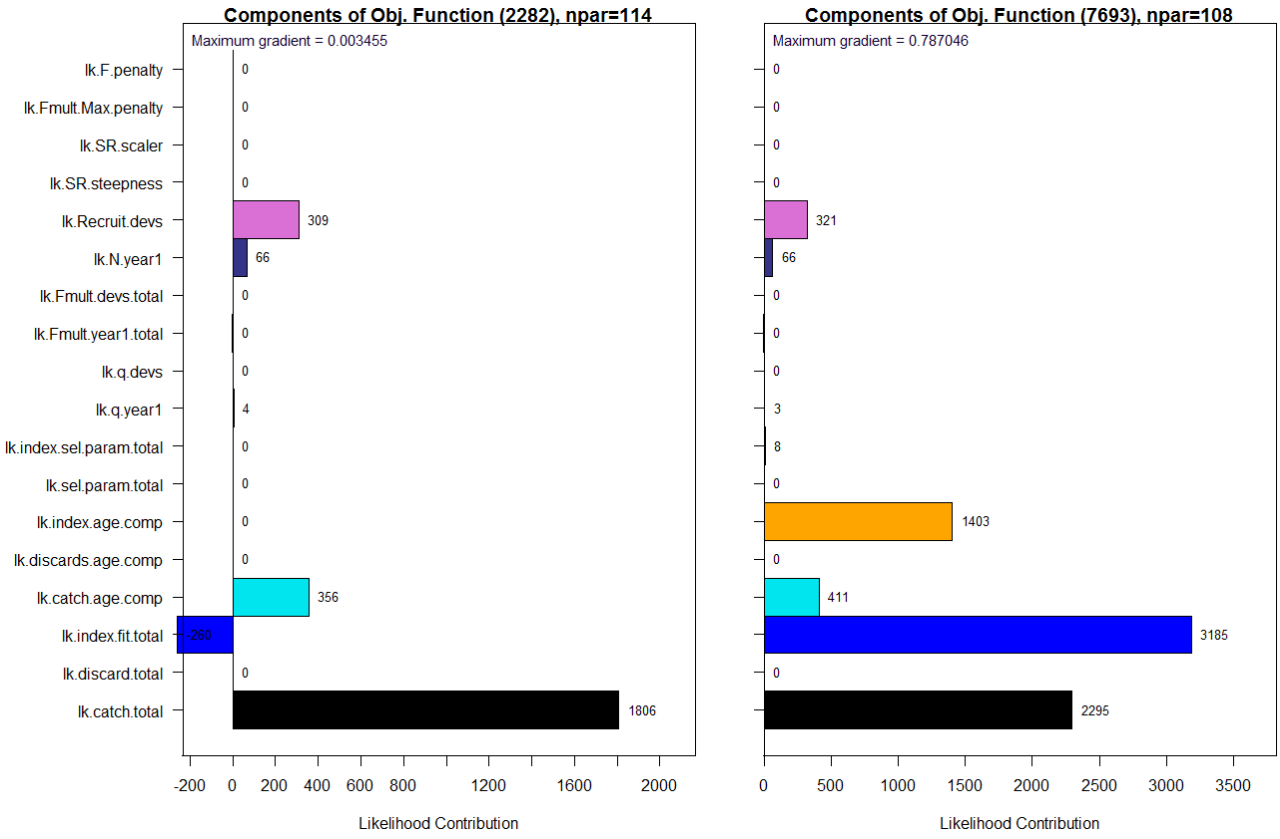

Figure B7.11. Overall contributions to the likelihood for components of model B004 (left) and B006 (right). Indices for model B006 are now input in catch-at-age format and age composition is estimated. The model is still heavily weighted to the catch, but the indices are now the majority of the objective function.

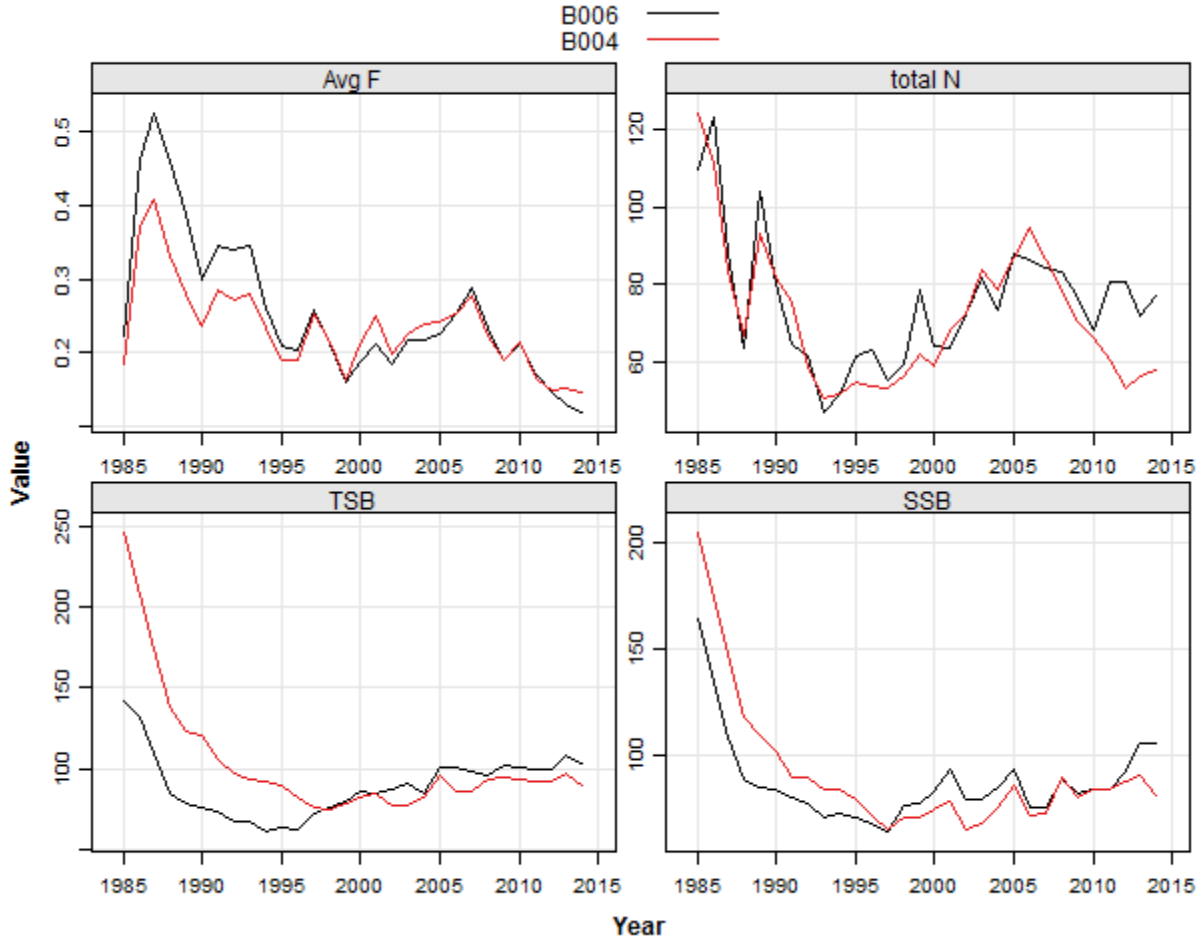

Figure B7.12. A comparison of bluefish fishing mortality, total stock numbers, total biomass, and spawning stock biomass between models B004 and B006. Estimating age composition for the survey indices results in a lower F, and higher 2014 estimates of TSN, TSB, and SSB. In addition, fitting to the age composition of the surveys decreases the scale of biomass at the beginning of the time series.

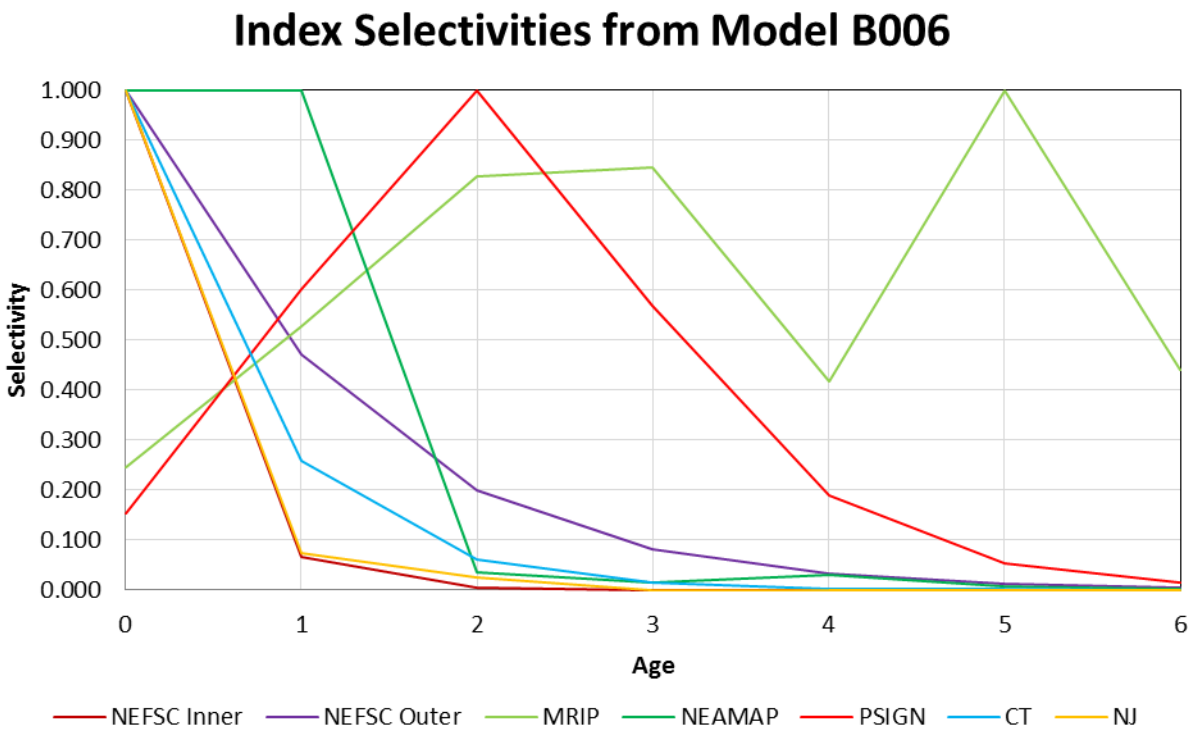

Figure B7.13. Index selectivity estimates from model B006, where the indices were input in a catch-at-age format to estimate age composition.

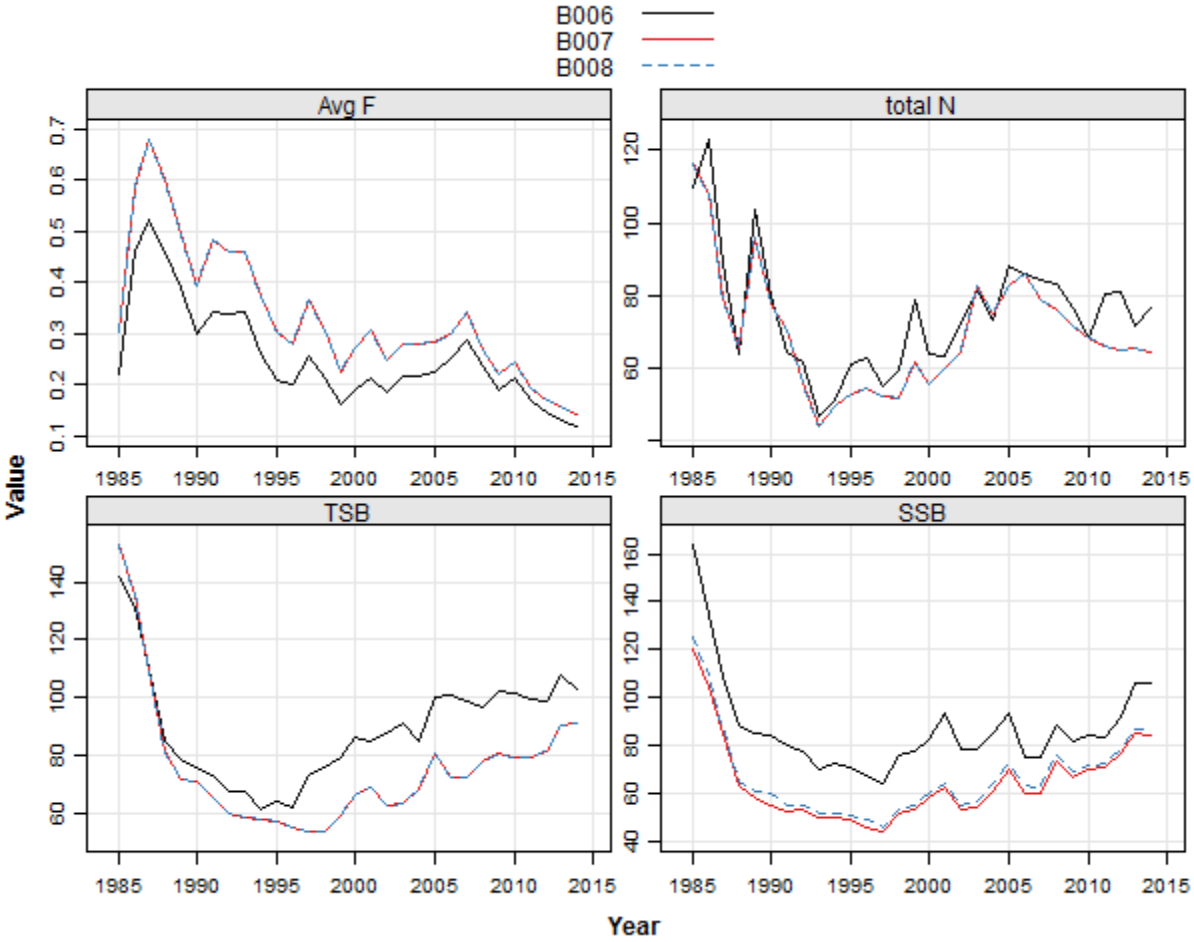

Figure B7.14. A comparison of bluefish fishing mortality, total stock numbers, total biomass, and spawning stock biomass between models B006, B007 (2 fleets) and B008 (new maturity-at-age). Separating the input data into separate commercial and recreational fleets increased the scale of fishing mortality and scaled down the time-series of total numbers and biomass. New maturity information in model B008 resulted in only a slight increase in SSB.

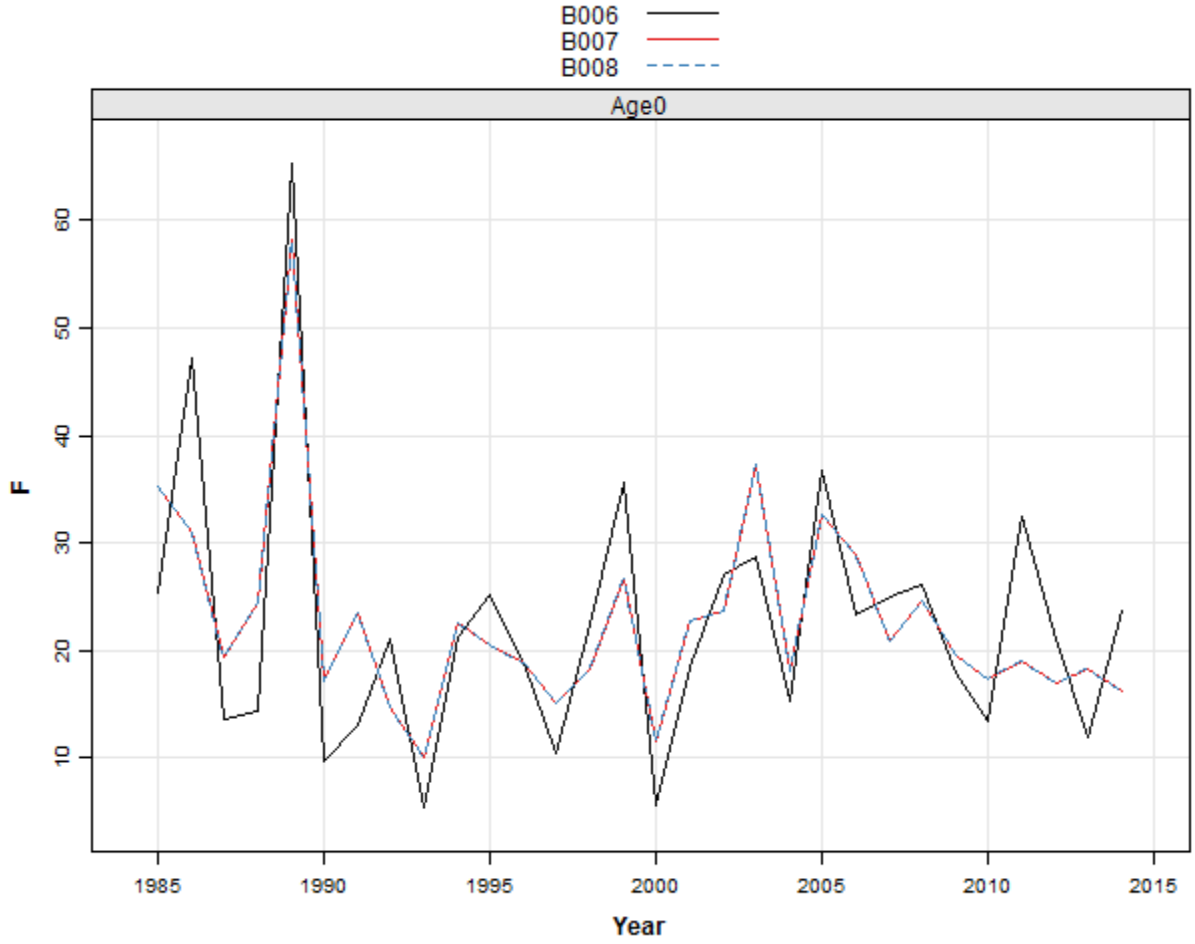

Figure B7.15. The separation of data into a commercial and recreational fleet did not change the recruitment time-series significantly but resulted in a smoother trend at the end of the B007 time-series.

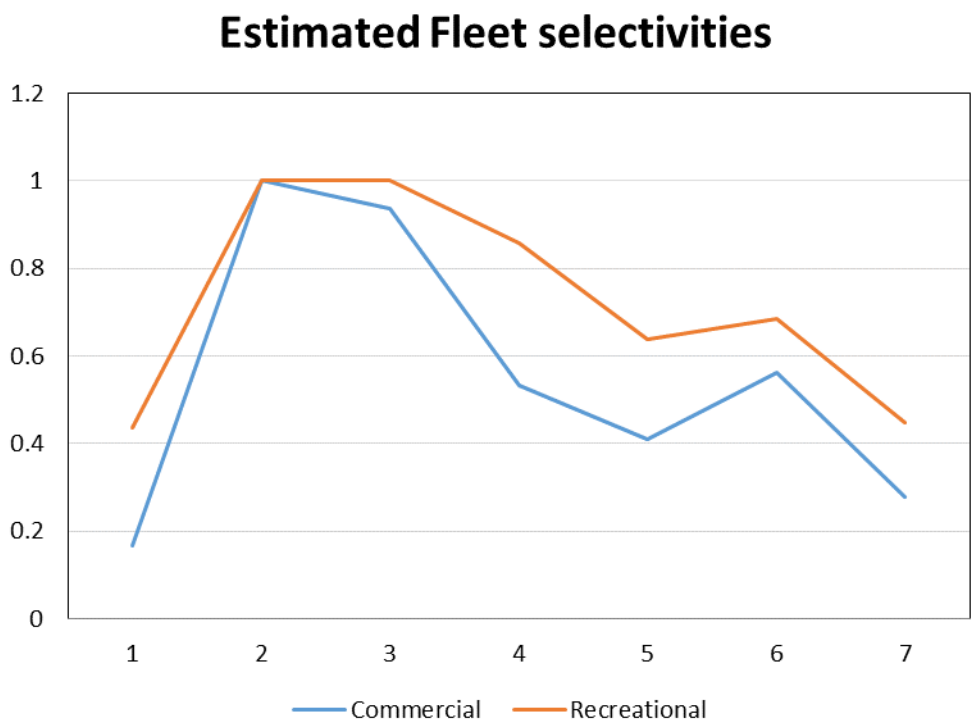

Figure B7.16. Estimated commercial and recreational fleet selectivities from model B011. Note that age class labels are 1 greater than the modeled age class, so that "age-1" corresponds to age 0, "age-2" corresponds to age 1, etc.

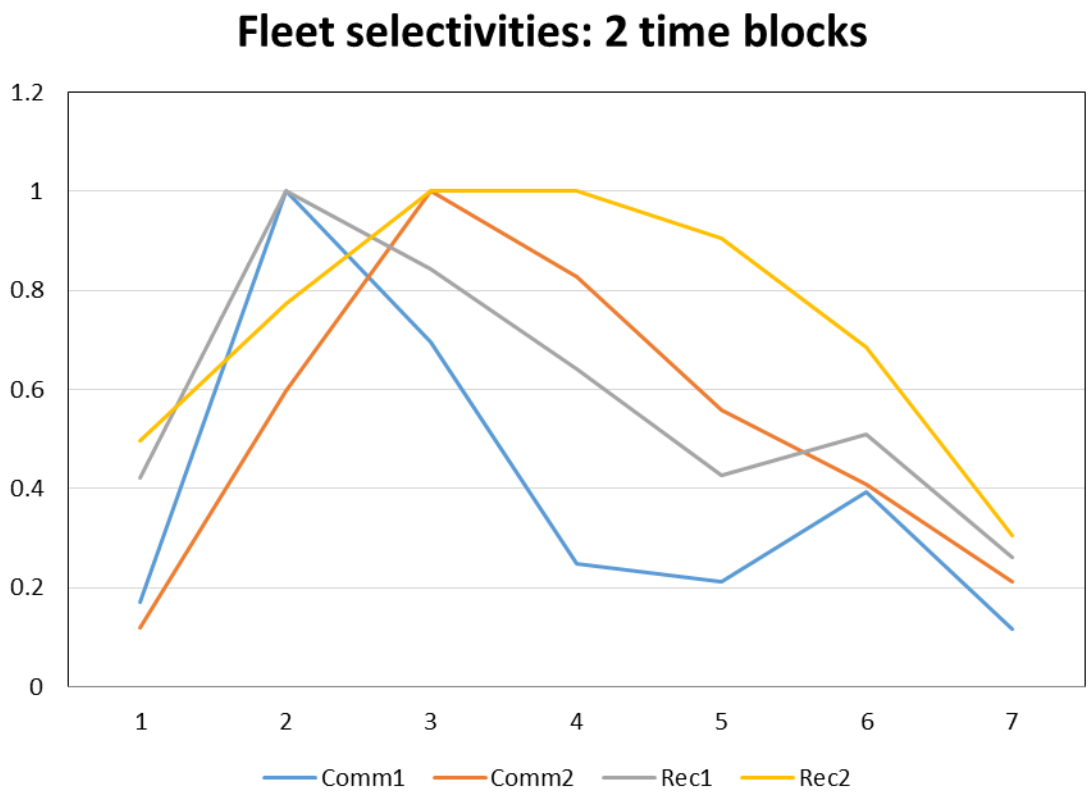

Figure B7.17. Estimated commercial and recreational fleet selectivities in two time blocks (1985-2005 and 2006-2014) from model B020. Note that age class labels are 1 greater than the modeled age class, so that "age-1" corresponds to age 0, "age-2" corresponds to age 1, etc.

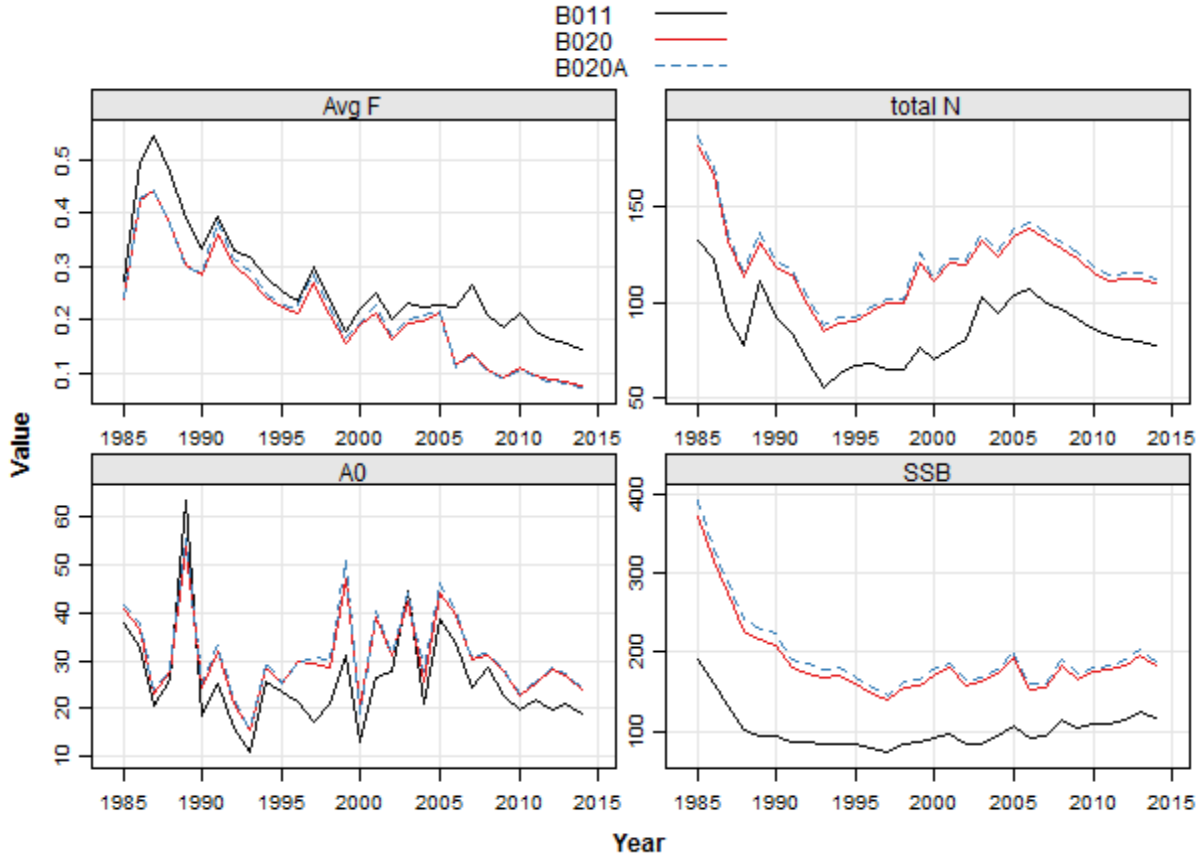

Figure B7.18. A comparison of bluefish fishing mortality, total stock numbers, recruitment, and spawning stock biomass between models B011, B020 (2 fleet selectivity blocks) and B020A (ESS = 0 for 1997-2005). Adding 2 selectivity blocks to the fleets decreases fishing mortality estimates and increases stock numbers, recruitment, and biomass estimates.

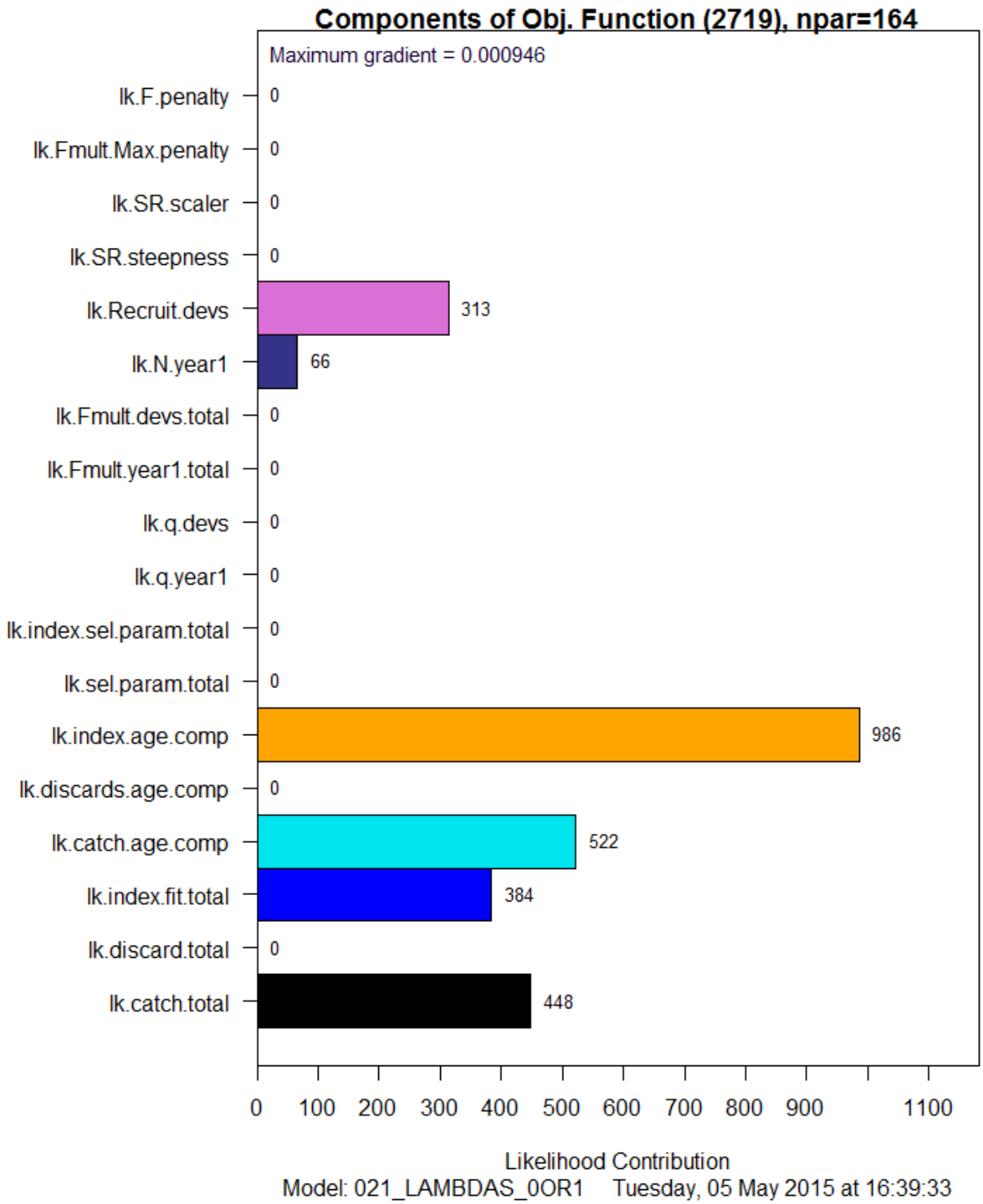

Figure B7.19. Overall contributions to the likelihood for components of model B021. This model shifted the lambdas to 1's or 0's, acting as switches to turn on or off the components of the objective function. If lambda is turned on for a component it is then included in the objective function and associated input CV is used as a weight (acting like a prior).

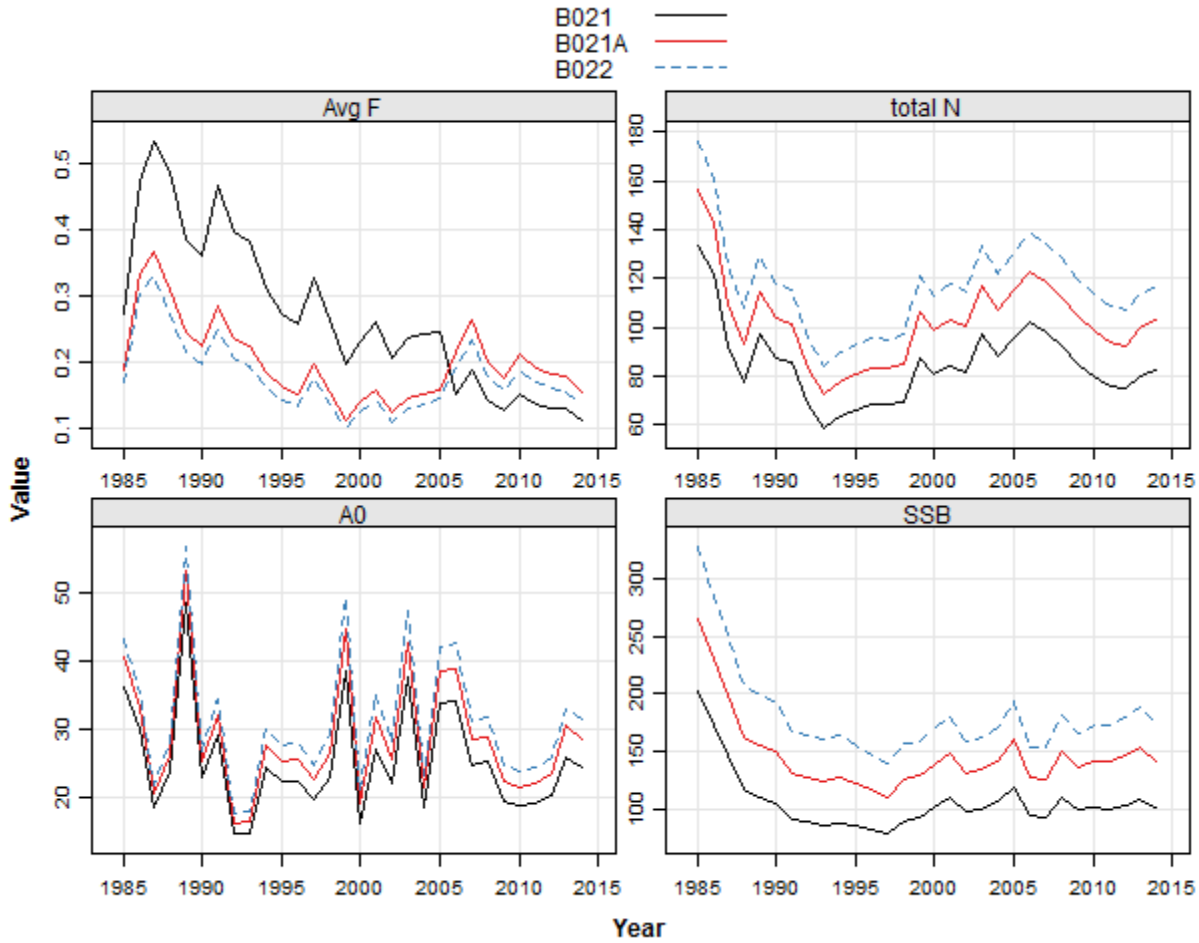

Figure B7.20. A comparison of bluefish fishing mortality, total stock numbers, recruitment, and spawning stock biomass between models B021 (new model weighting: Lambdas = 0 or 1), B021A (Likelihood constants off) and B022 (penalty on Nyear1 off).

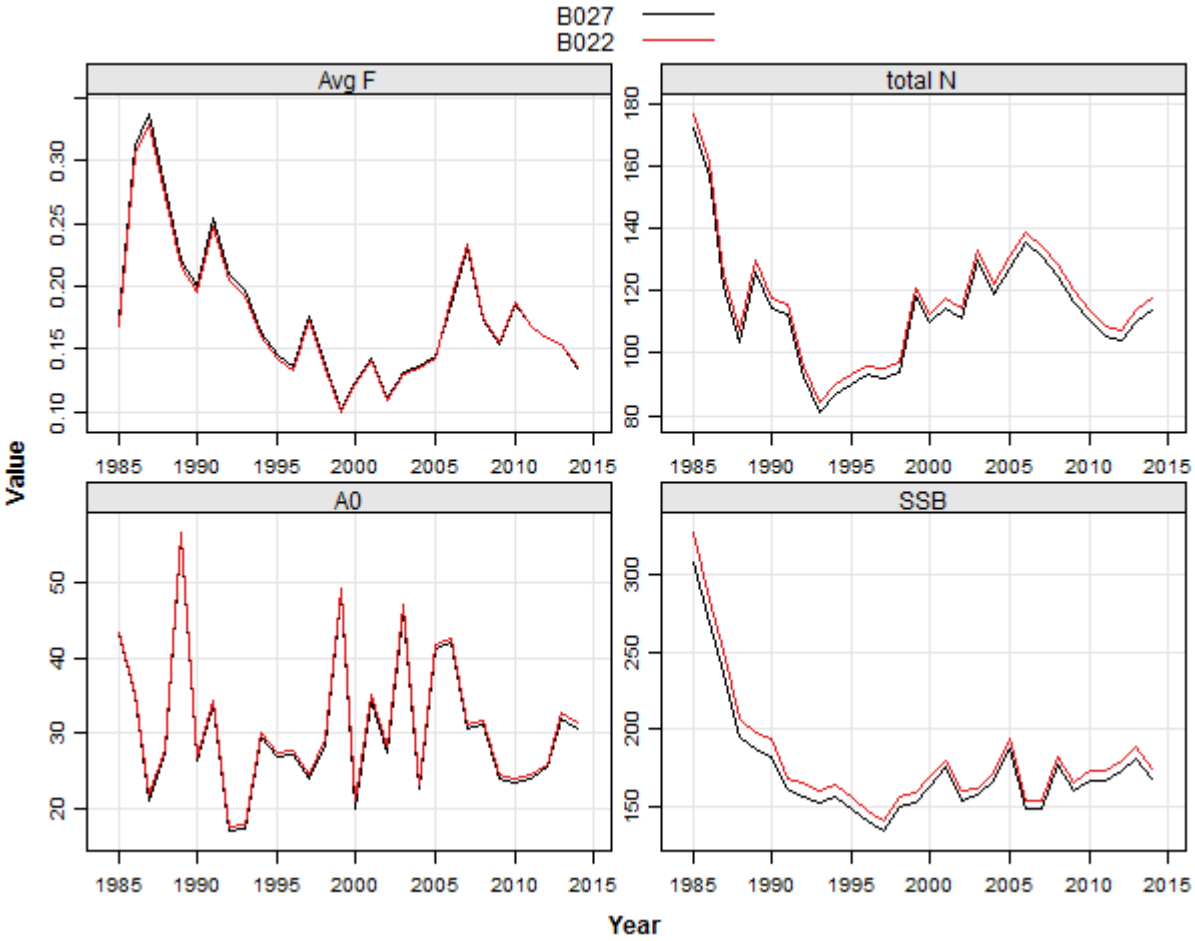

Figure B7.21. Minor changes were made to input CVs and selectivity estimates between model B022 and B027. The result of these changes was very little difference in the estimates of fishing mortality, total stock numbers, recruitment, and spawning stock biomass.

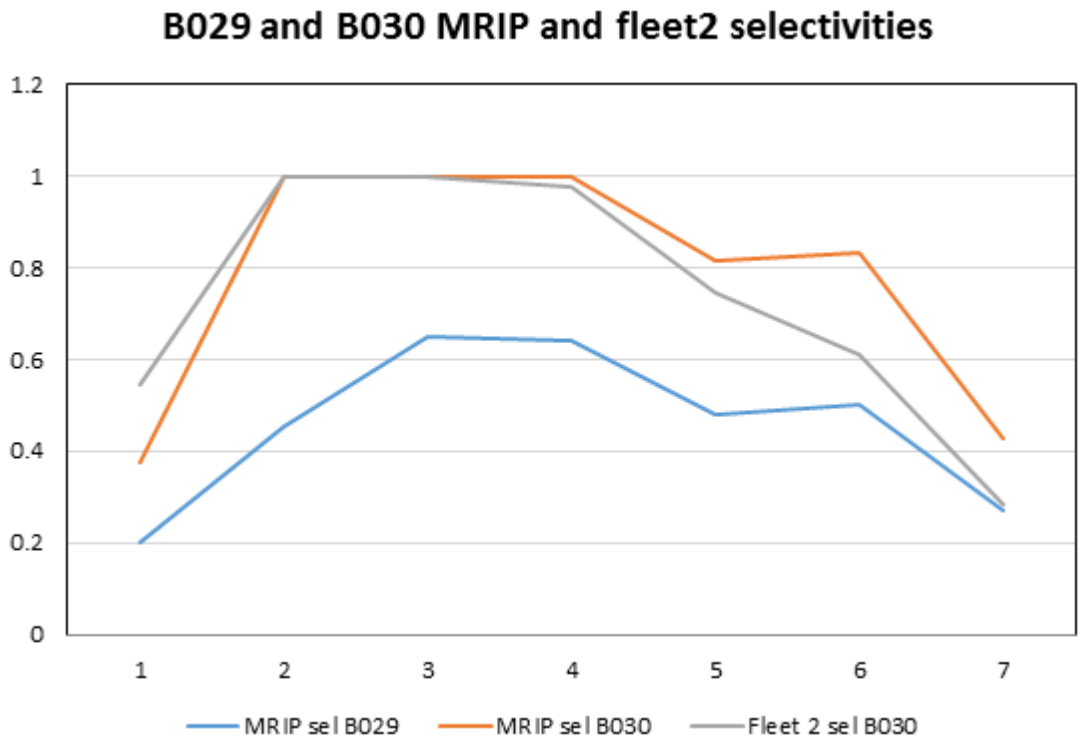

Figure B7.22. MRIP index selectivities and fleet 2 selectivity coming out of model B029 and B030. Note that age class labels are 1 greater than the modeled age class, so that "age-1" corresponds to age 0, "age-2" corresponds to age 1, etc.

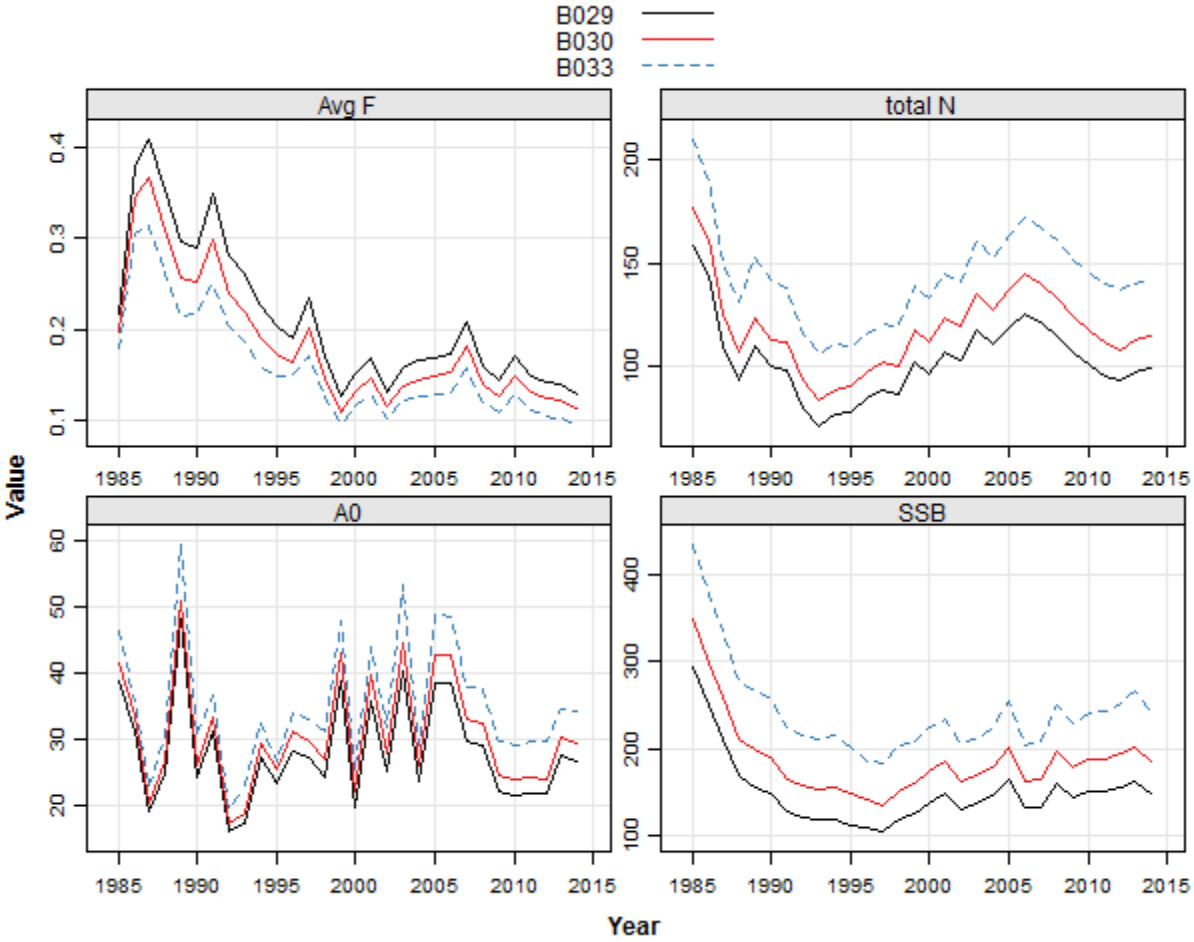

Figure B7.23. A comparison of bluefish fishing mortality, total stock numbers, recruitment, and spawning stock biomass between models B029 (Split off Bigelow survey), B030 (MRIP index selectivity to match fleet 2) and B033 (Corrected NC scale data).

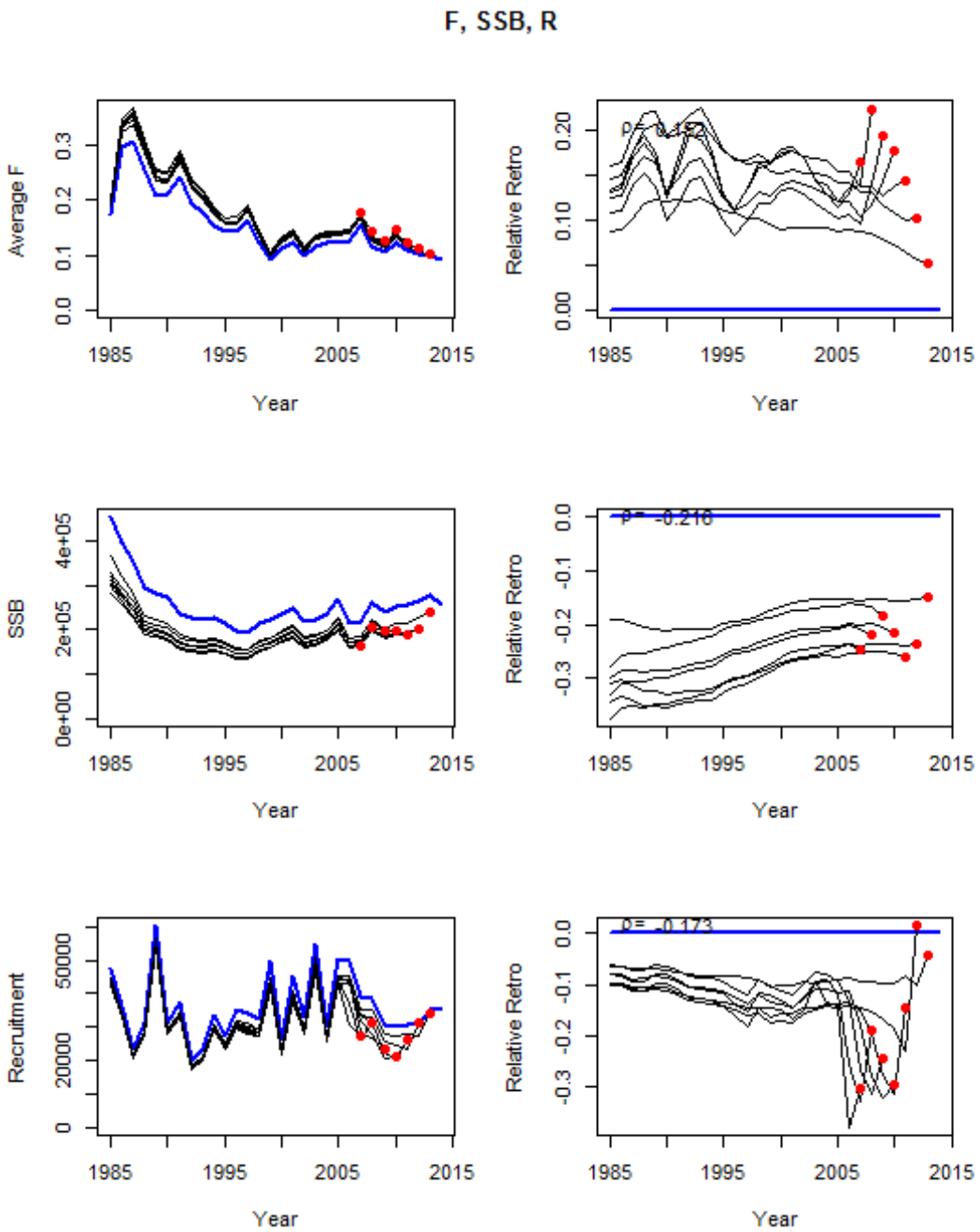

Figure B7.24. Significant retrospective bias in estimates of fishing mortality, spawning stock biomass and recruitment from model B035.

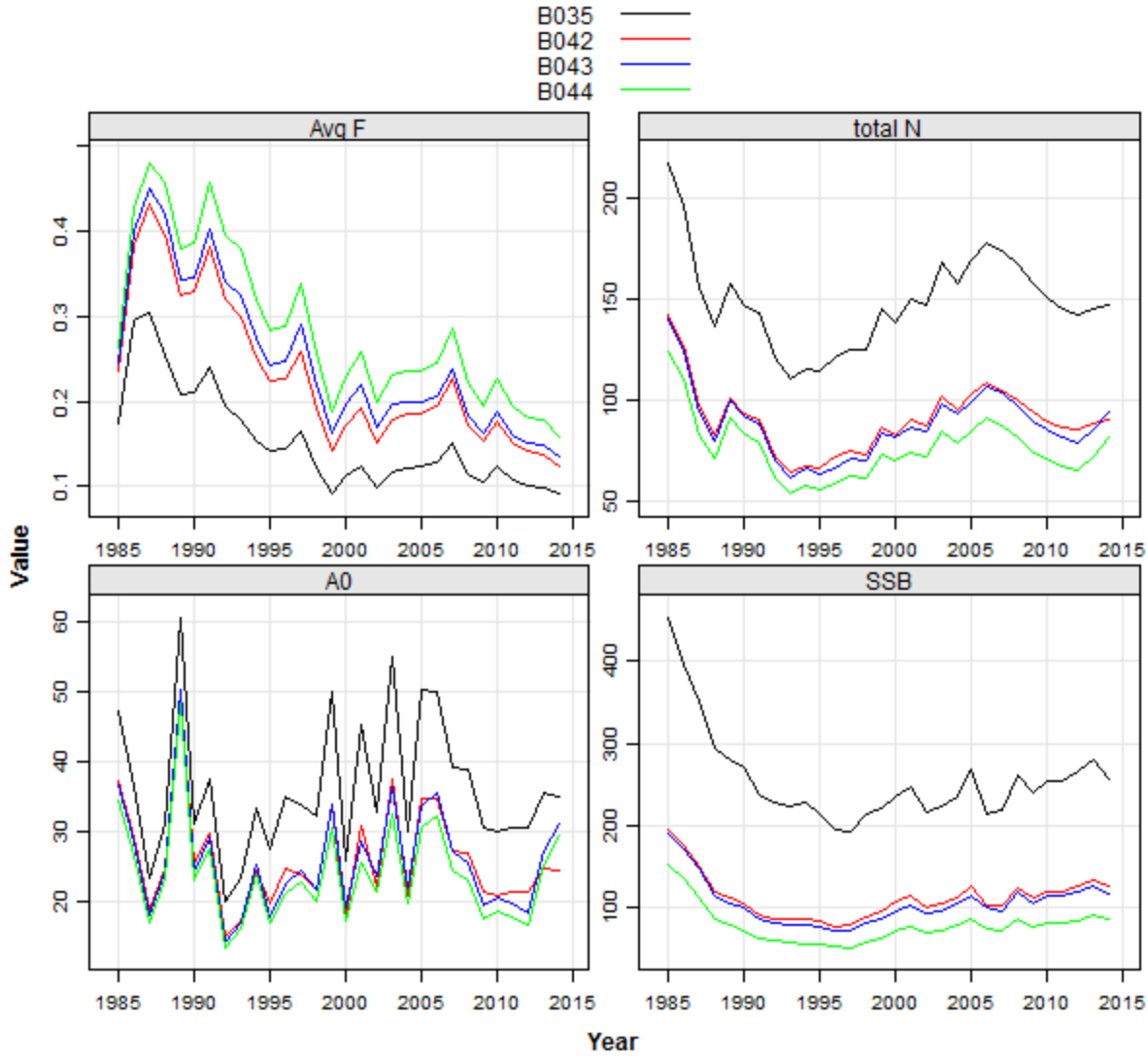

Figure B7.25. A comparison of bluefish fishing mortality, total stock numbers, recruitment, and spawning stock biomass between models B035 (PSIGN to sel-at-age), B042 (MRIP index selectivity to single logistic), B043 (adjustments to CVs and ESS), and B044 (final model accepted by SARC panel).

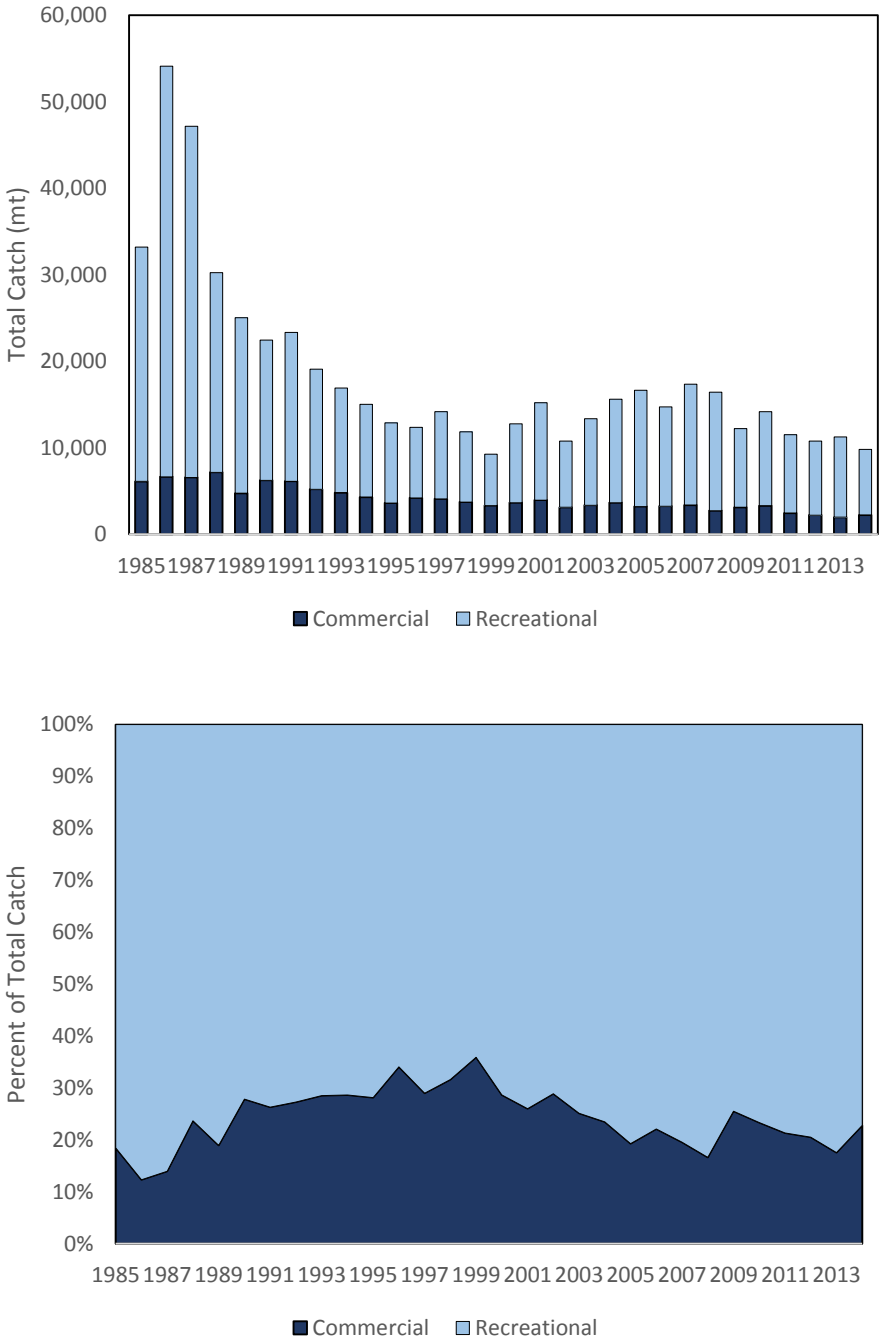

Figure B7.26. Bluefish catch by fleet in metric tons (top) and percent of total catch (bottom) from 1985 to 2014.

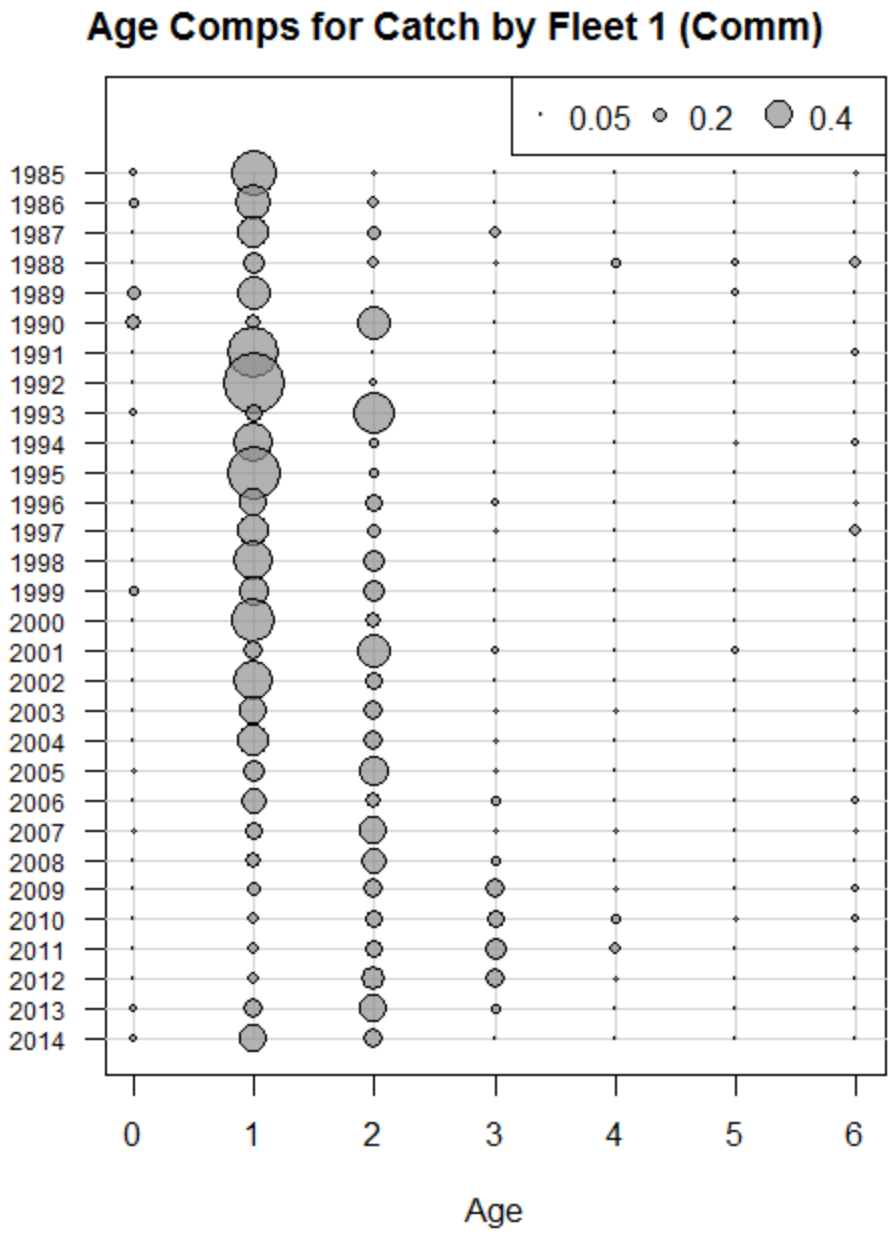

Figure B7.27. Bluefish age composition (catch-at-age) for the commercial fleet input into the final model run.

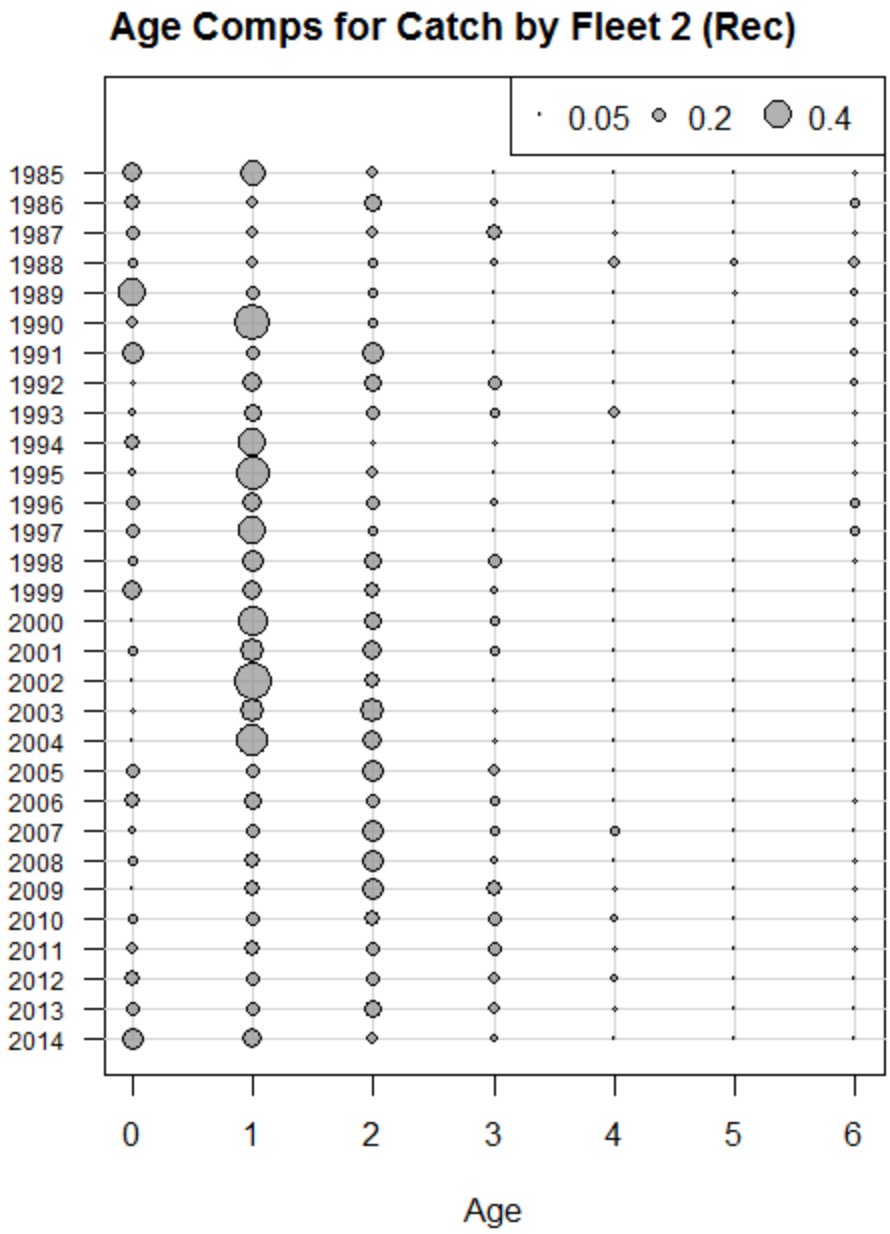

Figure B7.28. Bluefish age composition (catch-at-age) for the recreational fleet input into the final model run.

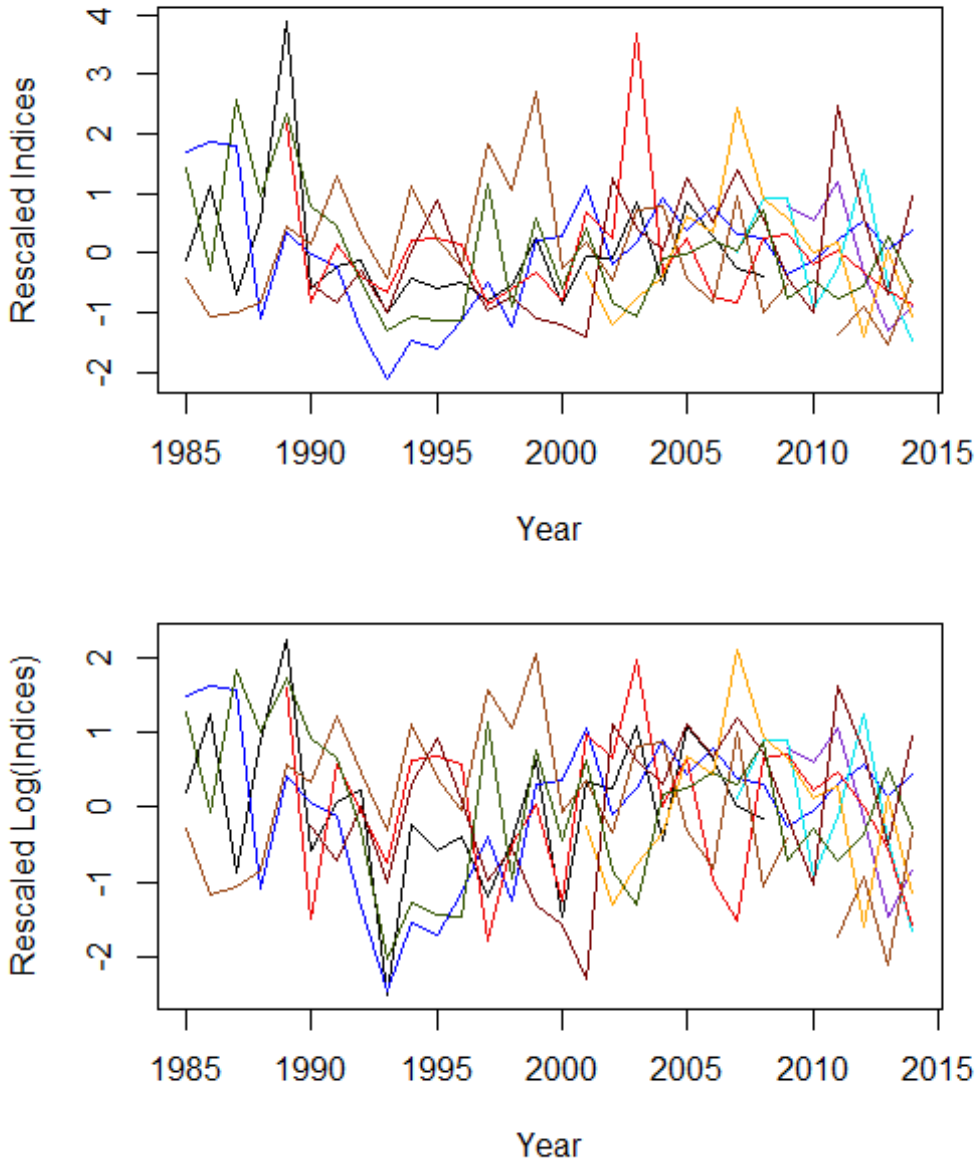

Figure B7.29. Bluefish survey indices re-scaled to their mean values and log-survey indices rescaled to their mean values.

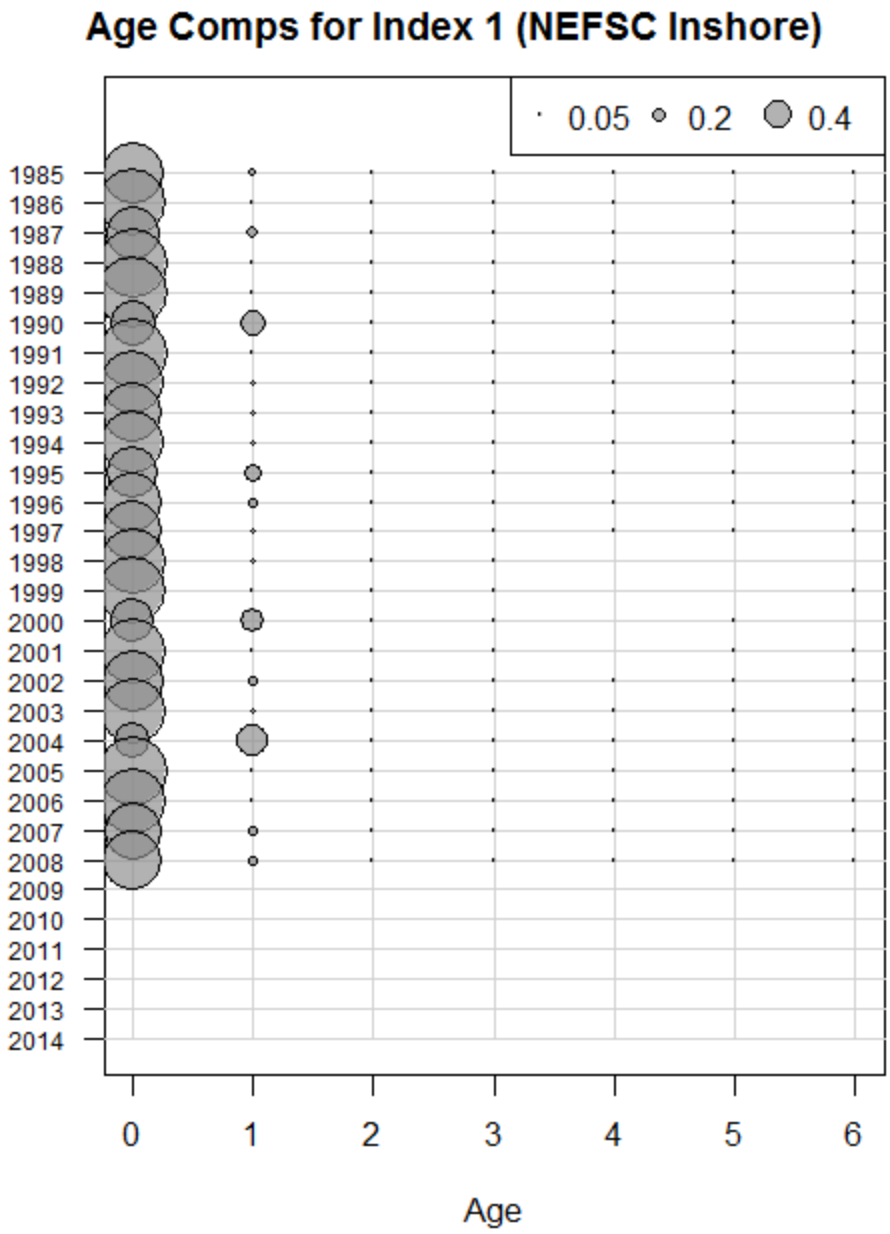

Figure B7.30. Input age composition for the NEFSC Inshore survey (Albatross survey from 1985 to 2008).

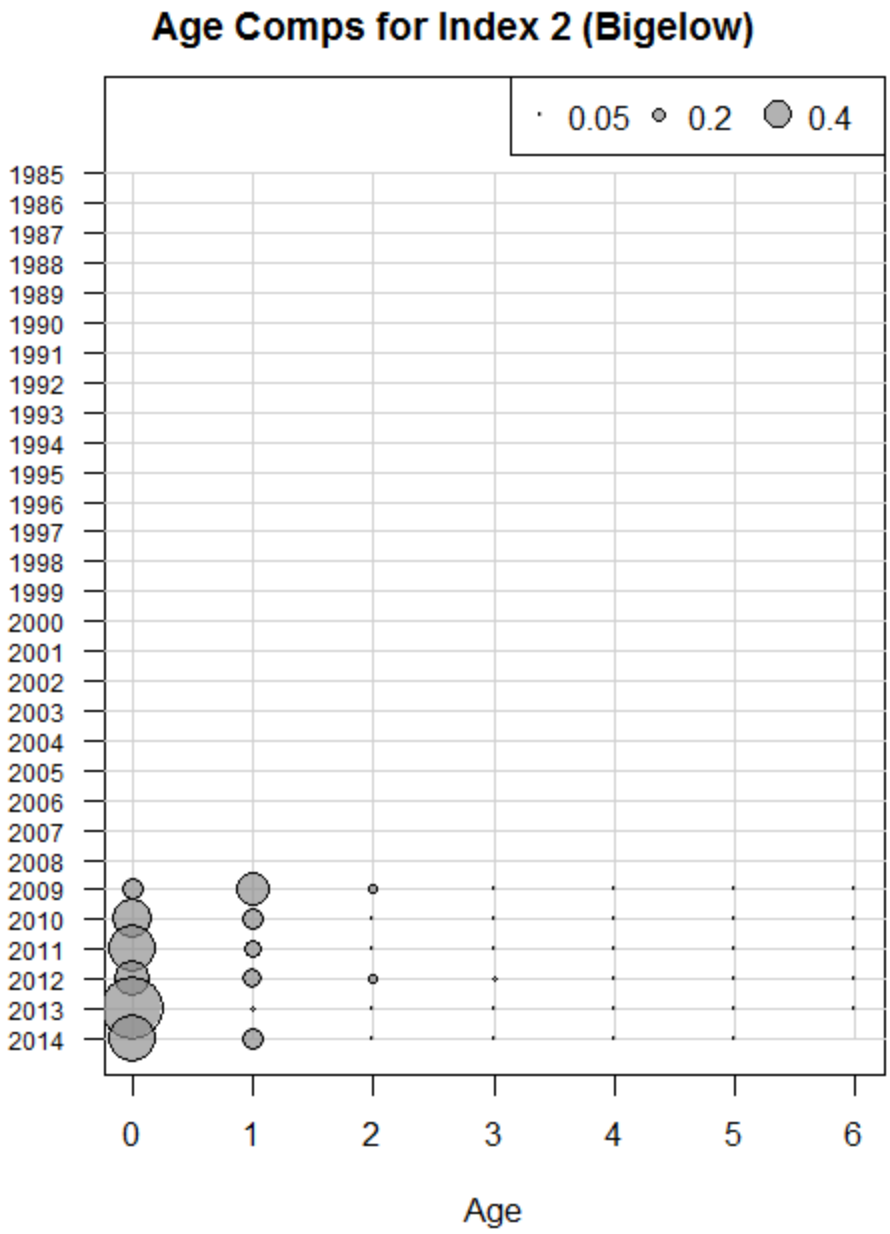

Figure B7.31. Input age composition for the NEFSC Bigelow survey (2009 to 2014).

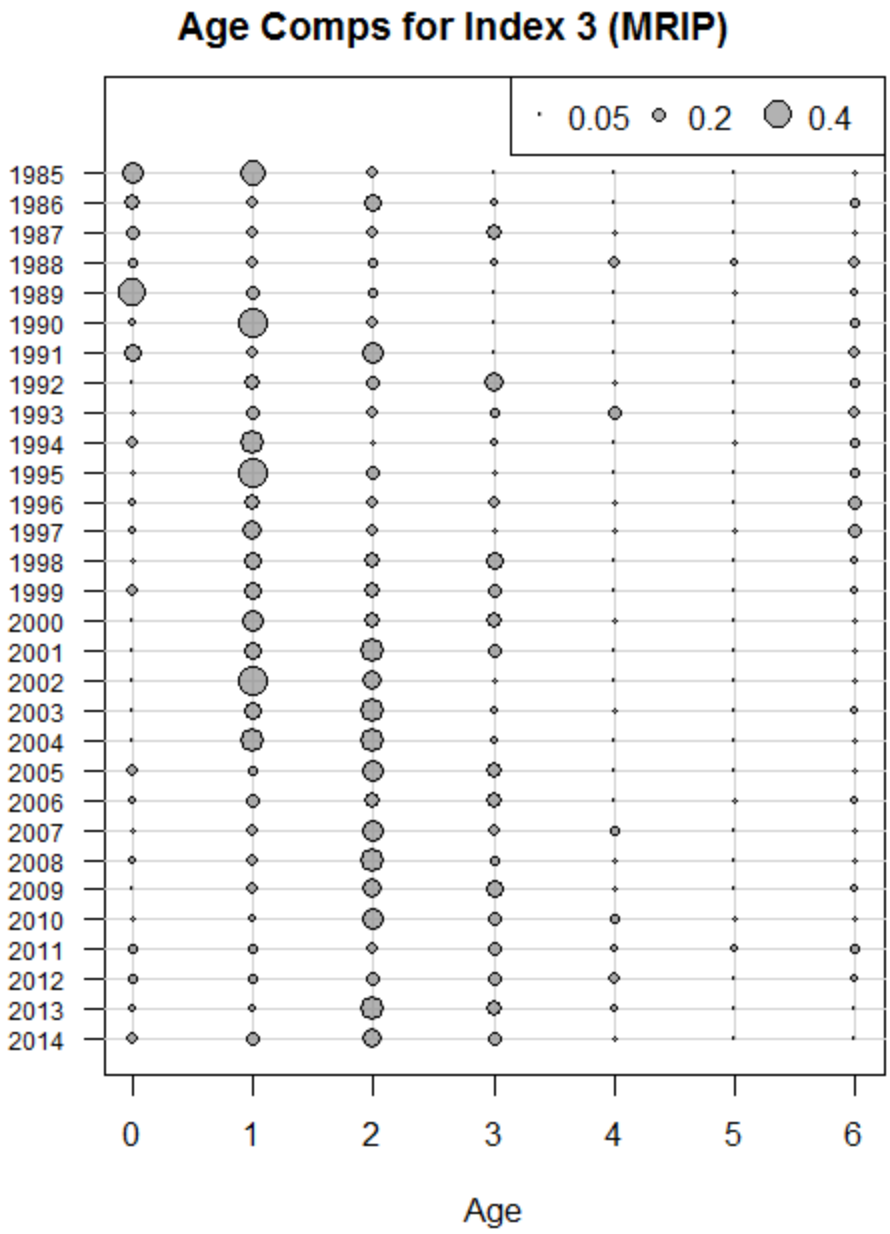

Figure B7.32. Input age composition for the MRIP recreation CPUE index from 1985 to 2014.

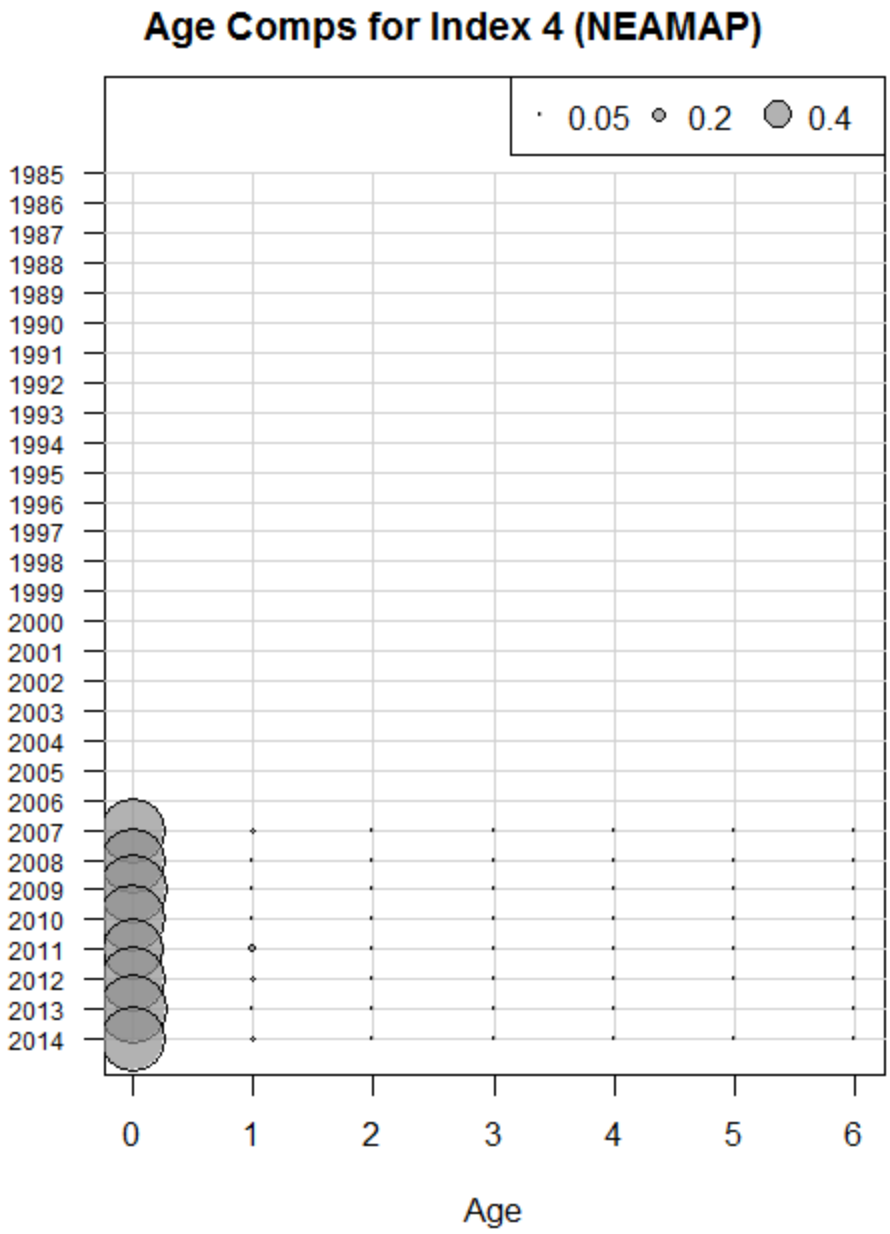

Figure B7.33. Input age composition for the NEAMAP trawl survey index from 2007 to 2014.

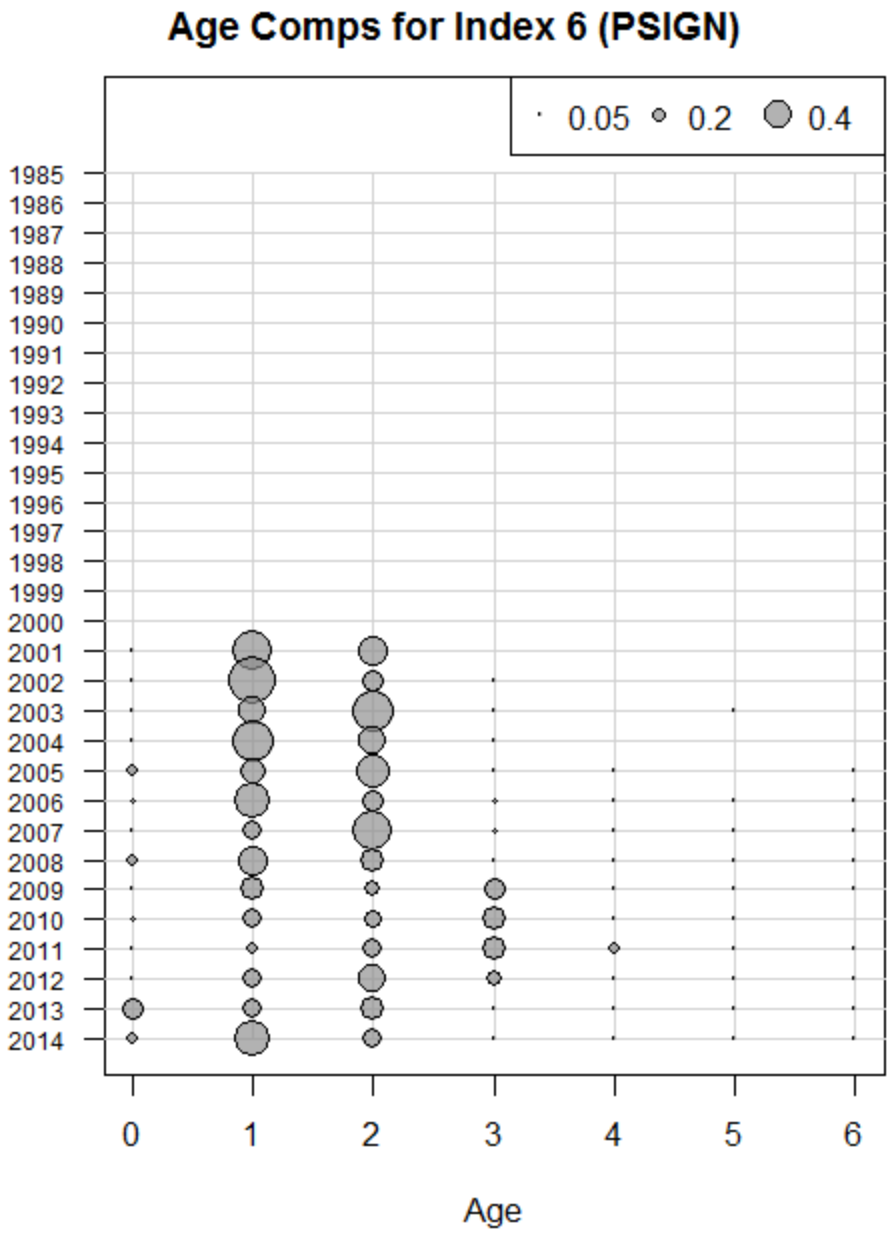

Figure B7.34. Input age composition for the PSIGN gillnet survey index from 2001 to 2014.

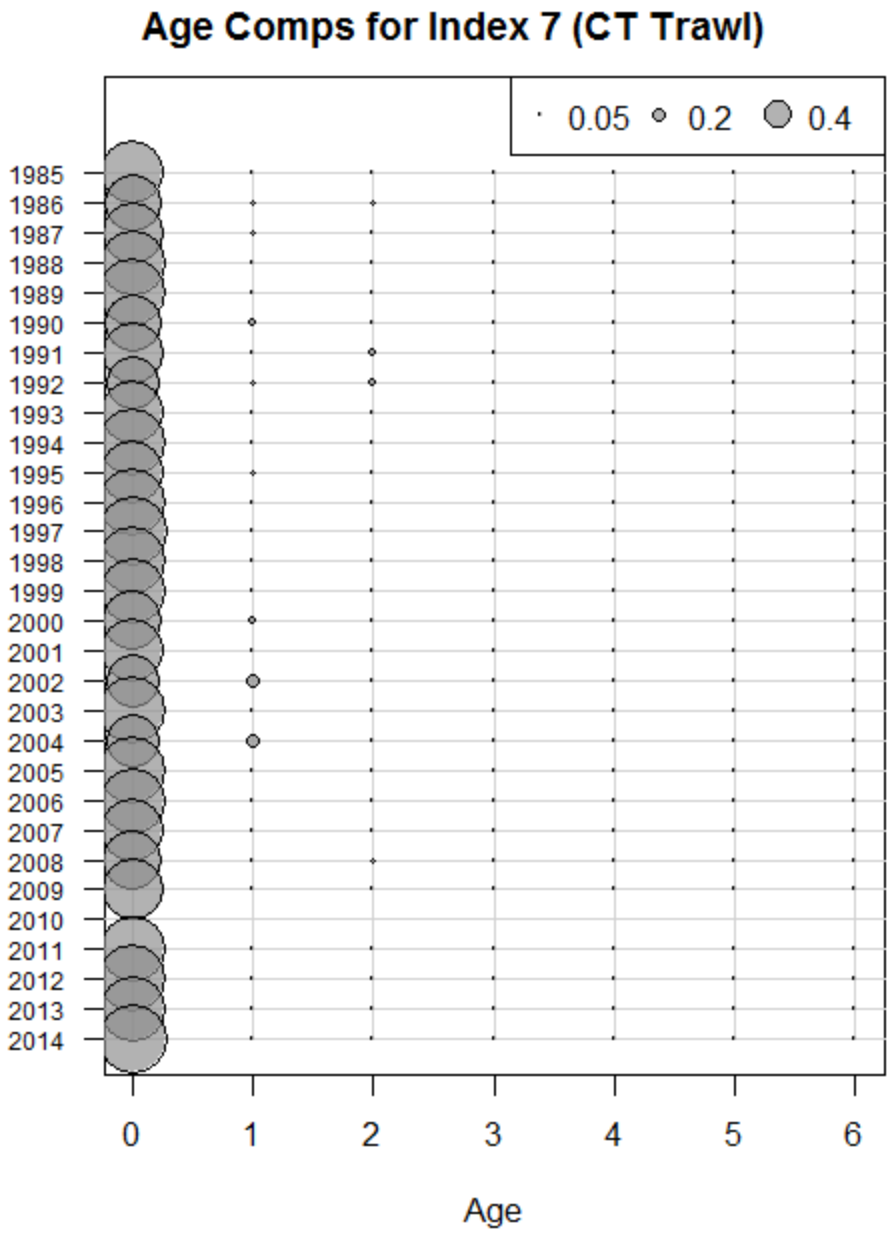

Figure B7.35. Input age composition for the CT LISTS trawl survey index from 1985 to 2014.

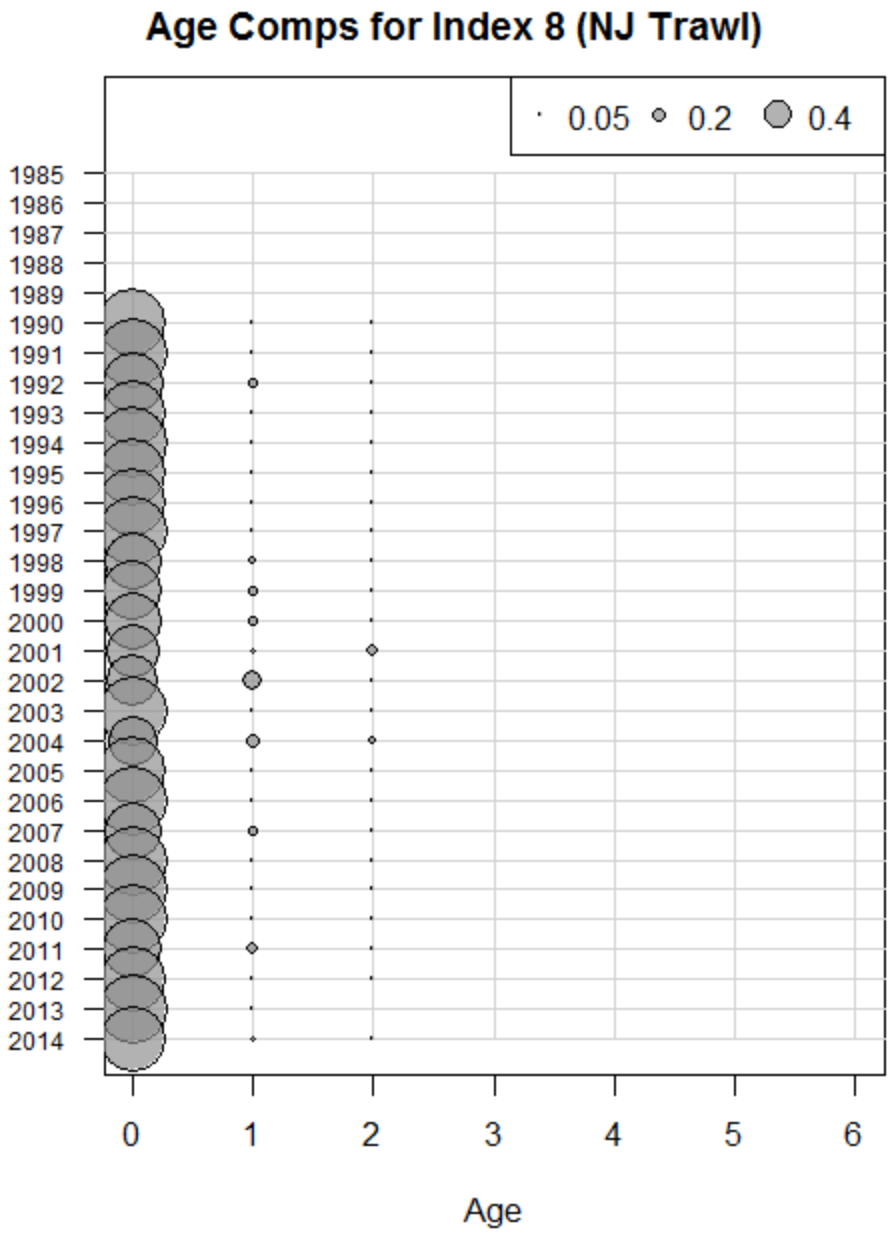

Figure B7.35A. Input age composition for the NJ Ocean trawl survey index from 1990 to 2014.

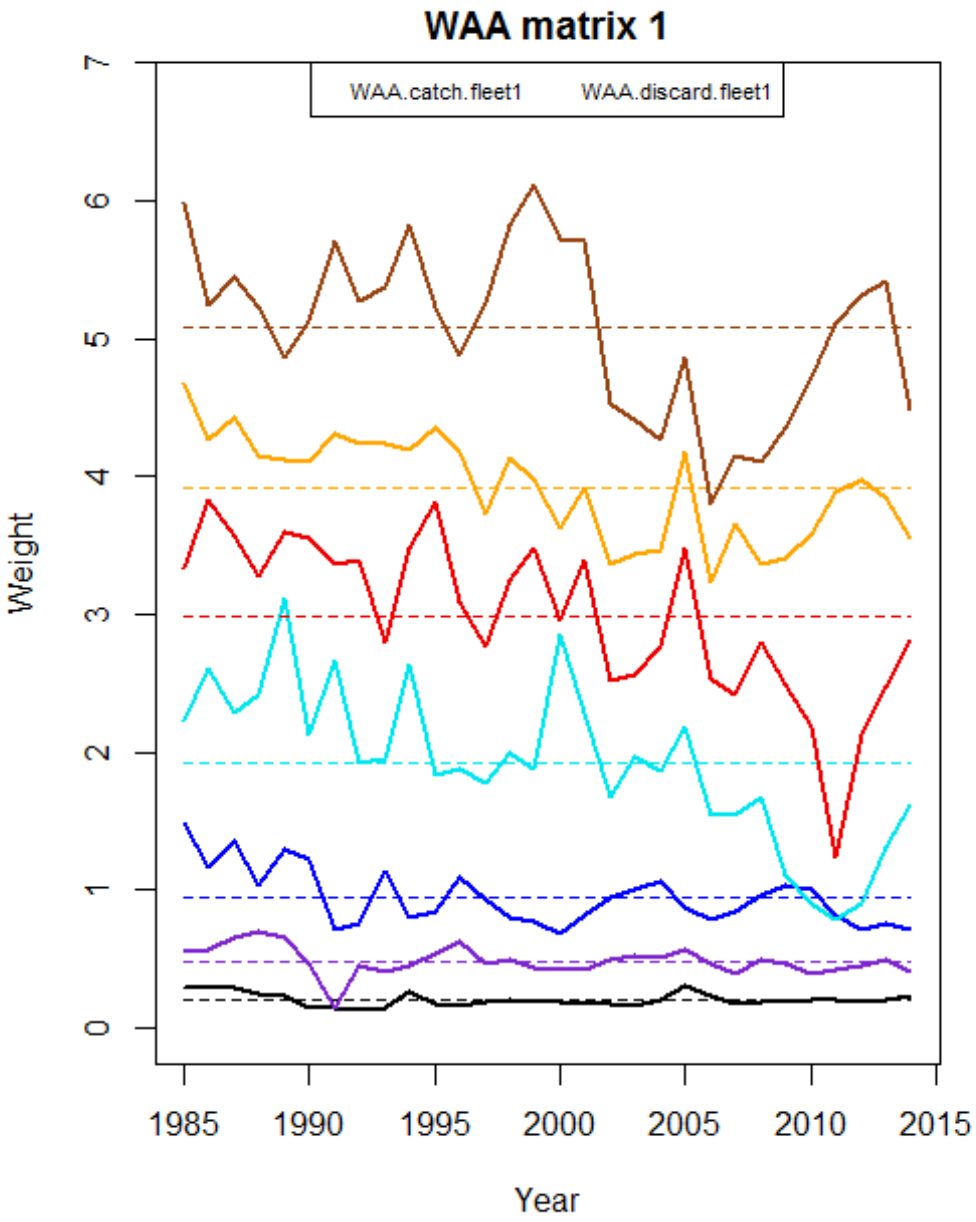

Figure B7.36. Bluefish weight-at-age (Ages 0-6+) for the commercial fleet from 1985 to 2014.

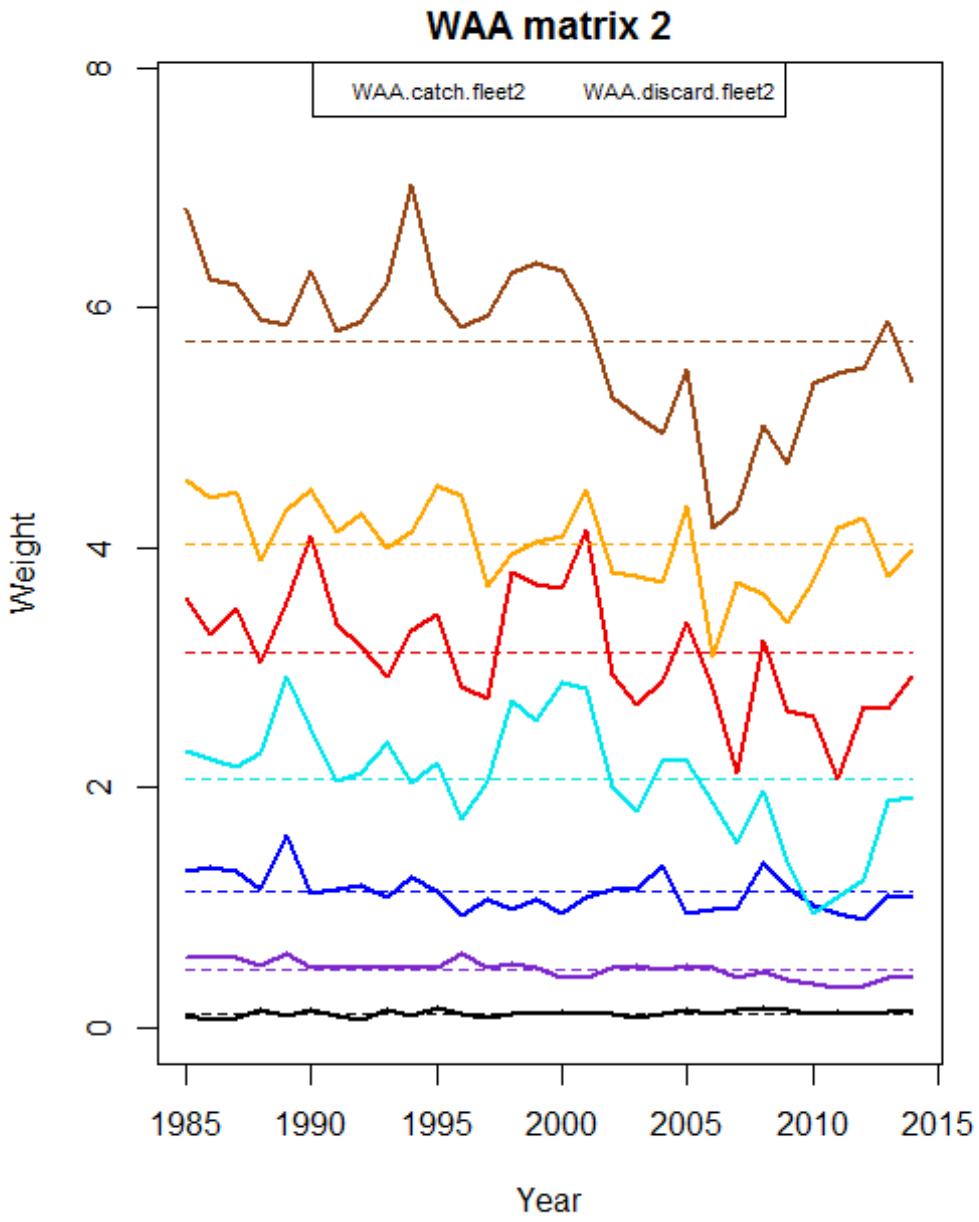

Figure B7.37. Bluefish weight-at-age (Ages 0-6+) for the recreational fleet from 1985 to 2014.

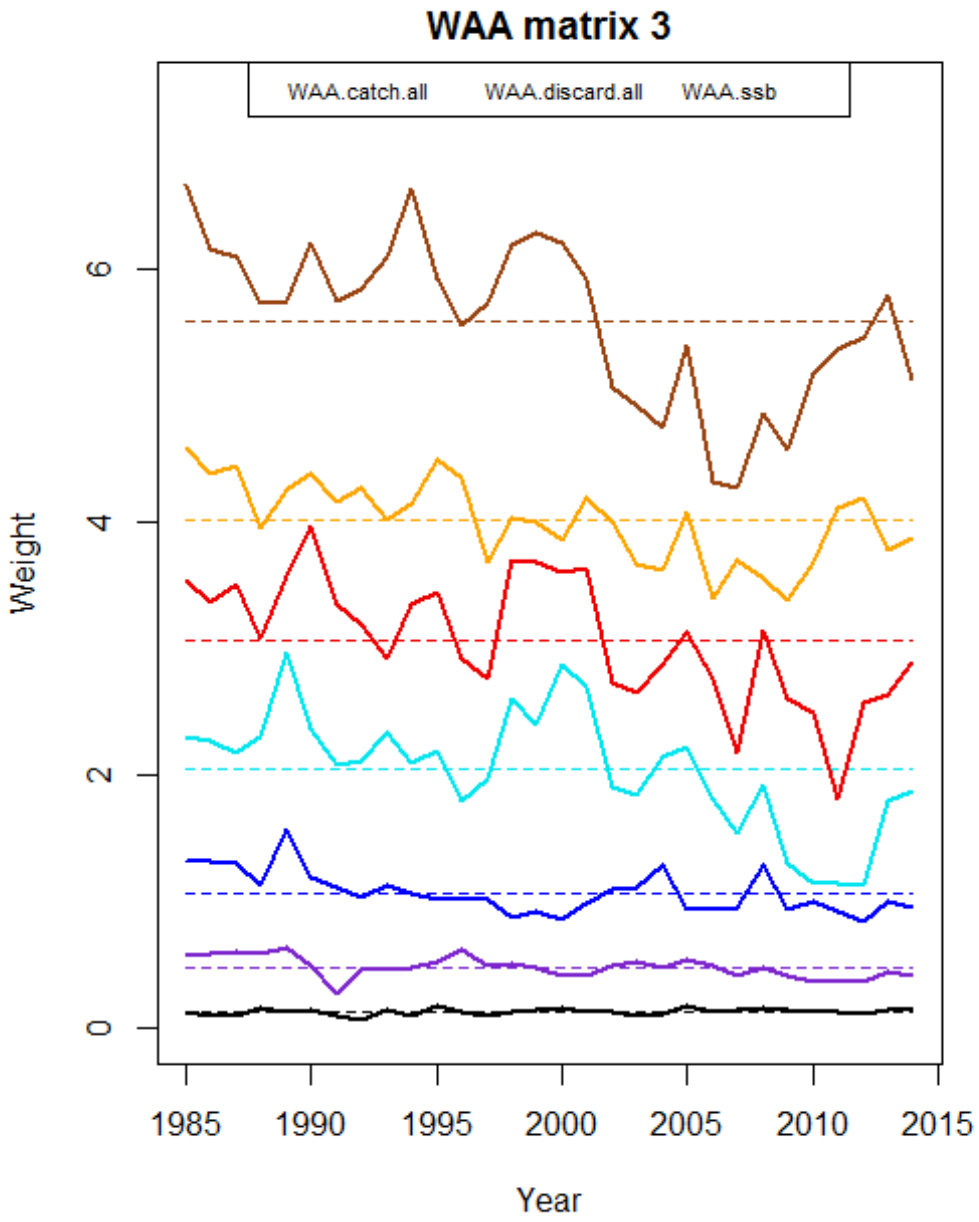

Figure B7.38. Bluefish weight-at-age (Ages 0-6+) for the catch (all fleets) from 1985 to 2014.

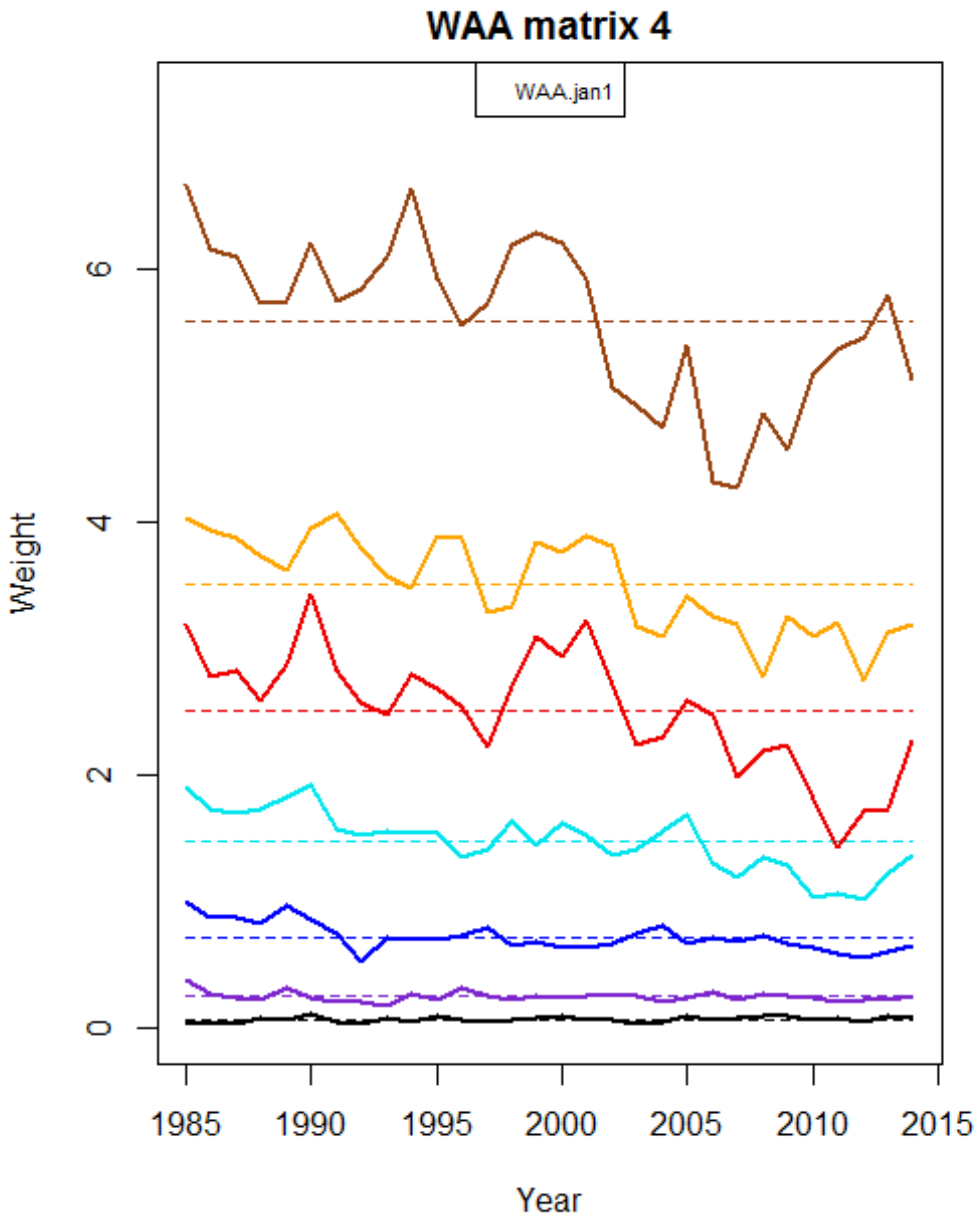

Figure B7.39. Bluefish Jan-1 weight-at-age (Ages 0-6+) for all fleets from 1985 to 2014.

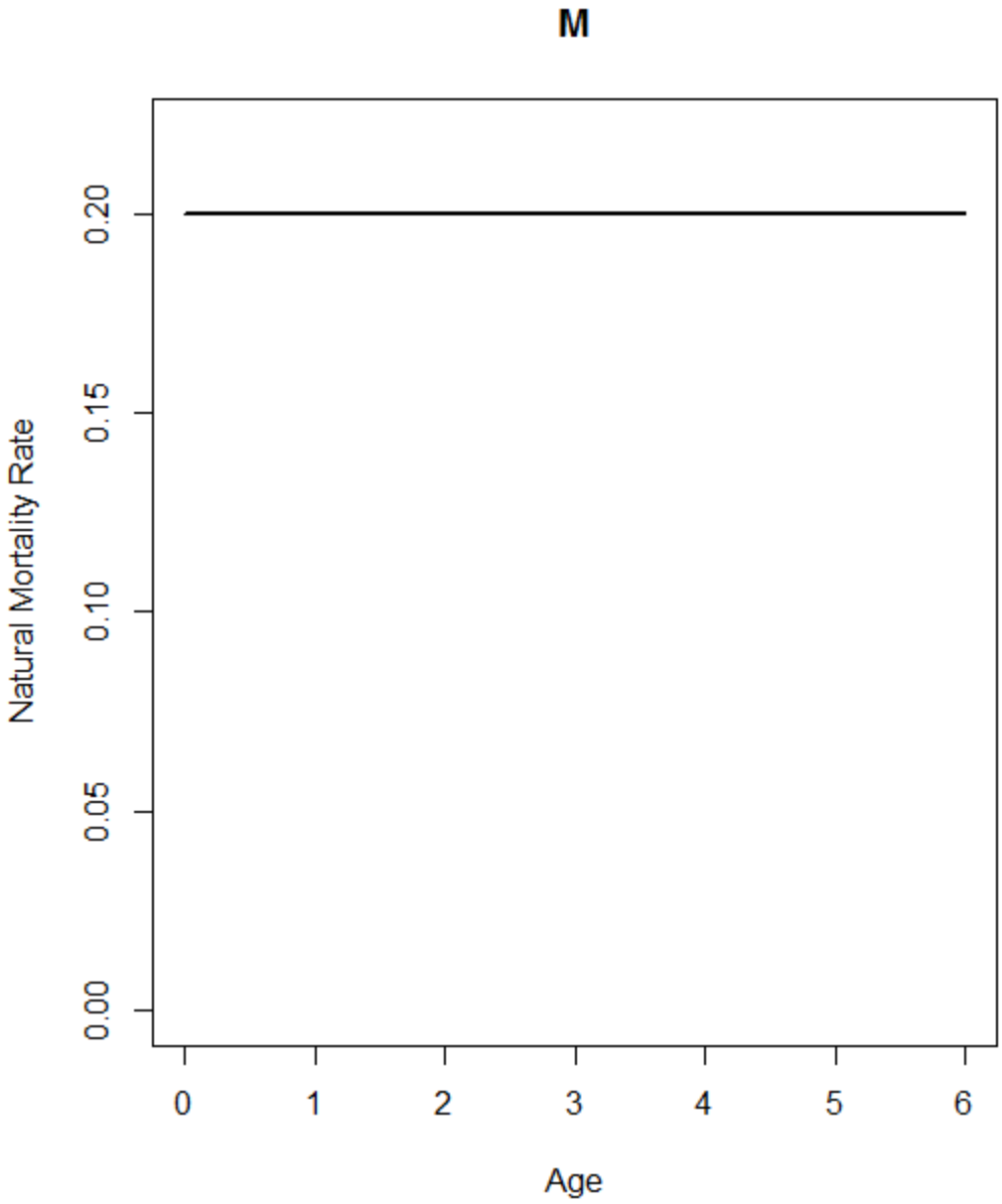

Figure B7.40. Bluefish natural mortality for the final model, kept constant at 0.2 for all ages across all years.

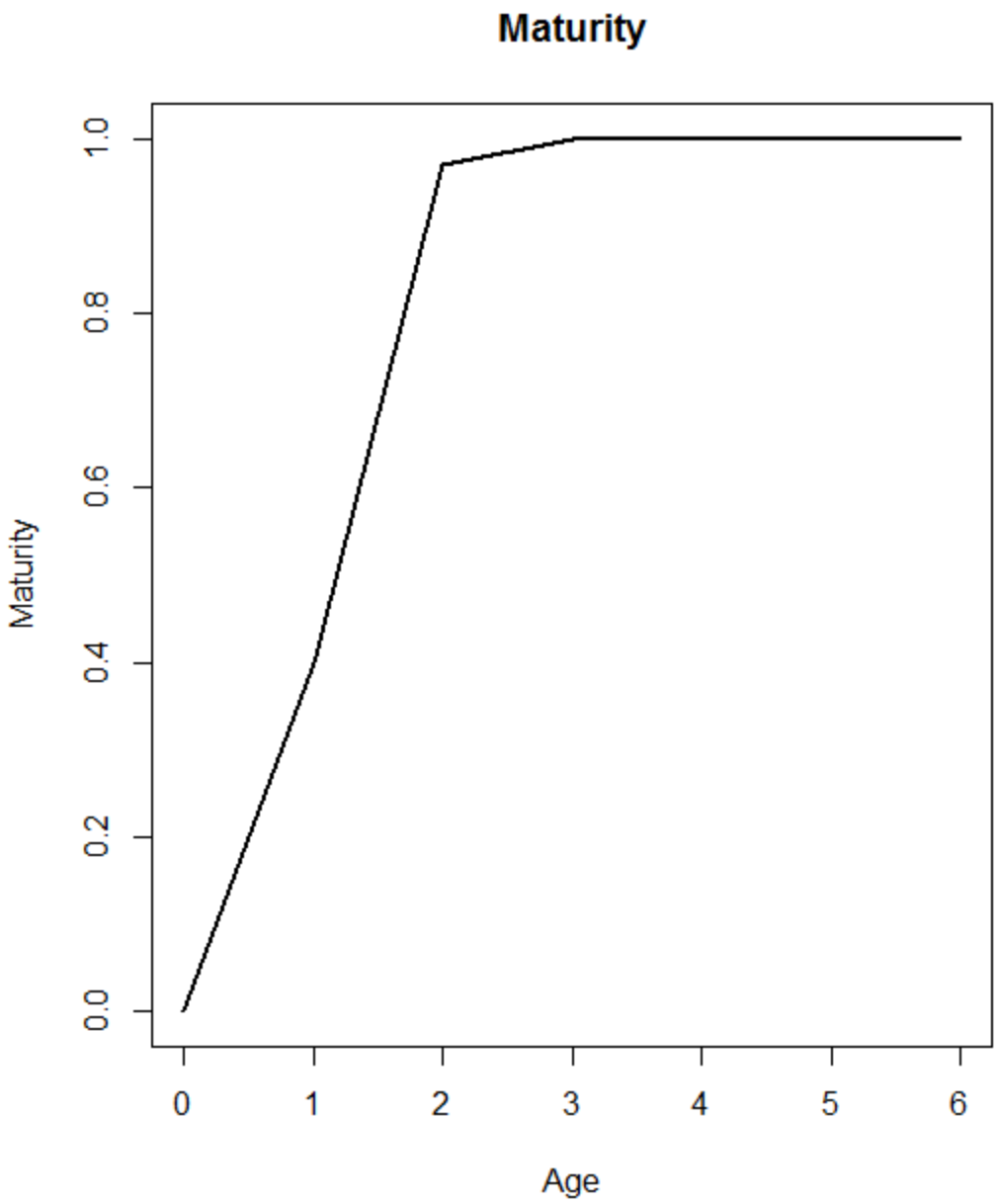

Figure B7.41. Bluefish maturity-at-age for the final model, kept constant across all years.

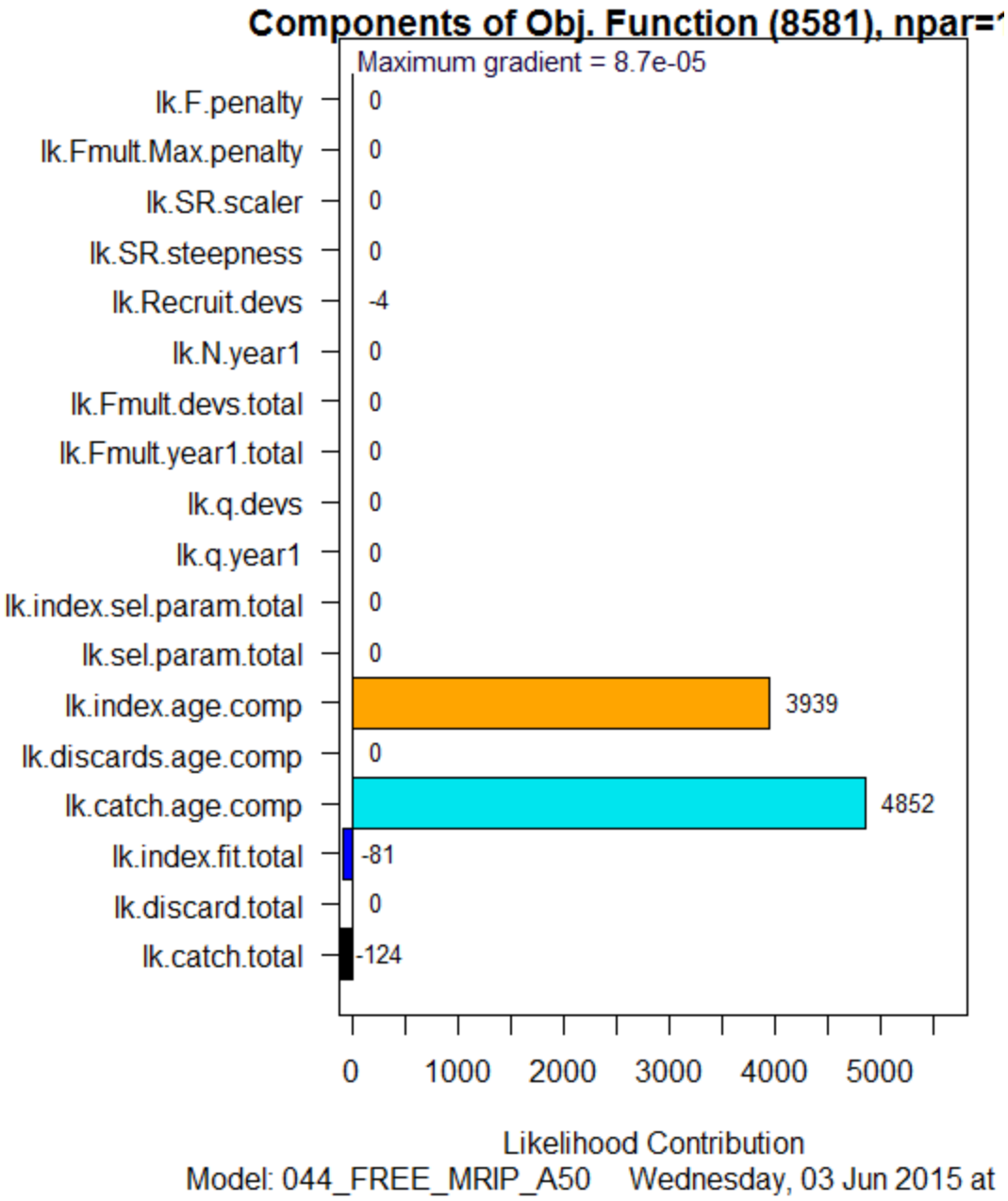

Figure B7.42. Objective function components of model BFINAL.

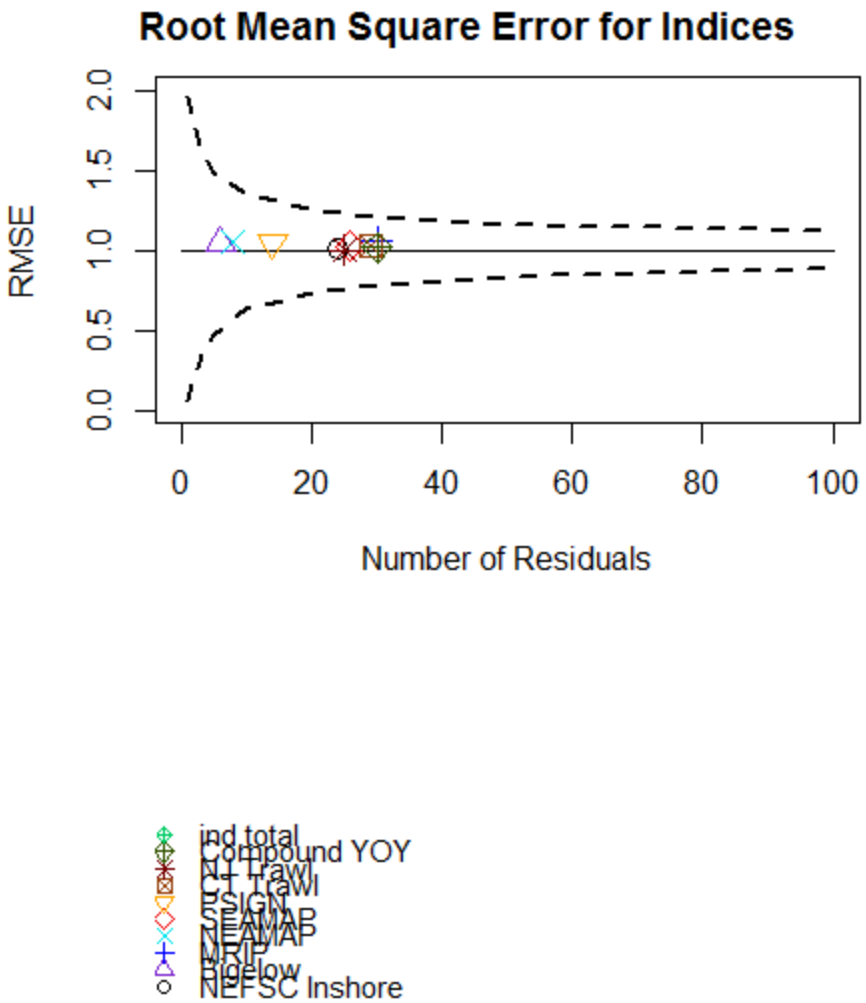

Figure B7.43. RMSE of the final indices after iterative adjustment of the input CVs.

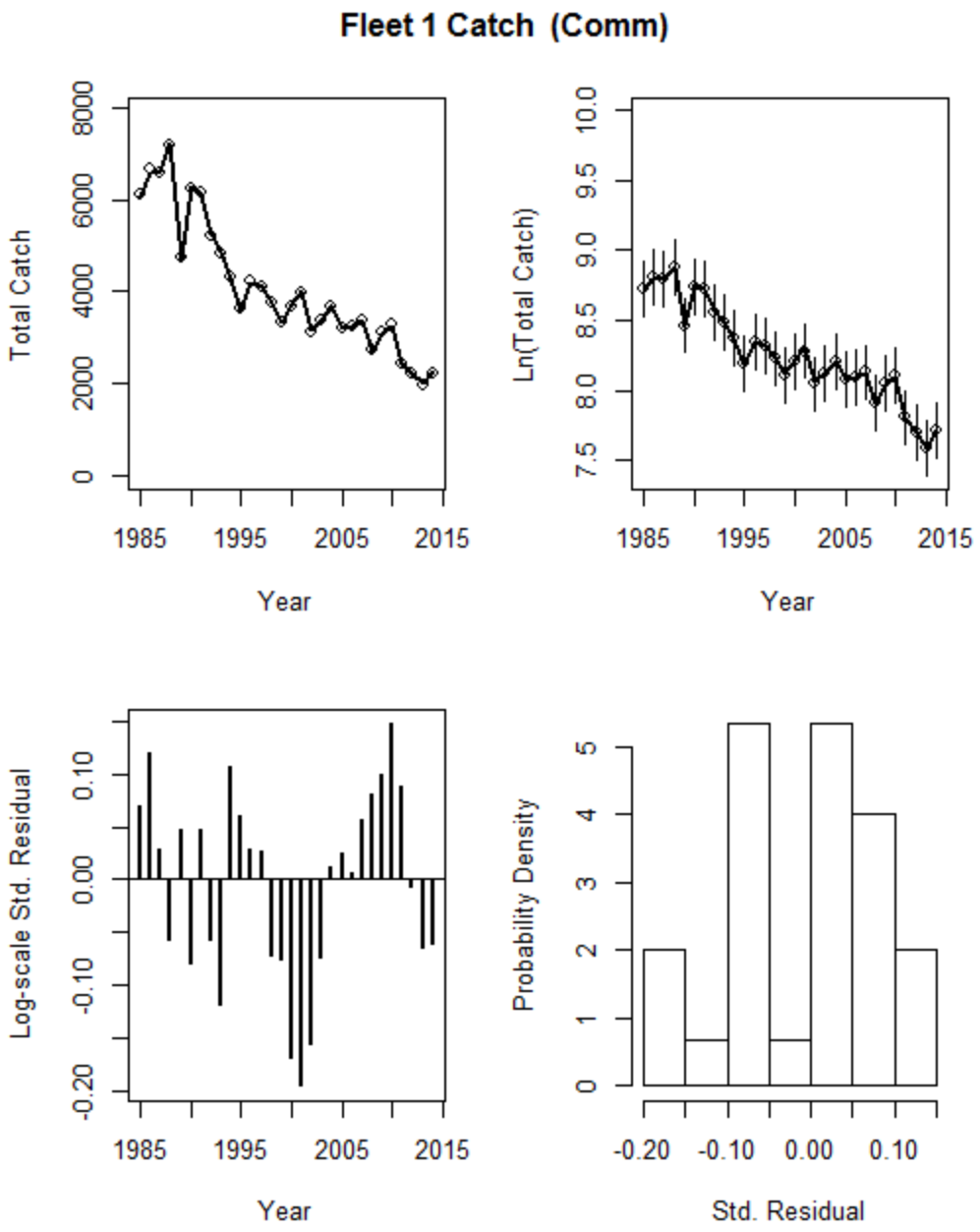

Figure B7.44. Final model fit to the commercial catch fleet with log-scale standardized residuals and residual probability density.

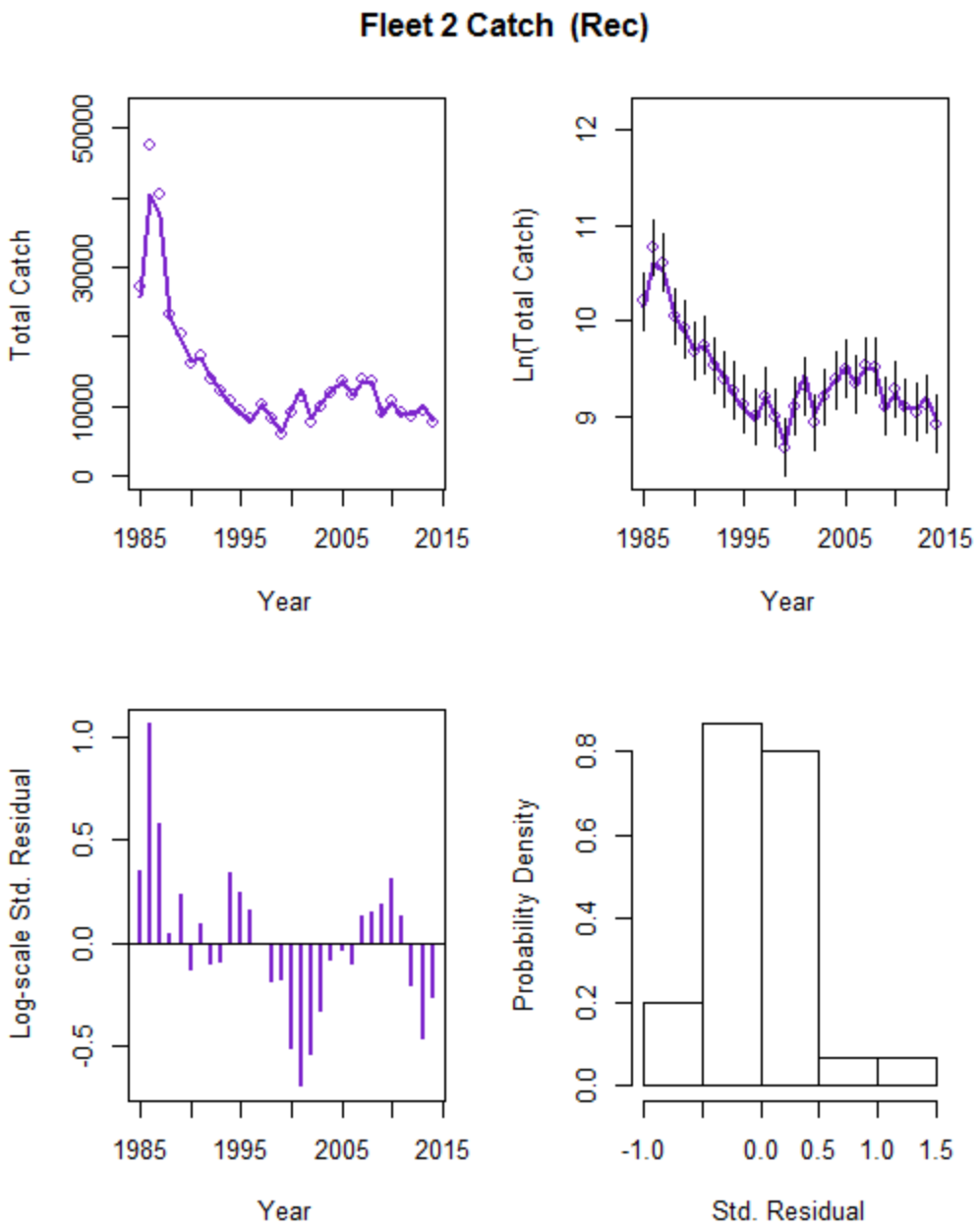

Figure B7.45. Final model fit to the recreational catch fleet with log-scale standardized residuals and residual probability density.

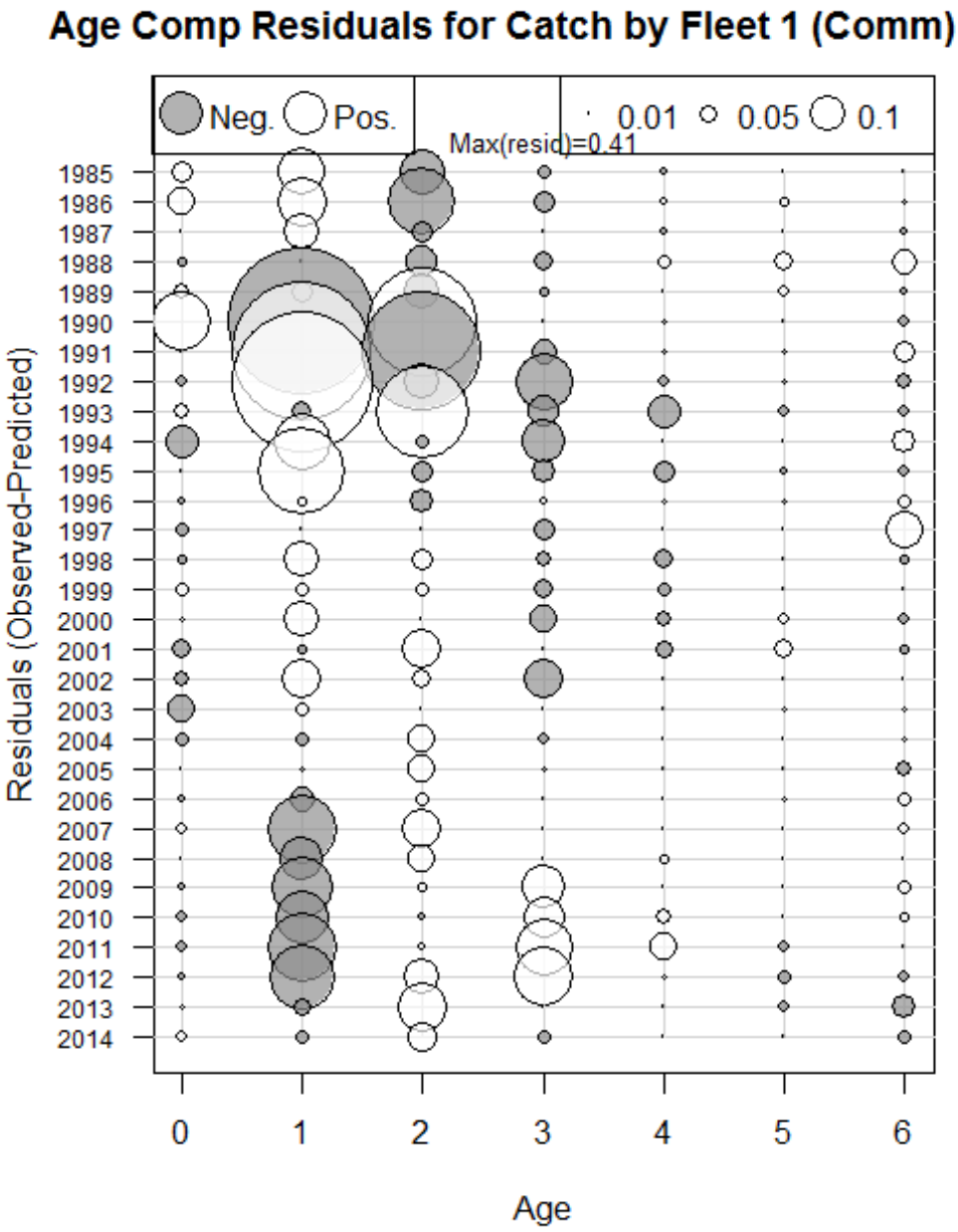

Figure B7.46. Age-composition residuals for the commercial catch fleet.

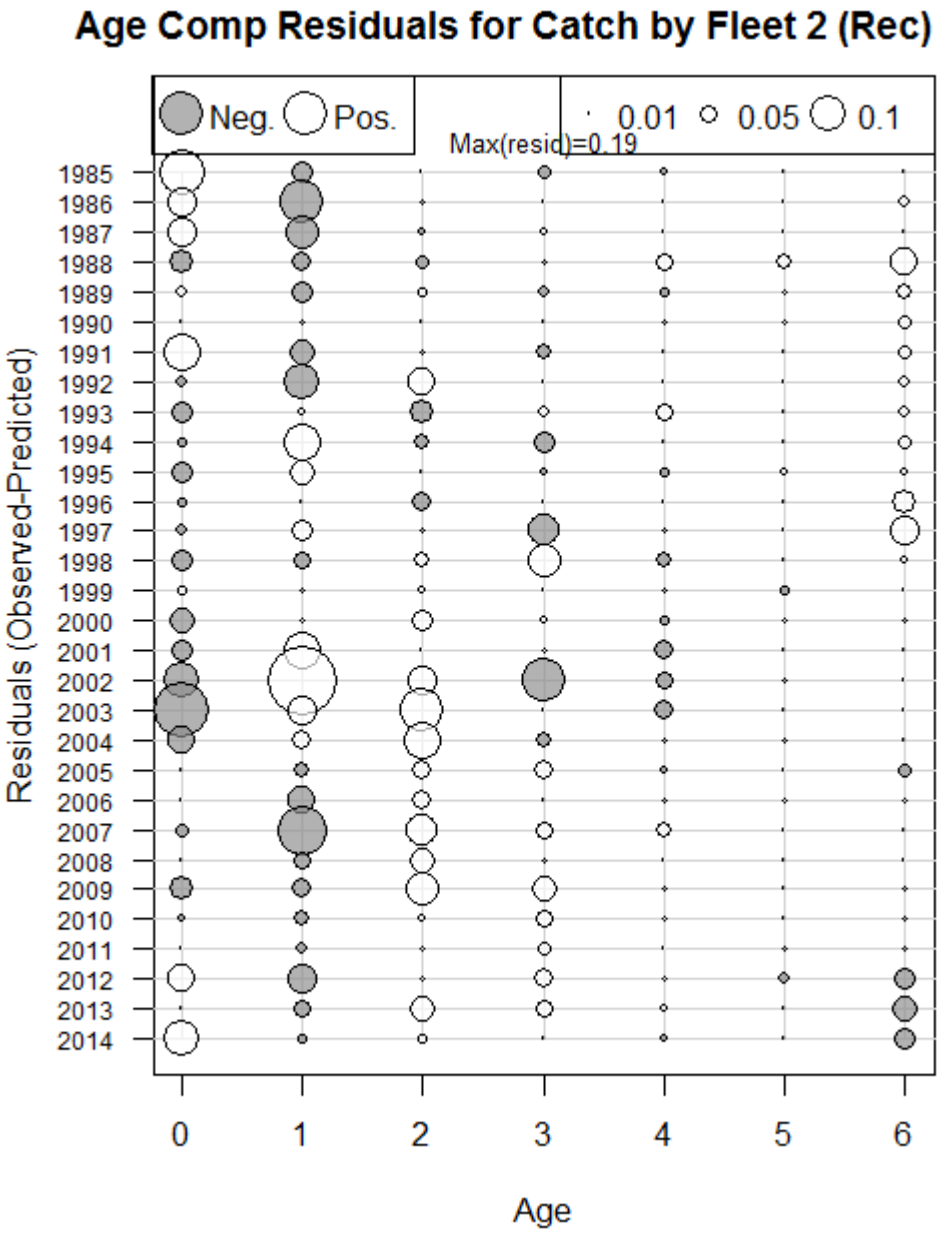

Figure B7.47. Age composition residuals for the recreational catch fleet.

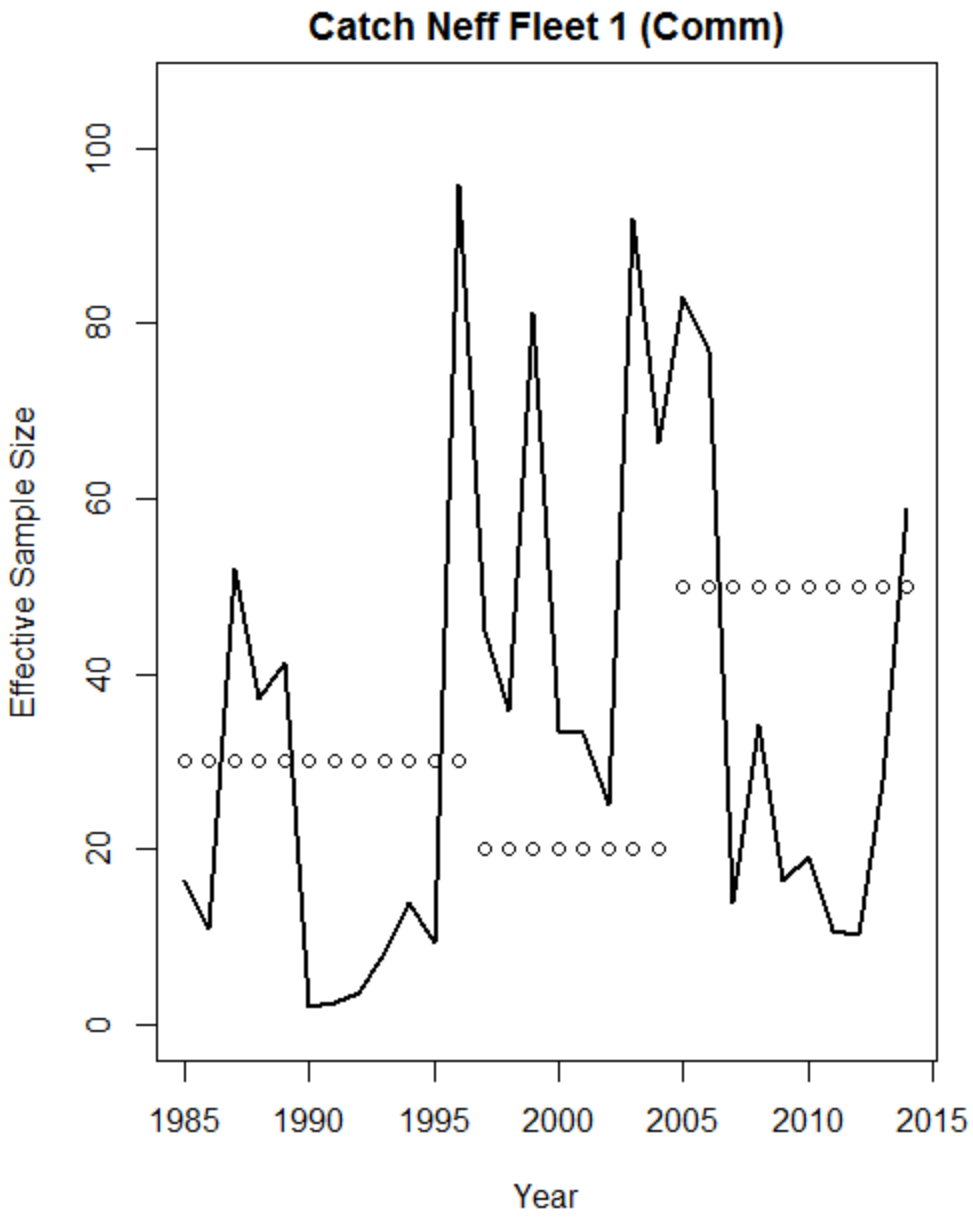

Figure B7.48. Input and estimated effective sample size for the commercial catch fleet.

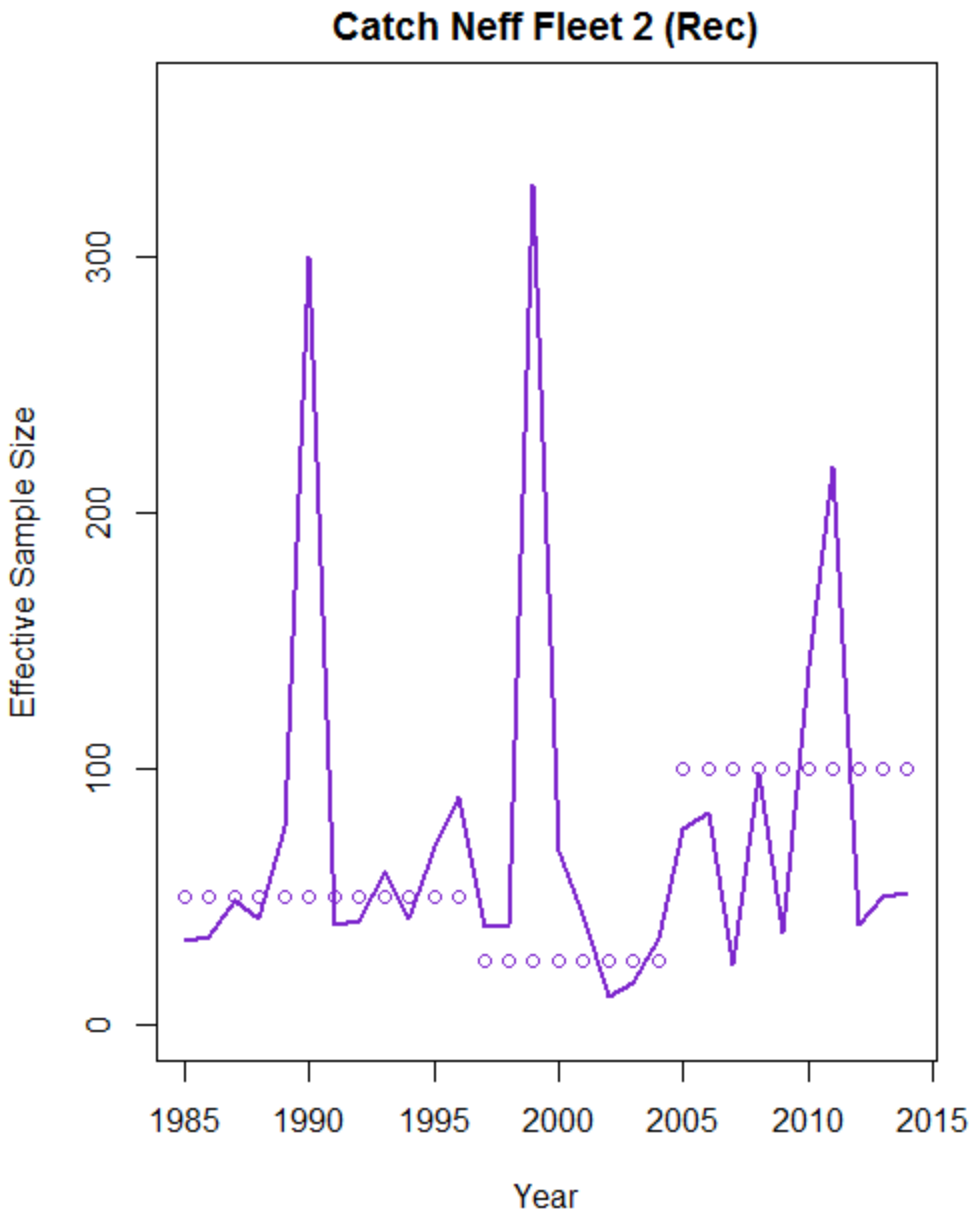

Figure B7.49. Input and estimated effective sample size for the recreational catch fleet.

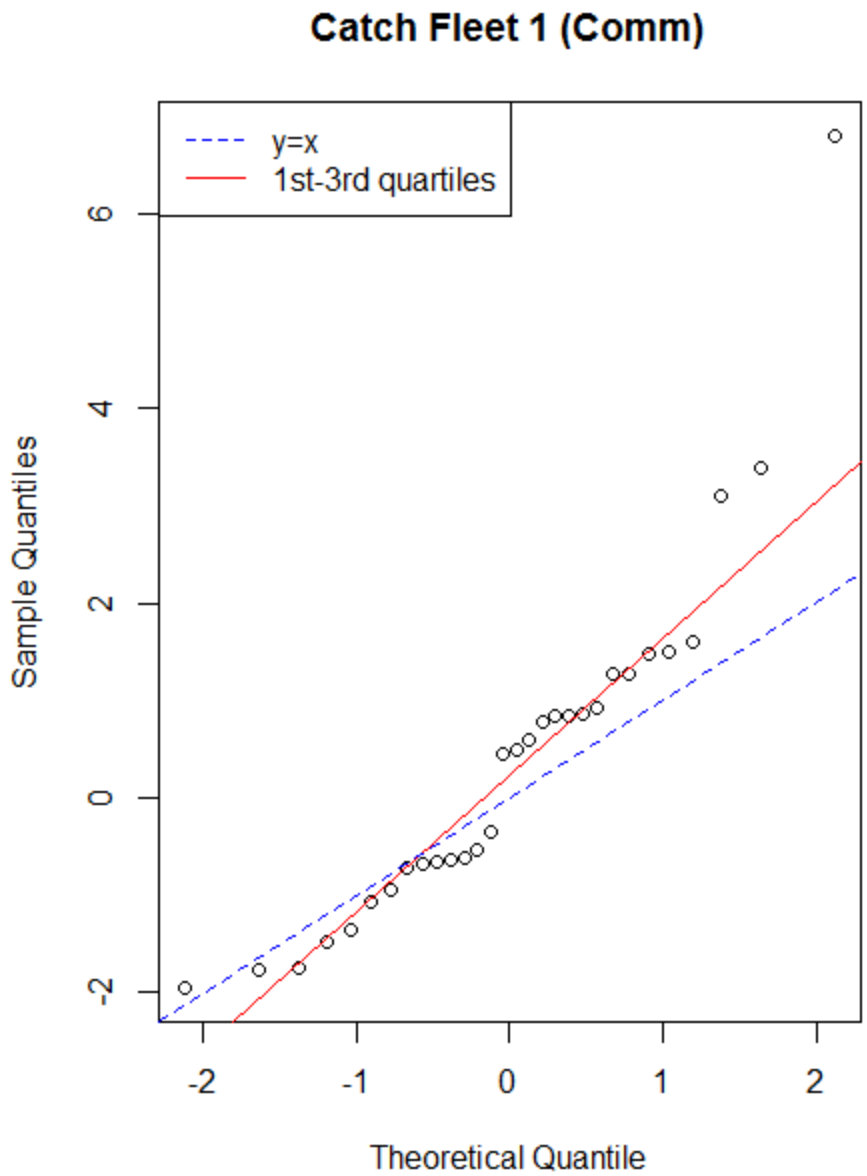

Figure B7.50. QQ-plot for the observed versus predicted mean catch for the commercial catch fleet.

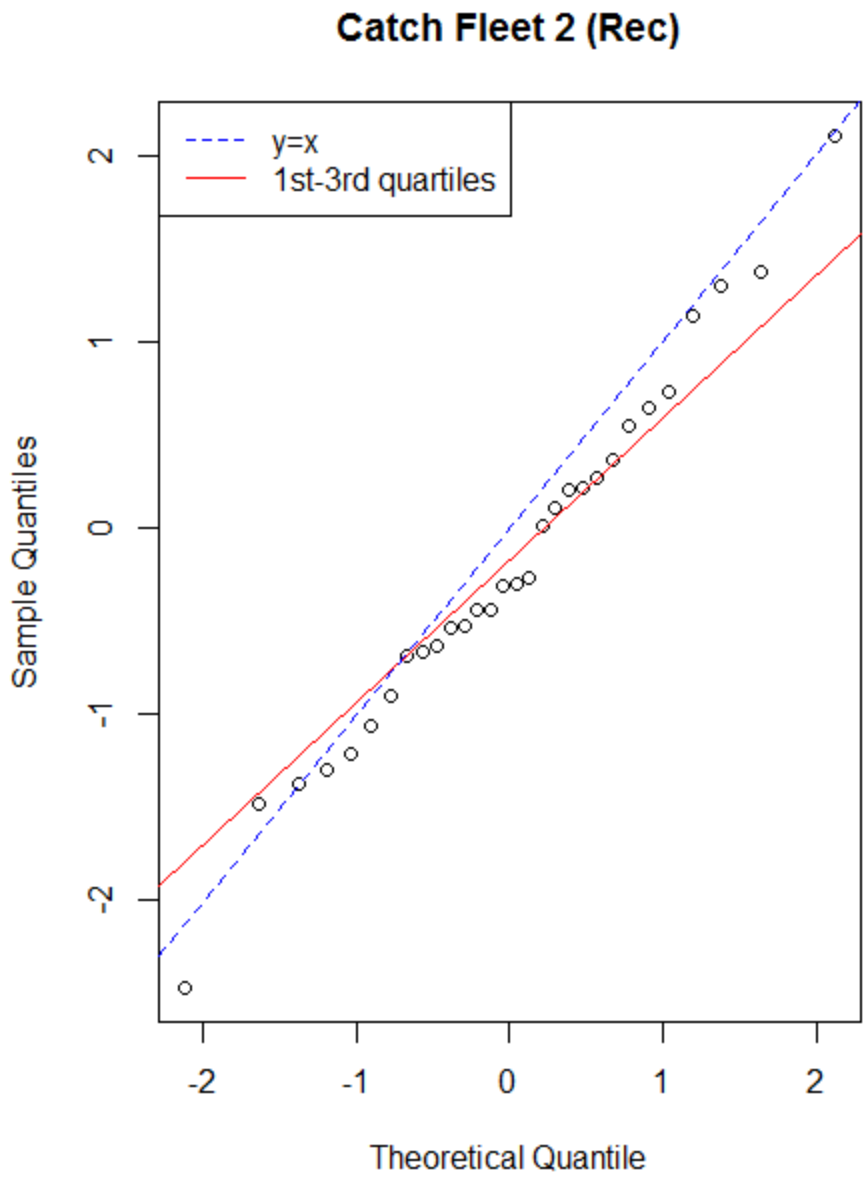

Figure B7.51. QQ-plot for the observed versus predicted mean catch for the recreational catch fleet.

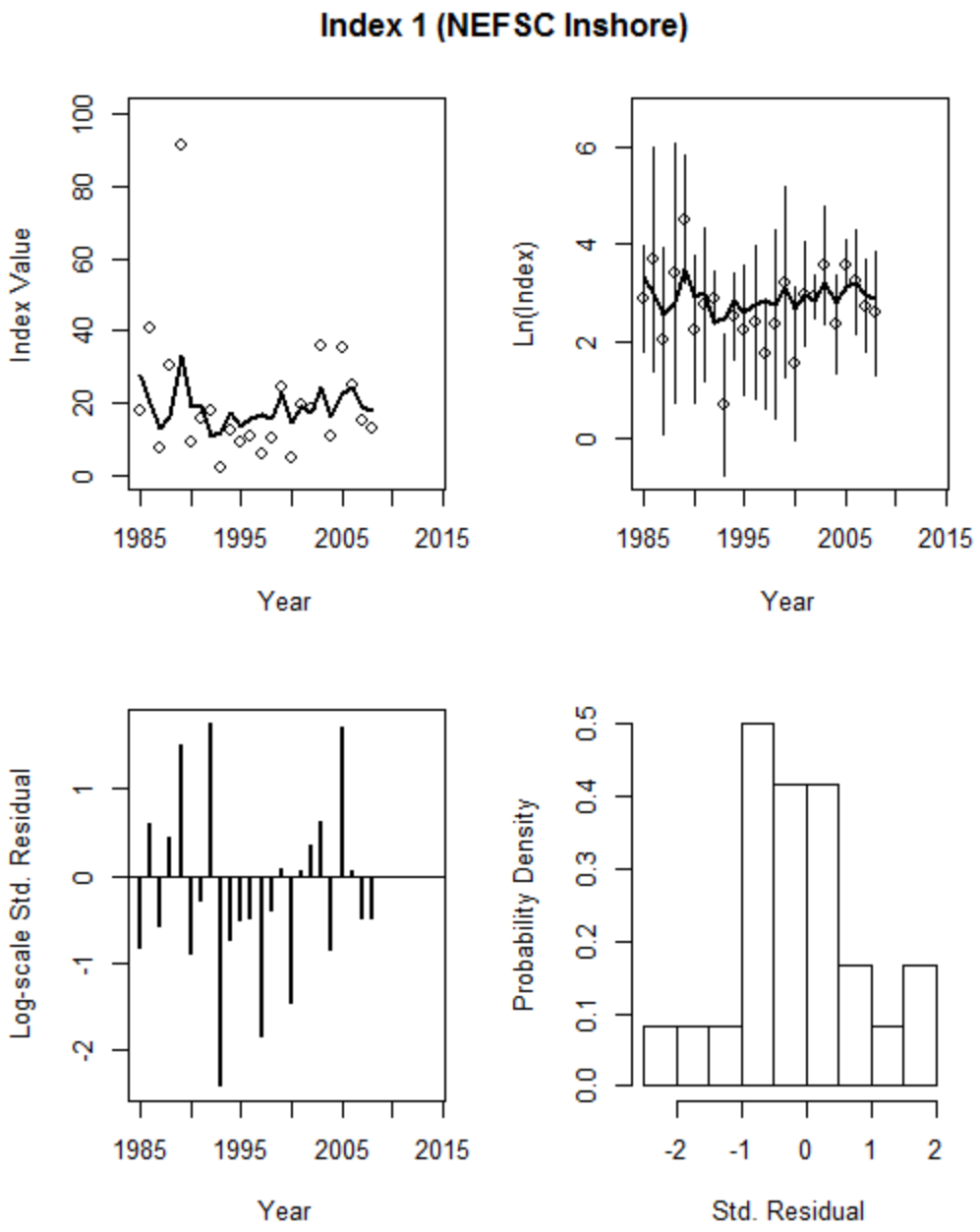

Figure B7.52. Final model fit to the NEFSC Inshore survey with log-scale standardized residuals and residual probability density.

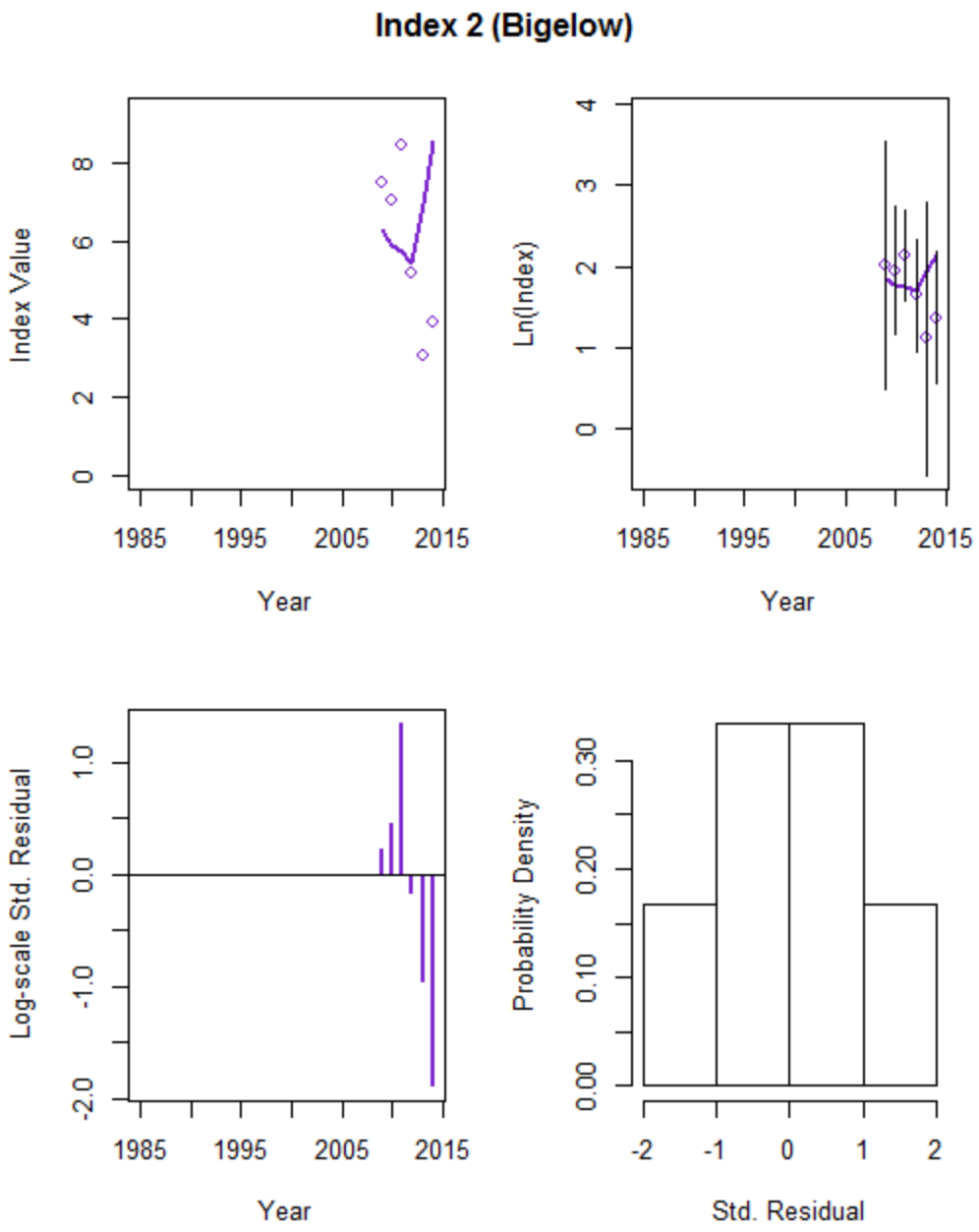

Figure B7.53. Final model fit to the NEFSC Bigelow survey with log-scale standardized residuals and residual probability density.

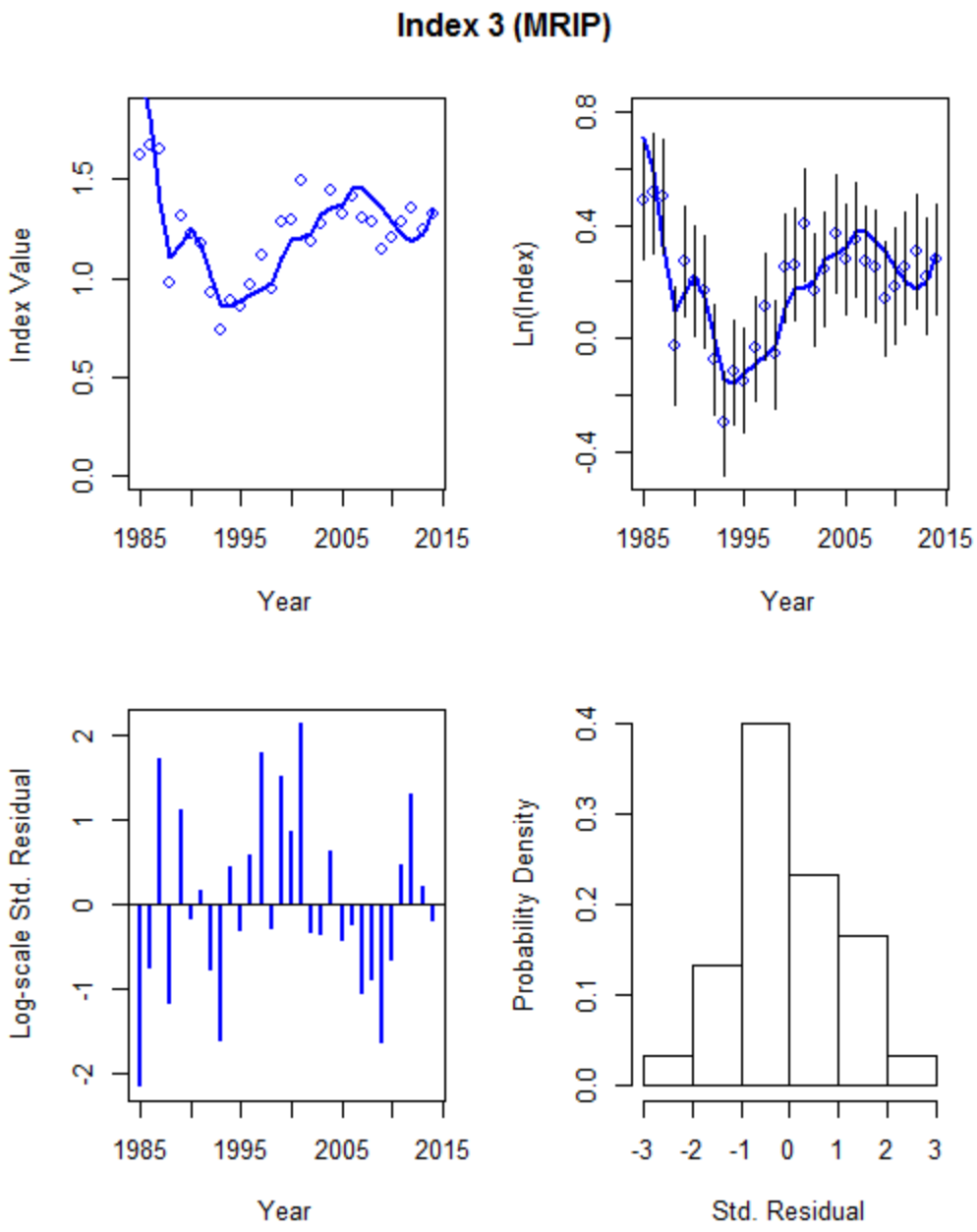

Figure B7.54. Final model fit to the MRIP recreational CPUE index with log-scale standardized residuals and residual probability density.

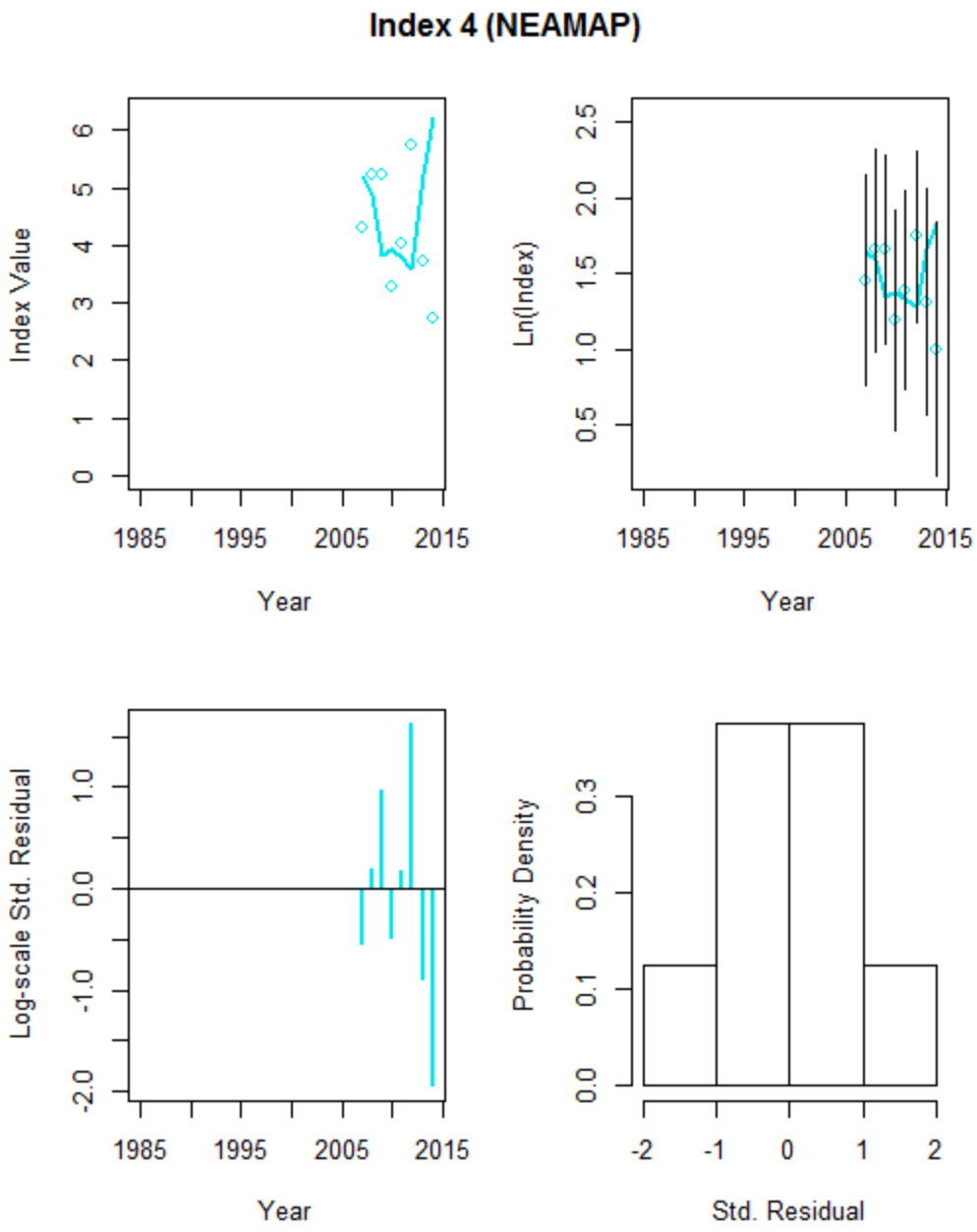

Figure B7.55. Final model fit to the NEAMAP survey with log-scale standardized residuals and residual probability density.

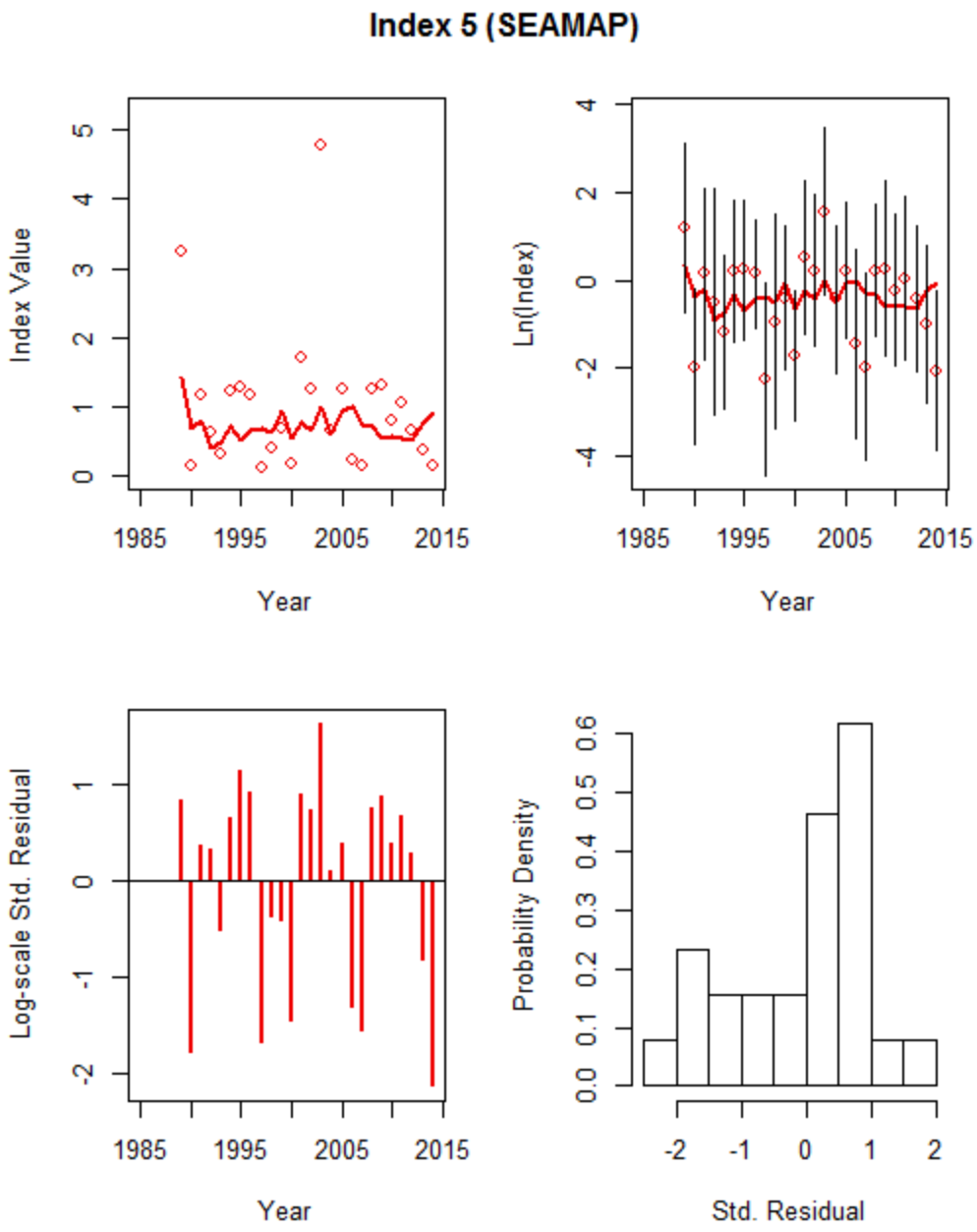

Figure B7.56. Final model fit to the SEAMAP Age 0 index with log-scale standardized residuals and residual probability density.

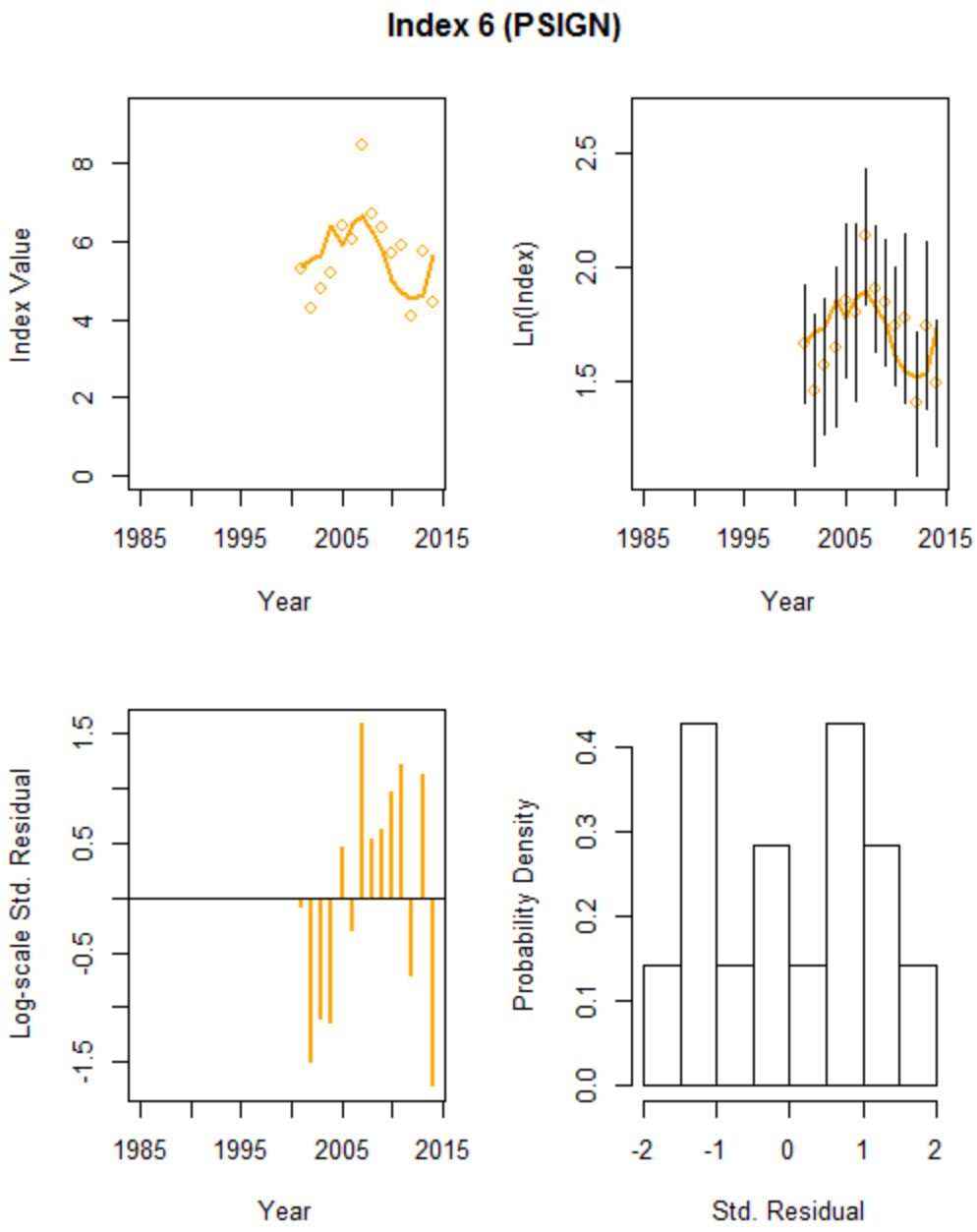

Figure B7.57. Final model fit to the PSIGNS gillnet survey with log-scale standardized residuals and residual probability density.

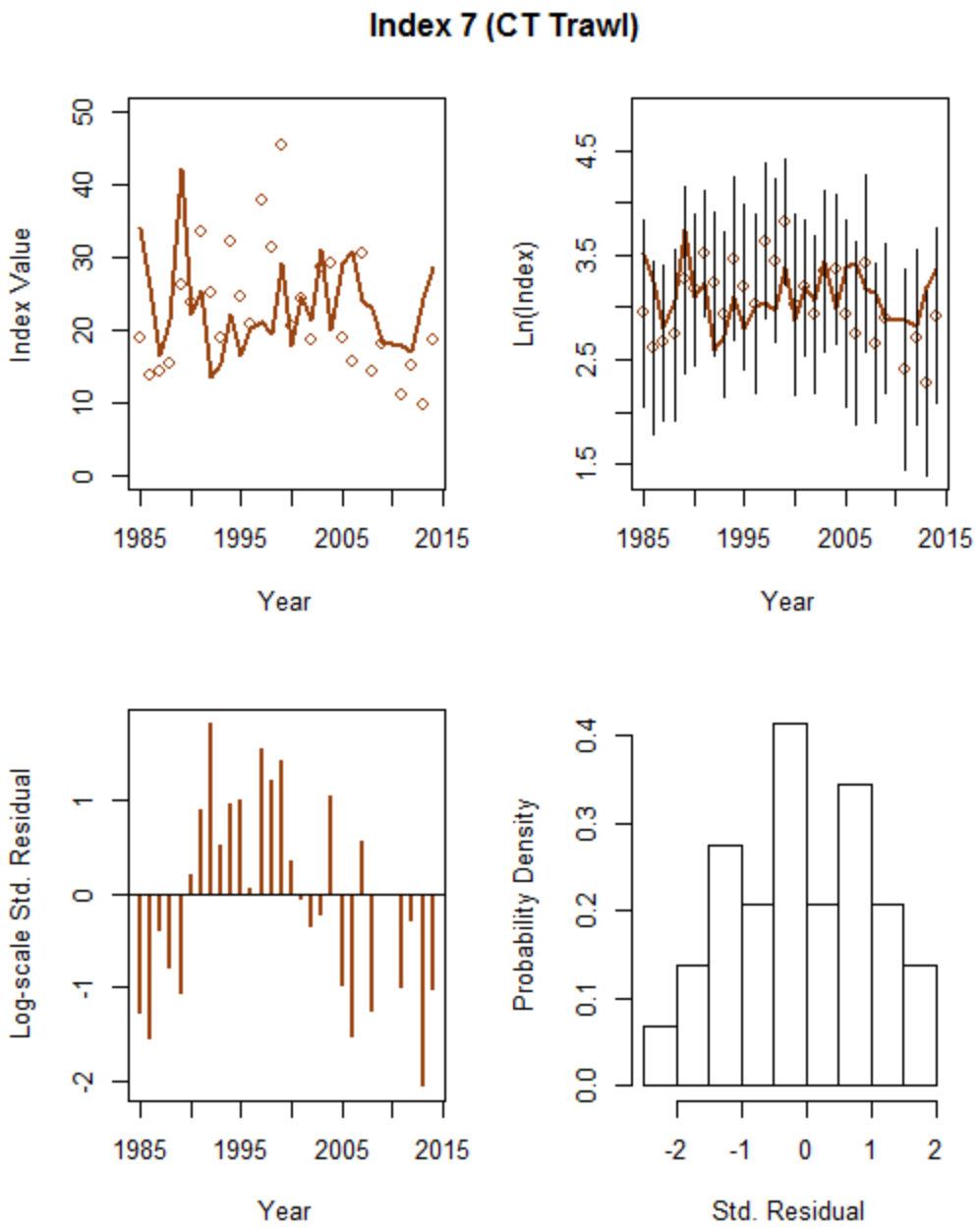

Figure B7.58. Final model fit to the CT LISTS trawl survey with log-scale standardized residuals and residual probability density.

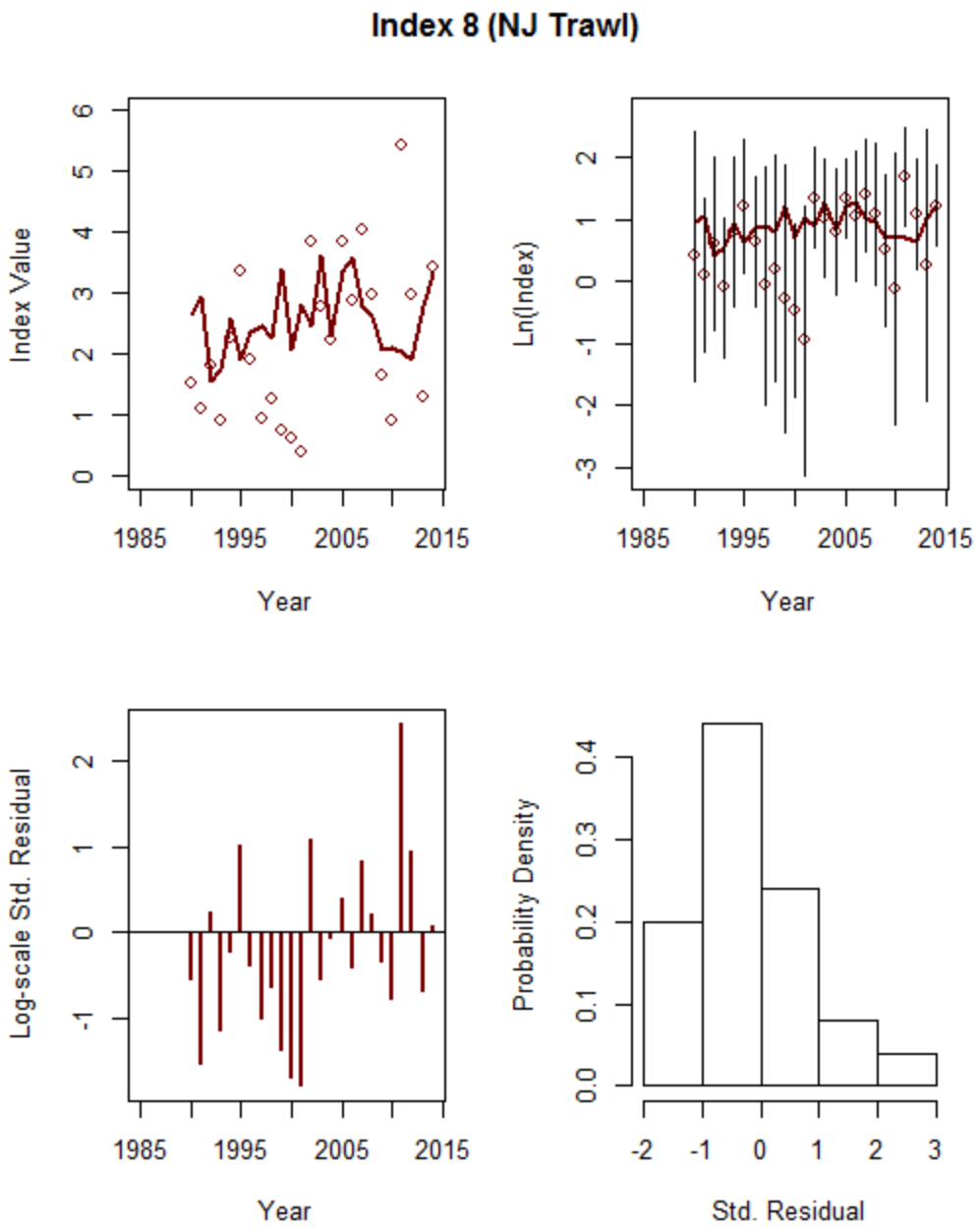

Figure B7.59. Final model fit to the NJ ocean trawl survey with log-scale standardized residuals and residual probability density.

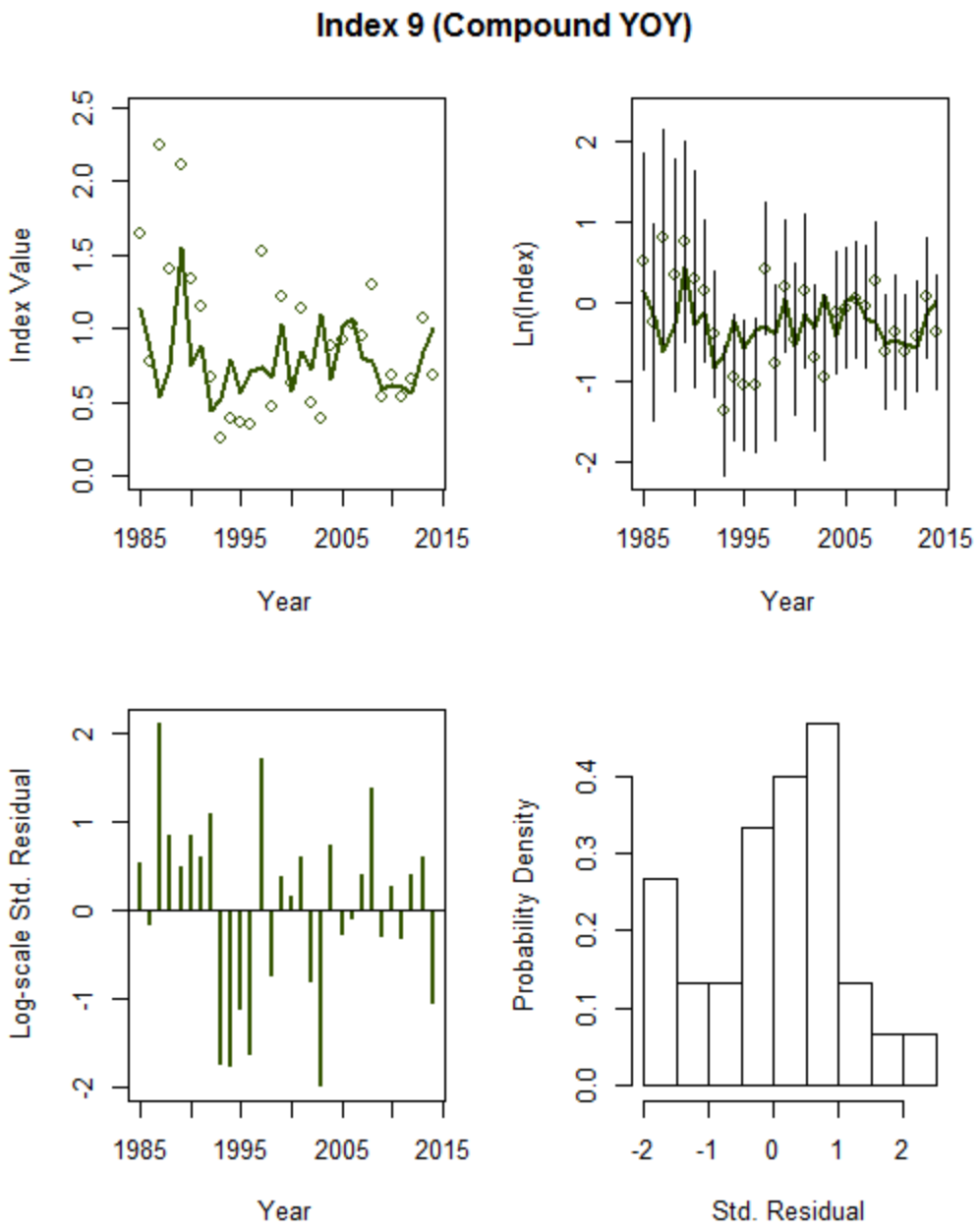

Figure B7.60. Final model fit to the composite YOY seine survey with log-scale standardized residuals and residual probability density.

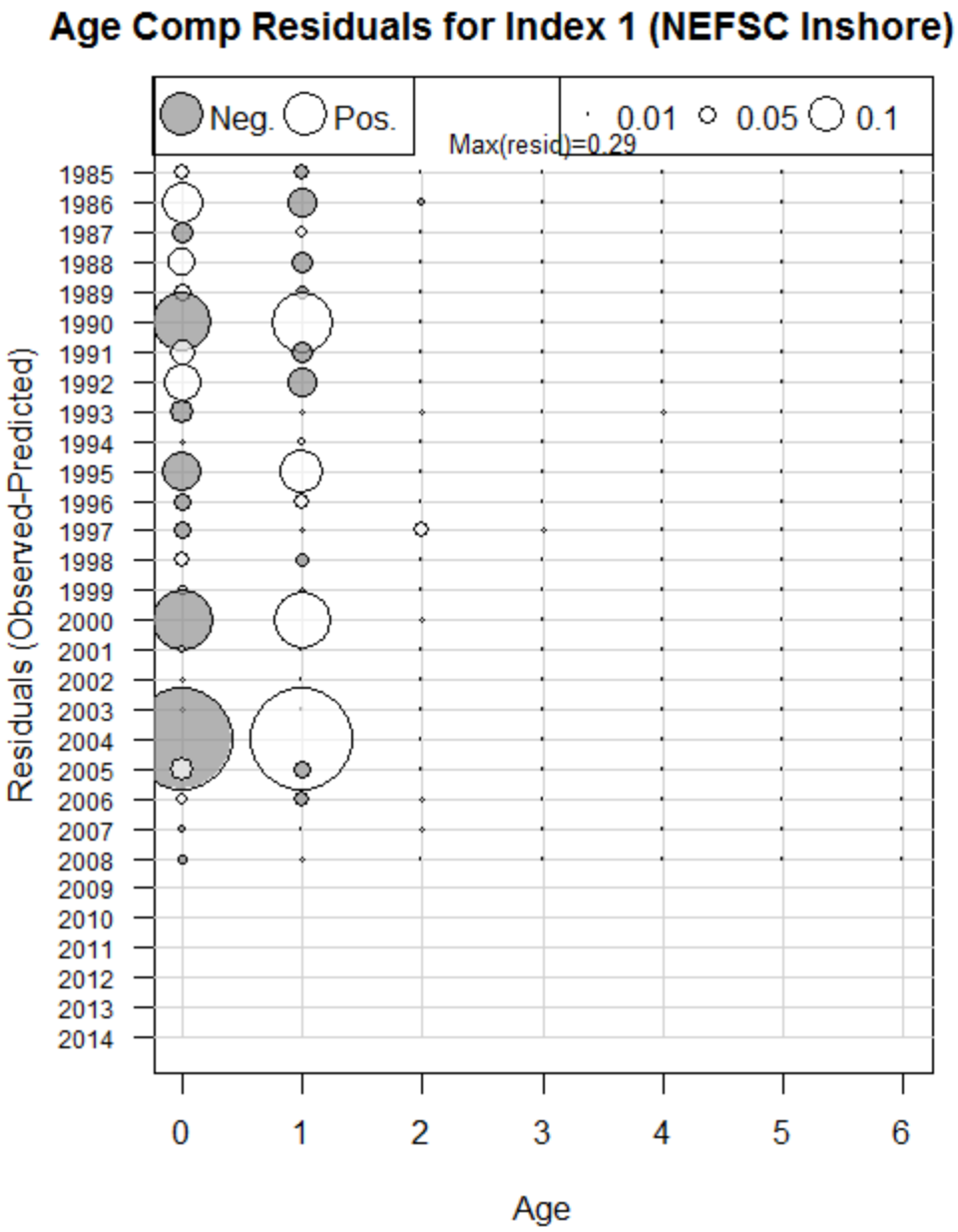

Figure B7.61. Age composition residuals for the NEFSC Inshore survey.

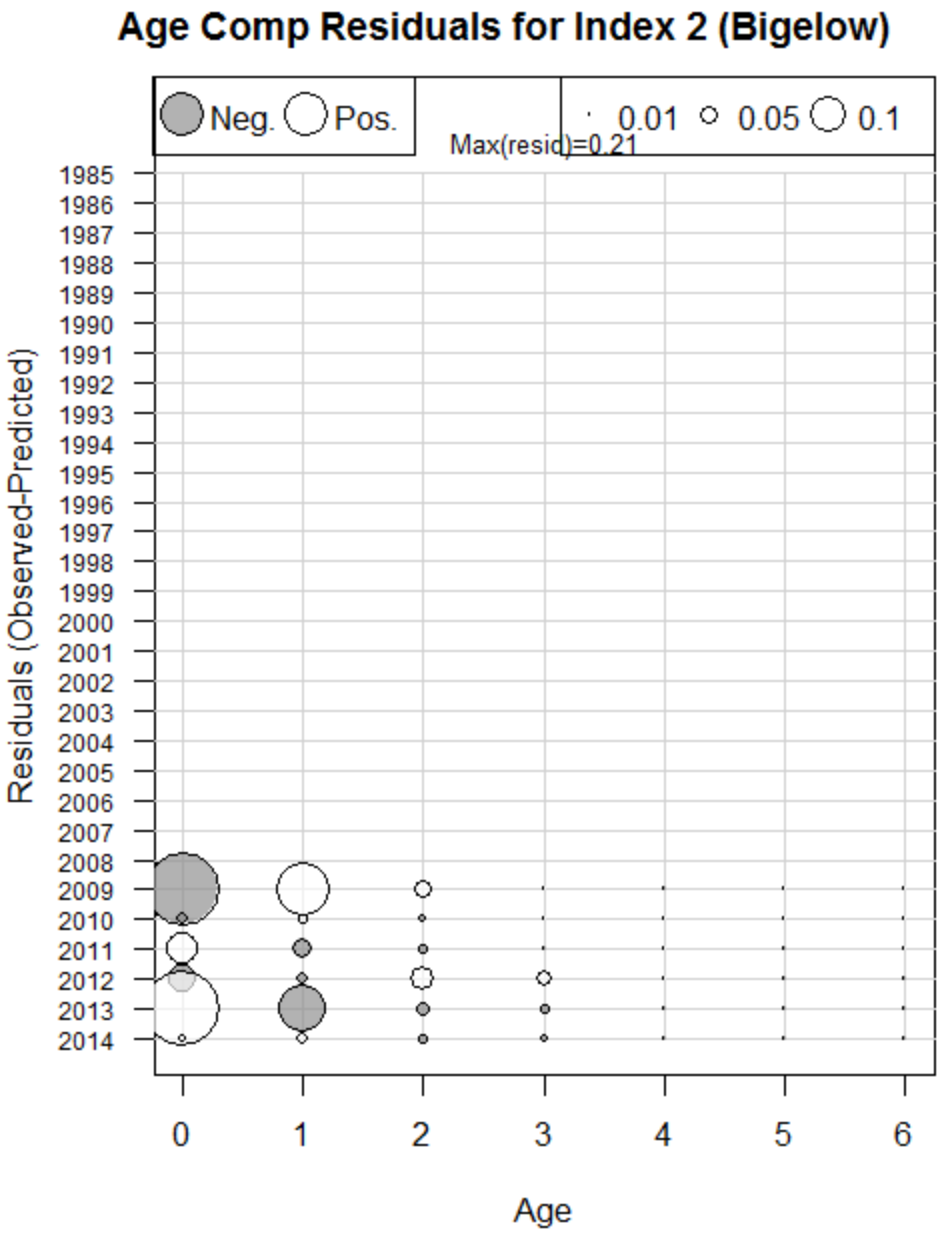

Figure B7.62. Age composition residuals for the NEFSC Bigelow survey.

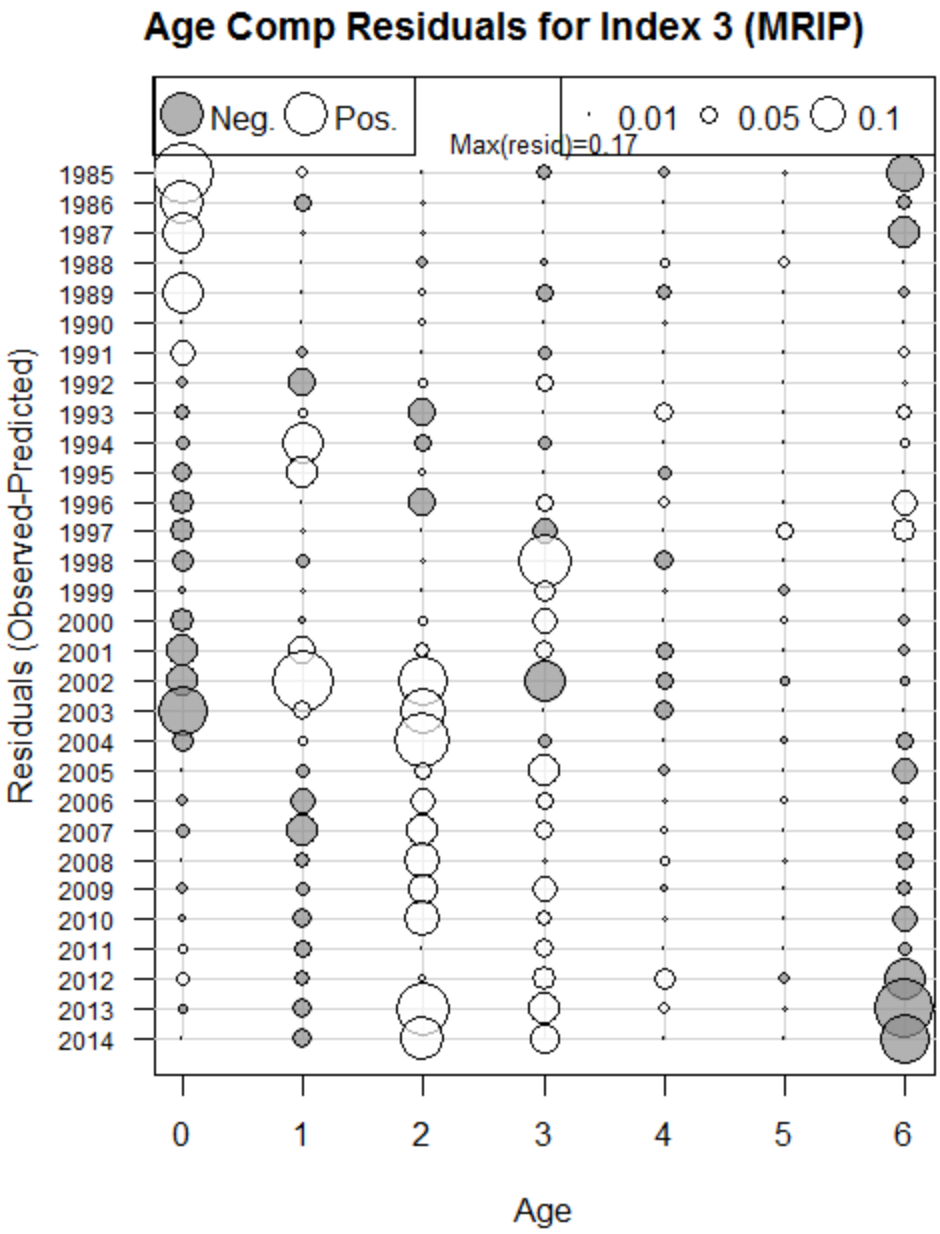

Figure B7.63. Age composition residuals for the MRIP recreational CPUE index.

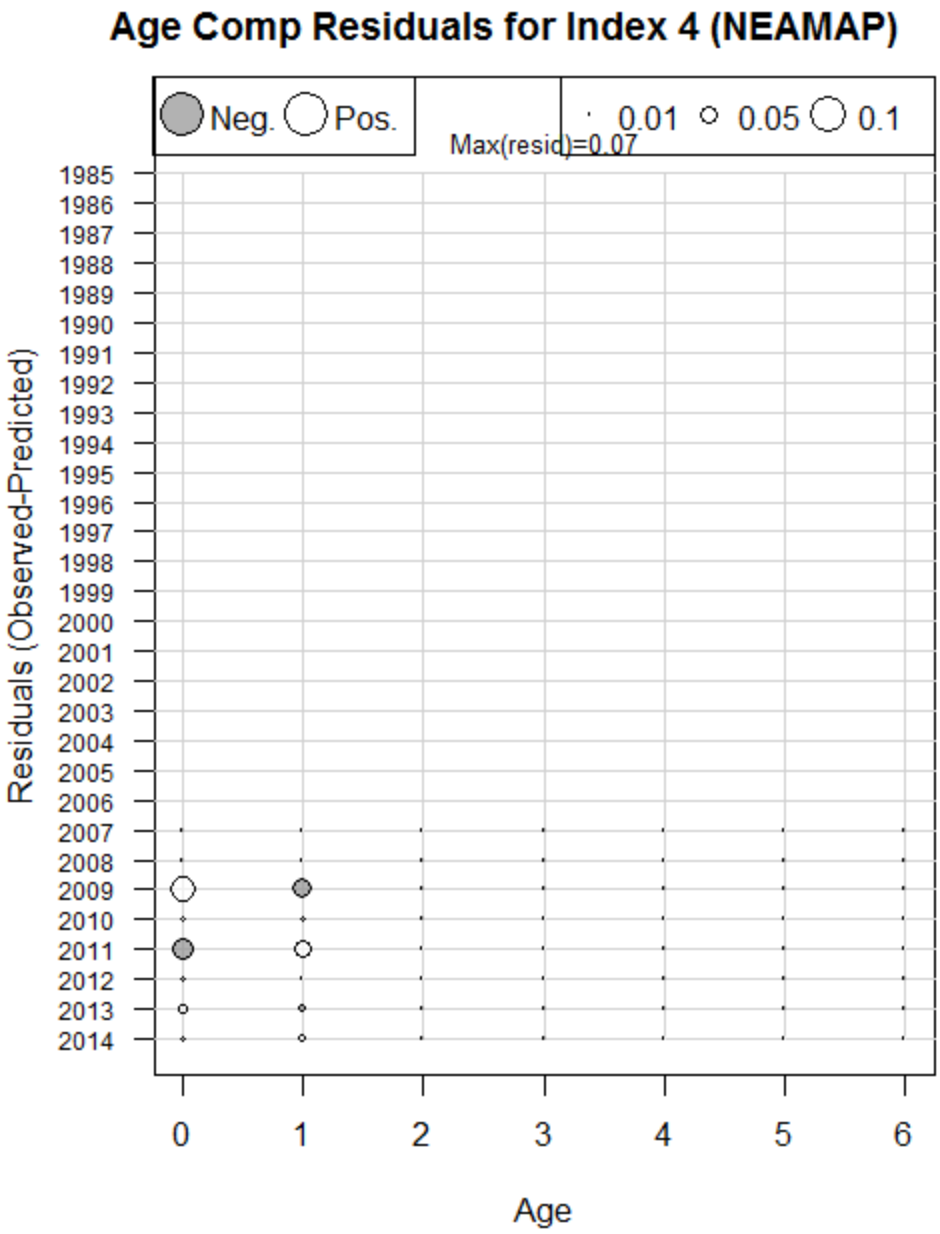

Figure B7.64. Age composition residuals for the NEAMAP survey.

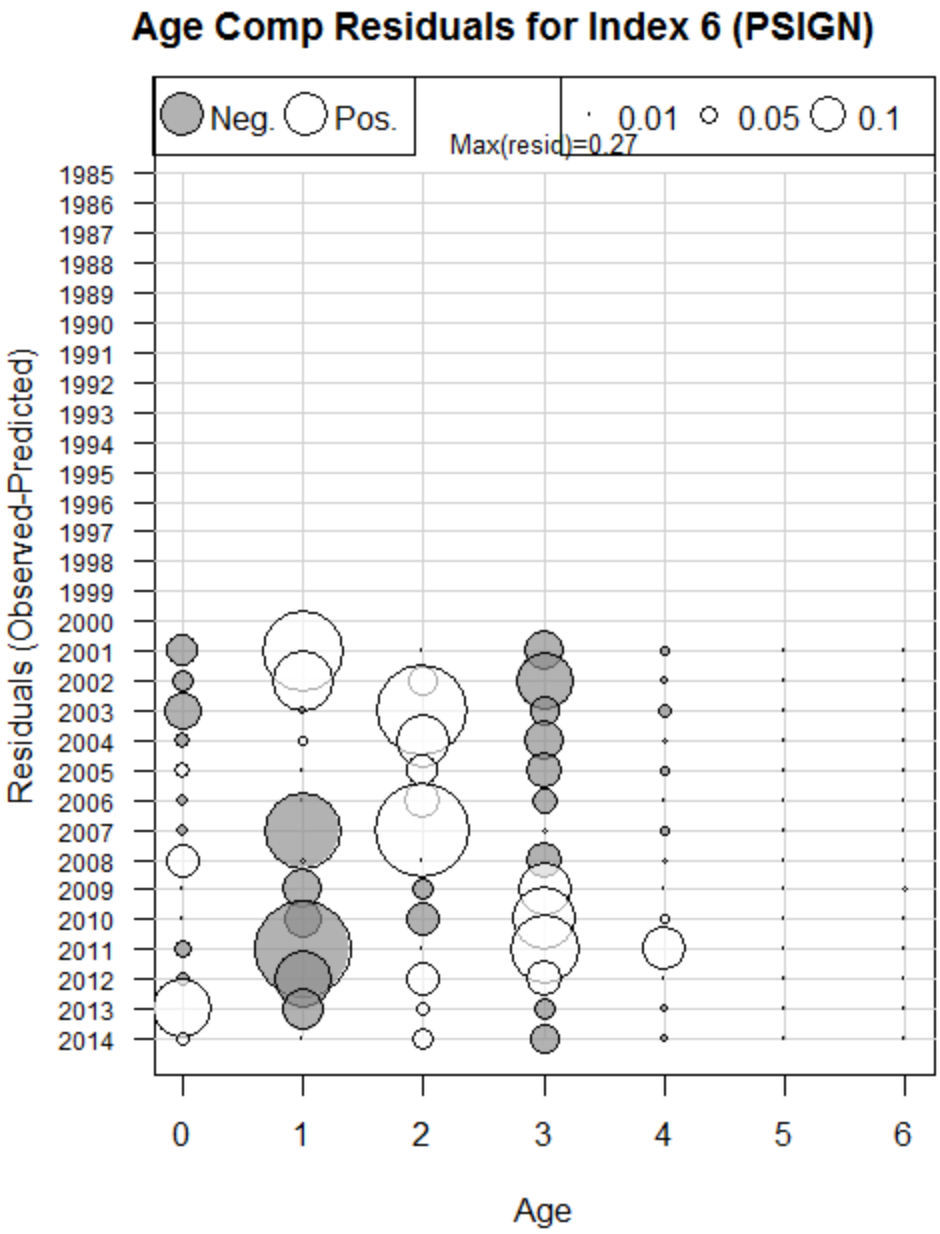

Figure B7.65. Age composition residuals for the PSIGNS gillnet survey.

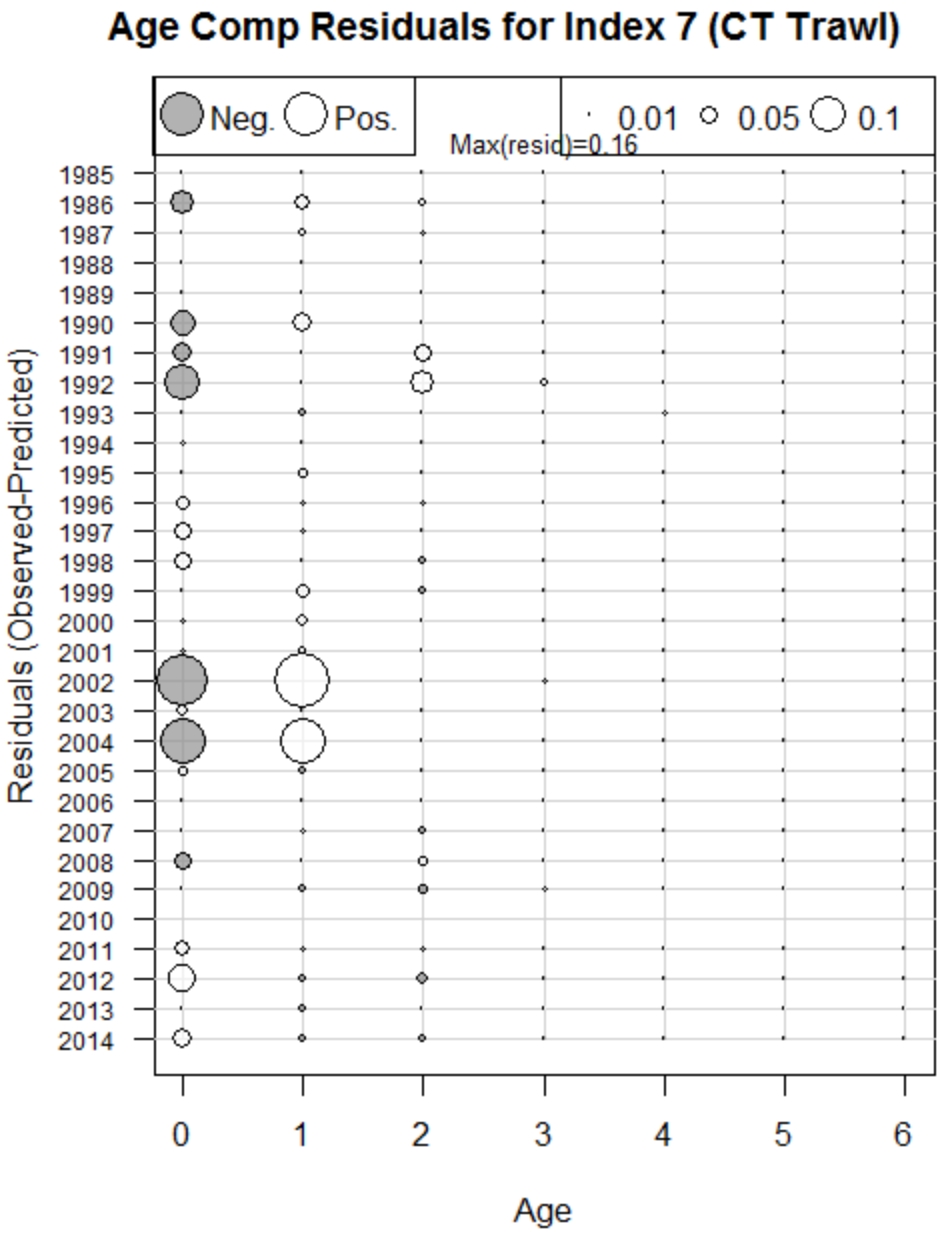

Figure B7.66. Age composition residuals for the CT LISTS trawl survey.

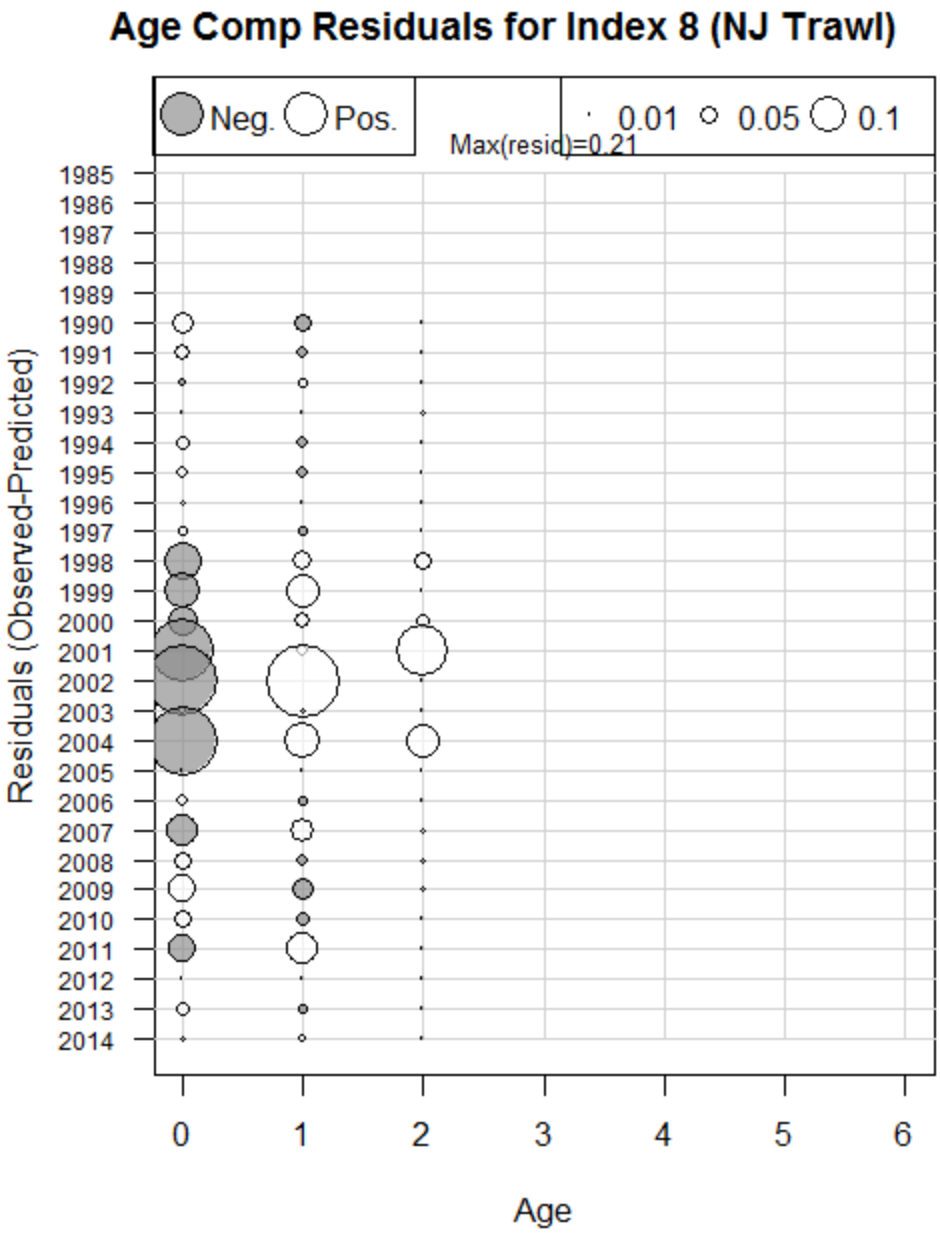

Figure B7.67. Age composition residuals for the NJ ocean trawl survey.

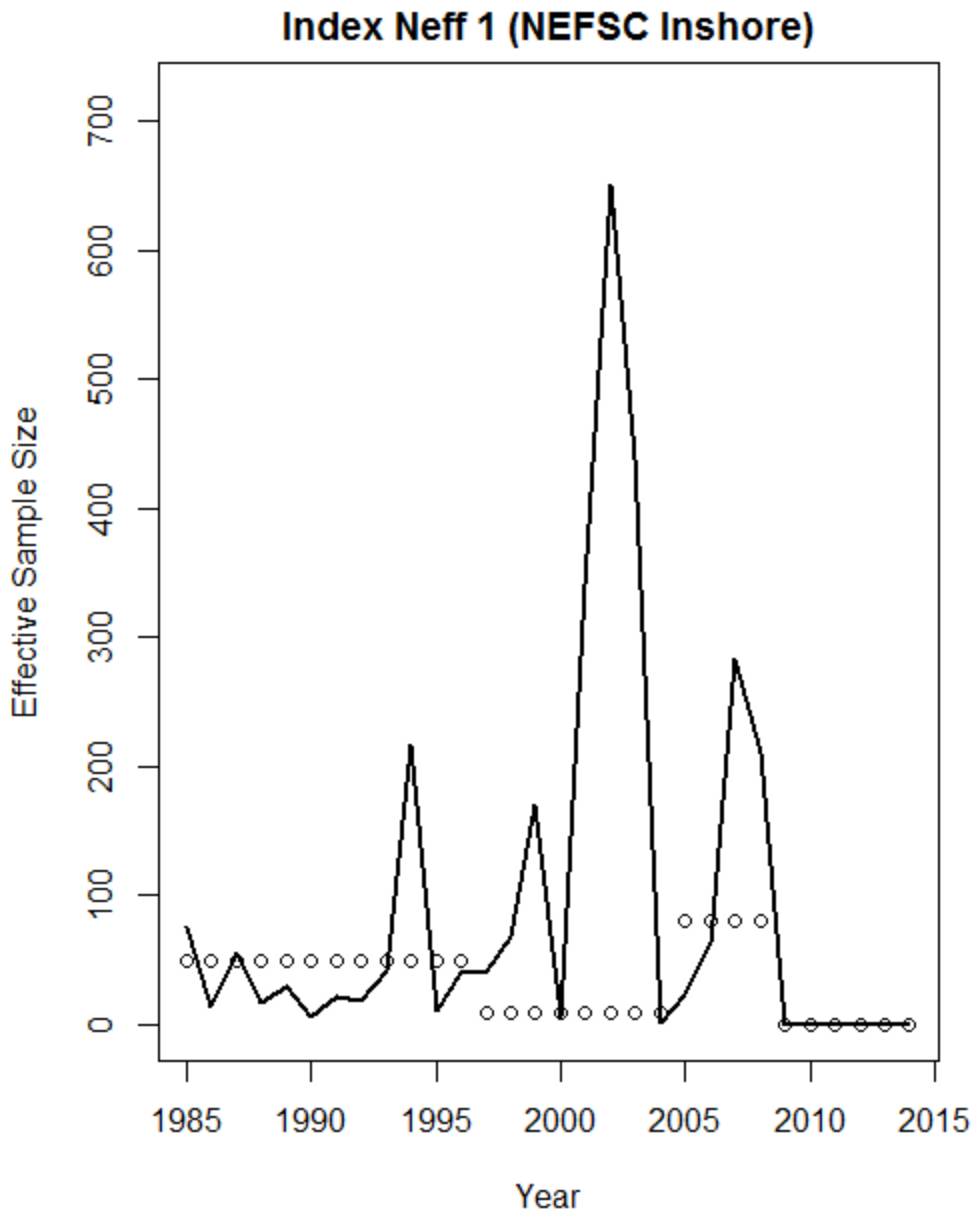

Figure B7.68. Input and estimated effective sample size for the NEFSC Inshore survey.

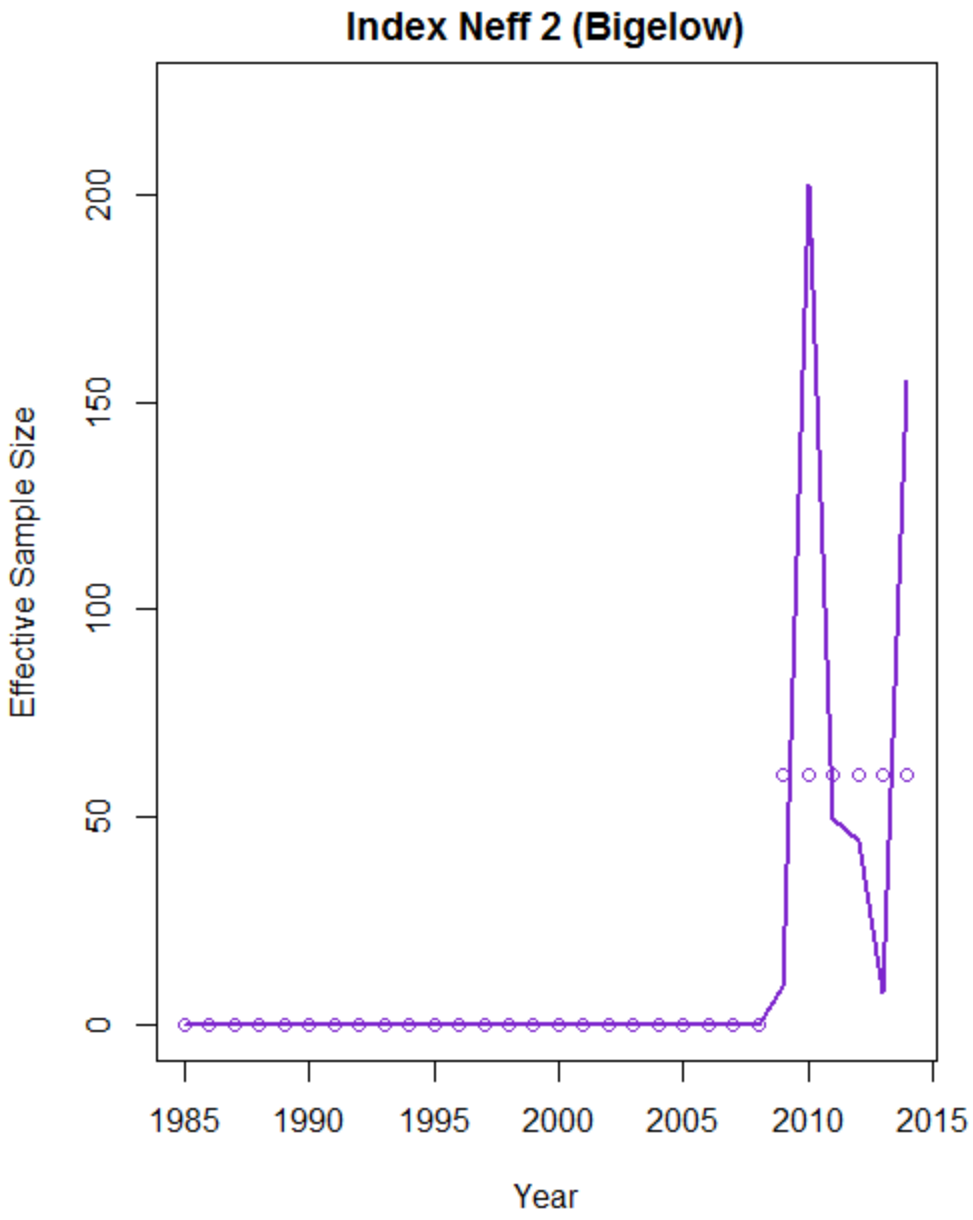

Figure B7.69. Input and estimated effective sample size for the NEFSC Bigelow survey.

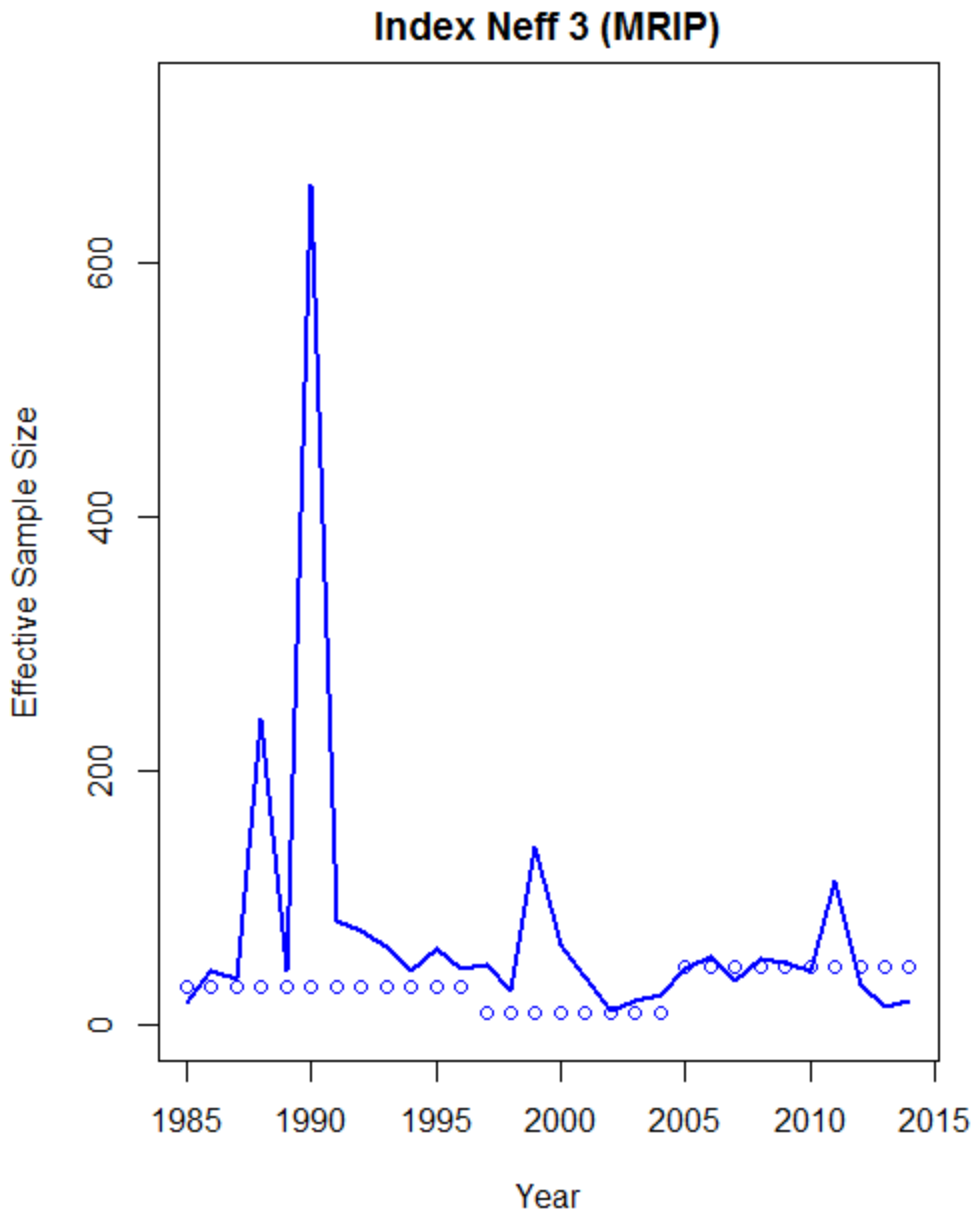

Figure B7.70. Input and estimated effective sample size for the MRIP recreational CPUE index.

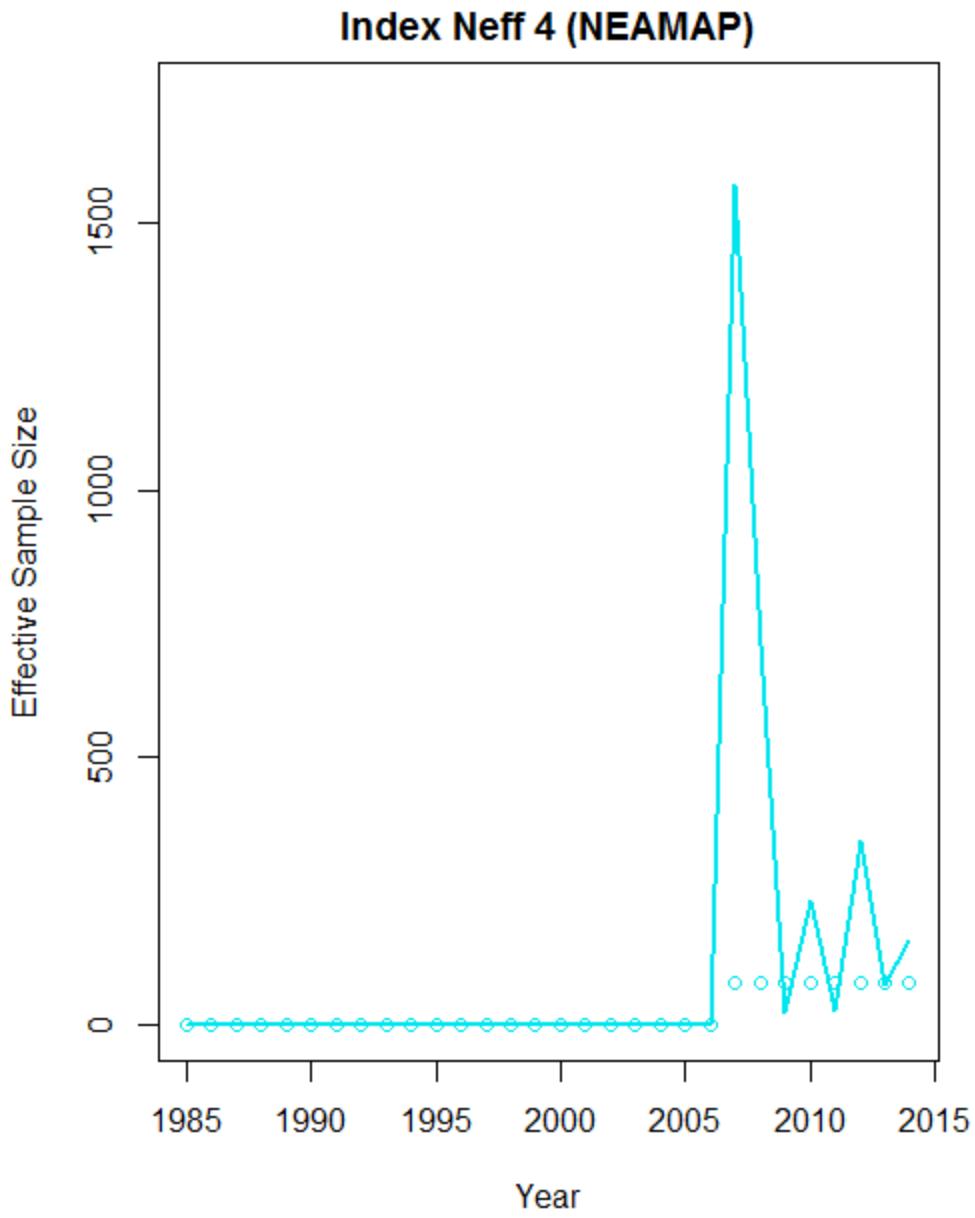

Figure B7.71. Input and estimated effective sample size for the NEAMAP survey.

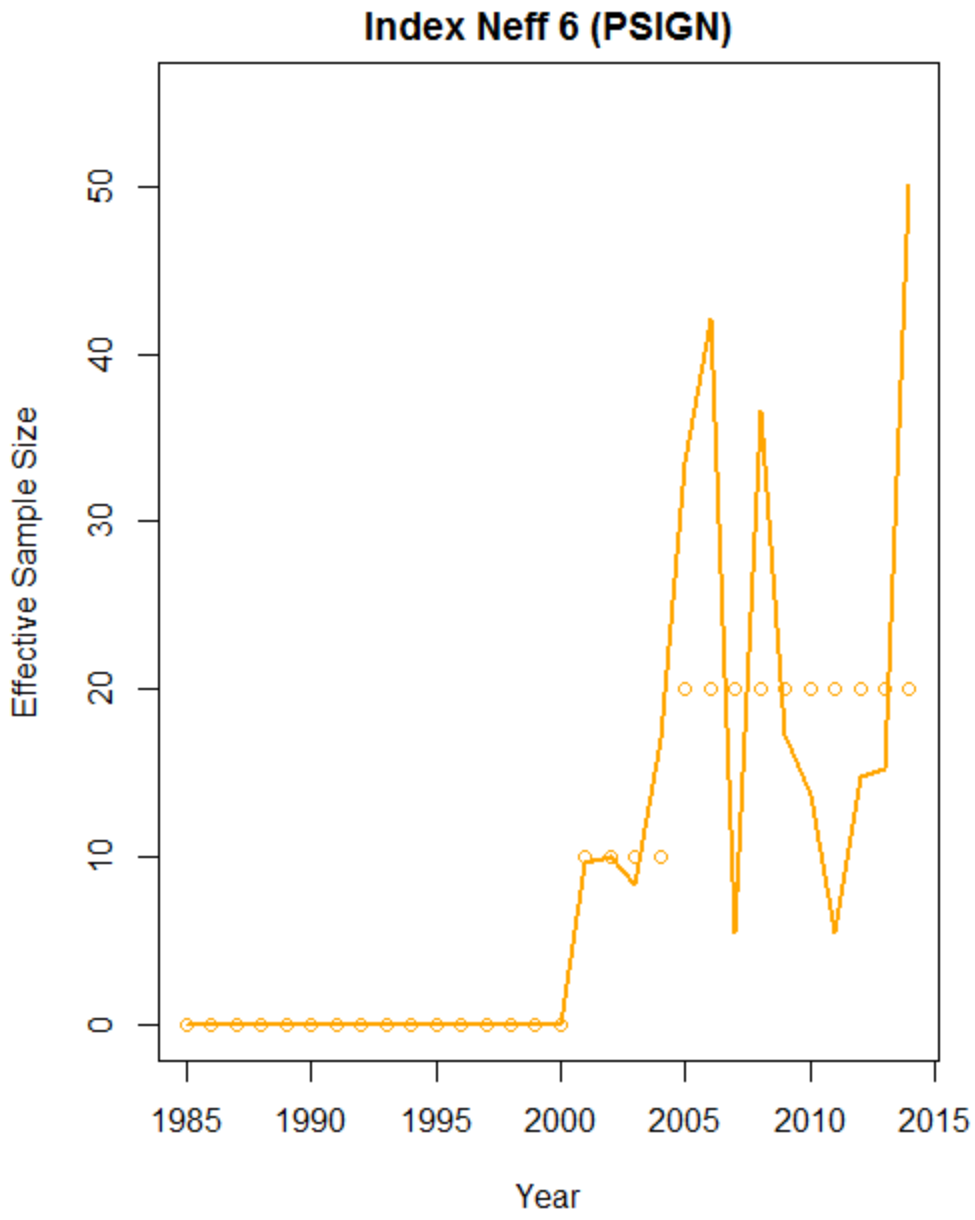

Figure B7.72. Input and estimated effective sample size for the PSIGNS gillnet survey.

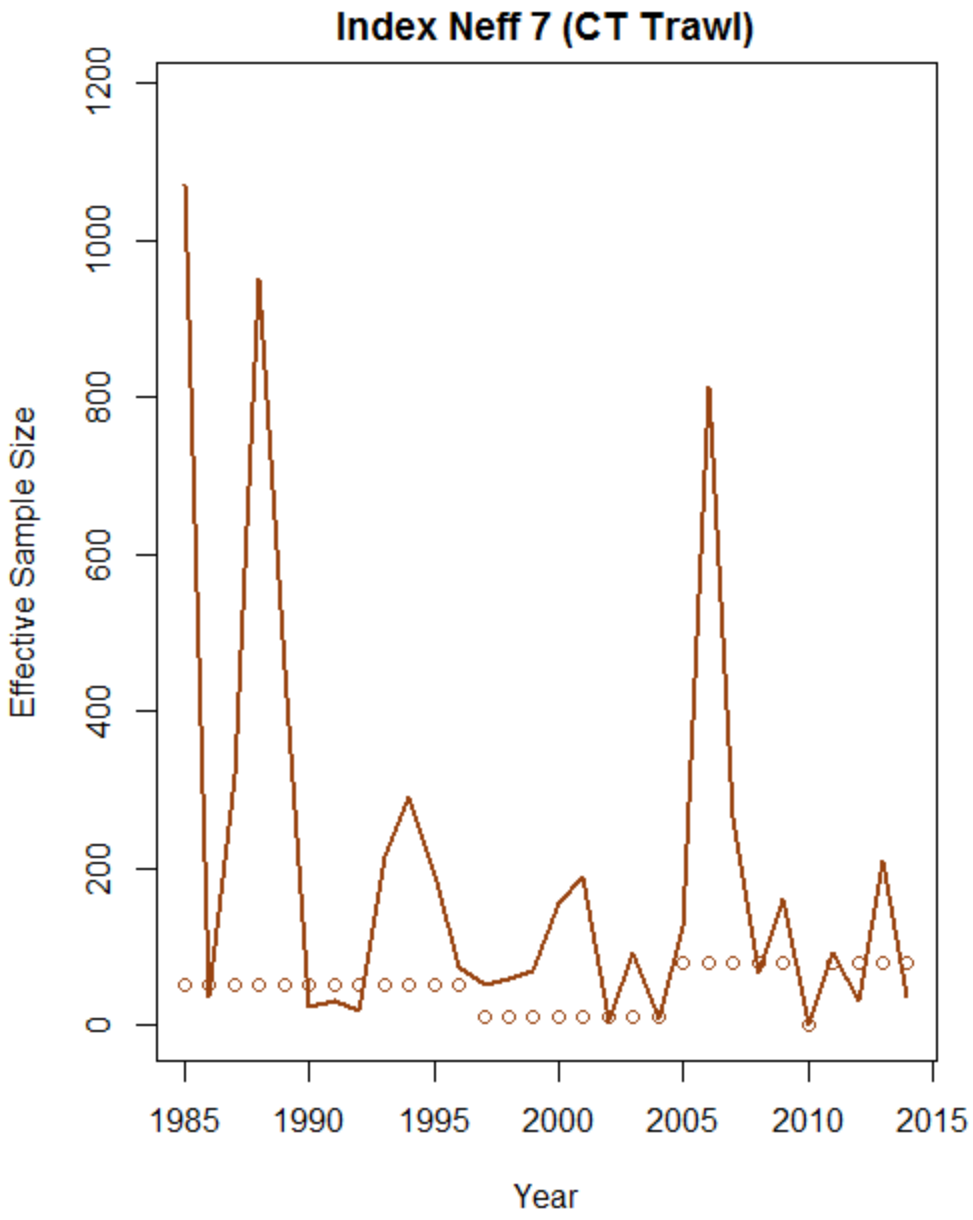

Figure B7.73. Input and estimated effective sample size for the CT LISTS trawl survey.

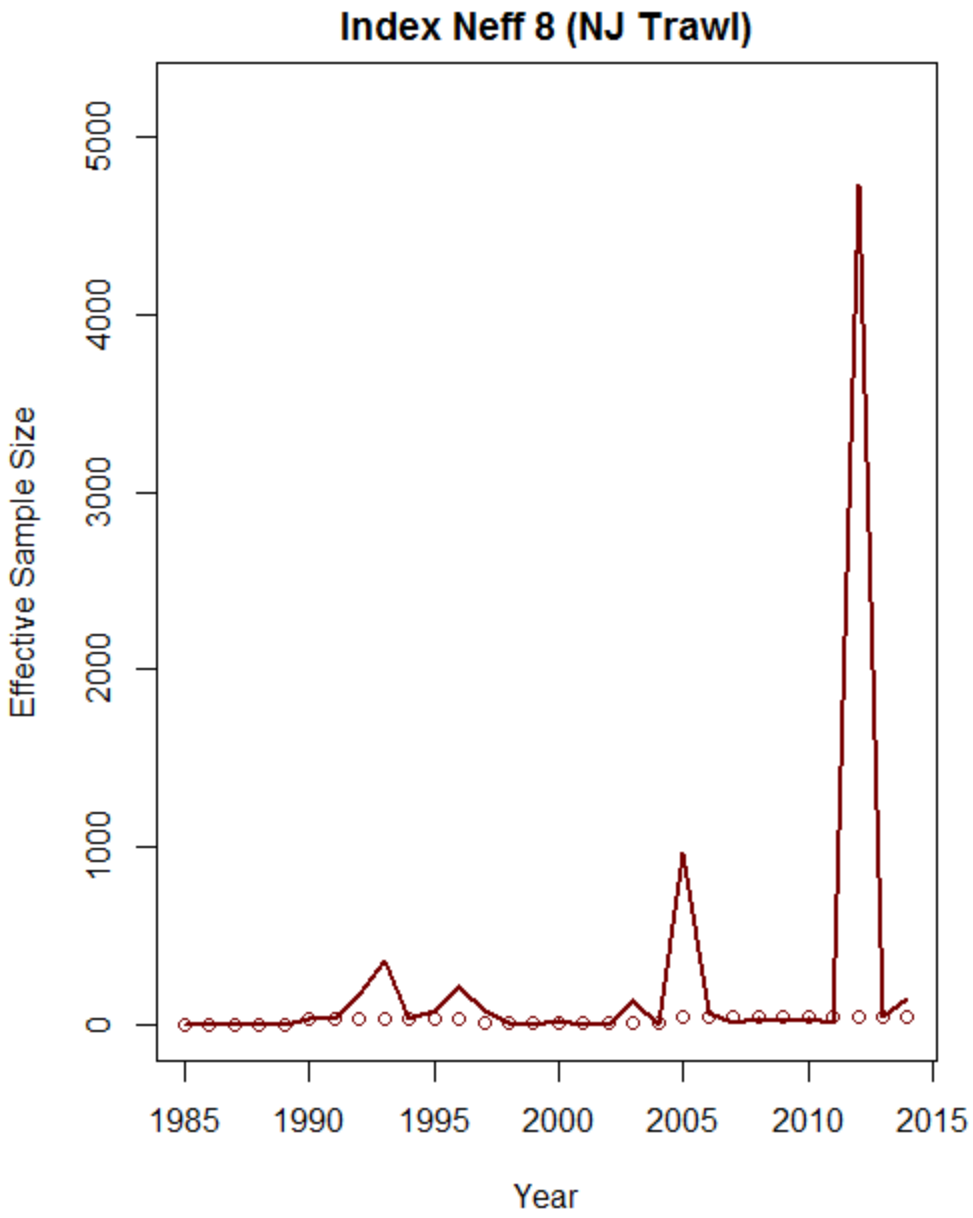

Figure B7.74. Input and estimated effective sample size for the NJ ocean trawl survey.

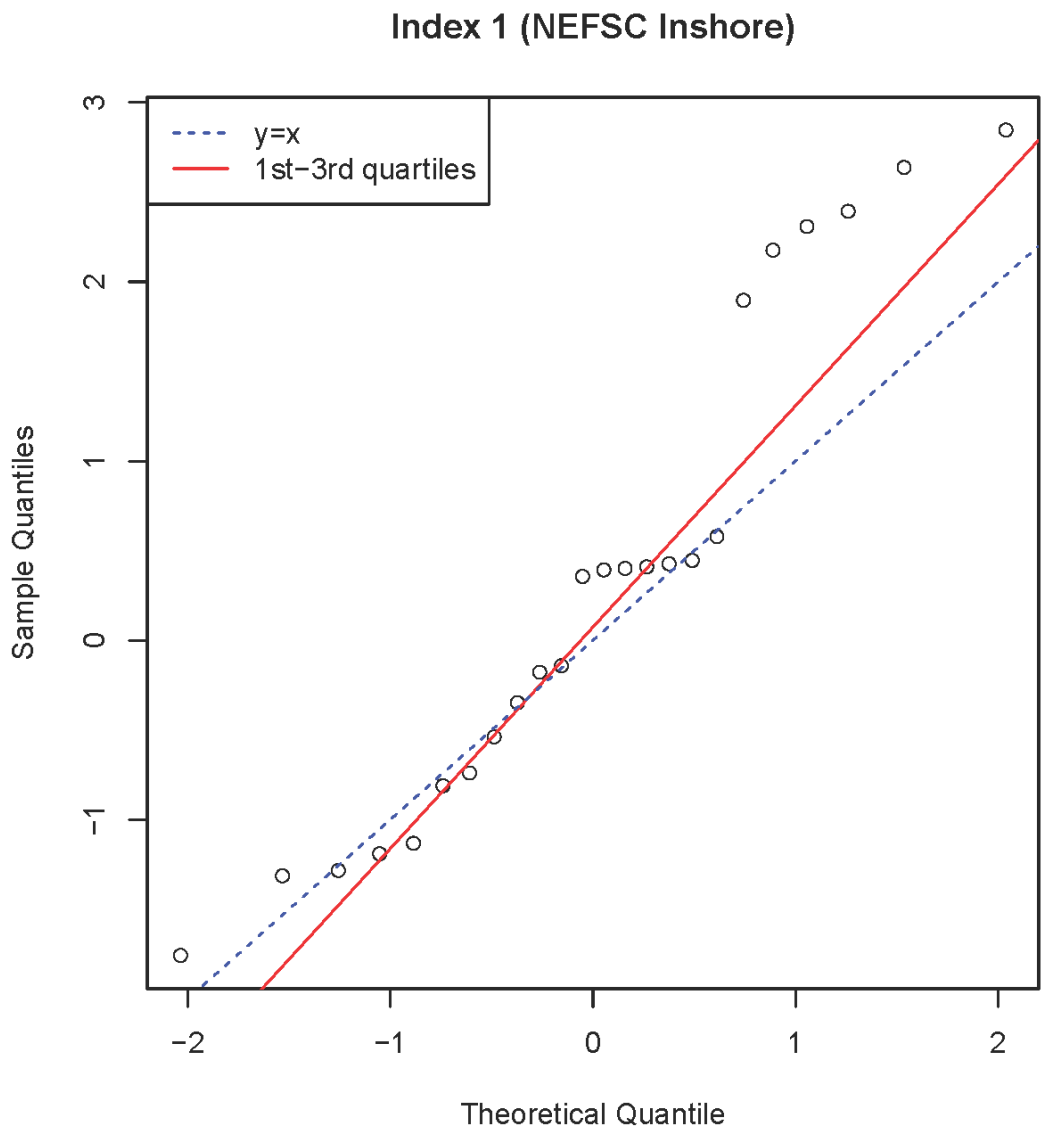

Figure B7.75. QQ-plot for the observed versus predicted mean catch for the NEFSC Inshore survey.

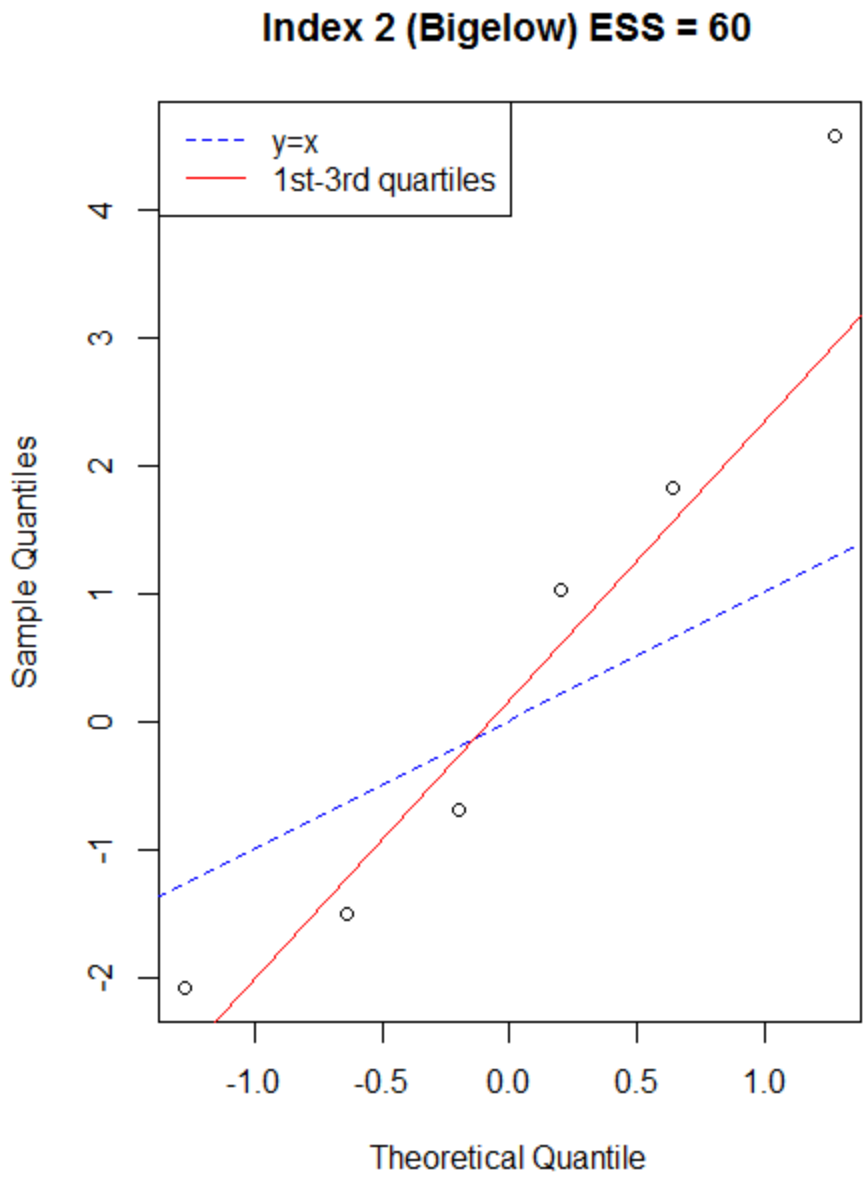

Figure B7.76. QQ-plot for the observed versus predicted mean catch for the NEFSC Bigelow survey.

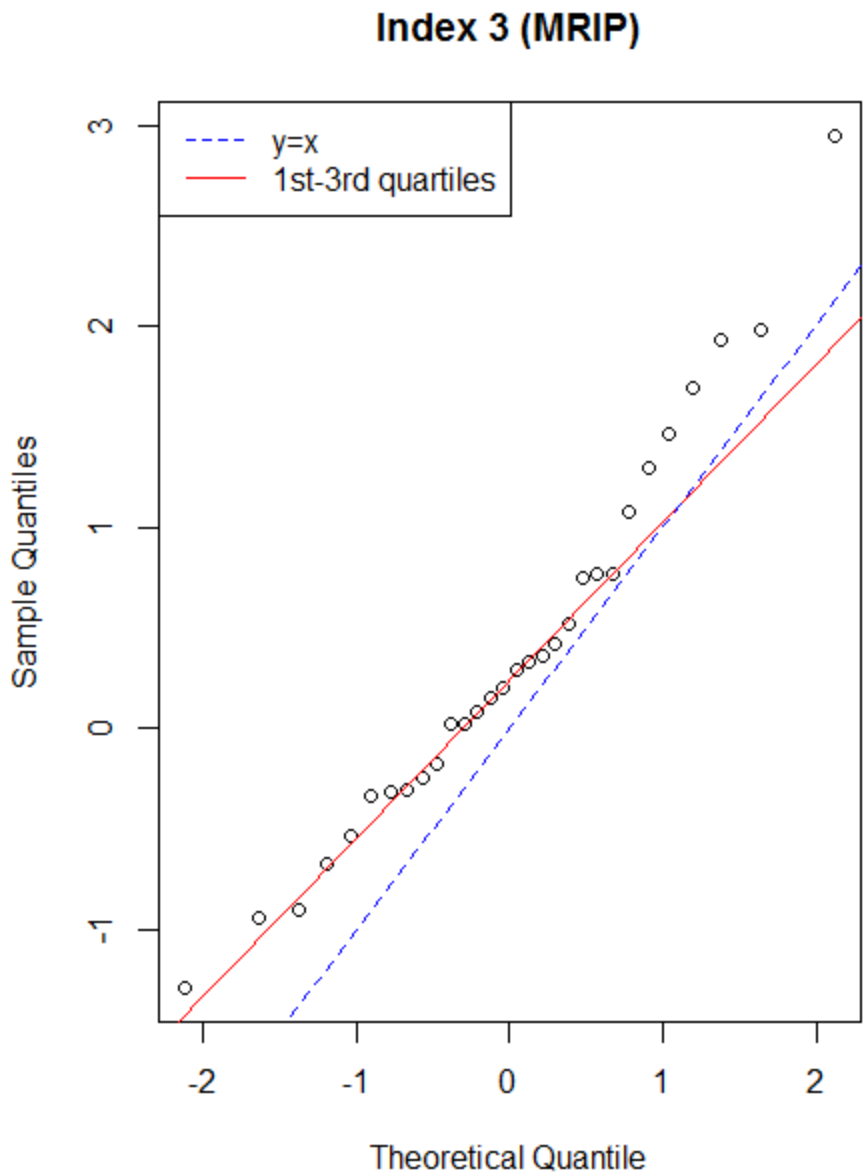

Figure B7.77. QQ-plot for the observed versus predicted mean catch for the MRIP recreational CPUE index.

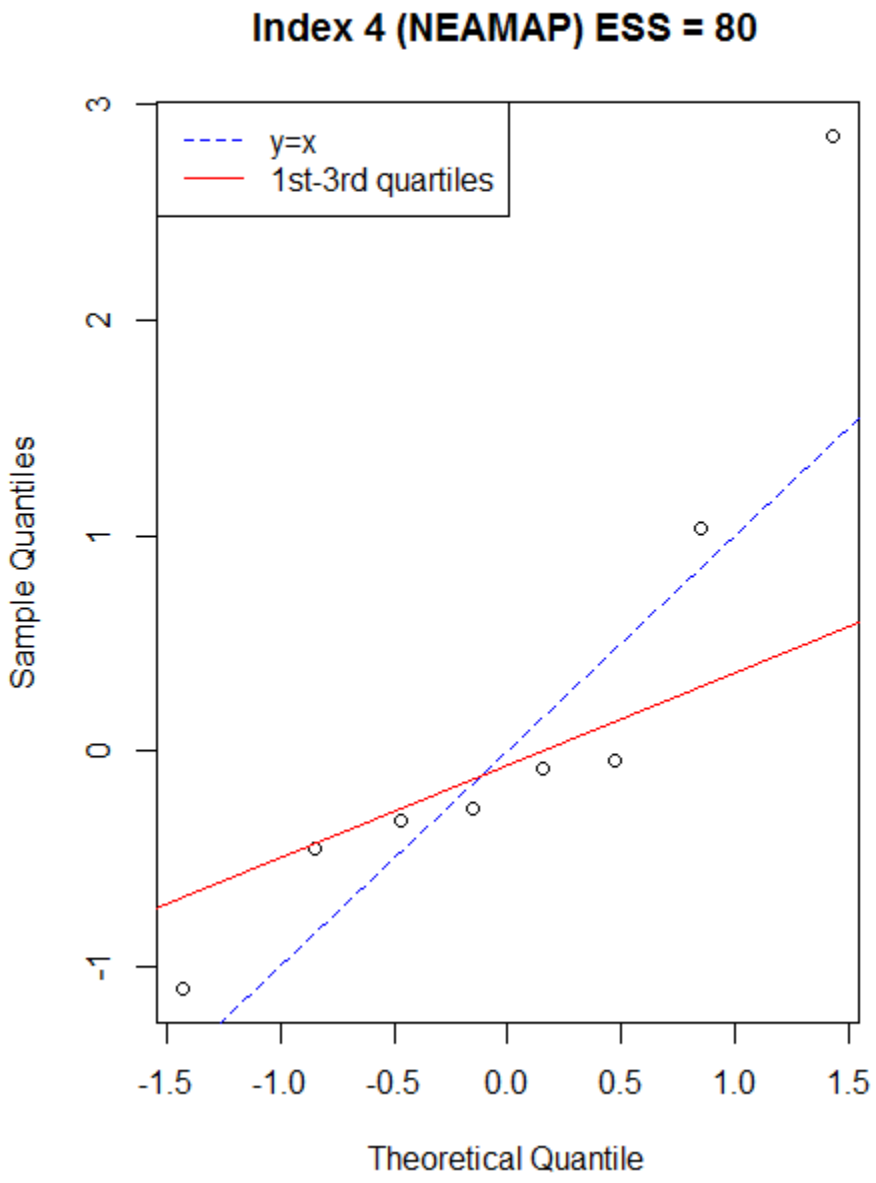

Figure B7.78. QQ-plot for the observed versus predicted mean catch for the NEAMAP survey.

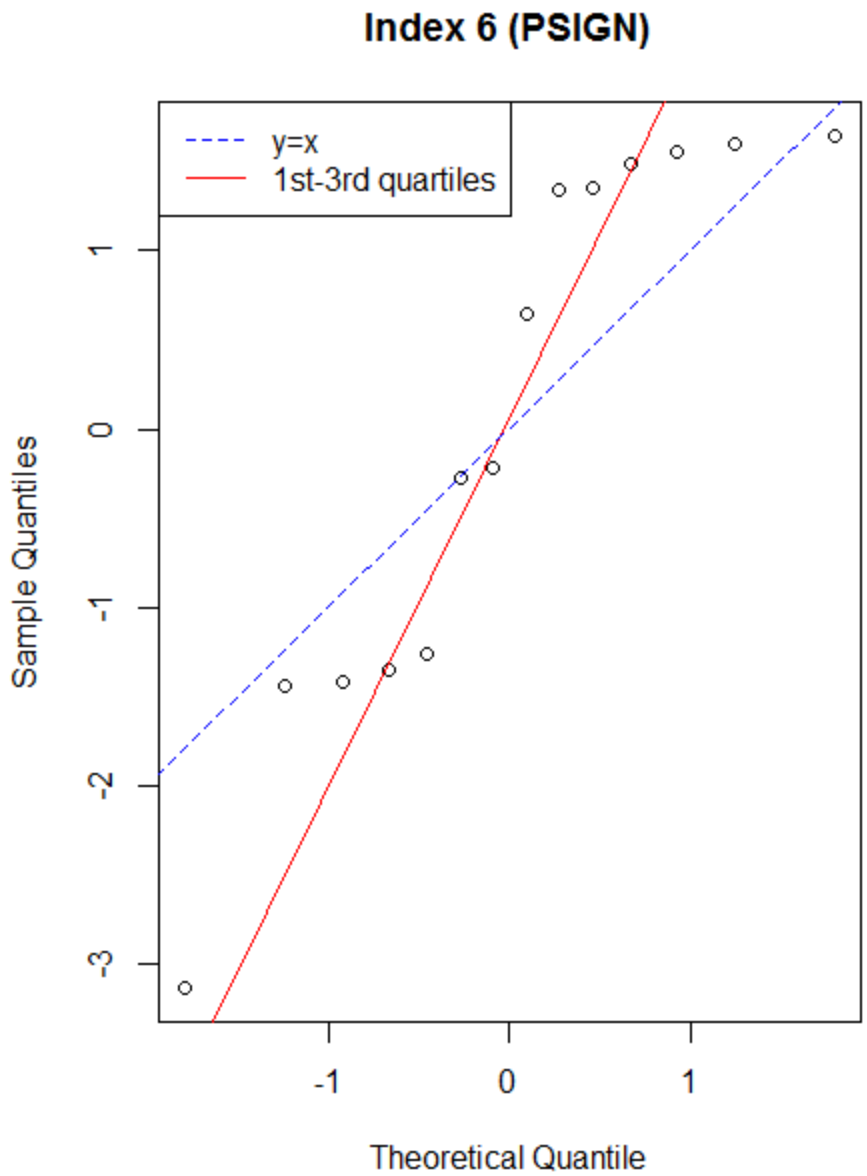

Figure B7.79. QQ-plot for the observed versus predicted mean catch for the PSIGNS gillnet survey.

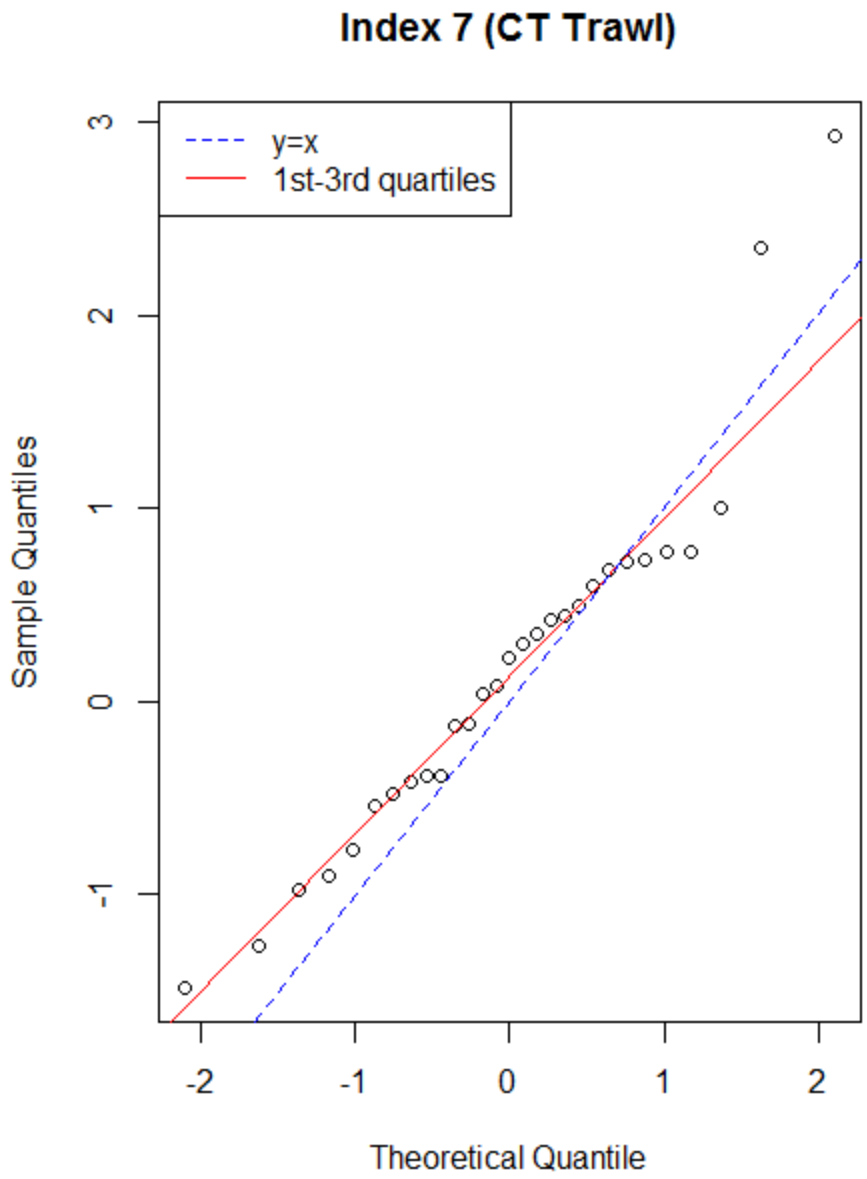

Figure B7.80. QQ-plot for the observed versus predicted mean catch for the CT LISTS trawl survey.

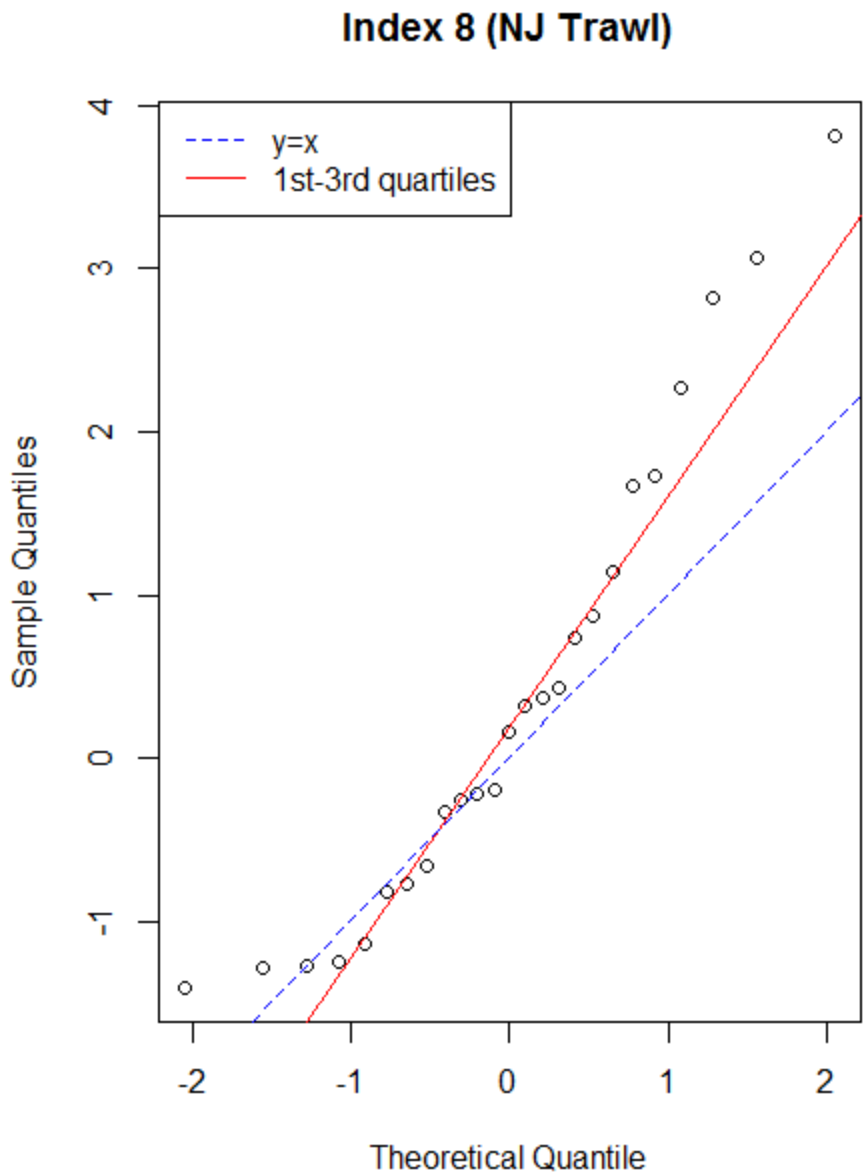

Figure B7.81. QQ-plot for the observed versus predicted mean catch for the NJ ocean trawl survey.

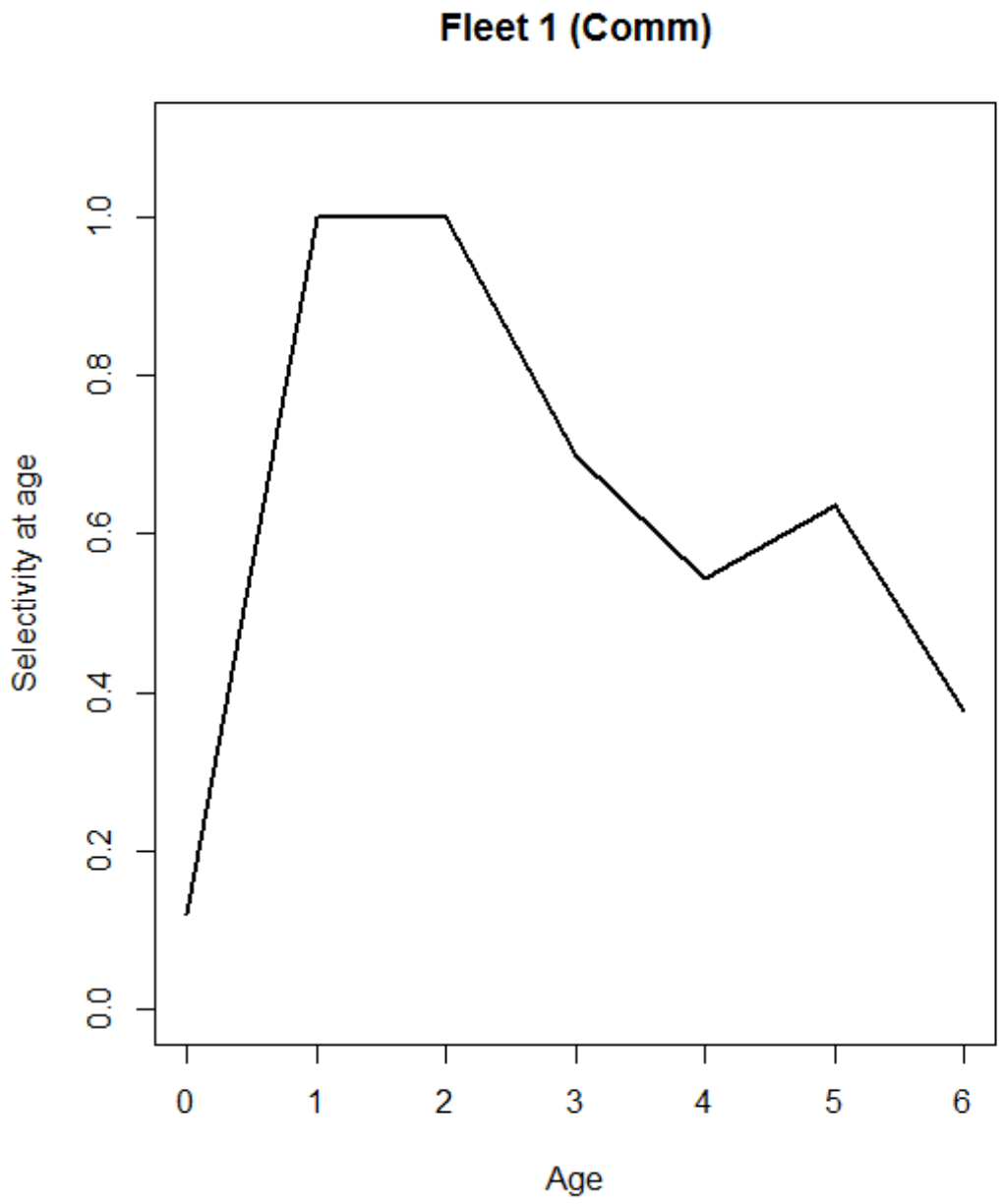

Figure B7.82. Estimated selectivity for the commercial fleet from the final model

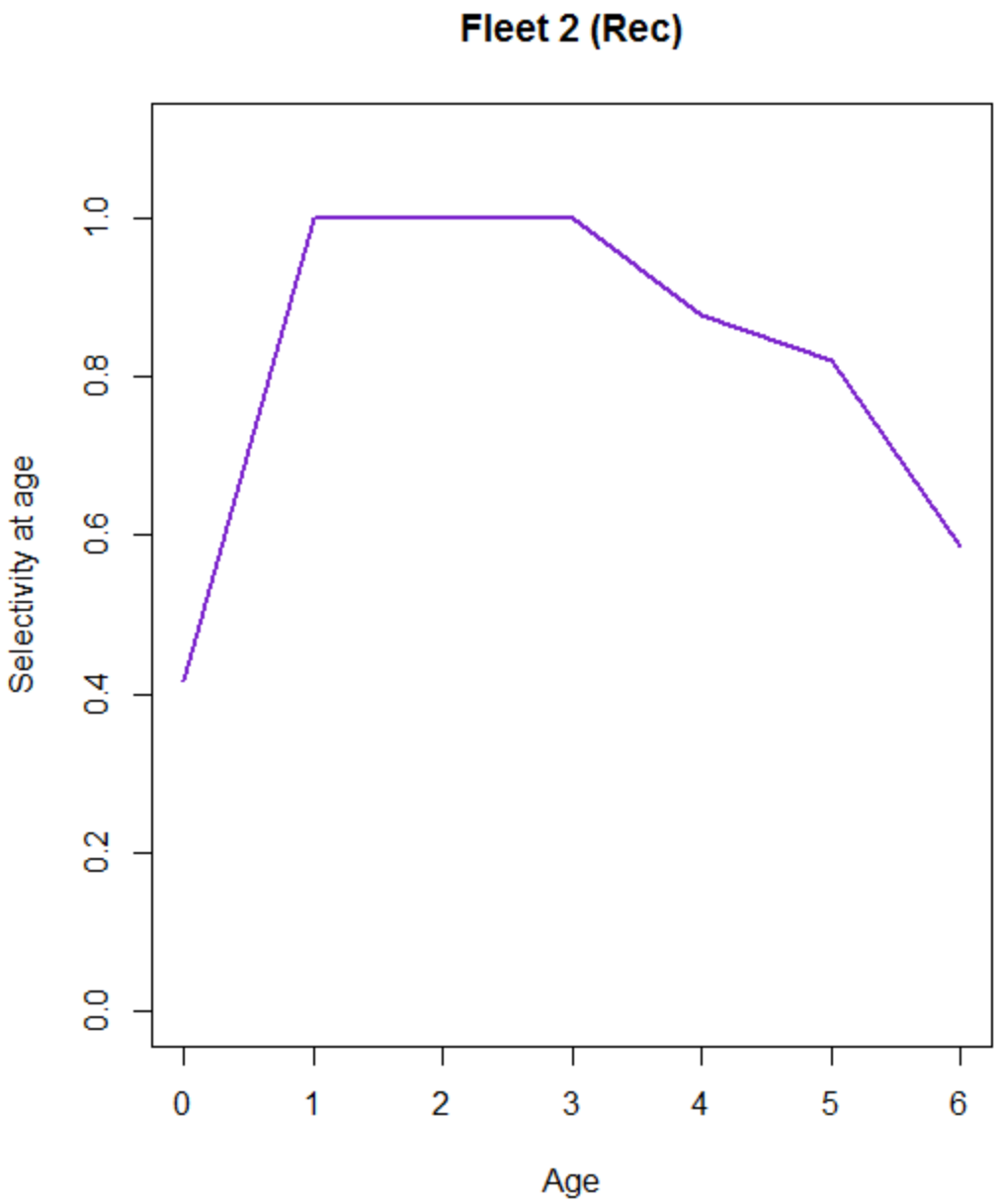

Figure B7.83. Estimated selectivity for the recreational fleet from the final model.

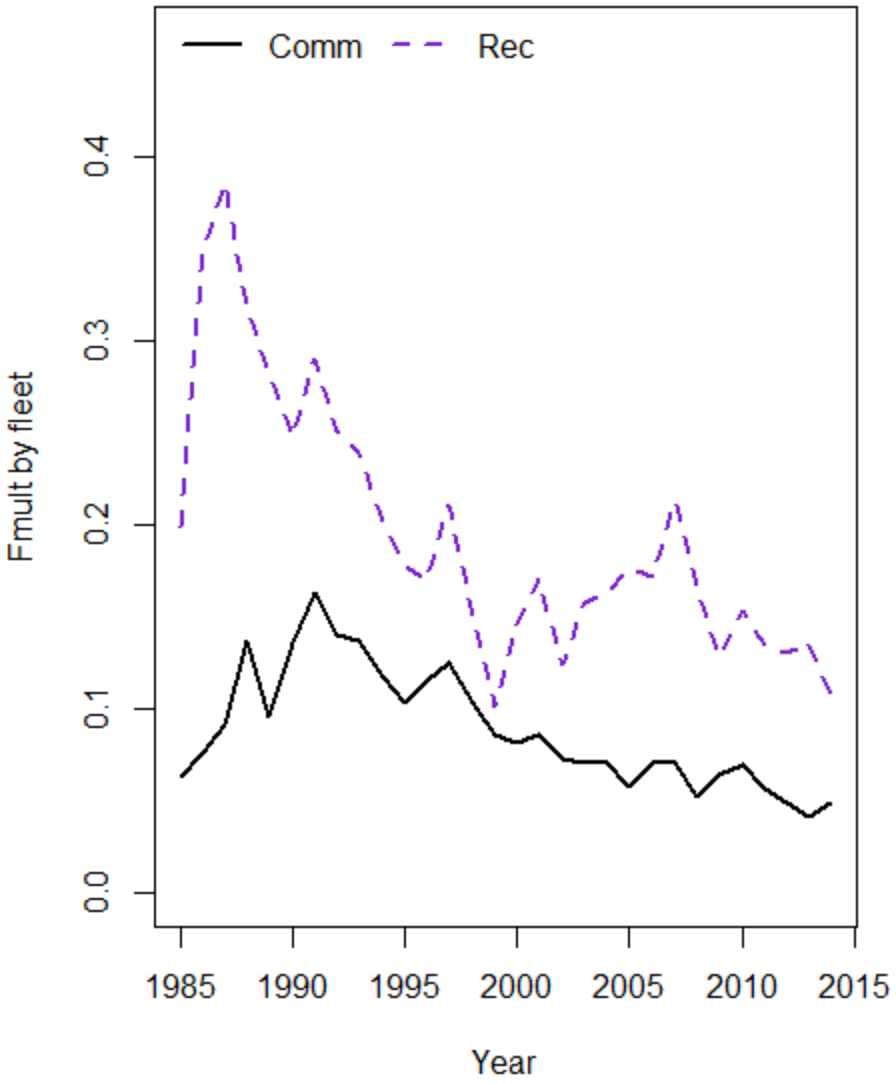

Figure B7.84. Full F (F_{mult}) estimates for the commercial (fleet 1) and recreational (fleet 2) fleets.

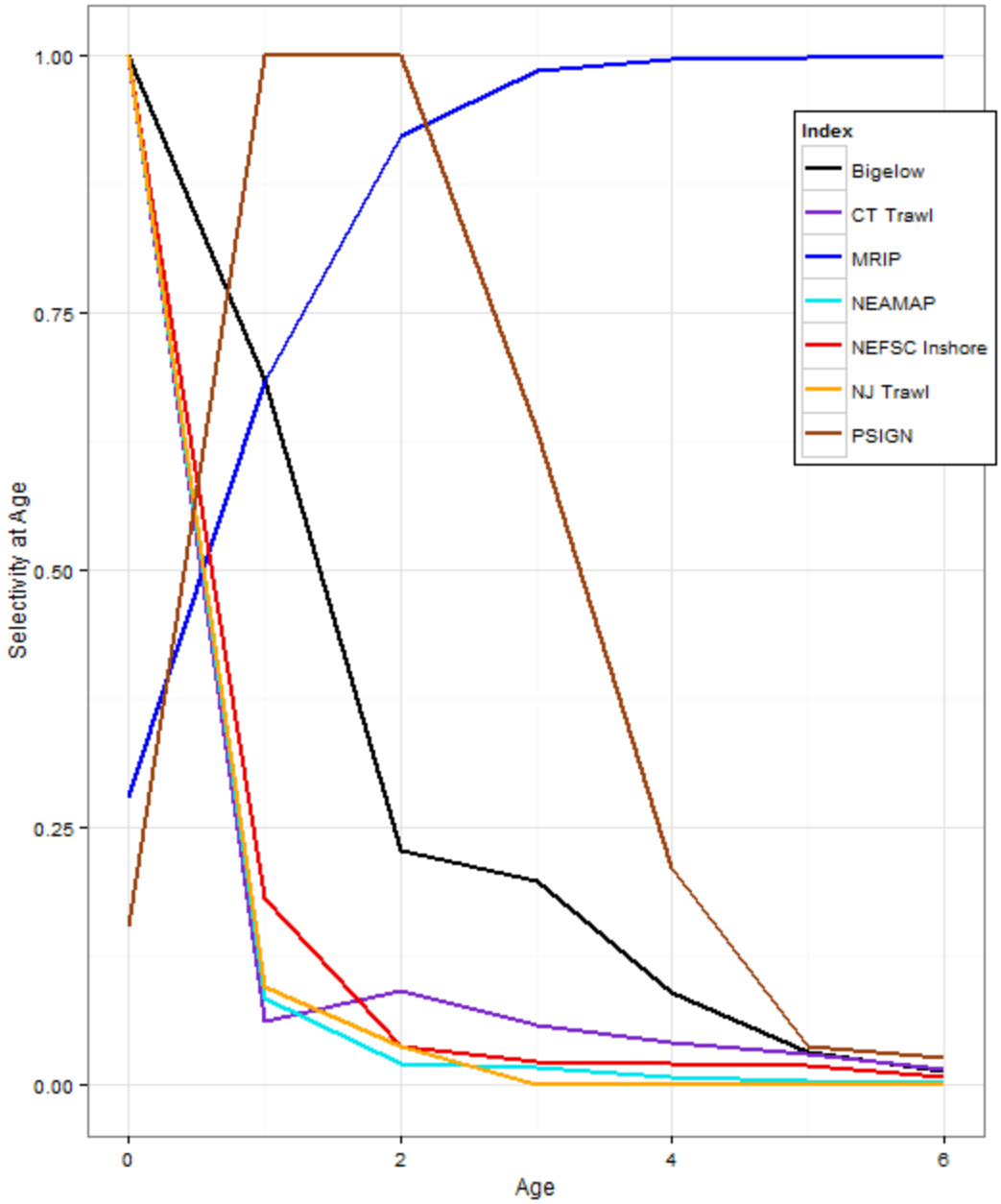

Figure B7.85. Estimated selectivities for the indices from the final model. Note the two age 0 indices are not plotted so only 7 selectivities are shown.

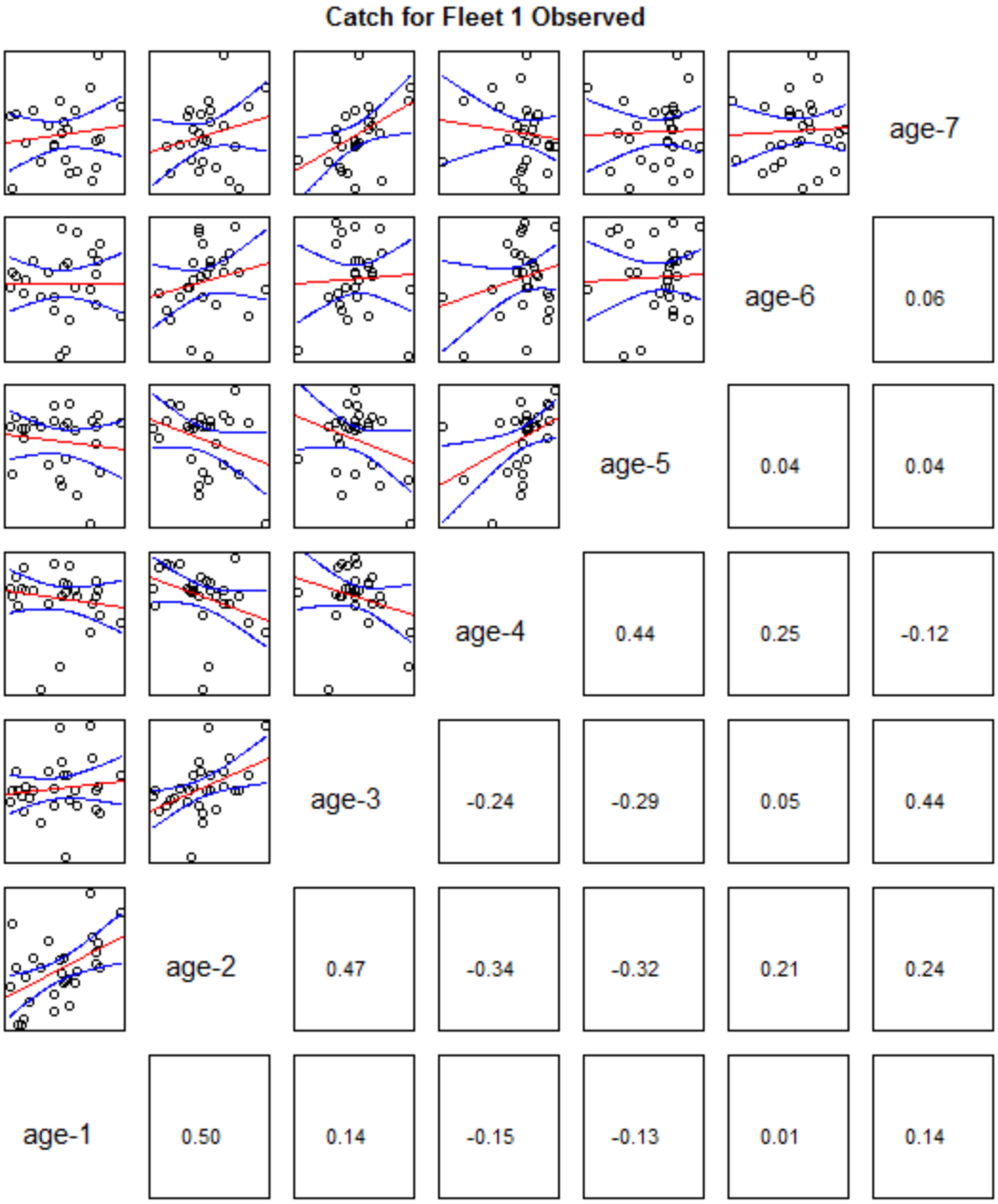

Figure B7.86. Observed catch for the commercial fleet. Note that age class labels are 1 greater than the modeled age class, so that "age-1" corresponds to age 0, "age-2" corresponds to age 1, etc.

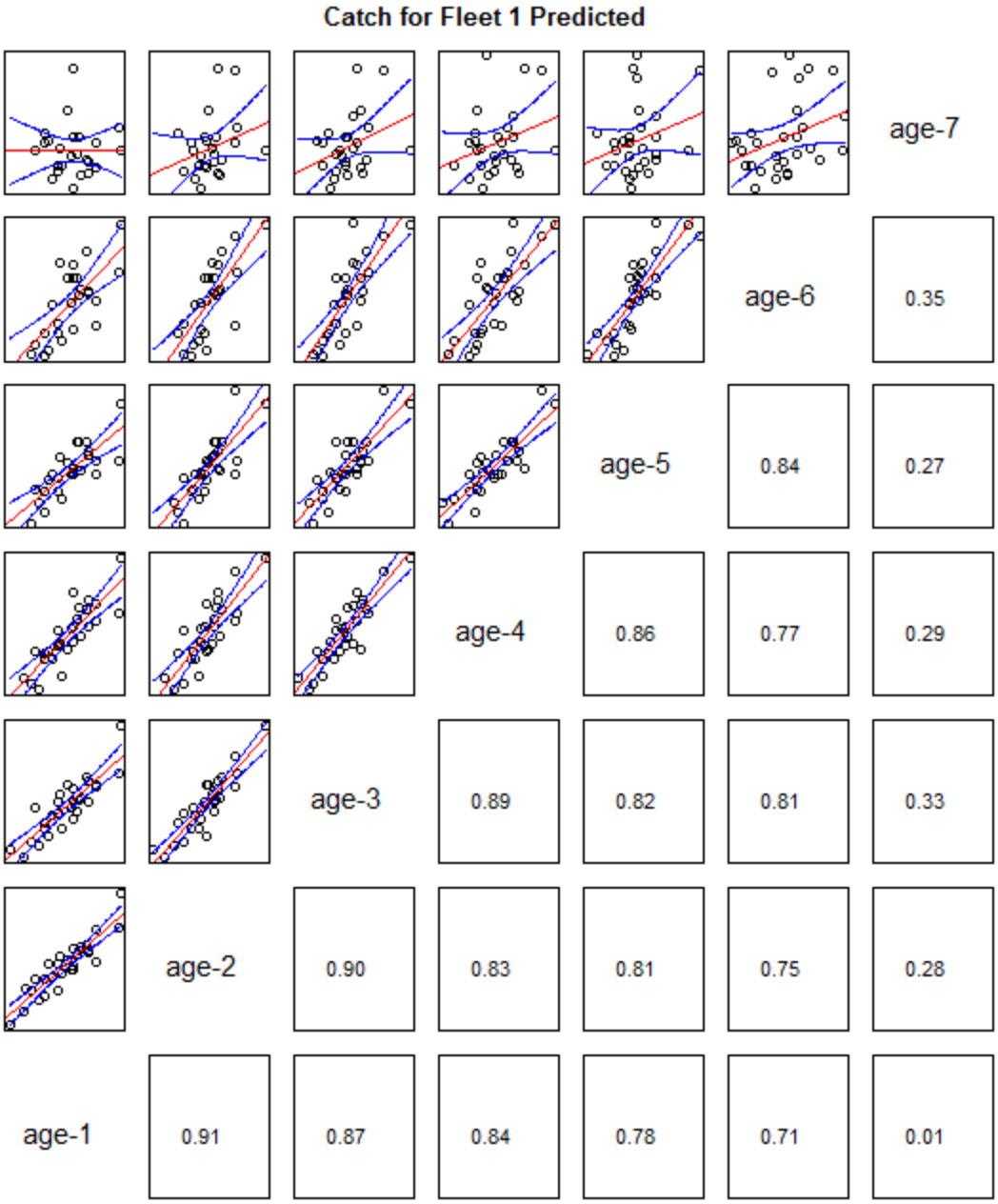

Figure B7.87. Predicted catch for the commercial fleet.
Note that age class labels are 1 greater than the modeled age class, so that "age-1" corresponds to age 0, "age-2" corresponds to age 1, etc.

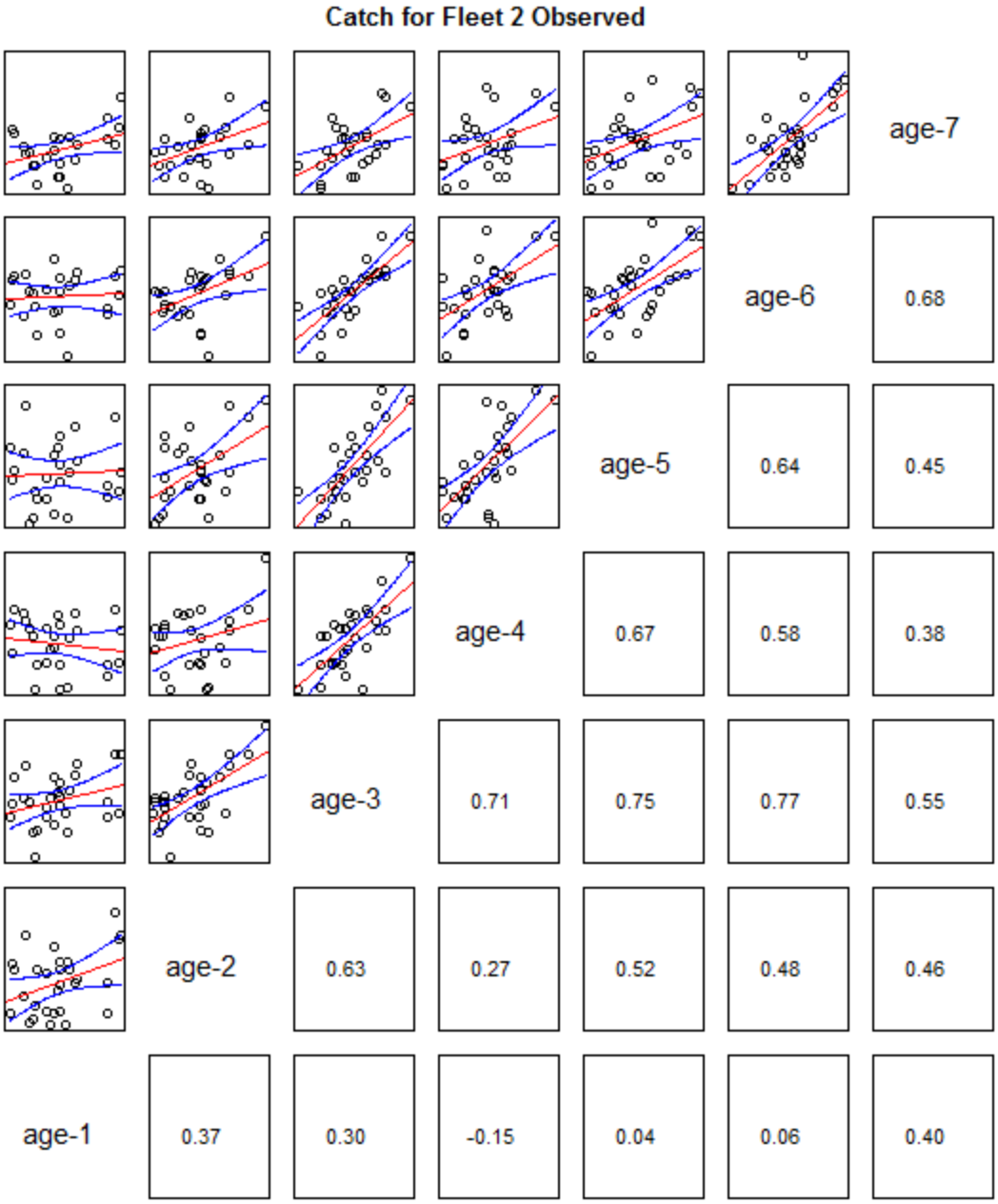

Figure B7.88. Observed catch for the recreational fleet. Note that age class labels are 1 greater than the modeled age class, so that "age-1" corresponds to age 0, "age-2" corresponds to age 1, etc.

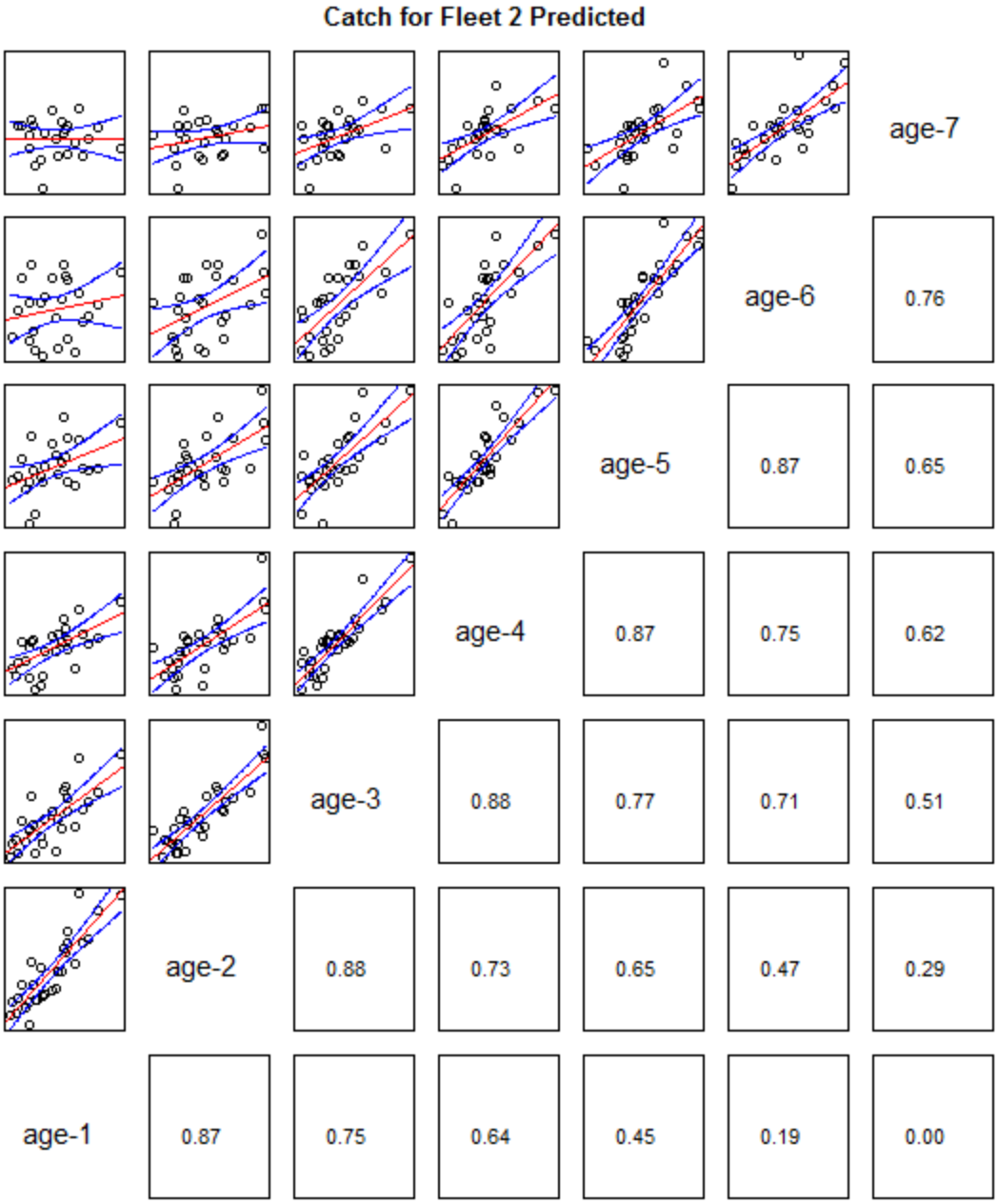

Figure B7.89. Predicted catch for the recreational fleet. Note that age class labels are 1 greater than the modeled age class, so that "age-1" corresponds to age 0, "age-2" corresponds to age 1, etc.

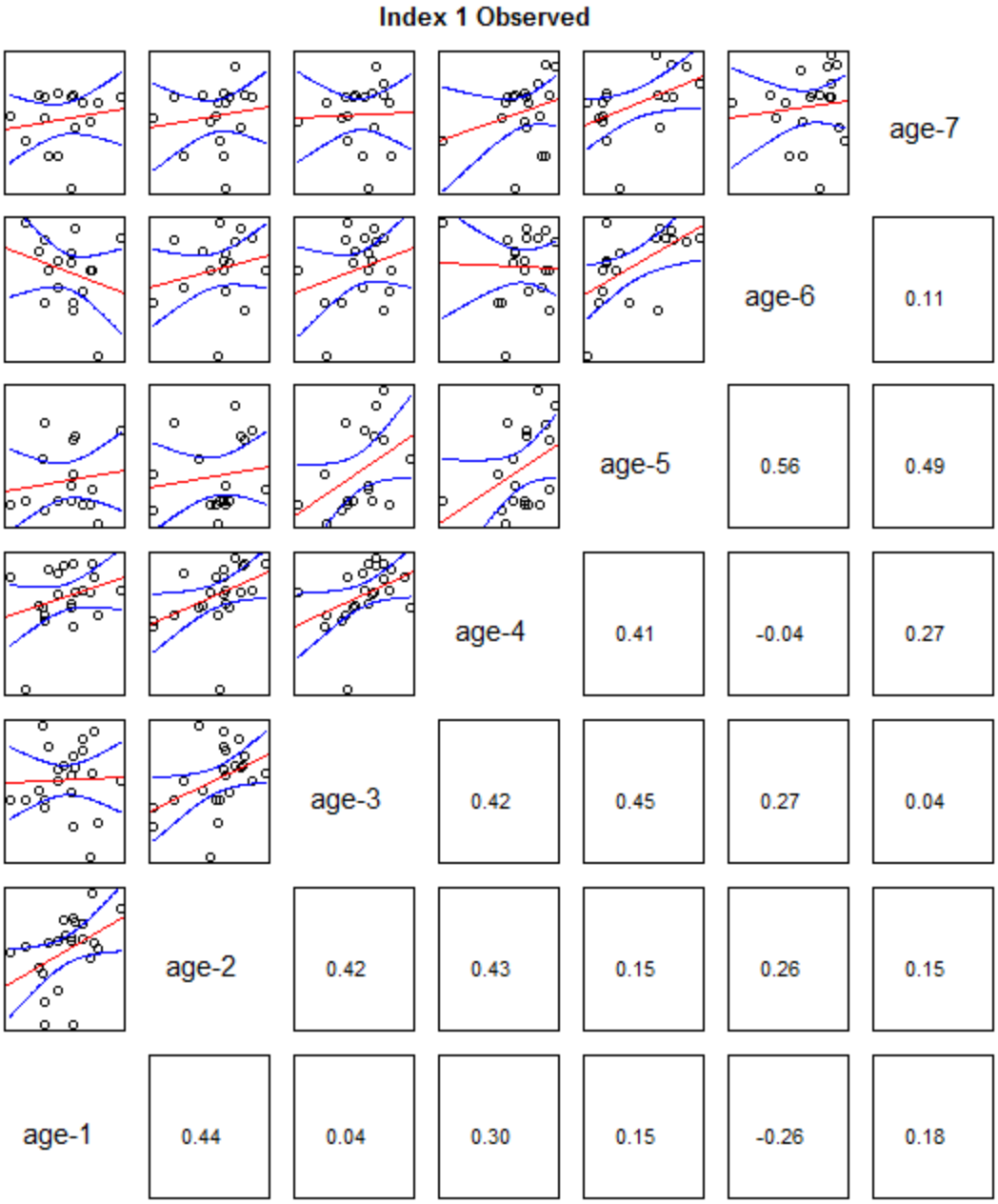

Figure B7.90. Observed catch for the NEFSC Inshore survey. Note that age class labels are 1 greater than the modeled age class, so that "age-1" corresponds to age 0, "age-2" corresponds to age 1, etc.

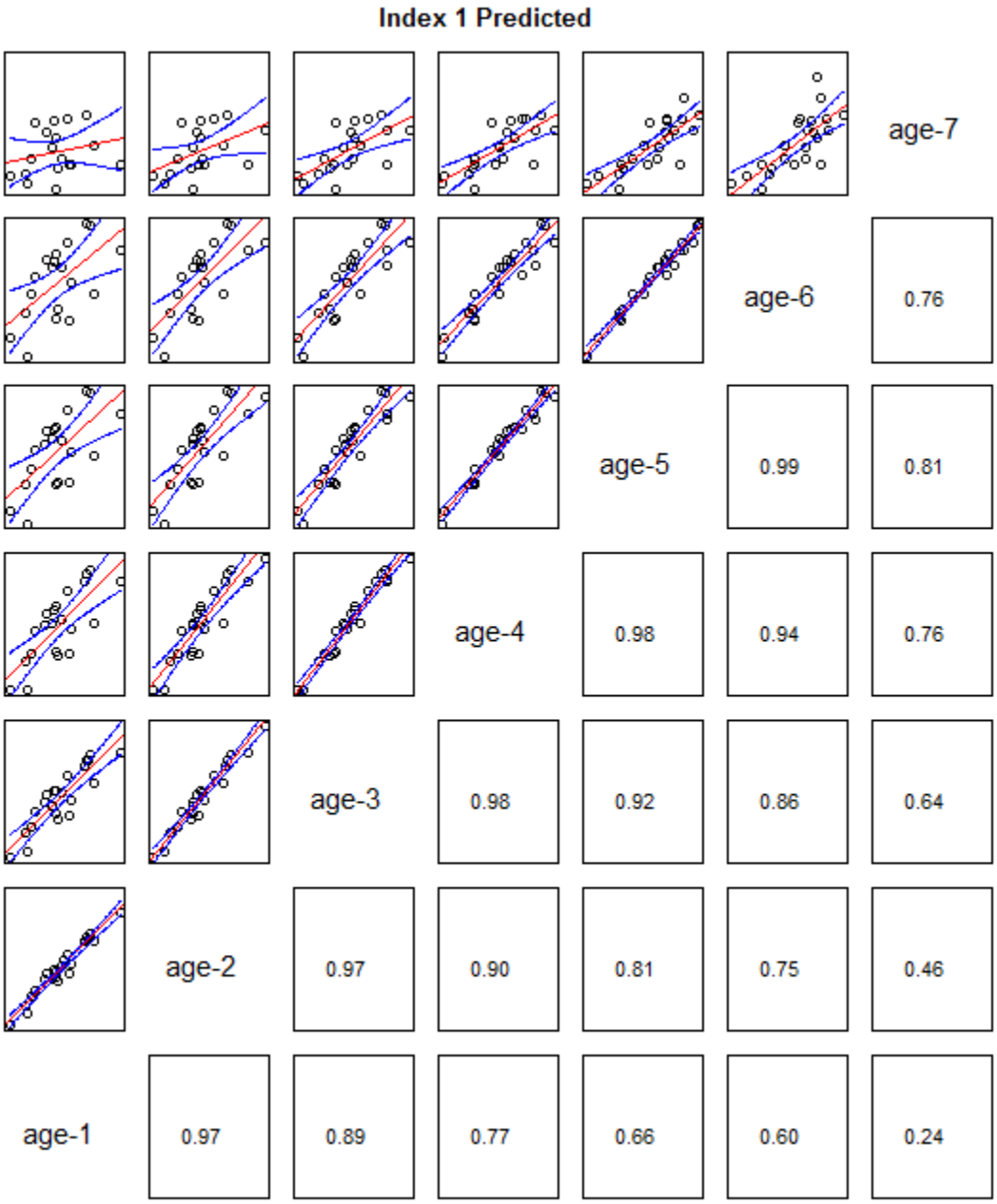

Figure B7.91. Predicted catch for the NEFSC Inshore survey. Note that age class labels are 1 greater than the modeled age class, so that "age-1" corresponds to age 0, "age-2" corresponds to age 1, etc.

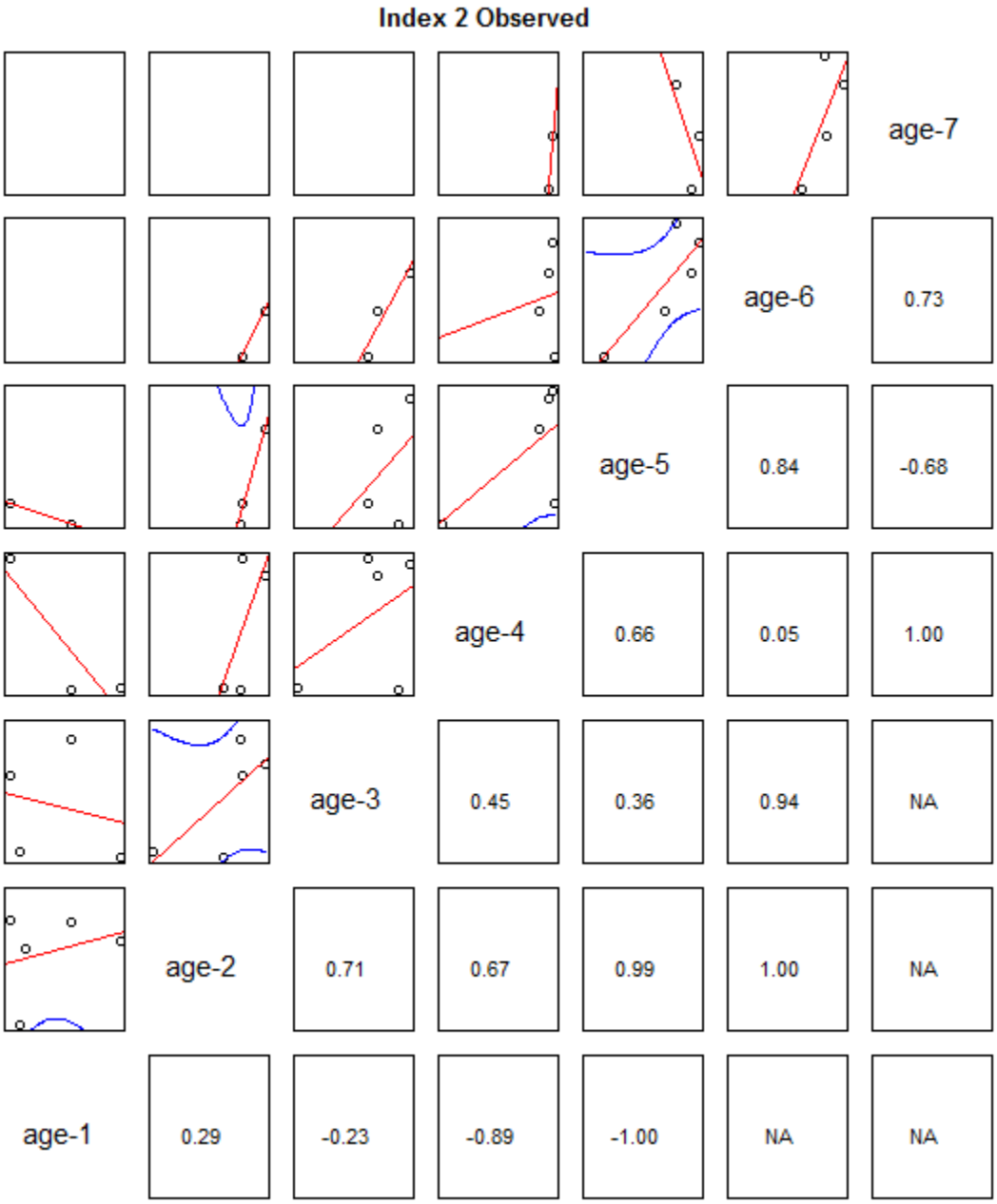

Figure B7.92. Observed catch for the NEFSC Bigelow survey. Note that age class labels are 1 greater than the modeled age class, so that "age-1" corresponds to age 0, "age-2" corresponds to age 1, etc.

Figure B7.93. Predicted catch for the NEFSC Bigelow survey. Note that age class labels are 1 greater than the modeled age class, so that "age-1" corresponds to age 0, "age-2" corresponds to age 1, etc.

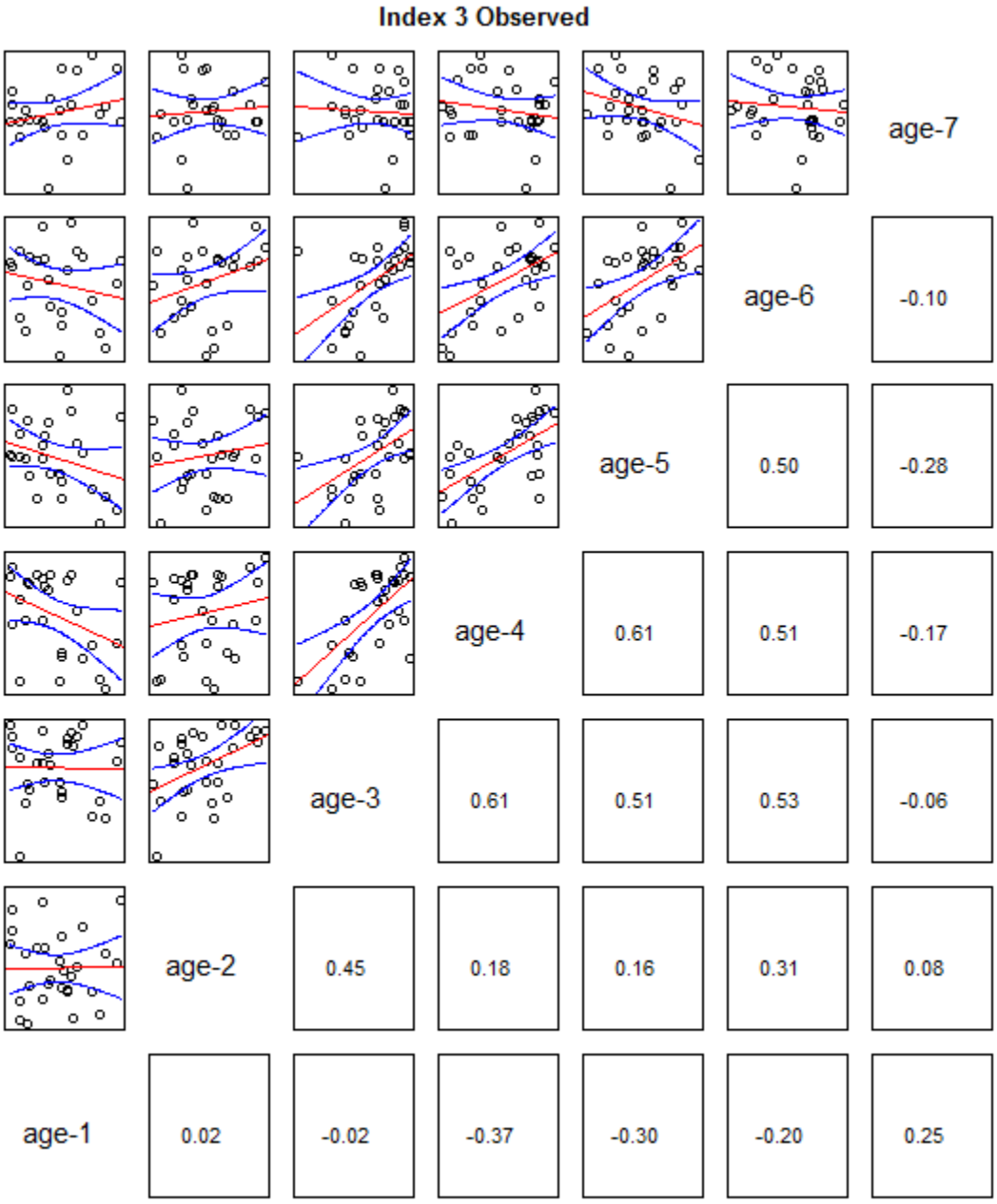

Figure B7.94. Observed catch for the MRIP recreational CPUE index. Note that age class labels are 1 greater than the modeled age class, so that "age-1" corresponds to age 0, "age-2" corresponds to age 1, etc.

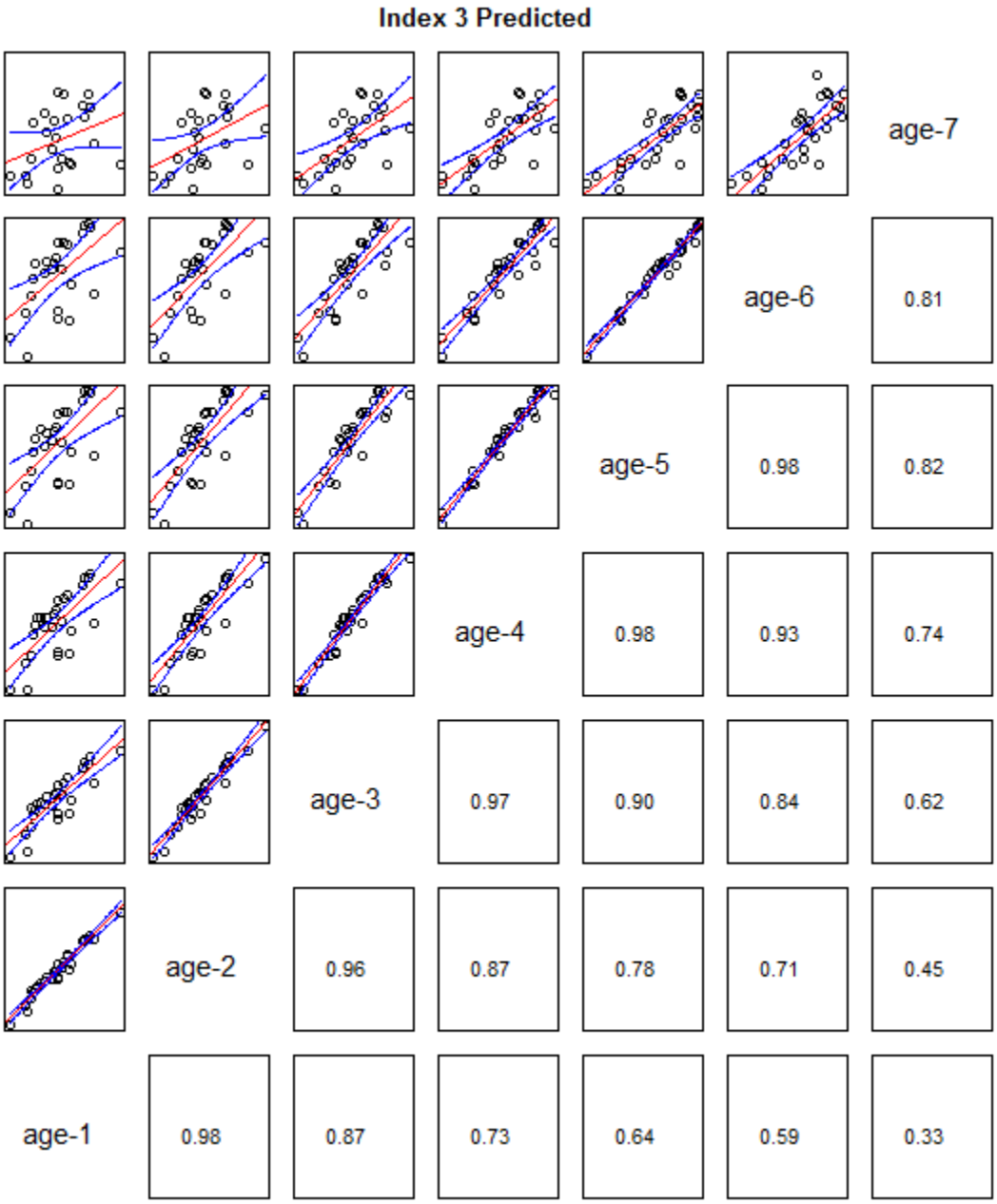

Figure B7.95. Predicted catch for the MRIP recreational CPUE index. Note that age class labels are 1 greater than the modeled age class, so that "age-1" corresponds to age 0, "age-2" corresponds to age 1, etc.

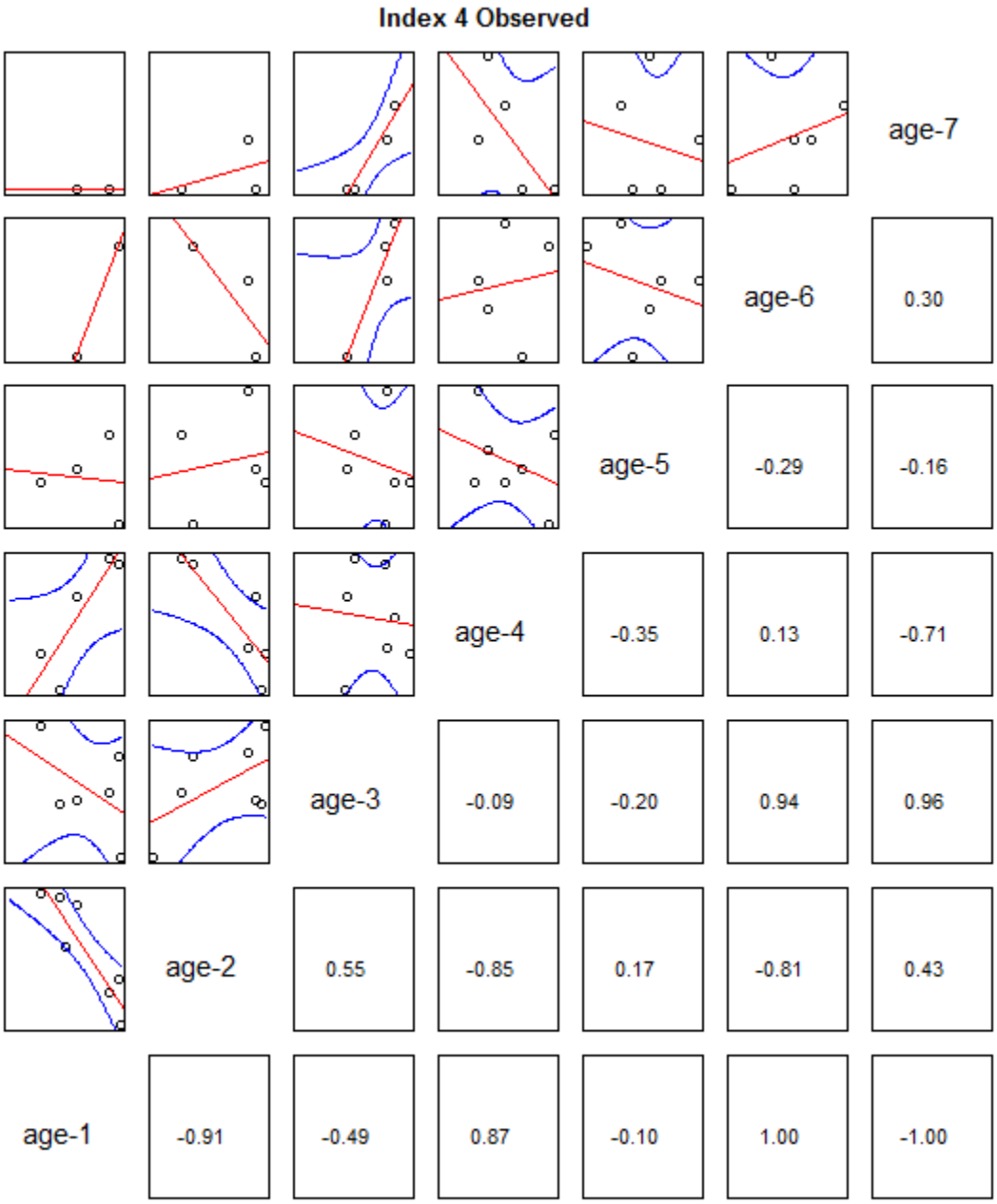

Figure B7.96. Observed catch for the NEAMAP survey. Note that age class labels are 1 greater than the modeled age class, so that "age-1" corresponds to age 0, "age-2" corresponds to age 1, etc.

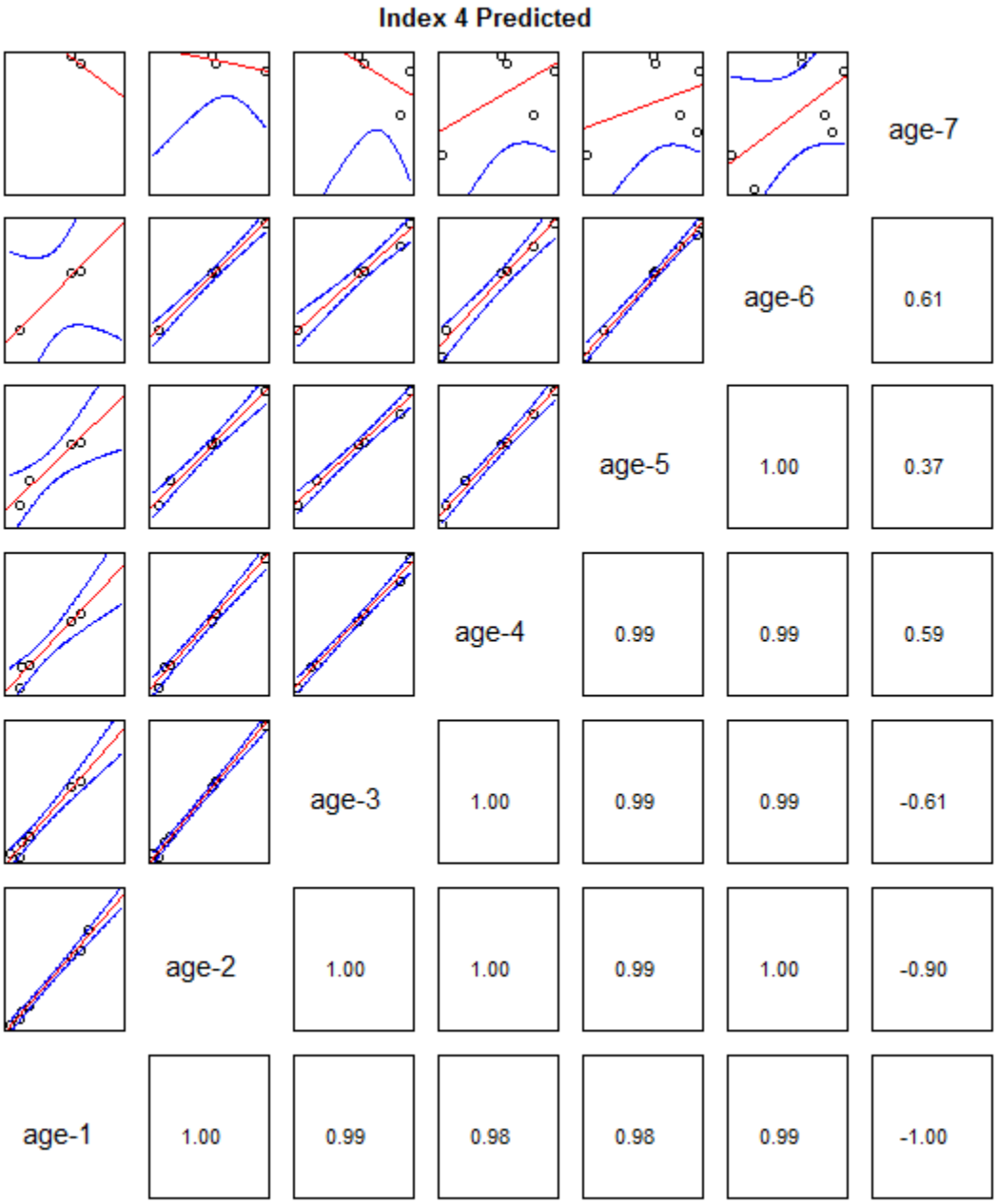

Figure B7.97. Predicted catch for the NEAMAP survey. Note that age class labels are 1 greater than the modeled age class, so that "age-1" corresponds to age 0, "age-2" corresponds to age 1, etc.

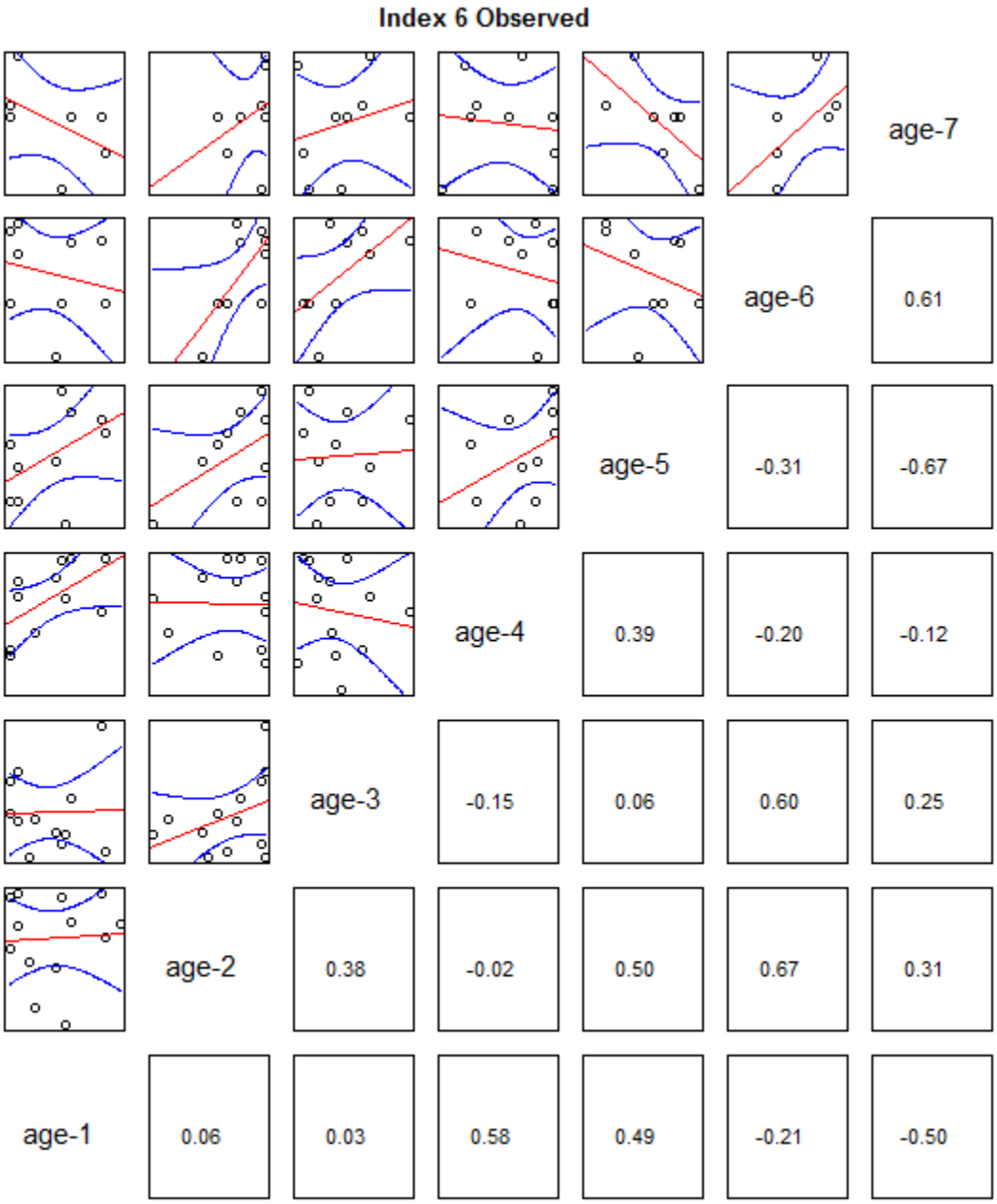

Figure B7.98. Observed catch for the PSIGNS gillnet survey. Note that age class labels are 1 greater than the modeled age class, so that "age-1" corresponds to age 0, "age-2" corresponds to age 1, etc.

Figure B7.99. Predicted catch for the PSIGNS gillnet survey. Note that age class labels are 1 greater than the modeled age class, so that "age-1" corresponds to age 0, "age-2" corresponds to age 1, etc.

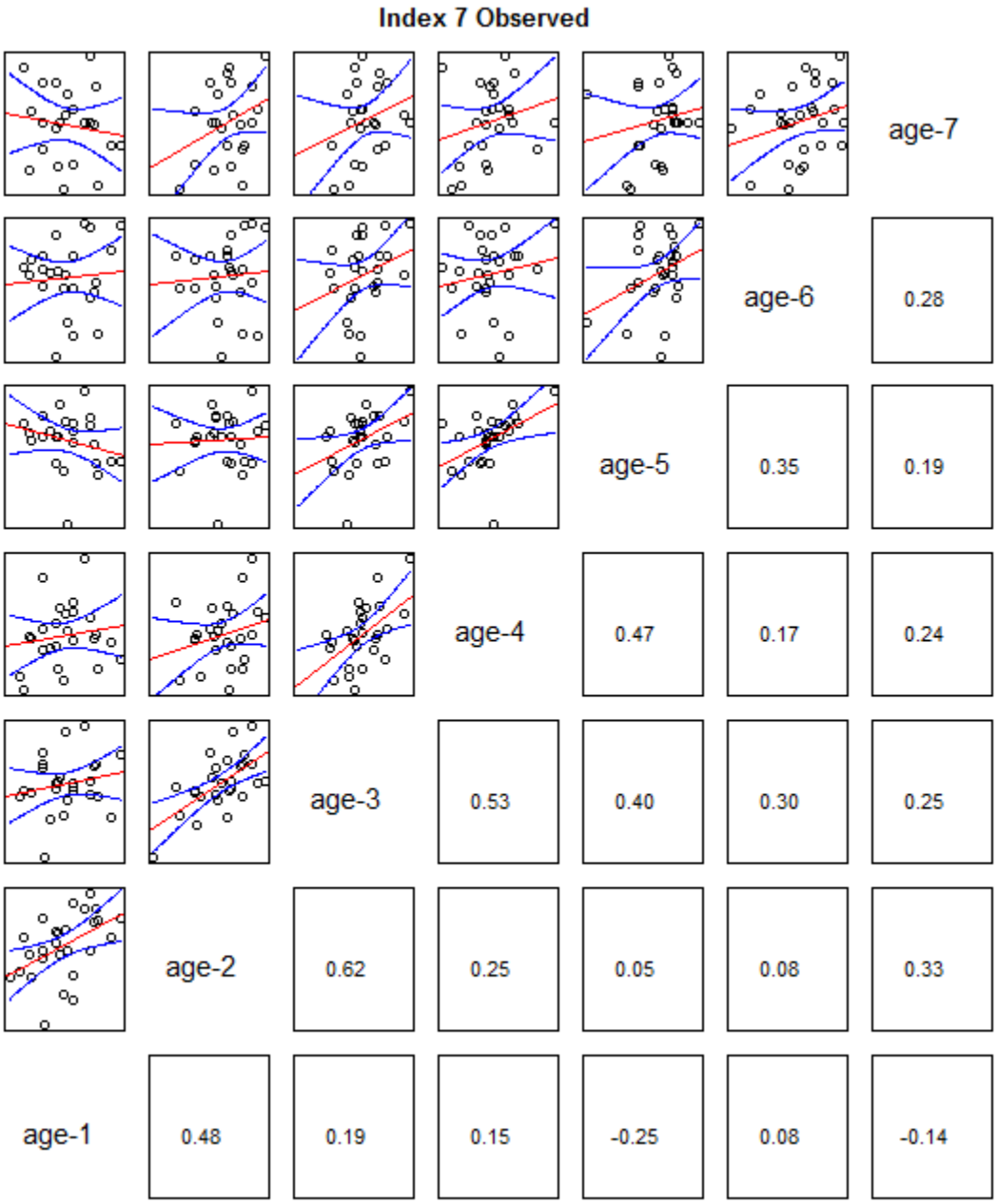

Figure B7.100. Observed catch for the CT LISTS trawl survey. Note that age class labels are 1 greater than the modeled age class, so that "age-1" corresponds to age 0, "age-2" corresponds to age 1, etc.

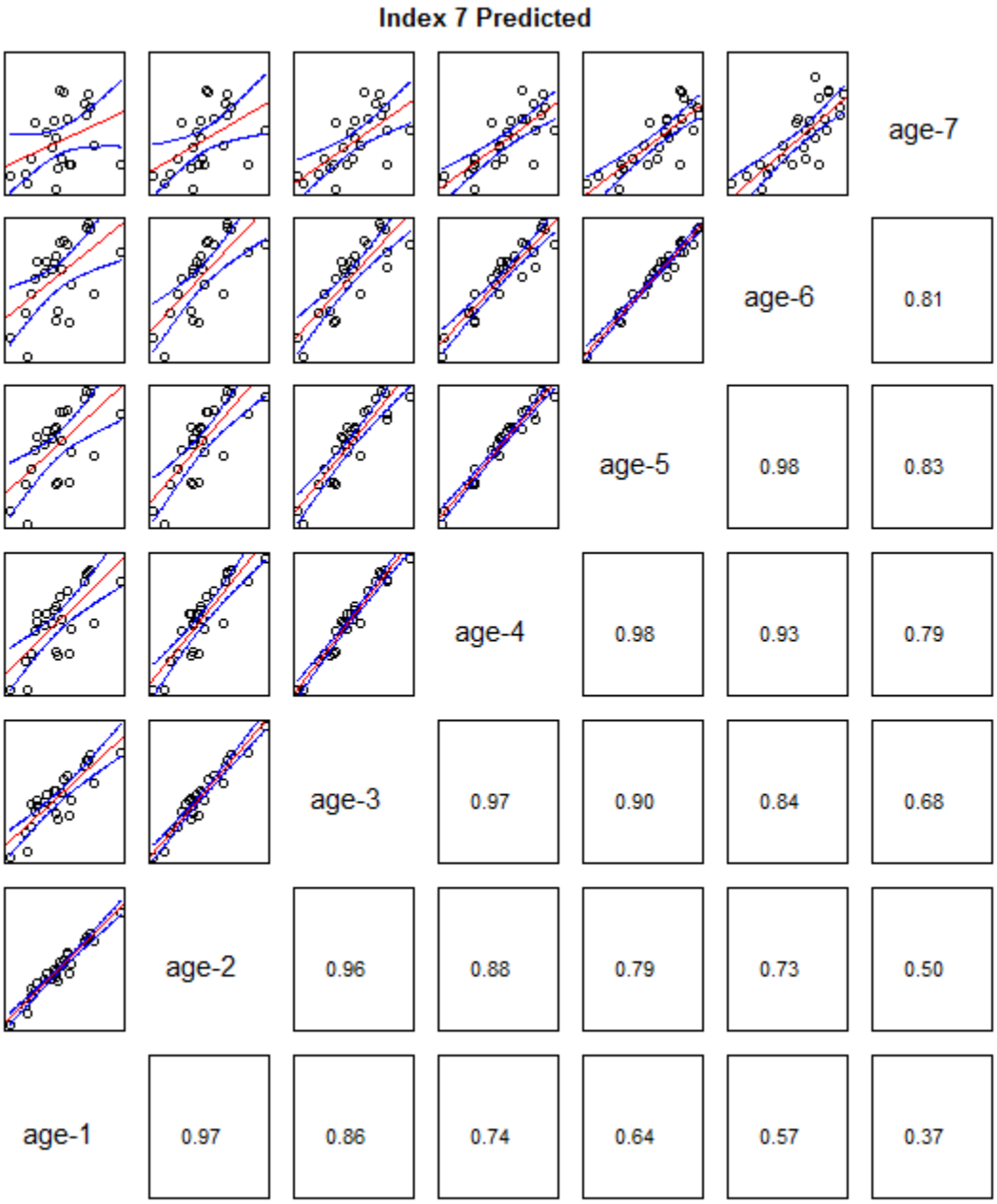

Figure B7.101. Predicted catch for the CT LISTS trawl survey. Note that age class labels are 1 greater than the modeled age class, so that "age-1" corresponds to age 0, "age-2" corresponds to age 1, etc.

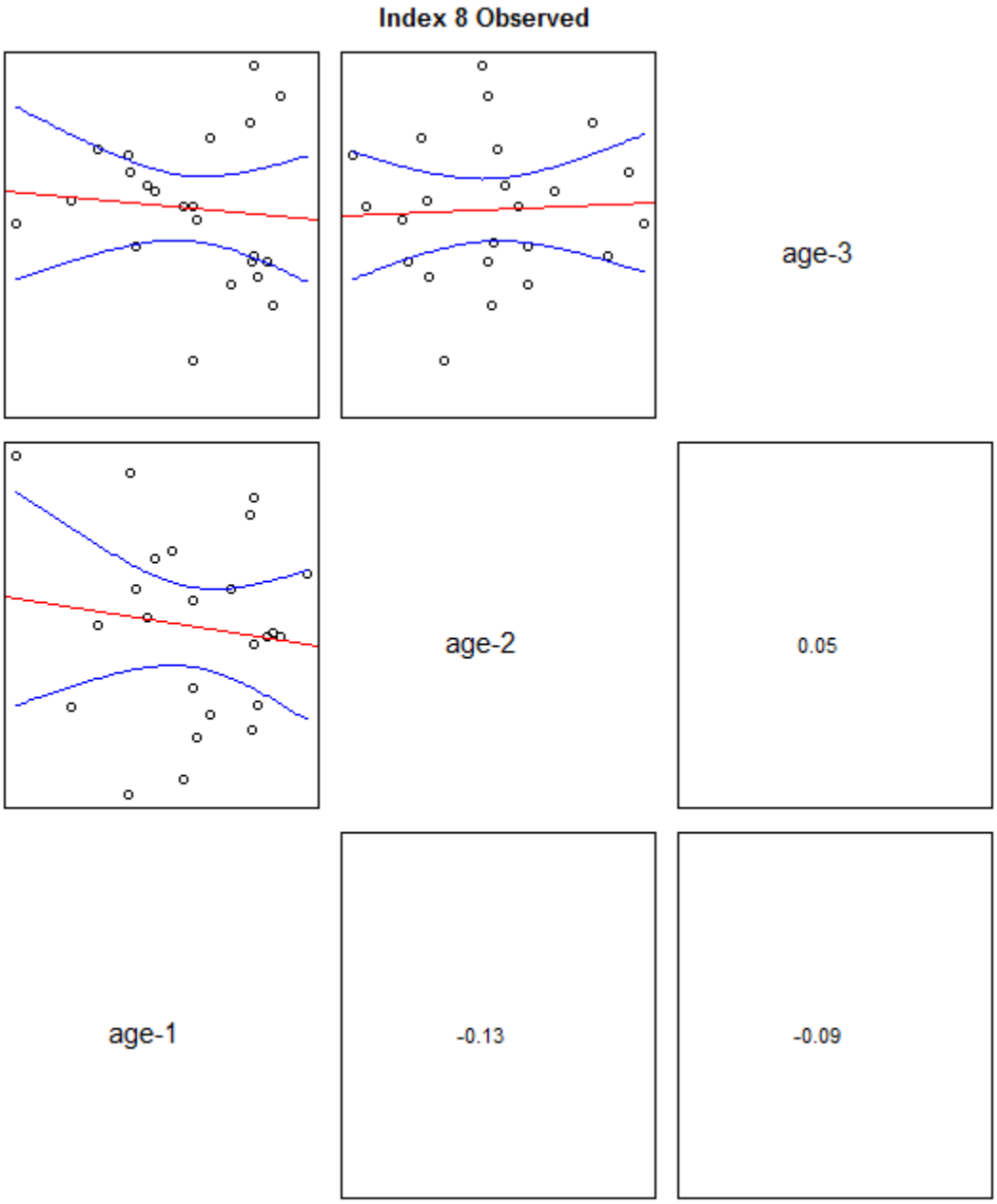

Figure B7.102. Observed catch for the NJ ocean trawl survey. Note that age class labels are 1 greater than the modeled age class, so that "age-1" corresponds to age 0, "age-2" corresponds to age 1, etc.

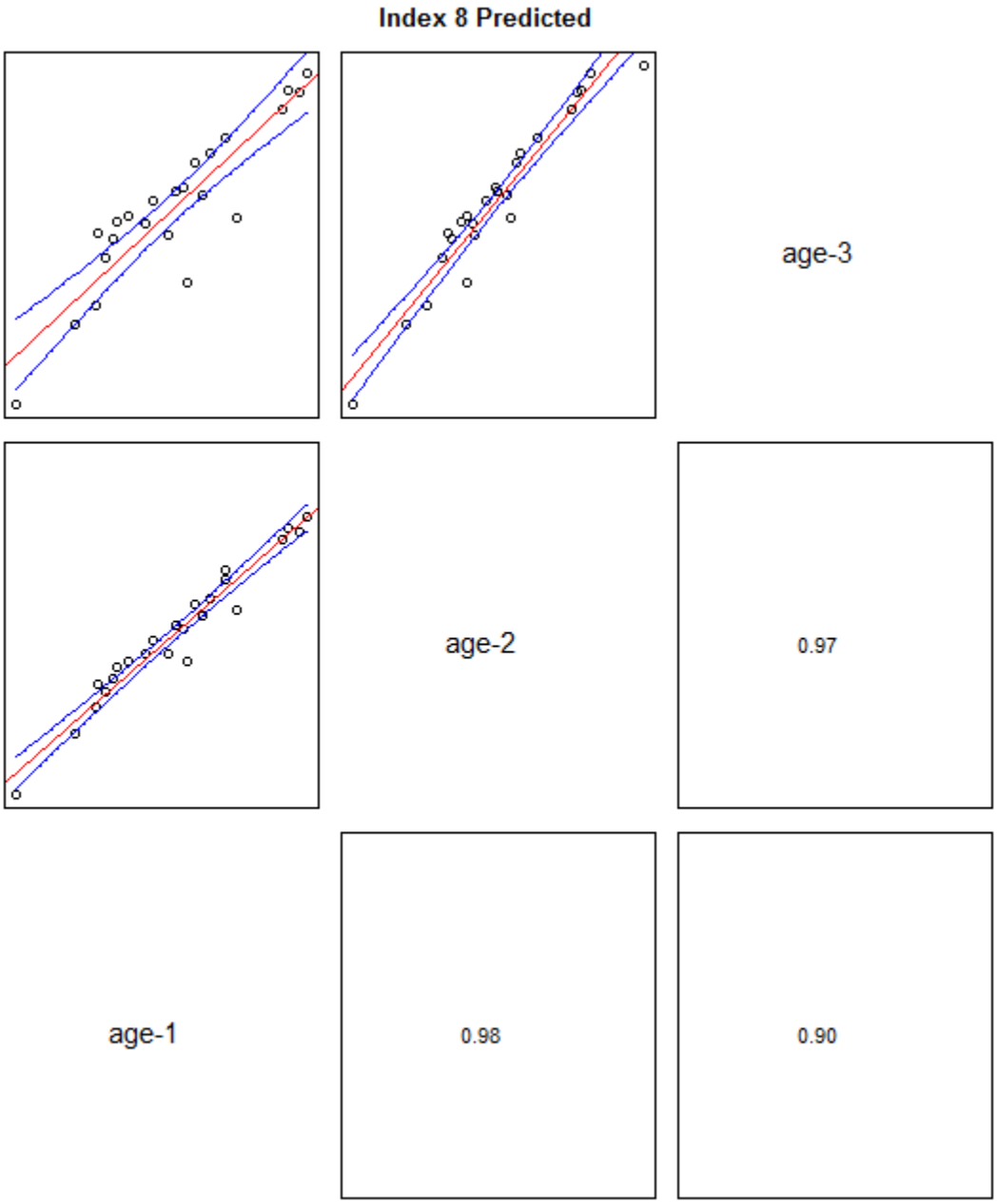

Figure B7.103. Predicted catch for the NJ ocean trawl survey. Note that age class labels are 1 greater than the modeled age class, so that "age-1" corresponds to age 0, "age-2" corresponds to age 1, etc.

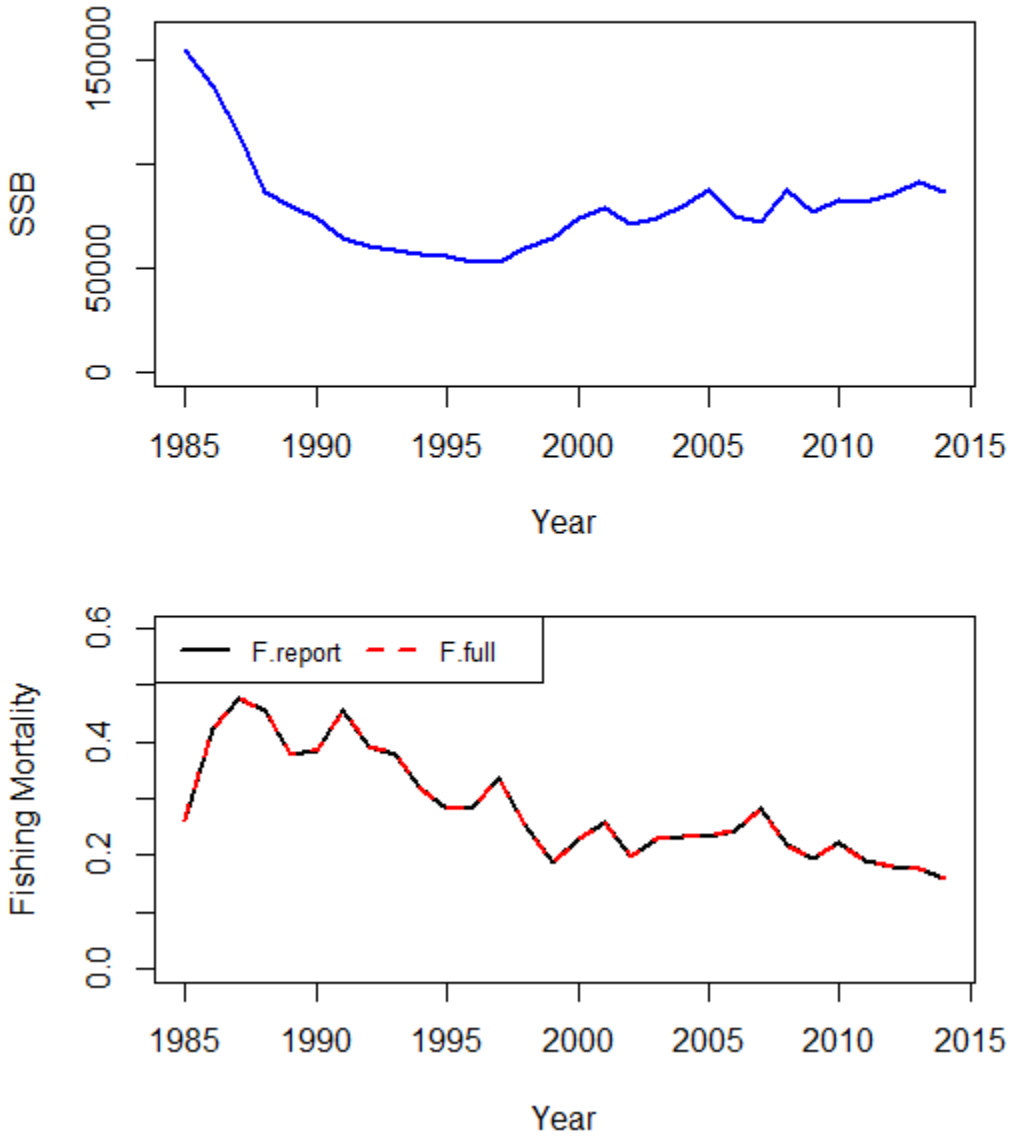

Figure B7.104. Estimated spawning stock biomass (top) and full fishing mortality (bottom) from 1985 to 2014 from the revised final model.

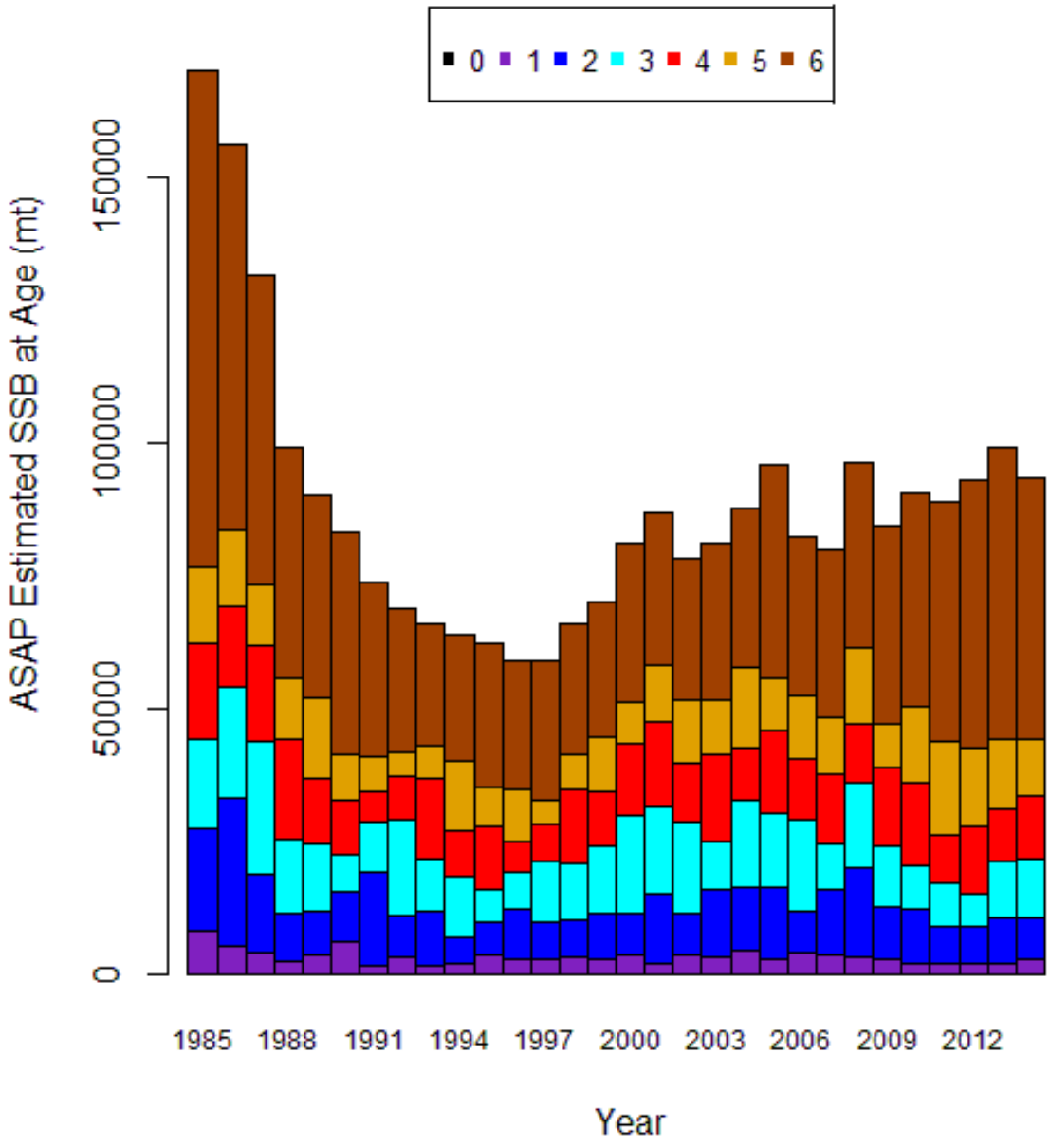

Figure B7.105. Age composition of the spawning stock biomass from 1985 to 2014.

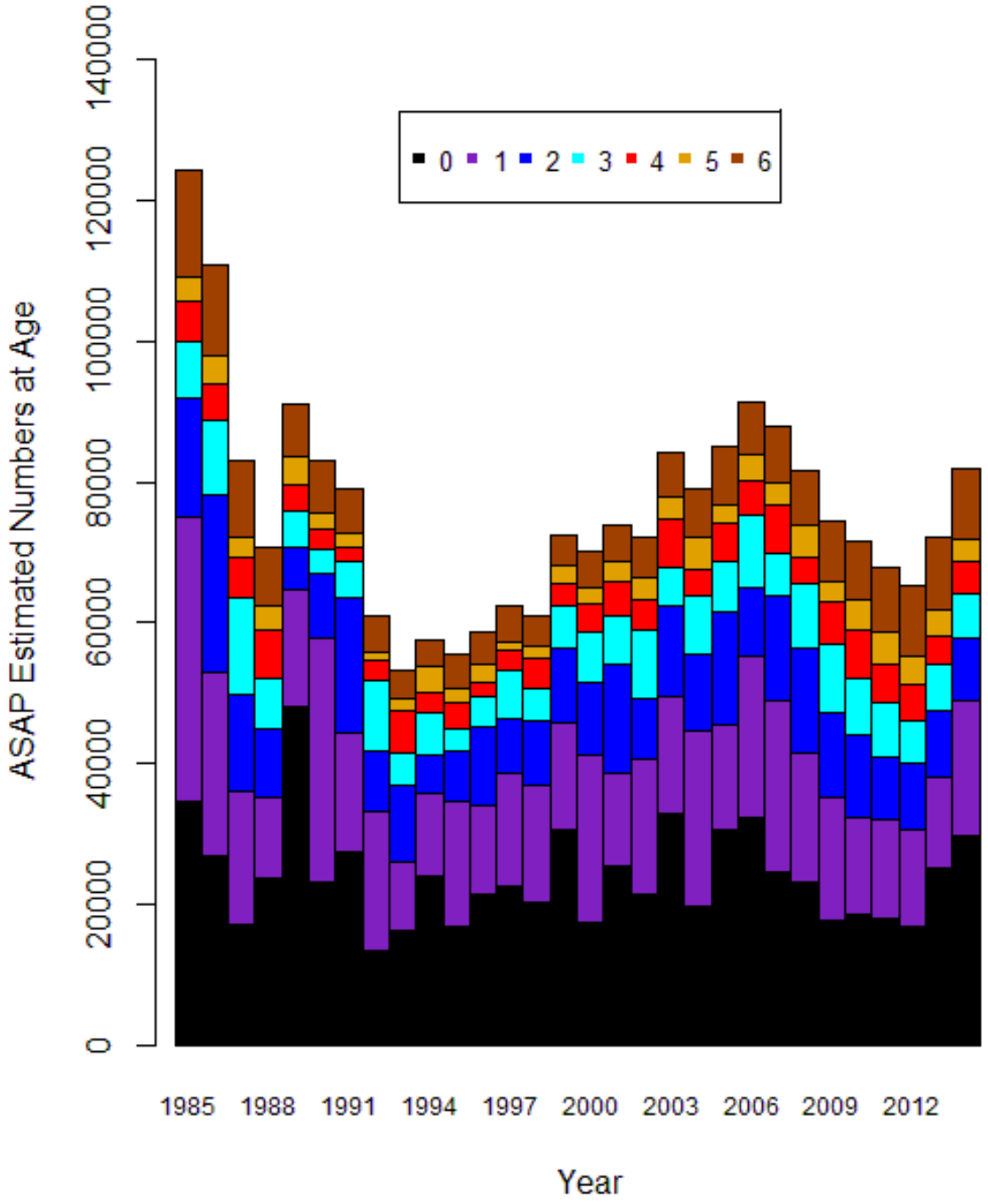

Figure B7.106. Estimated total numbers at age from 1985 to 2014.

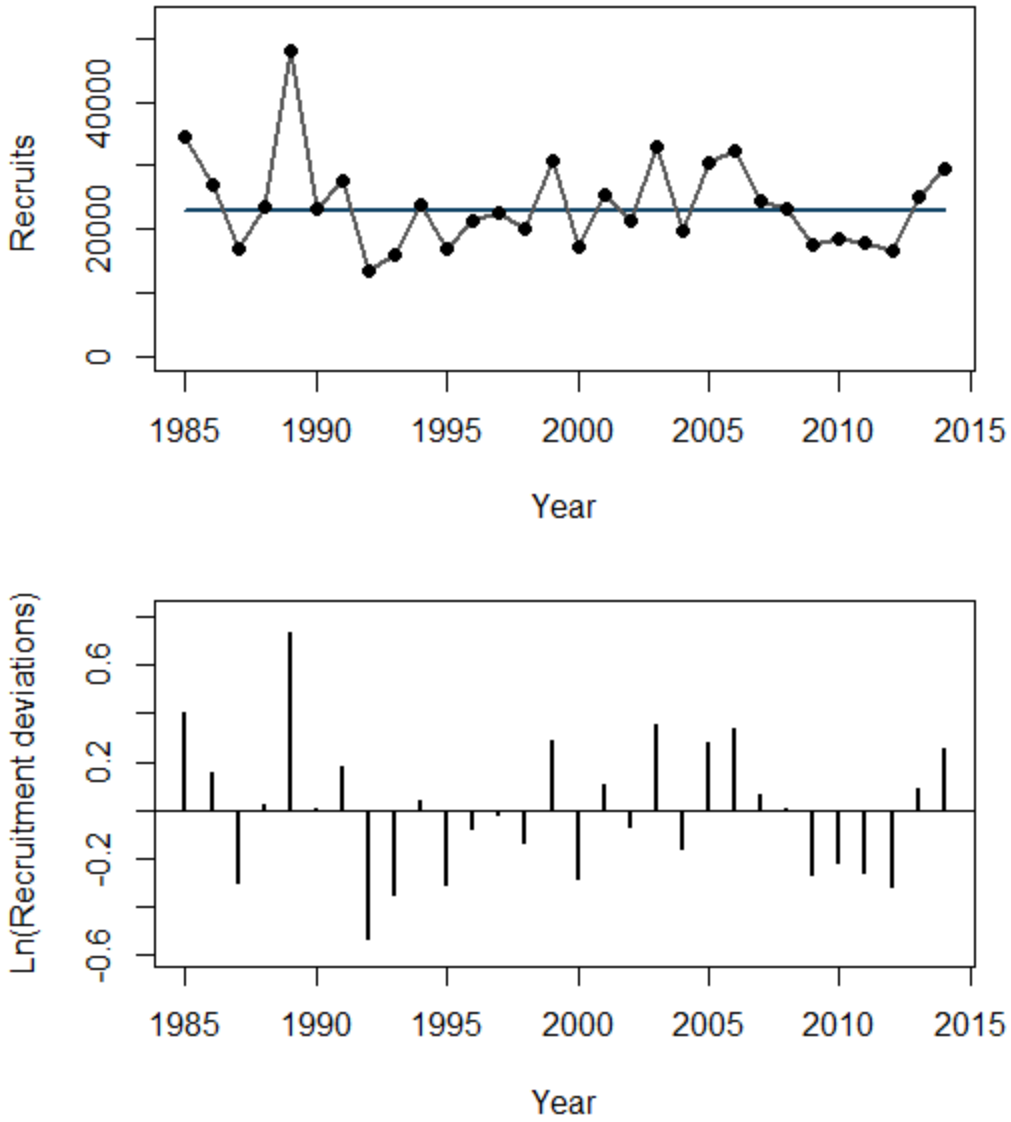

Figure B7.107. Recruitment estimates, mean recruitment, and recruitment deviations (log) from 1985 to 2014 from the final model.

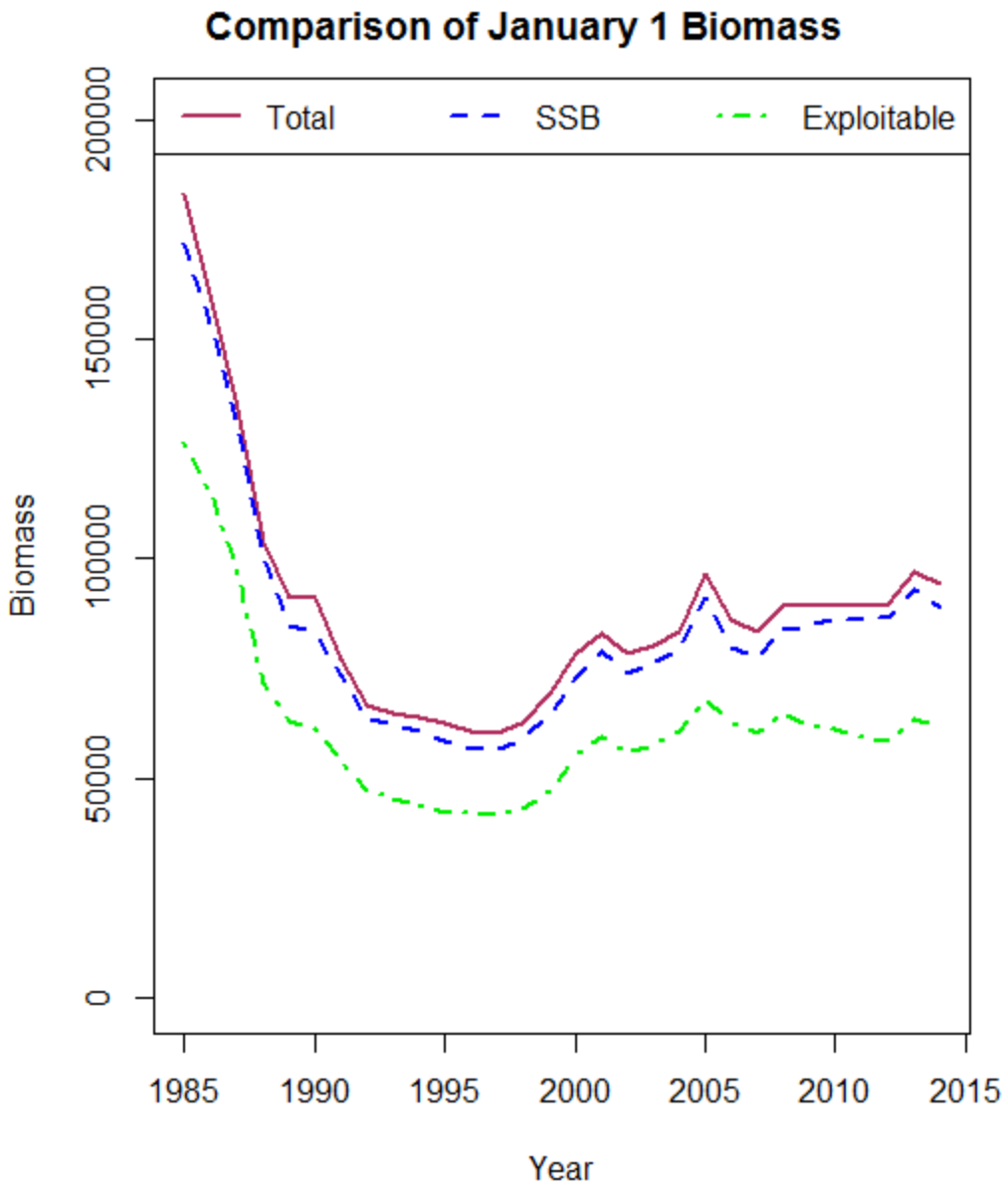

Figure B7.108. A comparison of total, spawning stock, and exploitable biomass from 1985 to 2014 from the final model.

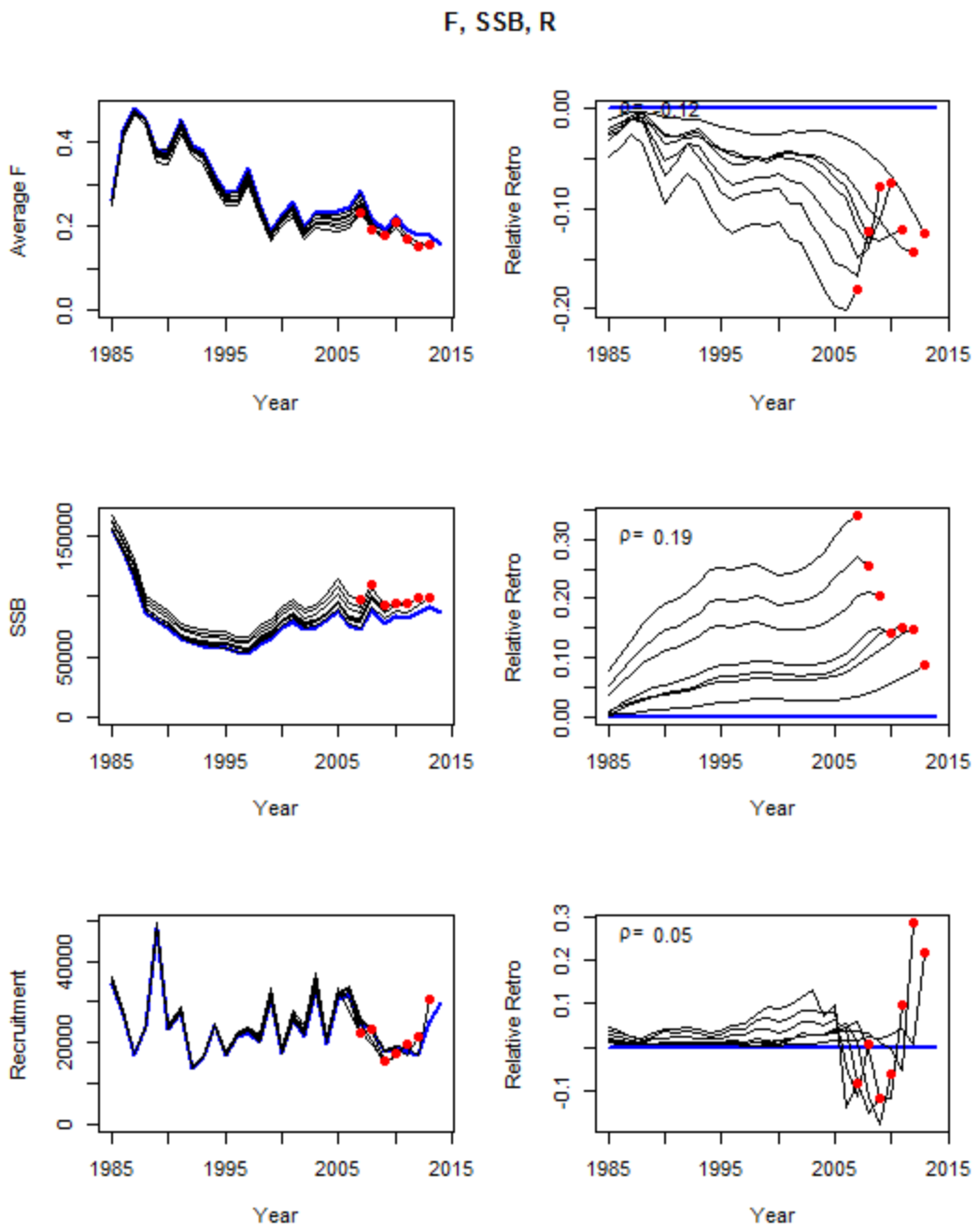

Figure B7.109. Retrospective plots for average fishing mortality, spawning stock biomass and recruitment from a 7 year peel carried out on the revised final model.

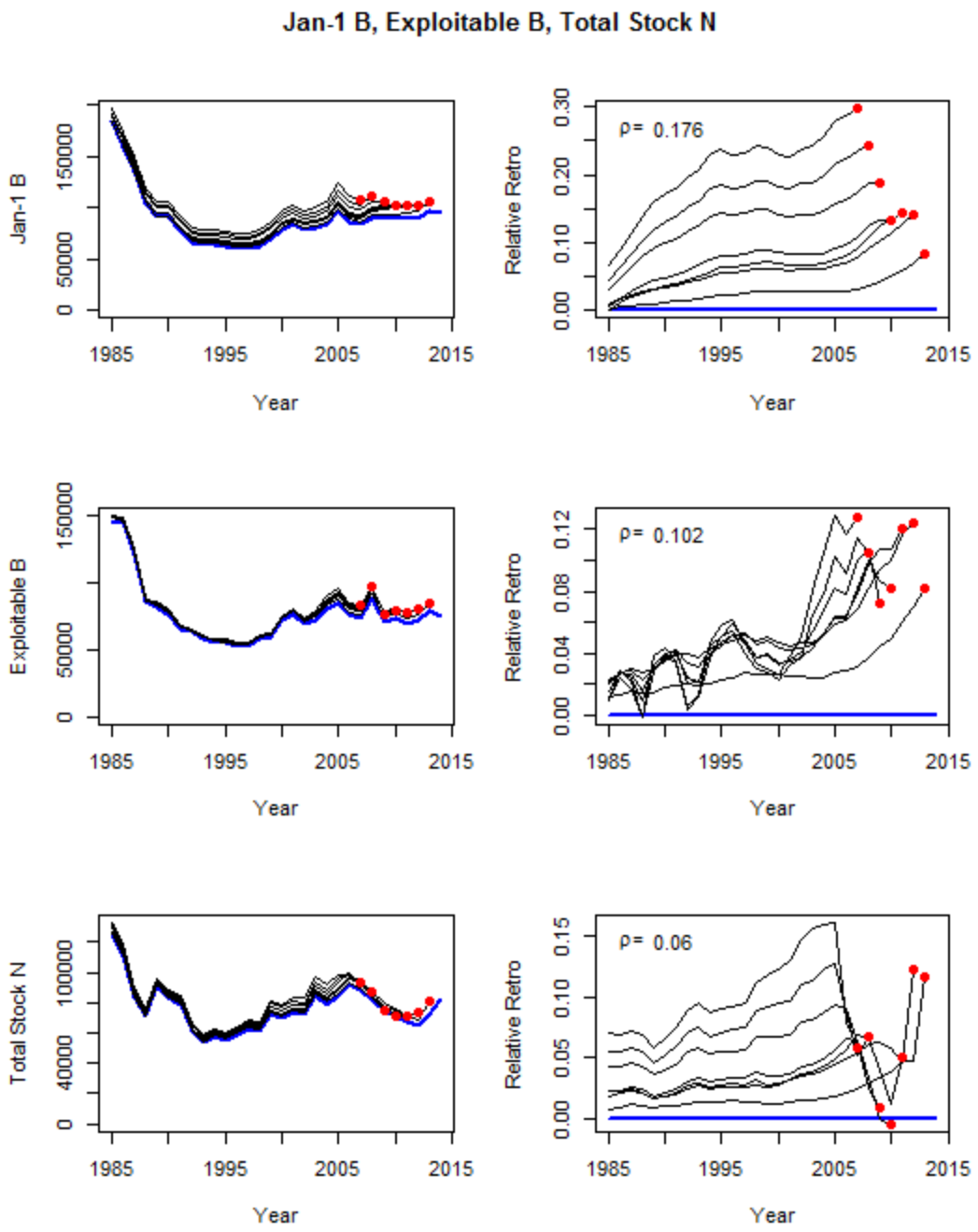

Figure B7.110. Retrospective plots for January-1 biomass, total biomass, and total stock numbers, from a 7 year peel carried out on the revised final model.

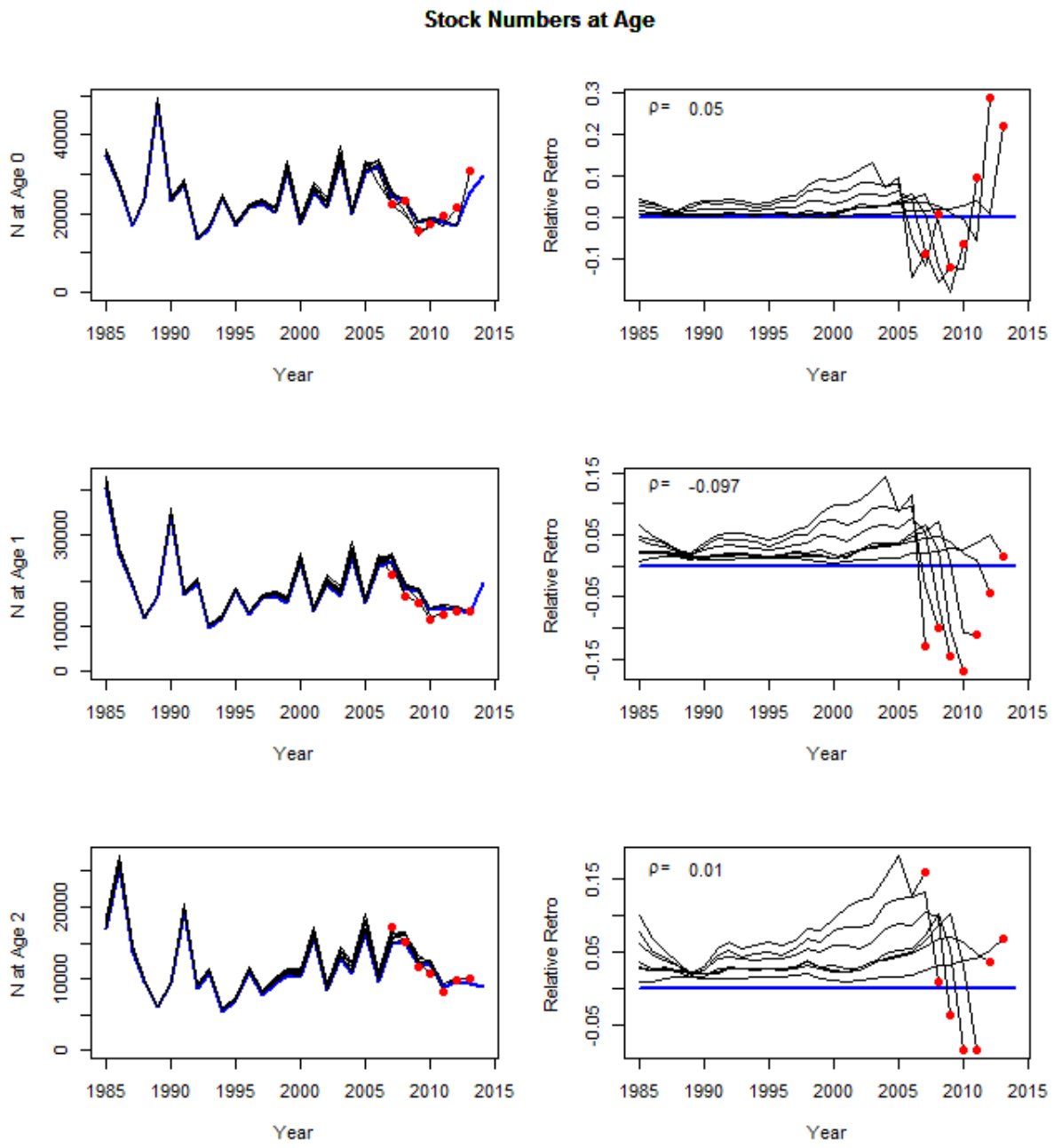

Figure B7.111. Retrospective plots for ages 0-2 from a 7 year peel carried out on the final model.

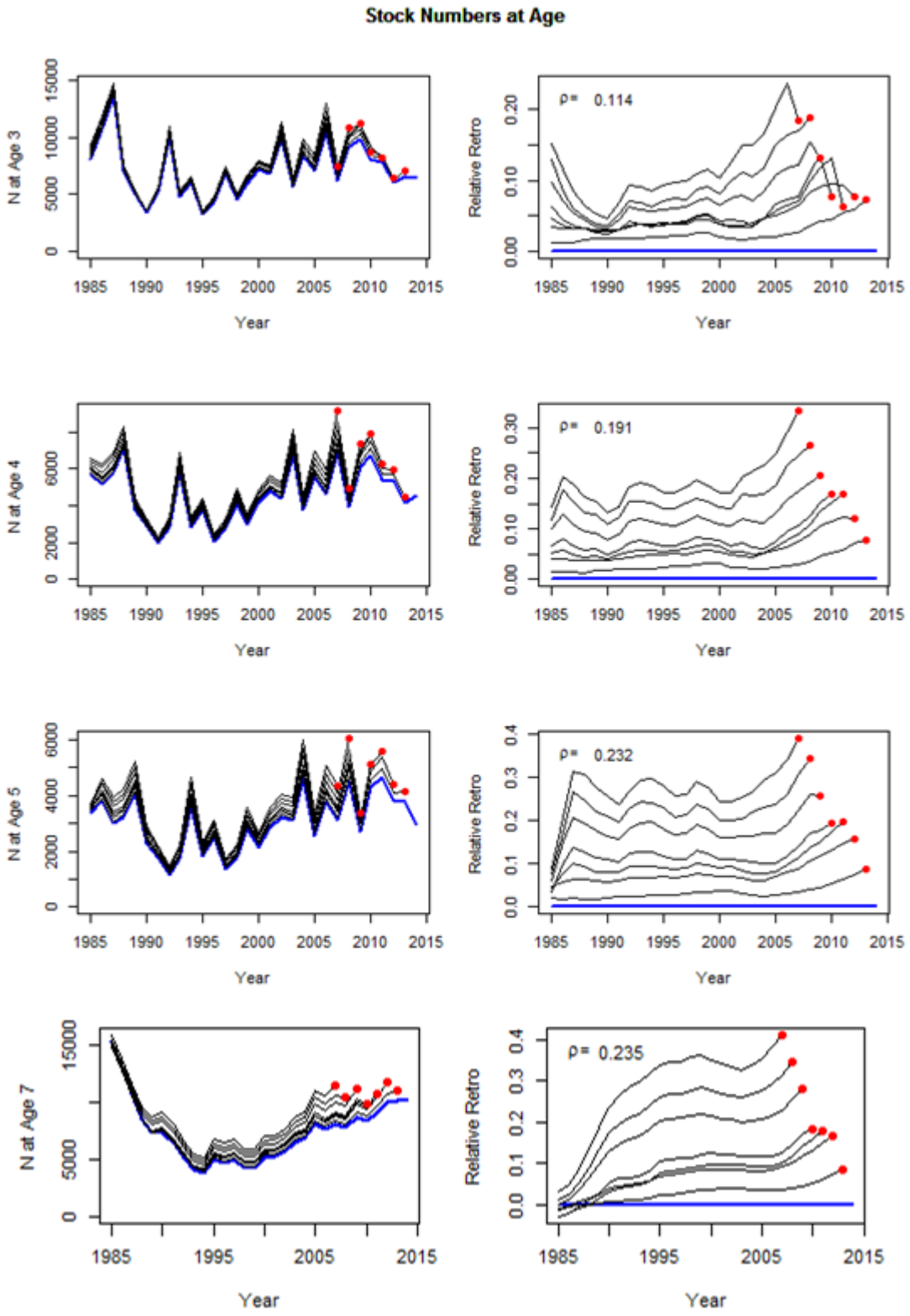

Figure B7.112. Retrospective plots for ages 3-6+ from a 7 year peel carried out on the final model.

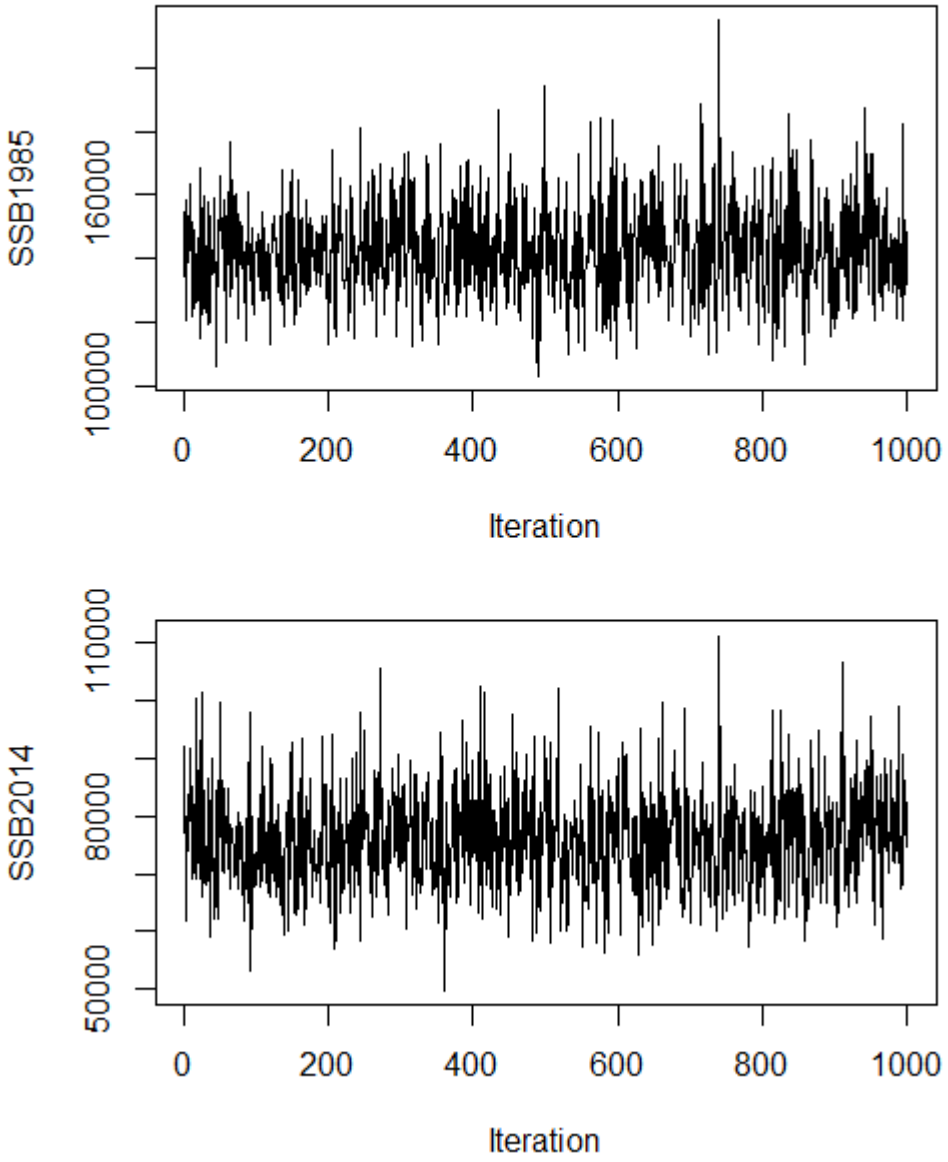

Figure B7.113. Trace plots for fishing mortality in 1985 and 2014 from 1000 MCMC and a thinning rate of 1000 (1,000,000 iterations).

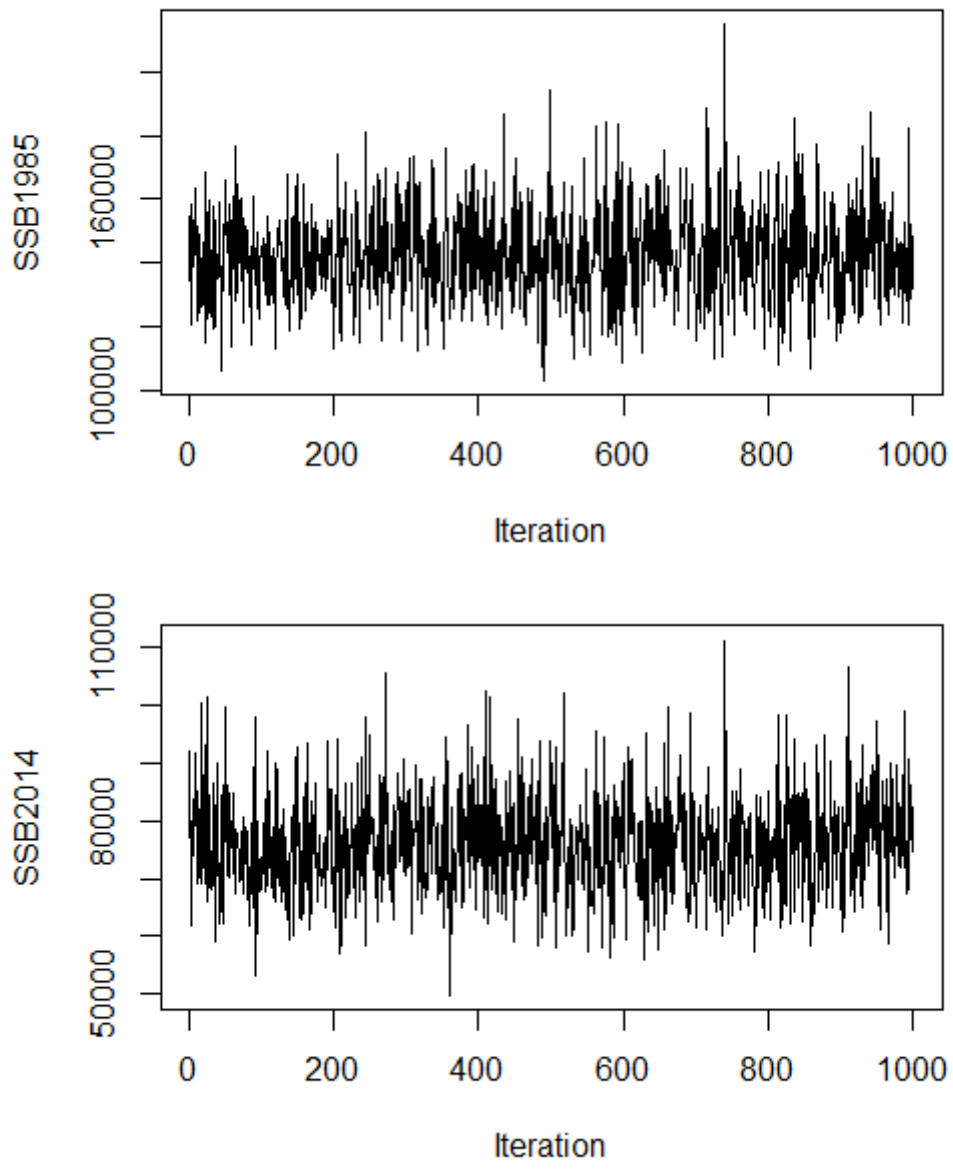

Figure B7.114. Trace plots for spawning stock biomass in 1985 and 2014 from 1000 MCMC and a thinning rate of 1000 (1,000,000 iterations).

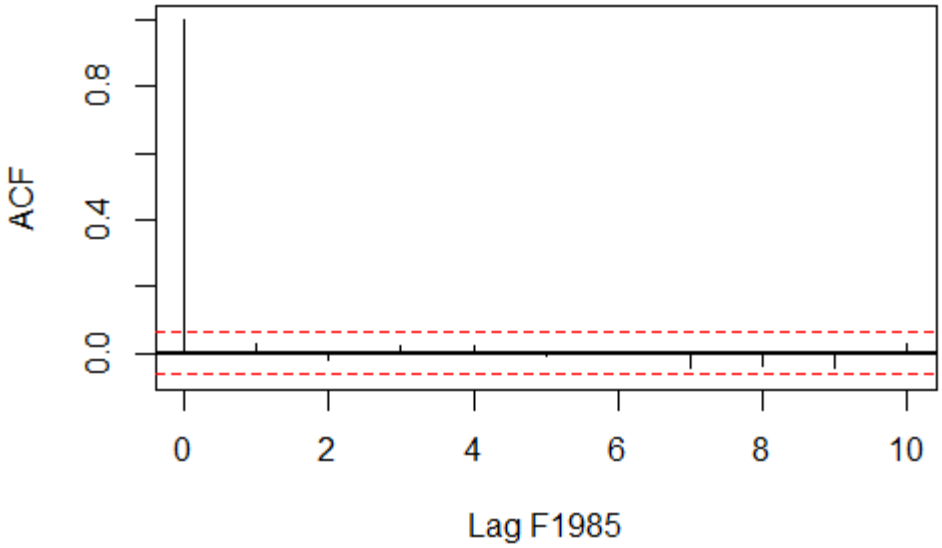

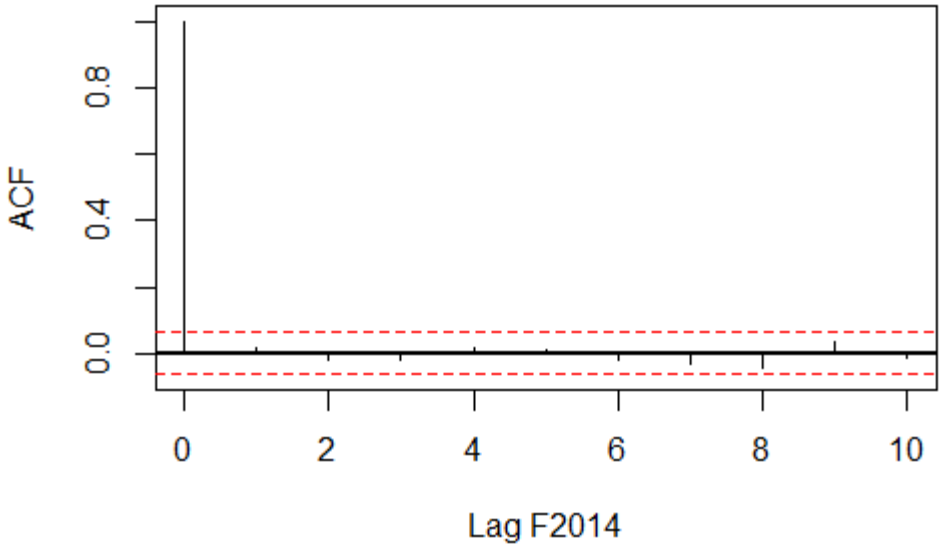

Figure B7.115. Autocorrelation for fishing mortality in the MCMC runs.

Figure B7.116. Autocorrelation for SSB in the MCMC runs.

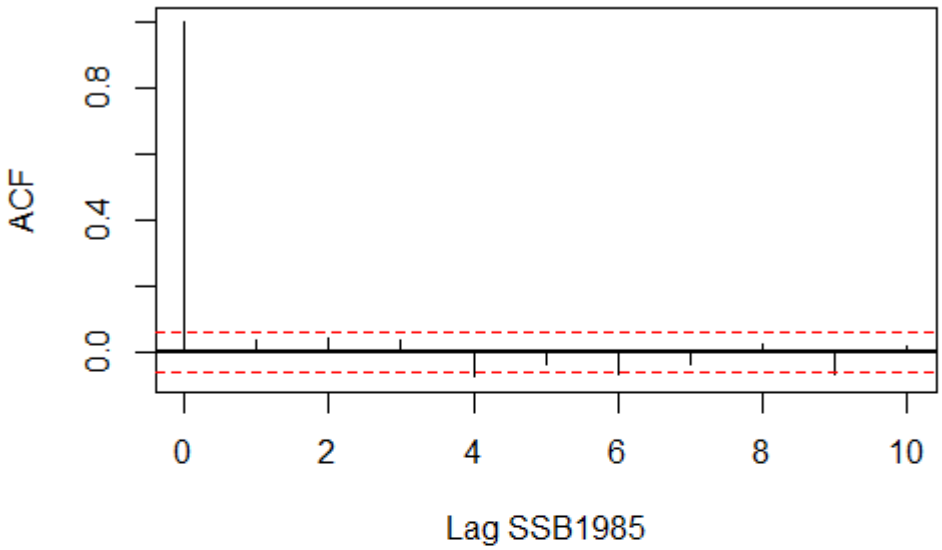

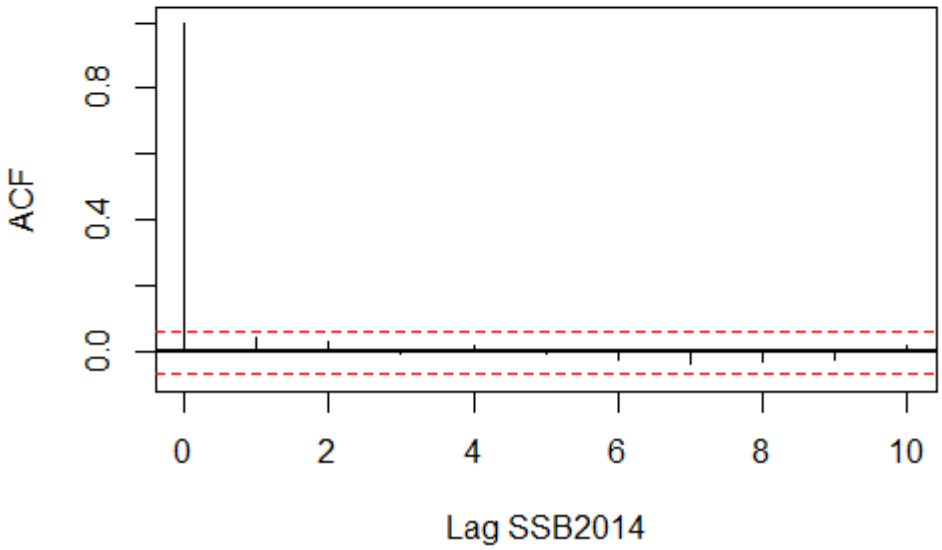

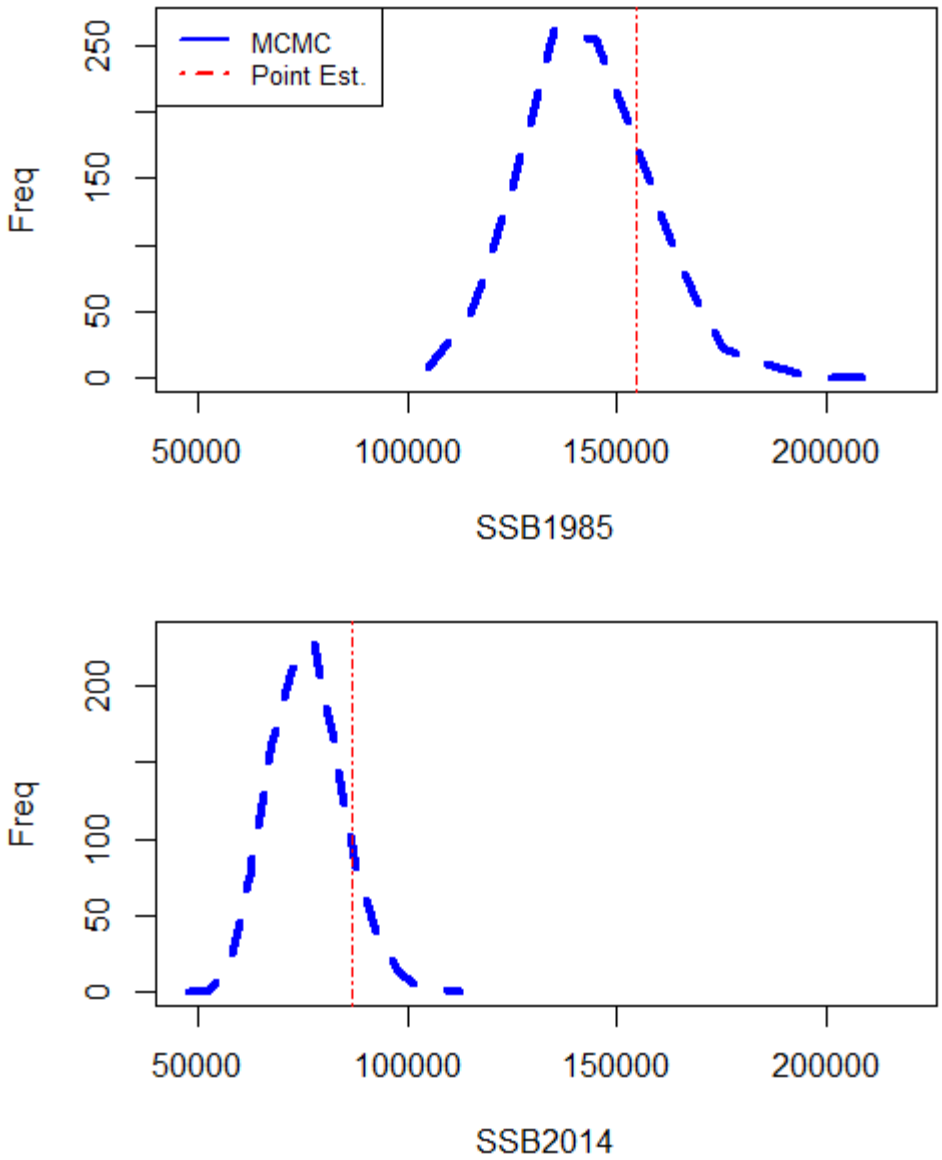

Figure B7.117. MCMC distribution plots for spawning stock biomass in 1985 and 2014 with point estimates from the revised final model.

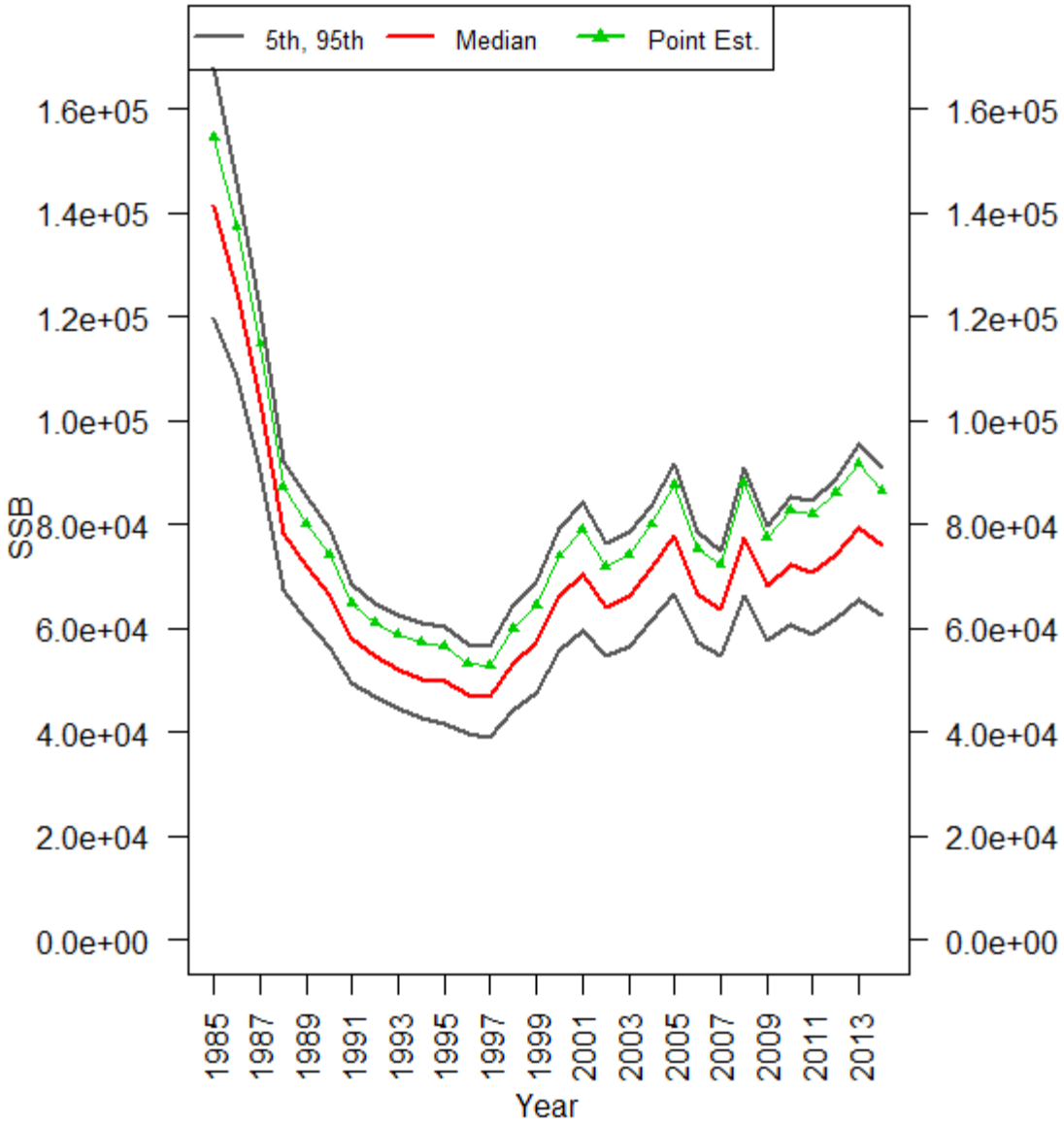

Figure B7.118. Median spawning stock biomass and 95 confidence intervals from the MCMC runs with point estimates from the revised final model.

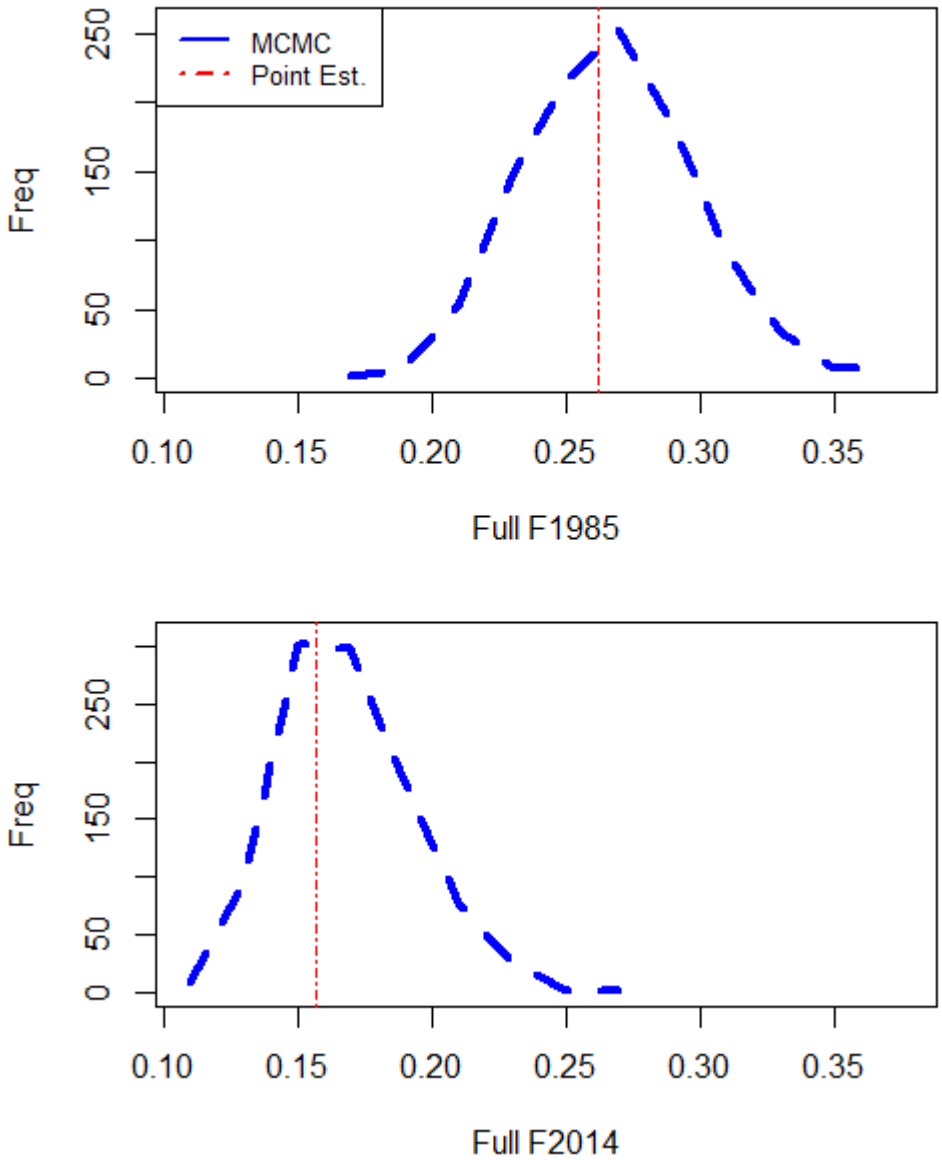

Figure B7.119. MCMC distribution plots for fishing mortality in 2985 and 2014 with point estimates from the revised final model.

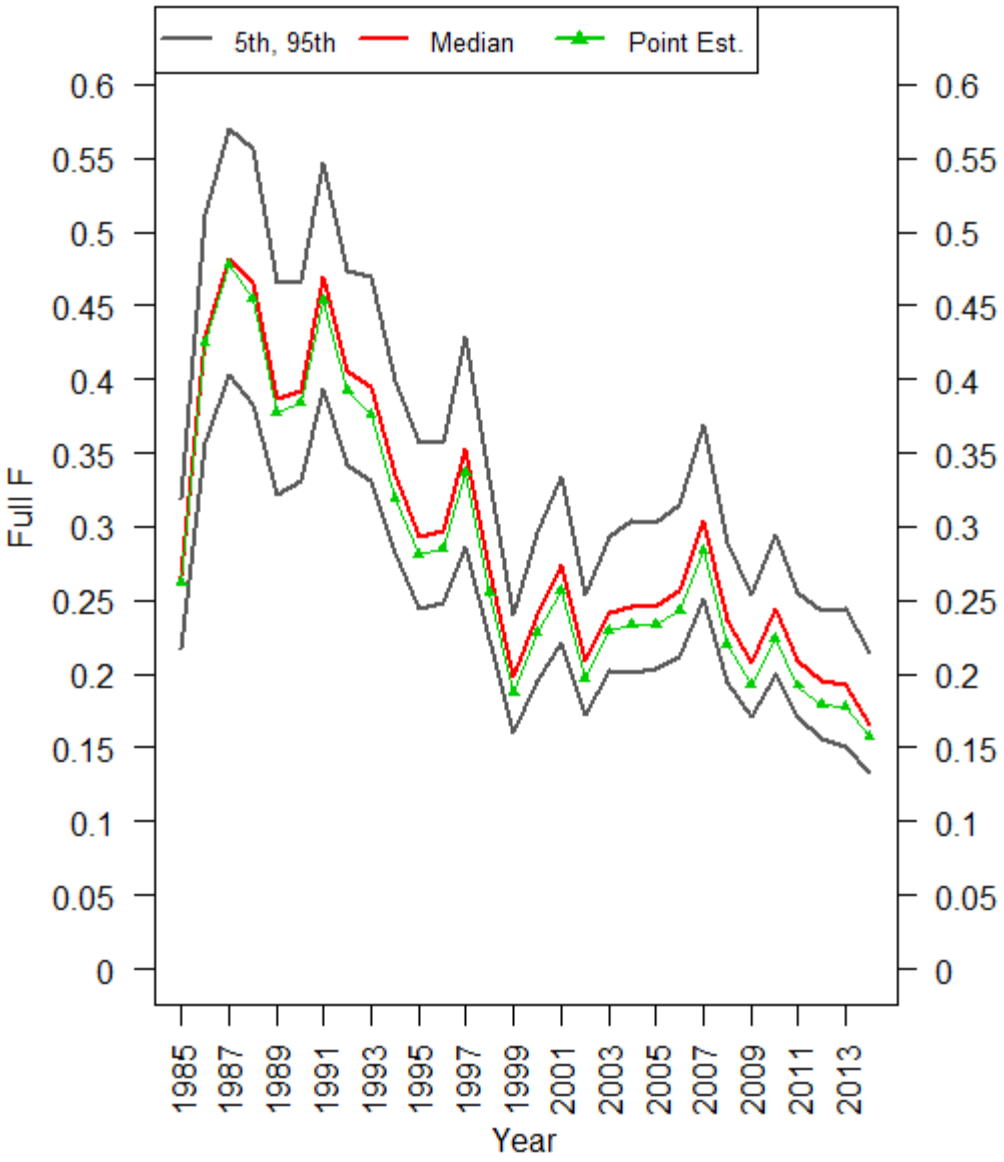

Figure B7.120. Median fishing mortality and 95% confidence intervals from the MCMC runs with point estimates from the revised final model.

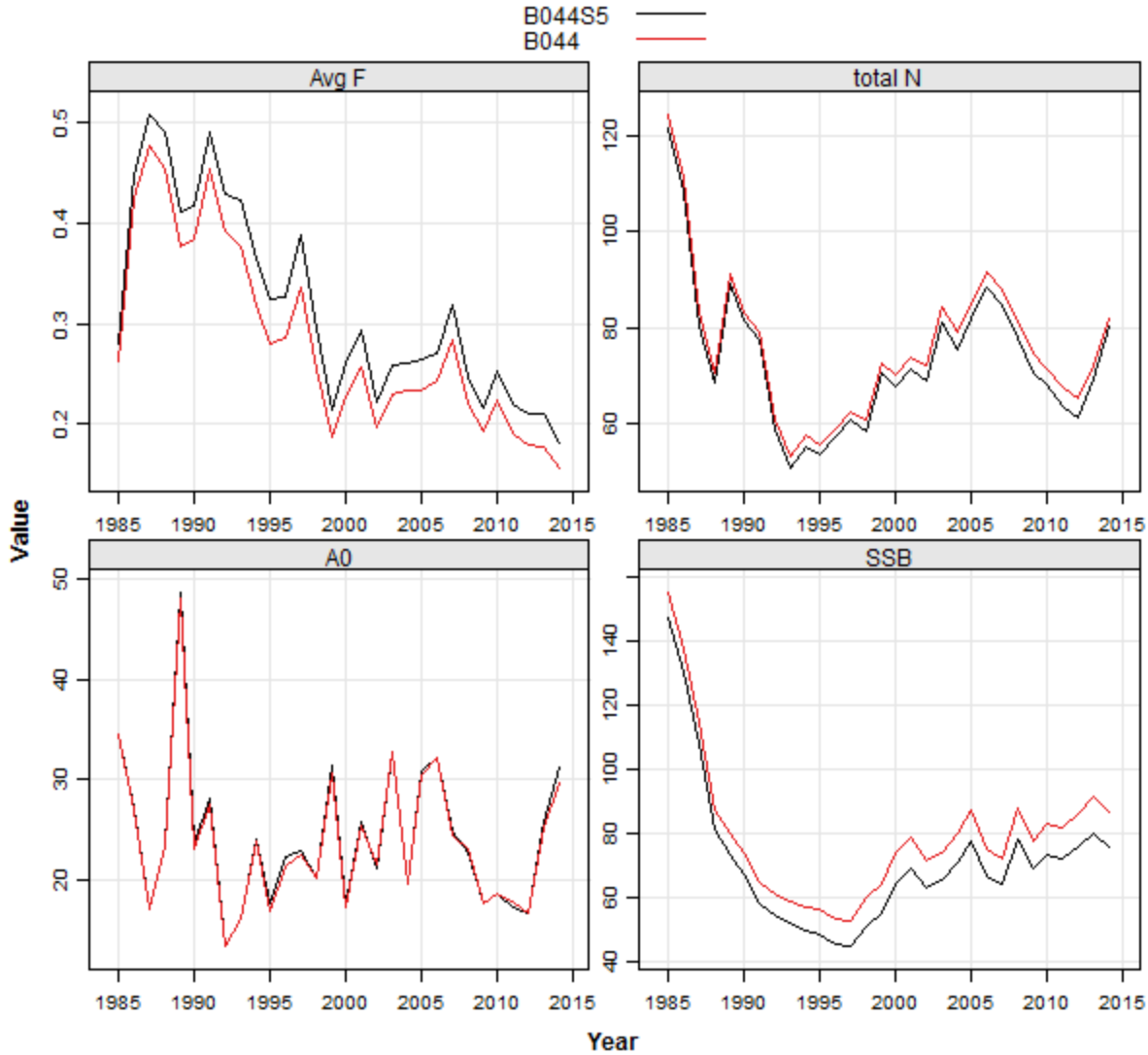

Figure B7.121. Final model sensitivity run assume AB1 lengths for the recreational discards. Trends for the revised final model (B044) estimates are represented by the red line, with sensitivity run estimates (B044S5) represented by the black line.

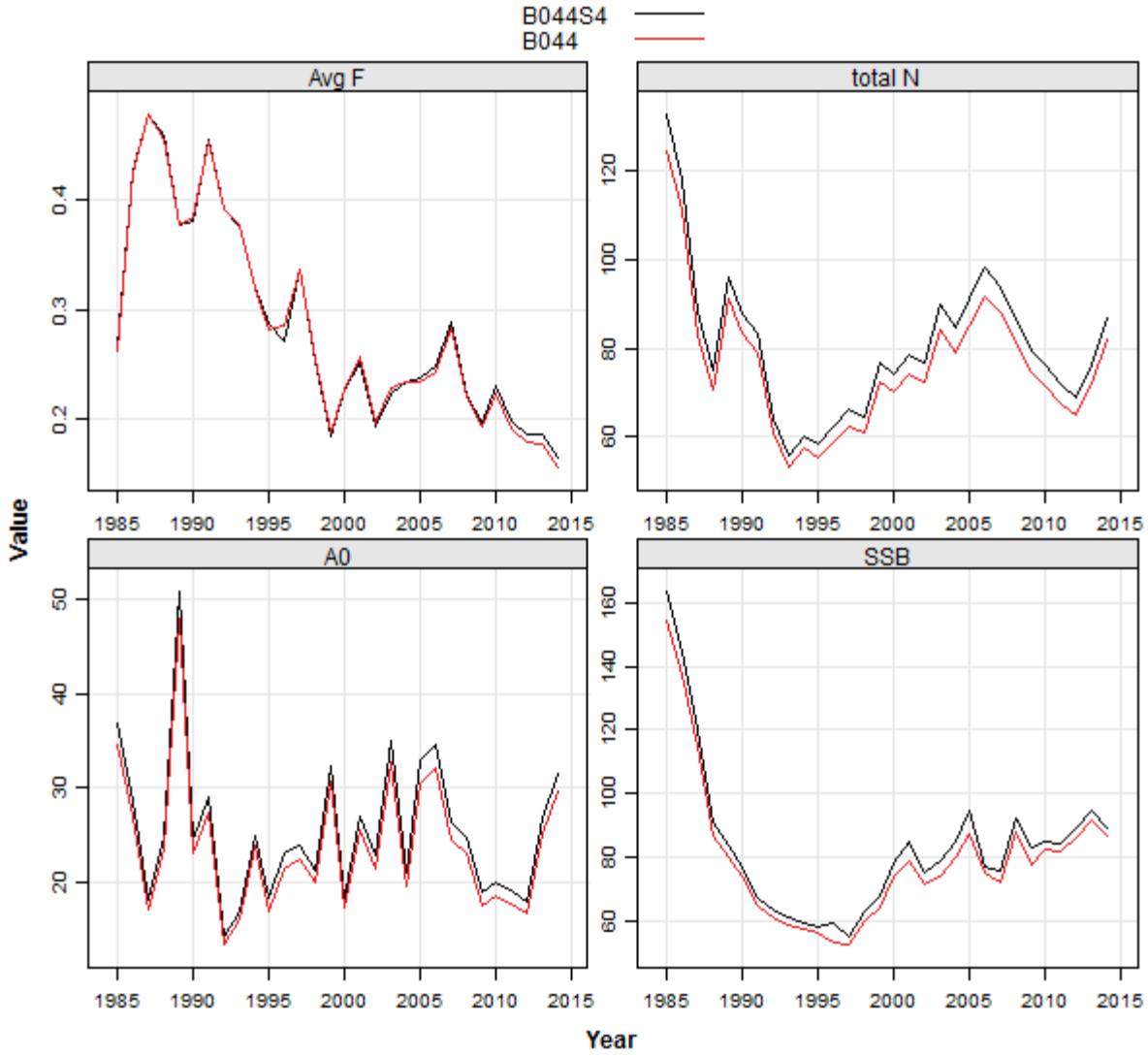

Figure B7.122. Final model sensitivity run assuming upper 95% CI for recreational catch.
Trends for the revised final model (B044) estimates are represented by the red line, with sensitivity run estimates (B044S4) represented by the black line.

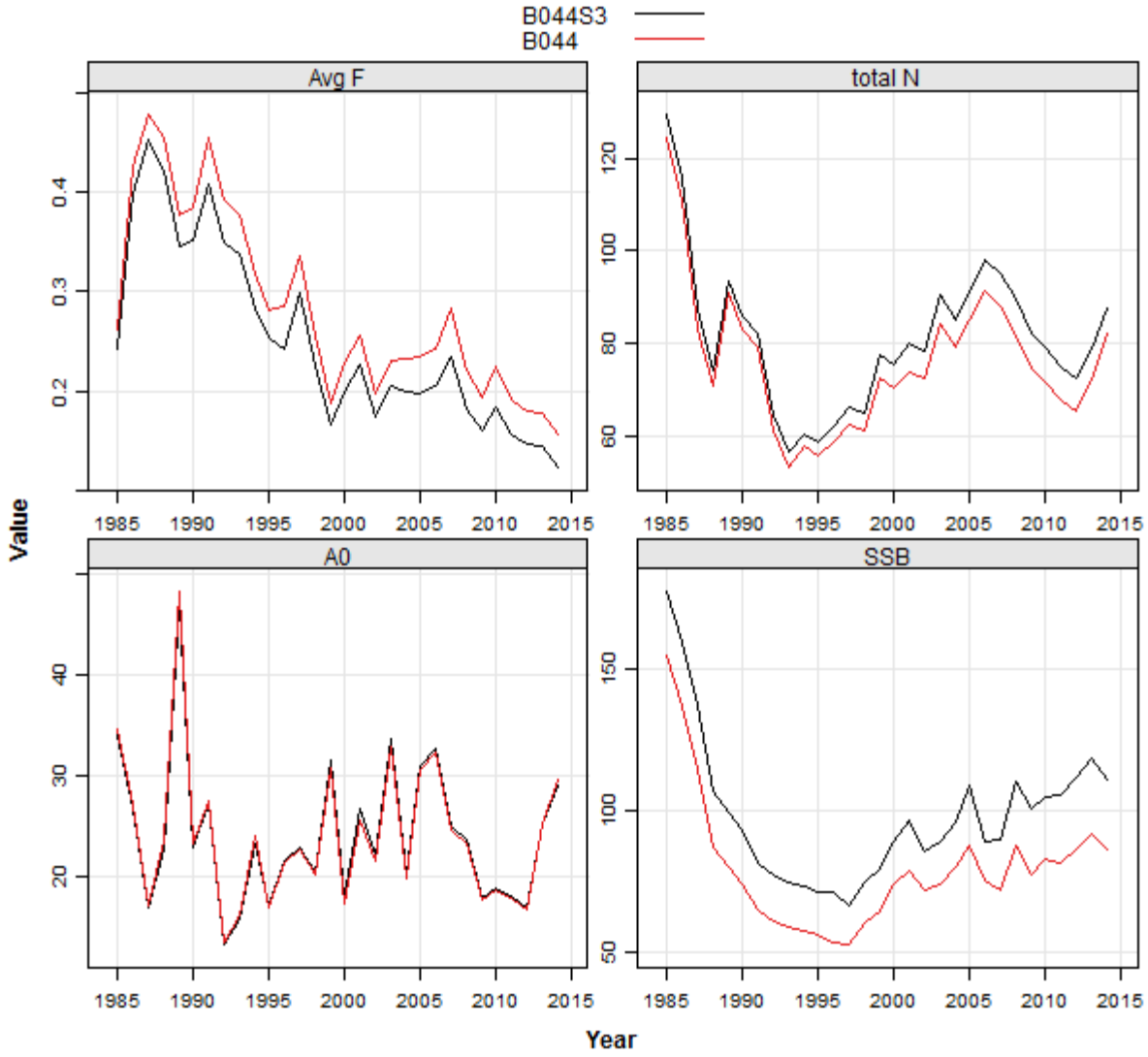

Figure B7.123. Final model sensitivity run assuming lower 95% CI for recreational catch.
Trends for the final model (B044) estimates are represented by the red line, with sensitivity run estimates (B044S3) represented by the black line.

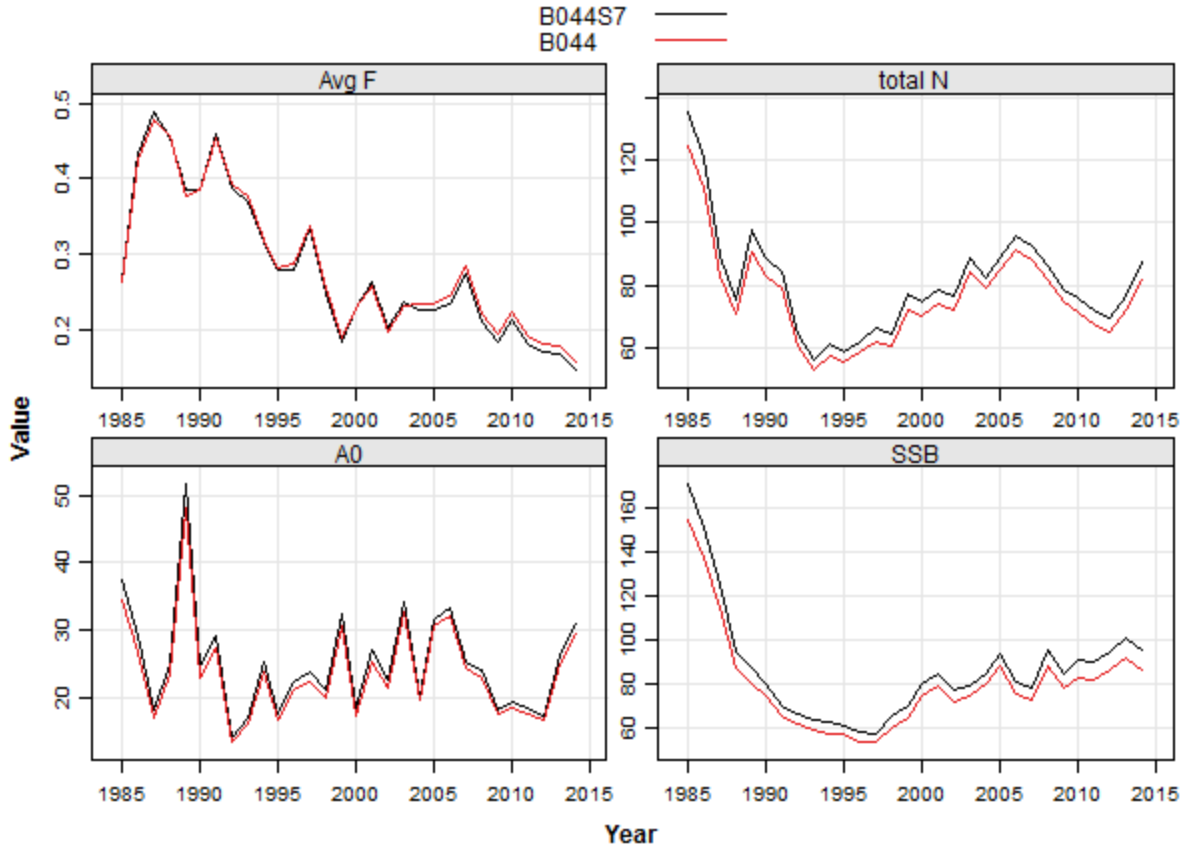

Figure B7.124. Final model sensitivity run assuming MRFSS number prior to 2004 for the recreational catch. Trends for the revised final model (B044) estimates are represented by the red line, with sensitivity run estimates (B044S7) represented by the black line.

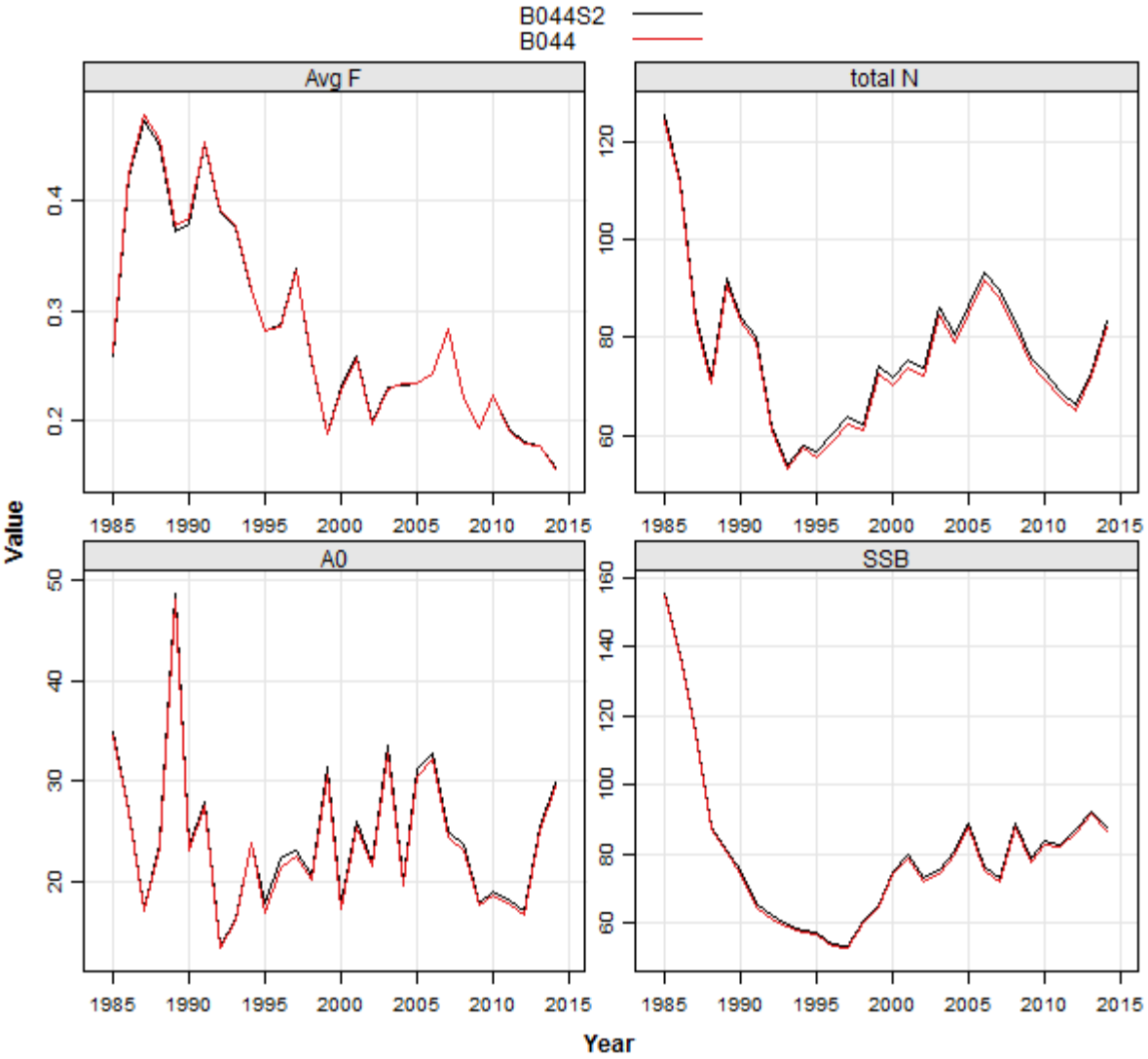

Figure B7.125. Final model sensitivity run assuming 17% mortality (instead of 15%) for the recreational discards. Trends for the final model (B044) estimates are represented by the red line, with sensitivity run estimates (B044S2) represented by the black line.

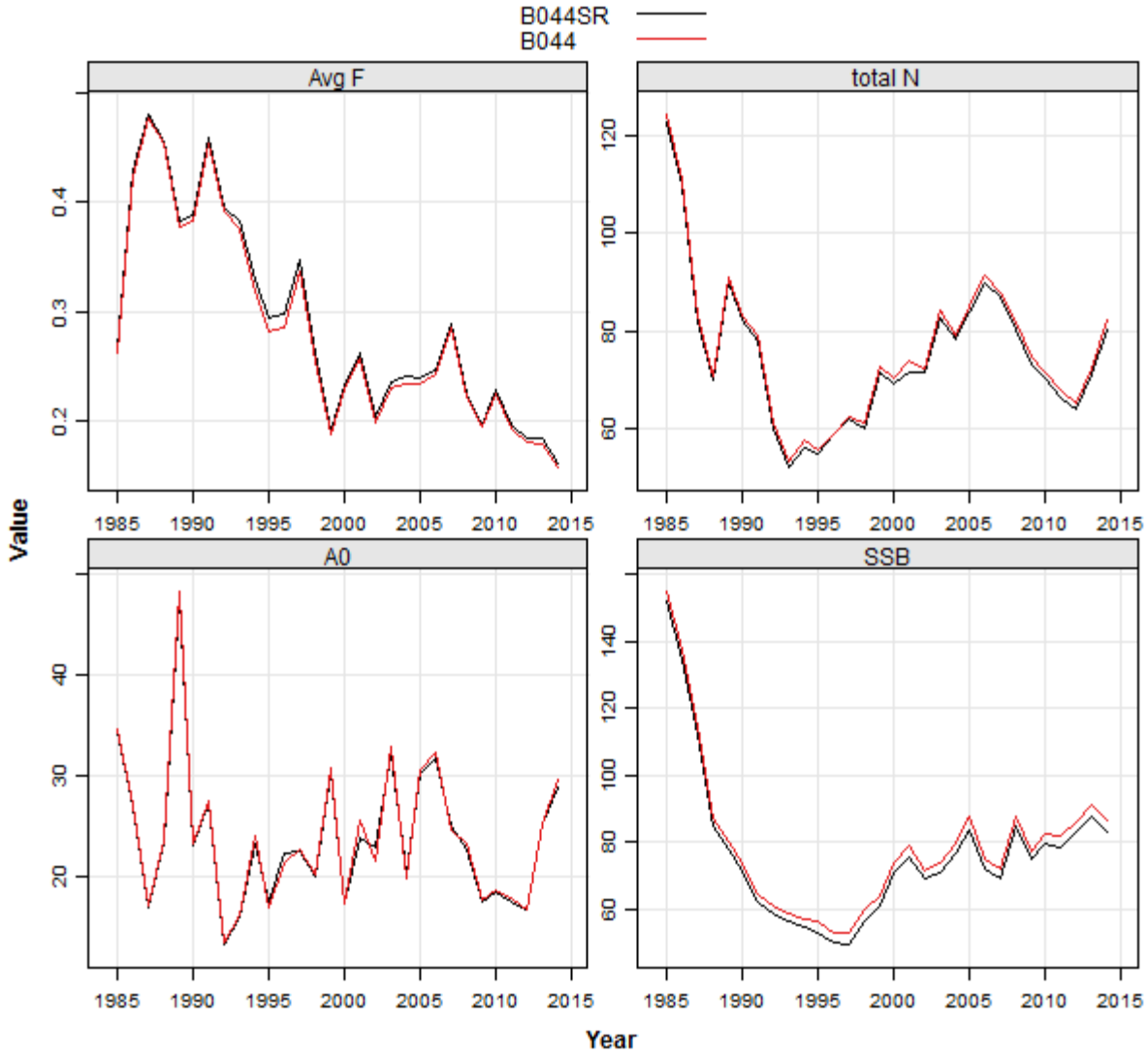

Figure B7.126. Final model sensitivity run assuming regional age-length keys from 2006 to 2014. Trends for the revised final model (B044) estimates are represented by the red line, with sensitivity run estimates (B044SR) represented by the black line.

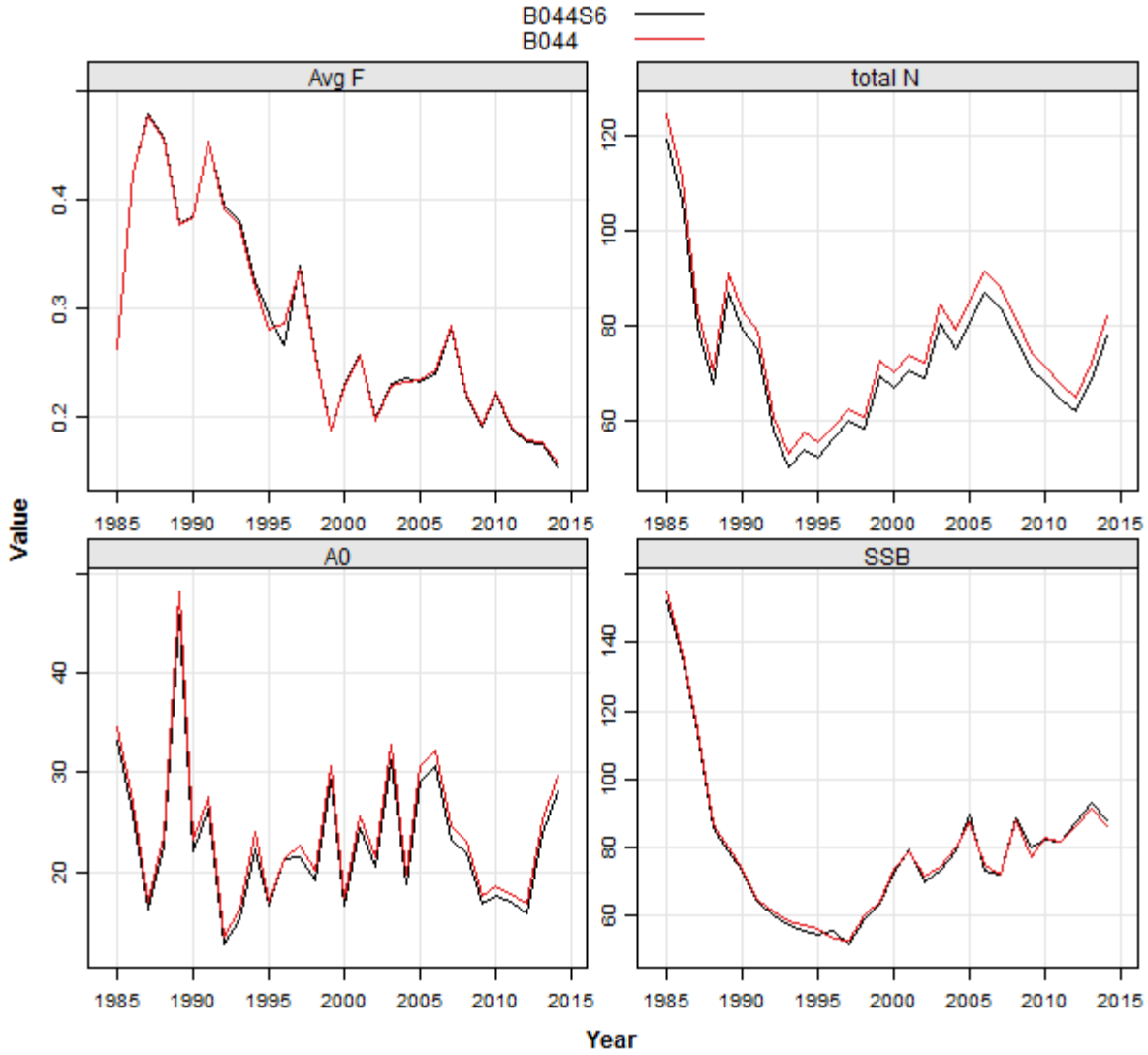

Figure B7.127. Final model sensitivity run assuming 3 time blocks for length-weight coefficients (1985-1994, 1995-2004, 2005-2014). Trends for the revised final model (B044) estimates are represented by the red line, with sensitivity run estimates (B044S6) represented by the black line.

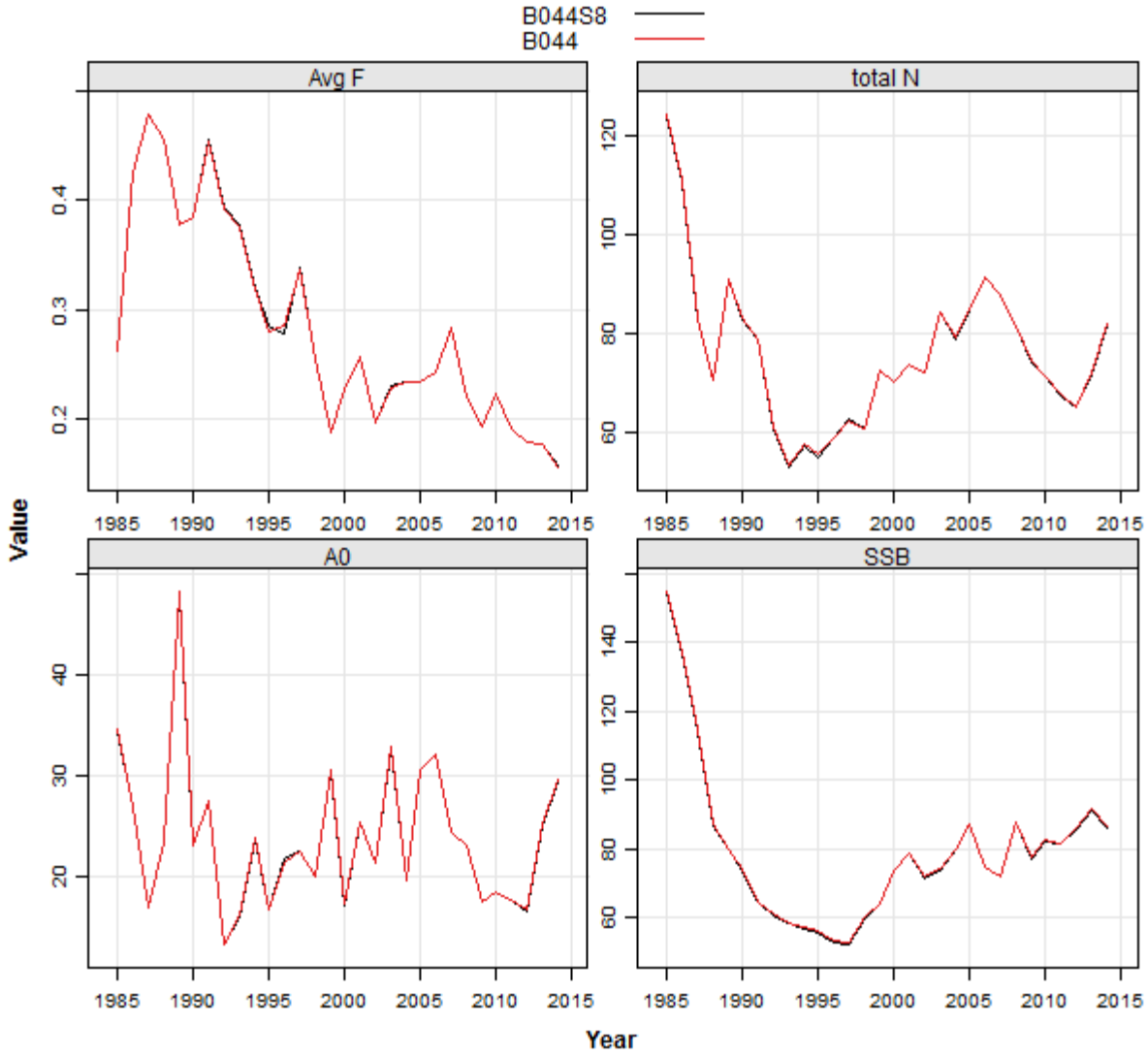

Figure B7.128. Final model sensitivity run assuming VA set 2 landings.
Trends for the revised final model (B044) estimates are represented by the red line, with sensitivity run estimates (B044S8) represented by the black line.

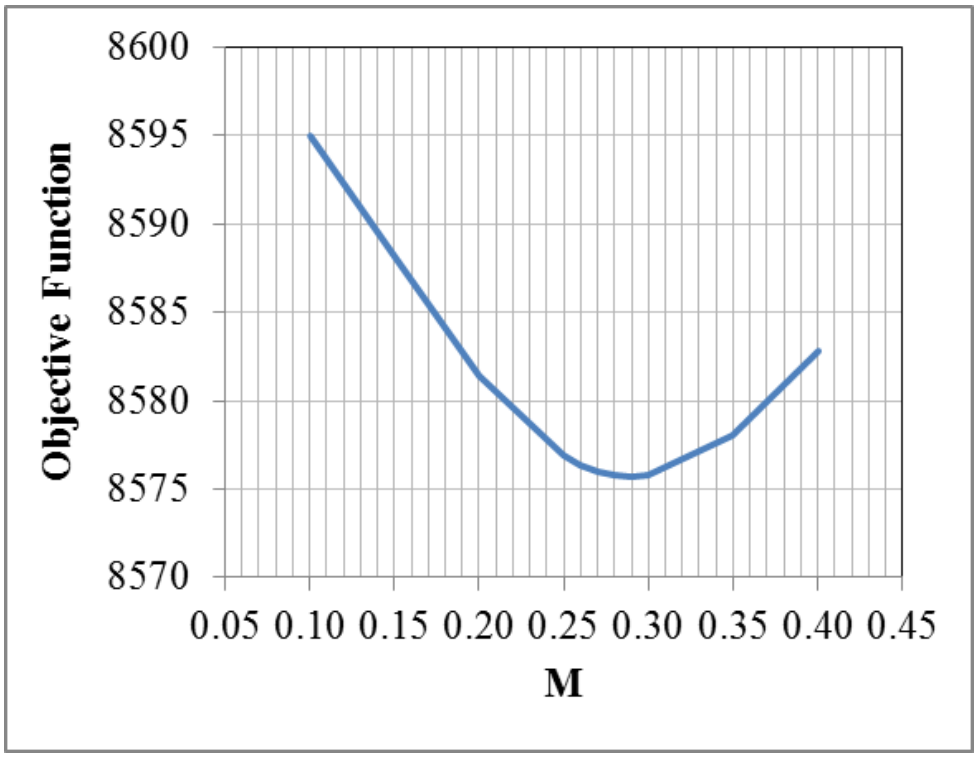

Figure B7.129. Final model objective function profile over different values of natural mortality.

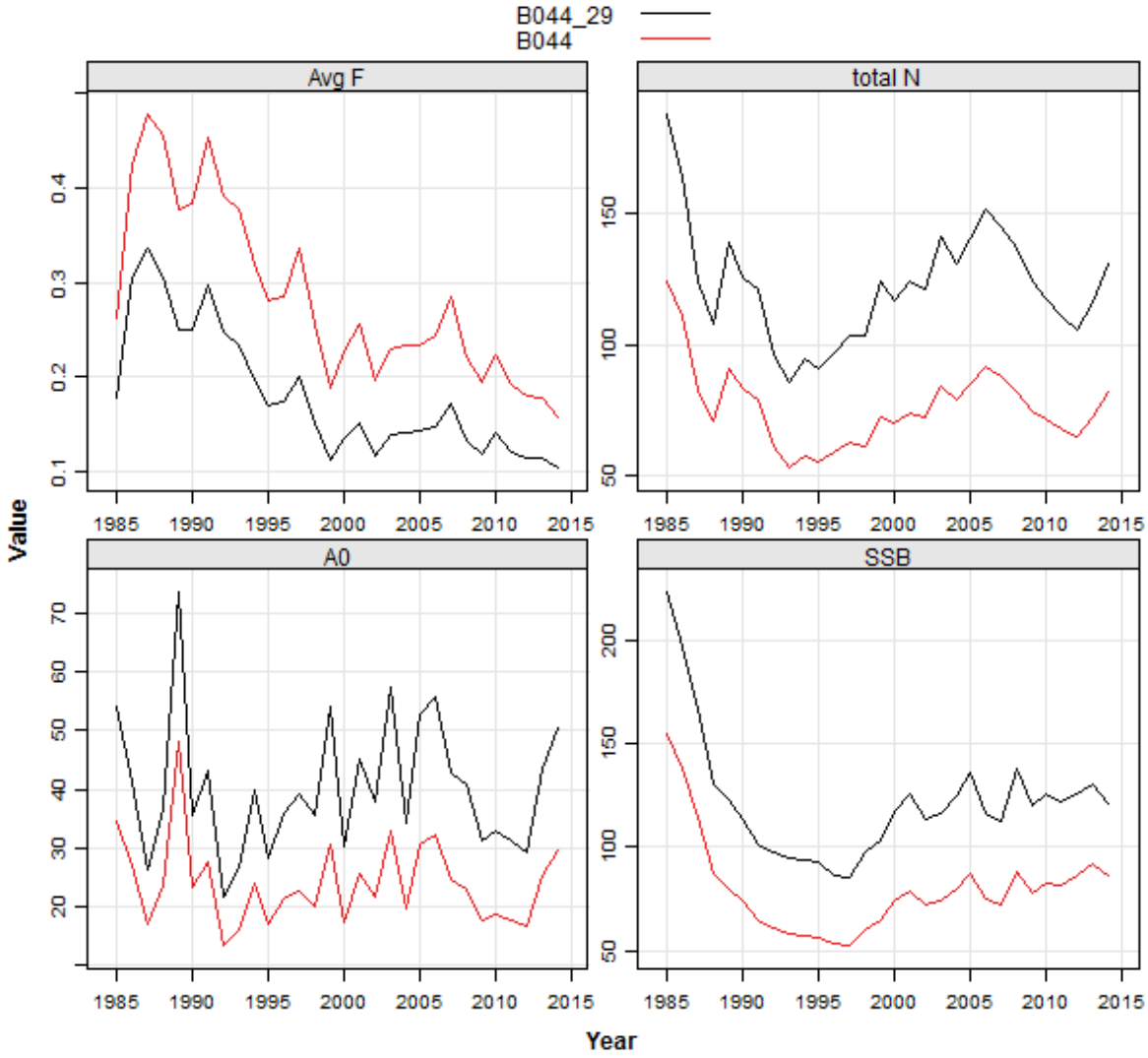

Figure B7.130. Final model sensitivity run assuming natural mortality equal to 0.29 (the value that minimizes the objective function). Trends for the final model (B044) estimates are represented by the blue line, with sensitivity run estimates (B044_29) represented by the black line.

Figure B7.131. Final model sensitivity run assuming age-based natural mortality estimates: Lorenzen scaled to Rule of Thumb (0.21) and Lorenzen scaled to (0.263: the value that minimizes the objective function. Trends for the revised final model (B044) estimates are represented by the blue line, with sensitivity run estimates from B043_LROT (Lorenzen scaled to rule of thumb: 0.21) represented by the red line and B043_L263 (Lorenzen scaled to 0.263) represented by the black line.

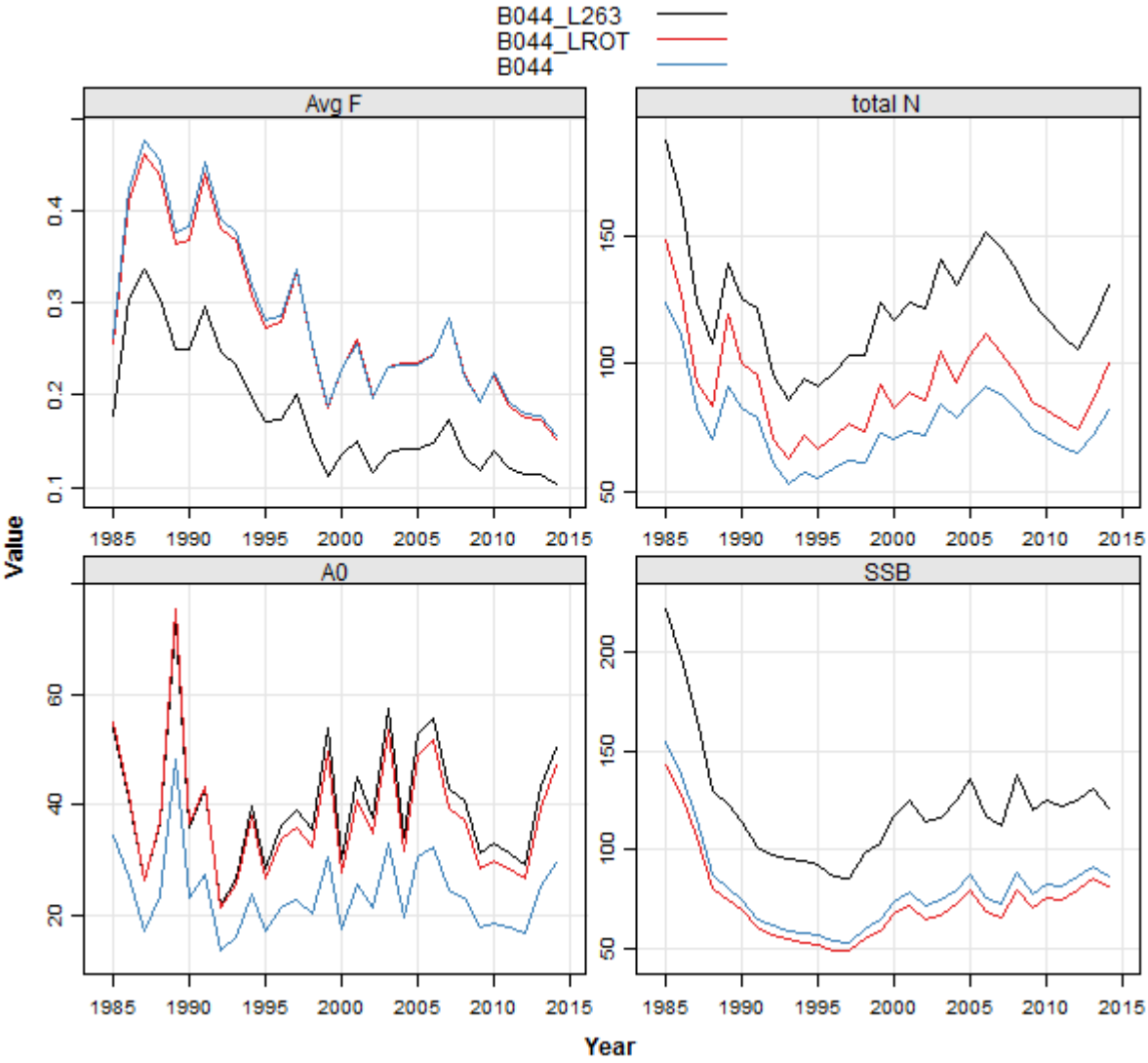

Figure B7.132. Final model sensitivity run exploring the effects of removing the MRIP index, and running the final model with only the fleets and MRIP index. Trends for the final model (B044) estimates are represented by the blue line, with sensitivity run estimates from B043MRIP (2 fleets+MRIP index) represented by the red line and B044.3 (no MRIP) represented by the black line.

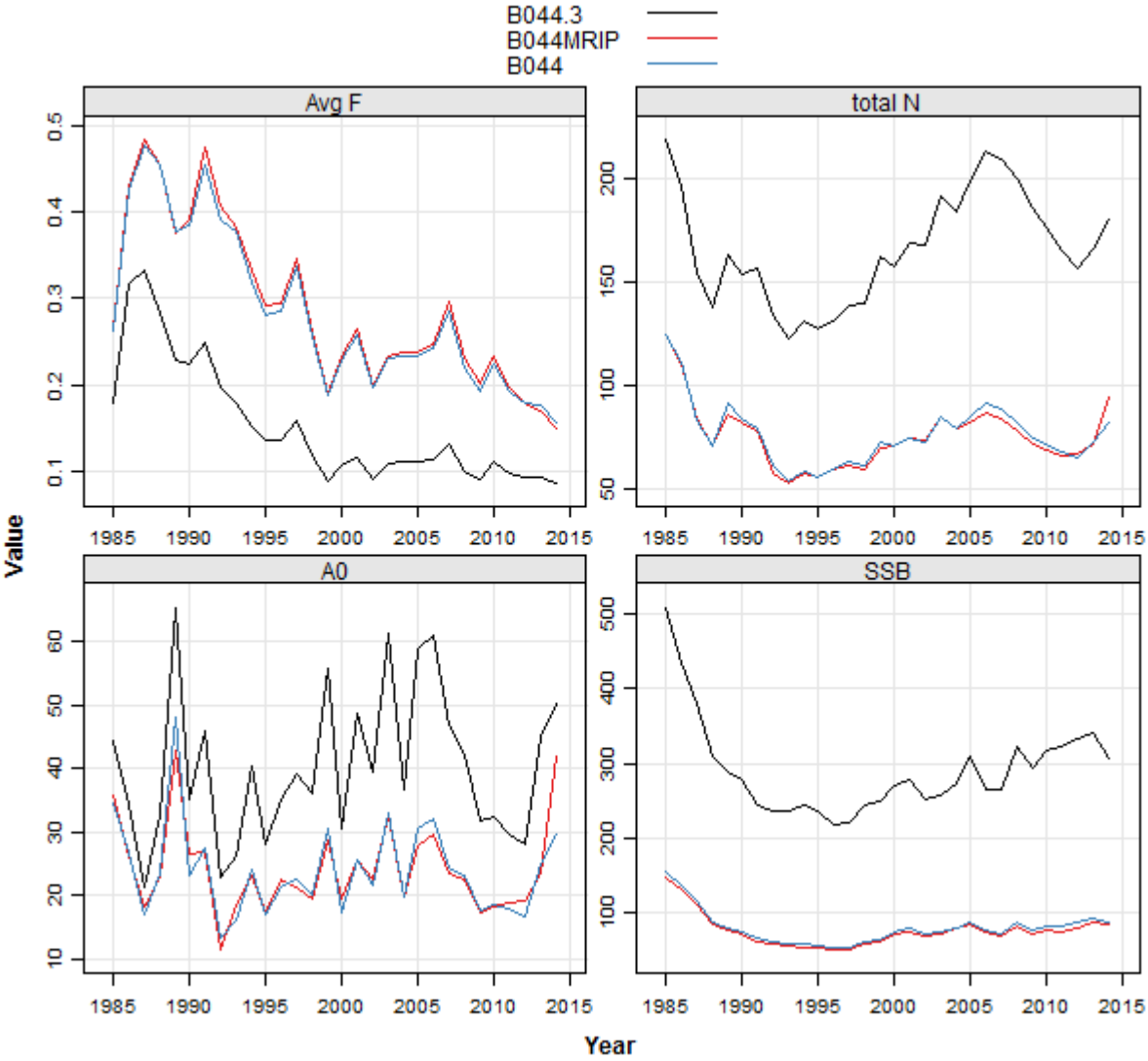

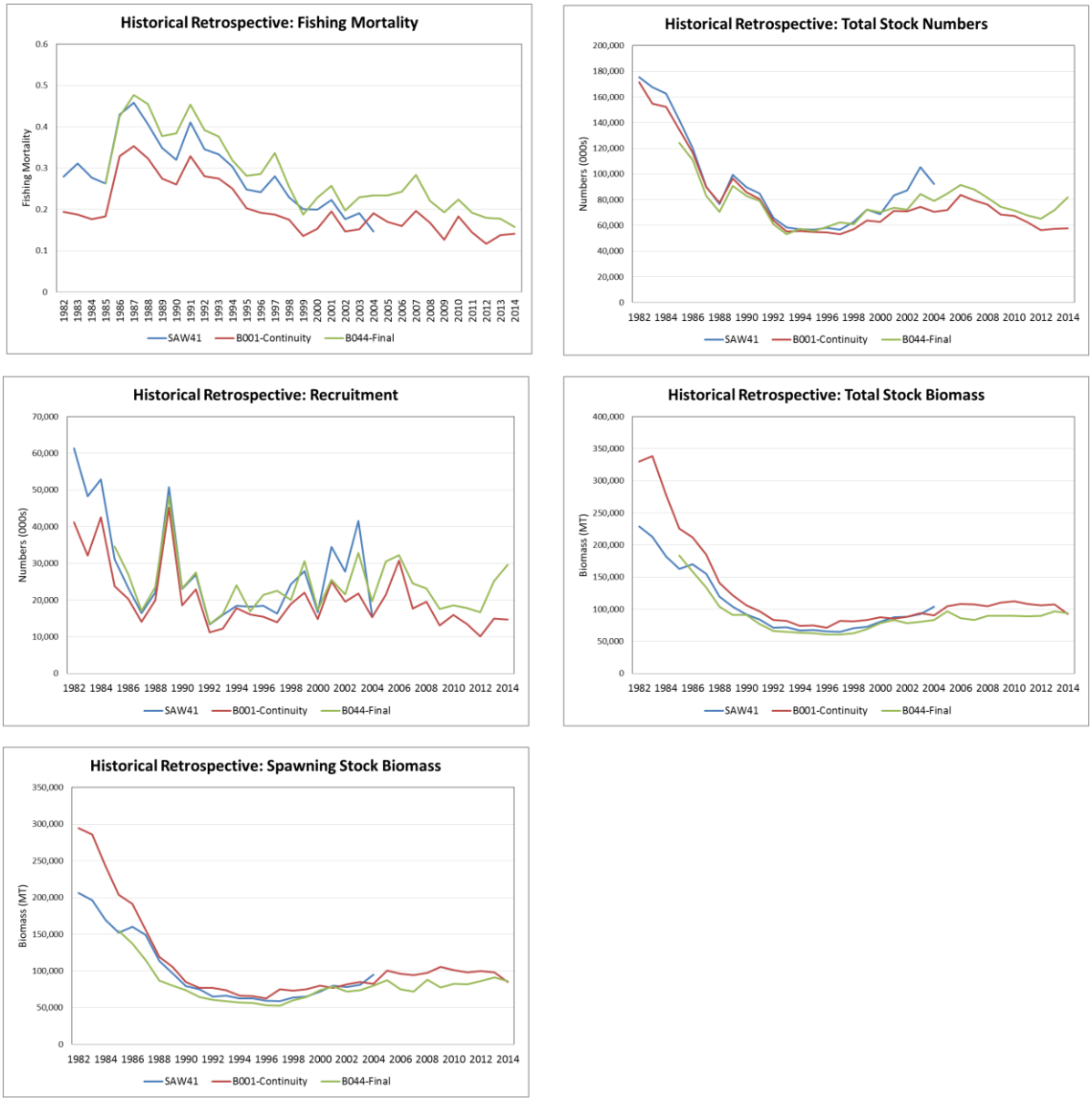

Figure B7.133. Historical retrospective plots comparing estimates of F, abundance, recruitment, total biomass and spawning stock biomass across the previous benchmark assessment model (SAW 41), the continuity run with updated data (B001) and the final preferred model from this assessment (BFinal).

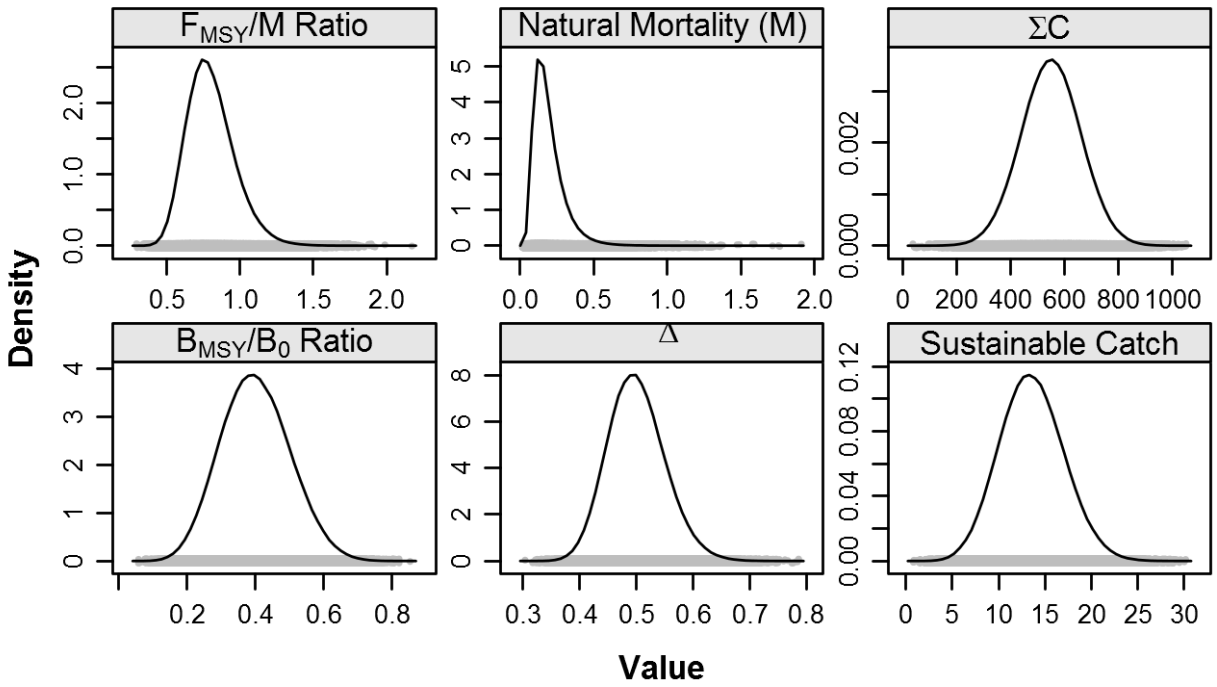

Figure B7.134: Density plot of individual parameter draws (top row panels; bottom row left & middle panels) and sustainable yield estimates (bottom right panel) based on 1,000,000 Monte Carlo simulations of the DCAC base model.

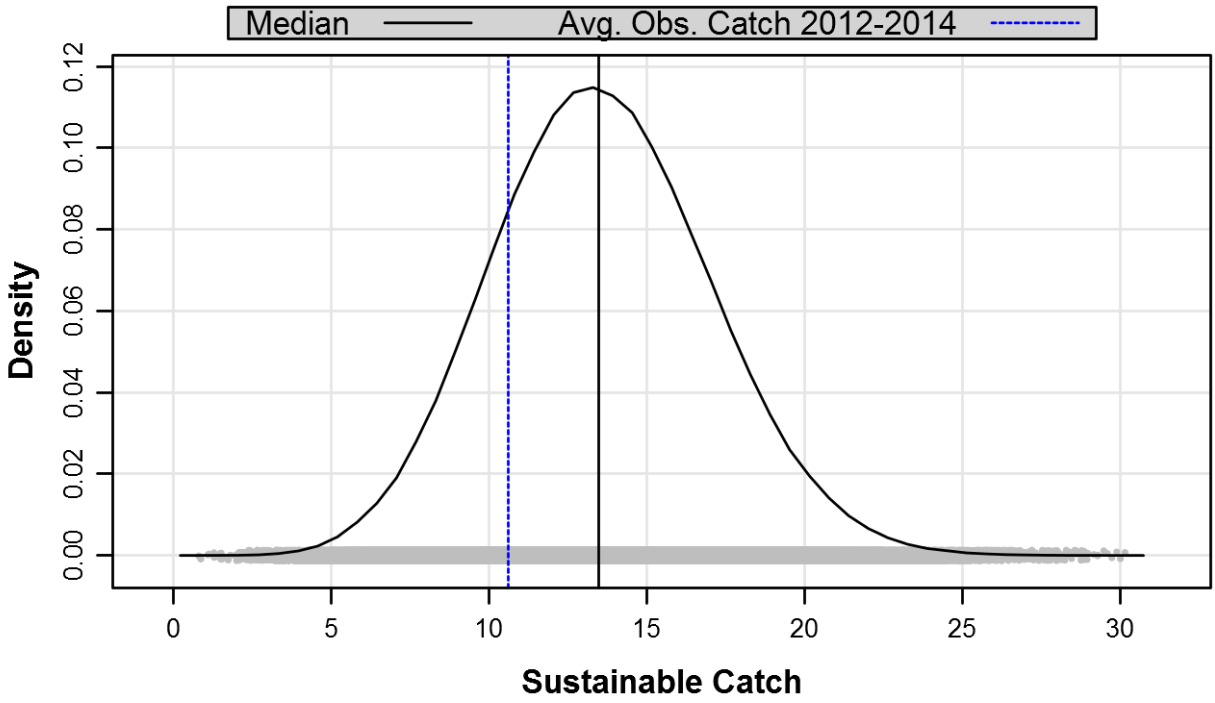

Figure B7.135: Density plot of sustainable yield based on 1,000,000 Monte Carlo simulations of the DCAC base model. Vertical lines represent the median sustainable yield estimate (black) and observed average catch (blue) during the three terminal years (2012-2014) of the assessment

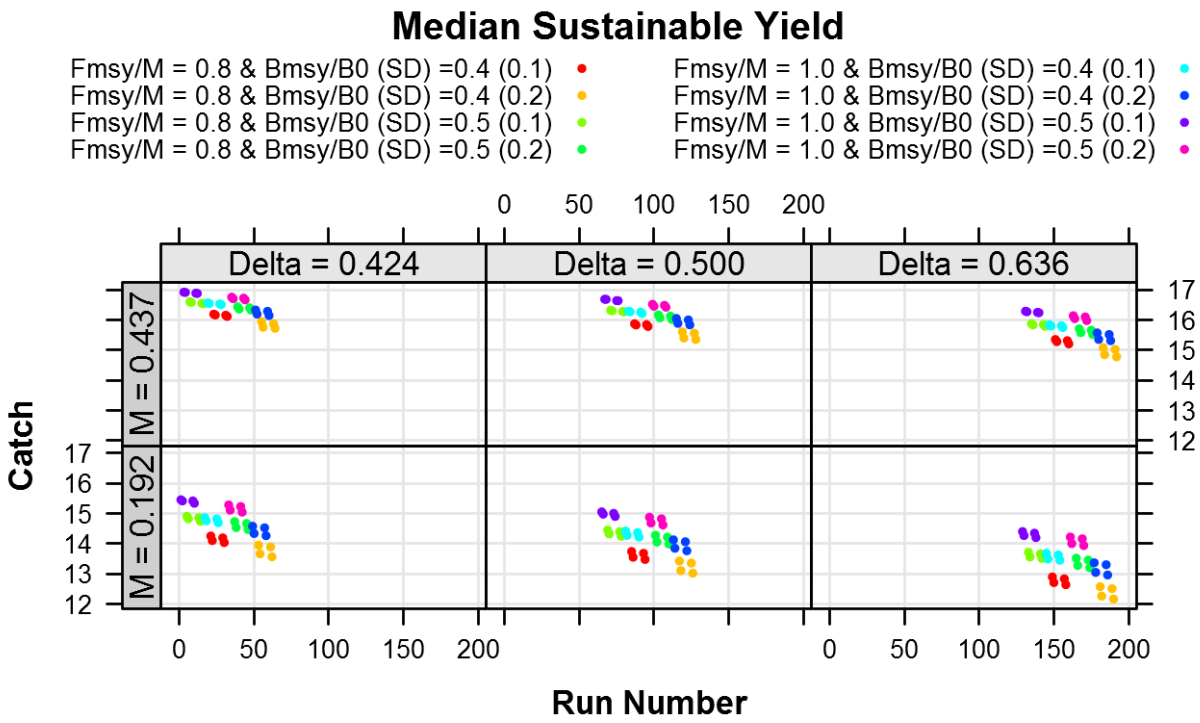

Figure B7.136: Y_{sust} median estimates (in mt) derived from each of the 192 different model configurations (including the base DCAC model).

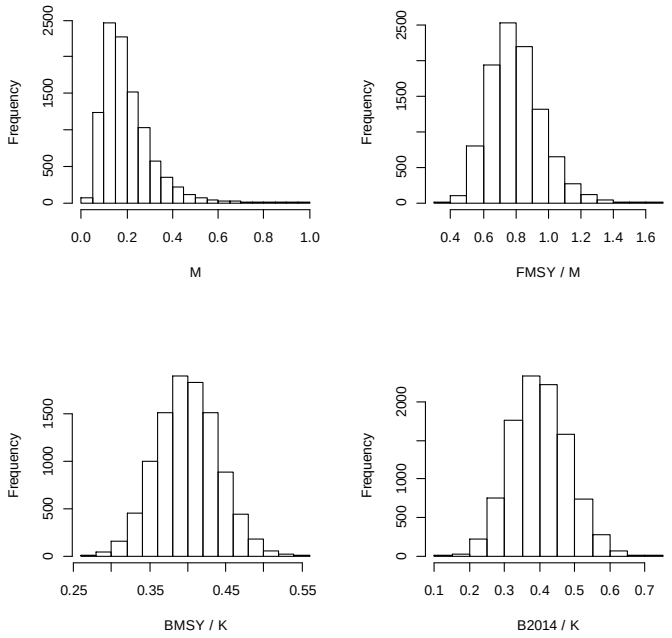

Figure B7.137. Distributions of drawn parameters for DBSRA model.

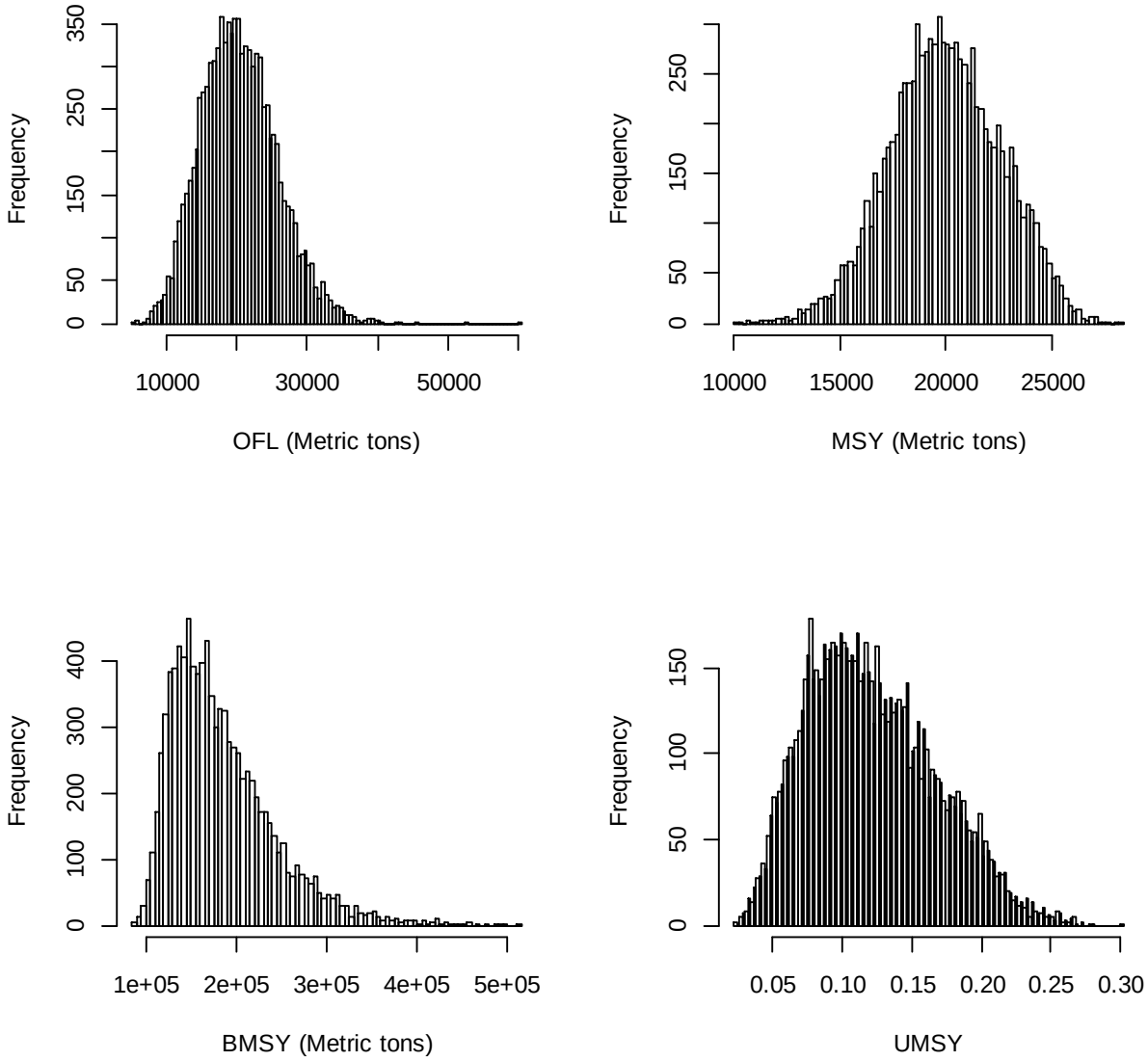

Figure B7.138. Distribution of management parameters from successful DBSRA model runs.

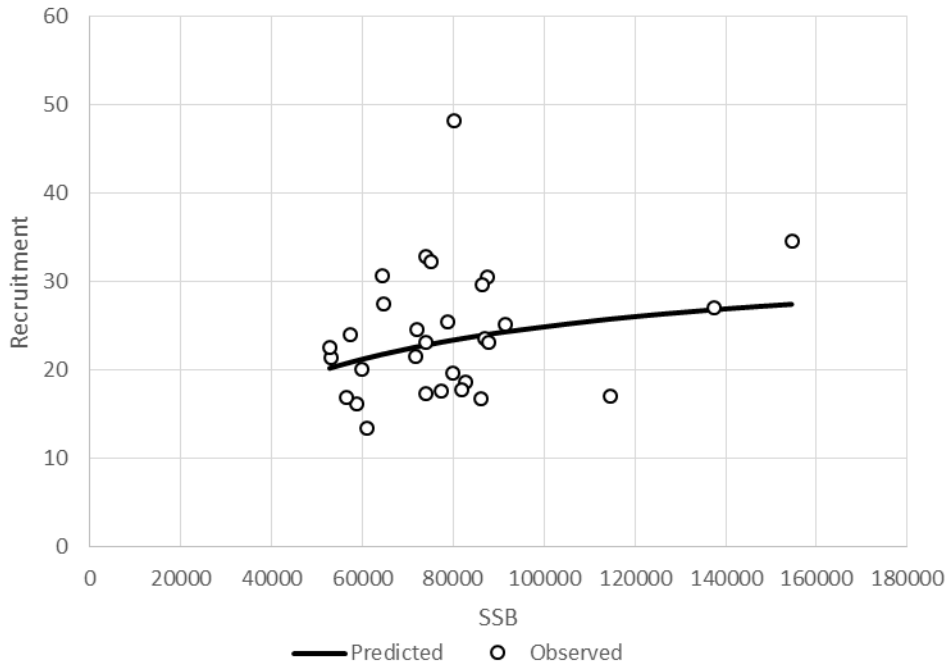

Figure B8.1. Observed stock-recruitment relationship plotted with a fitted curve.

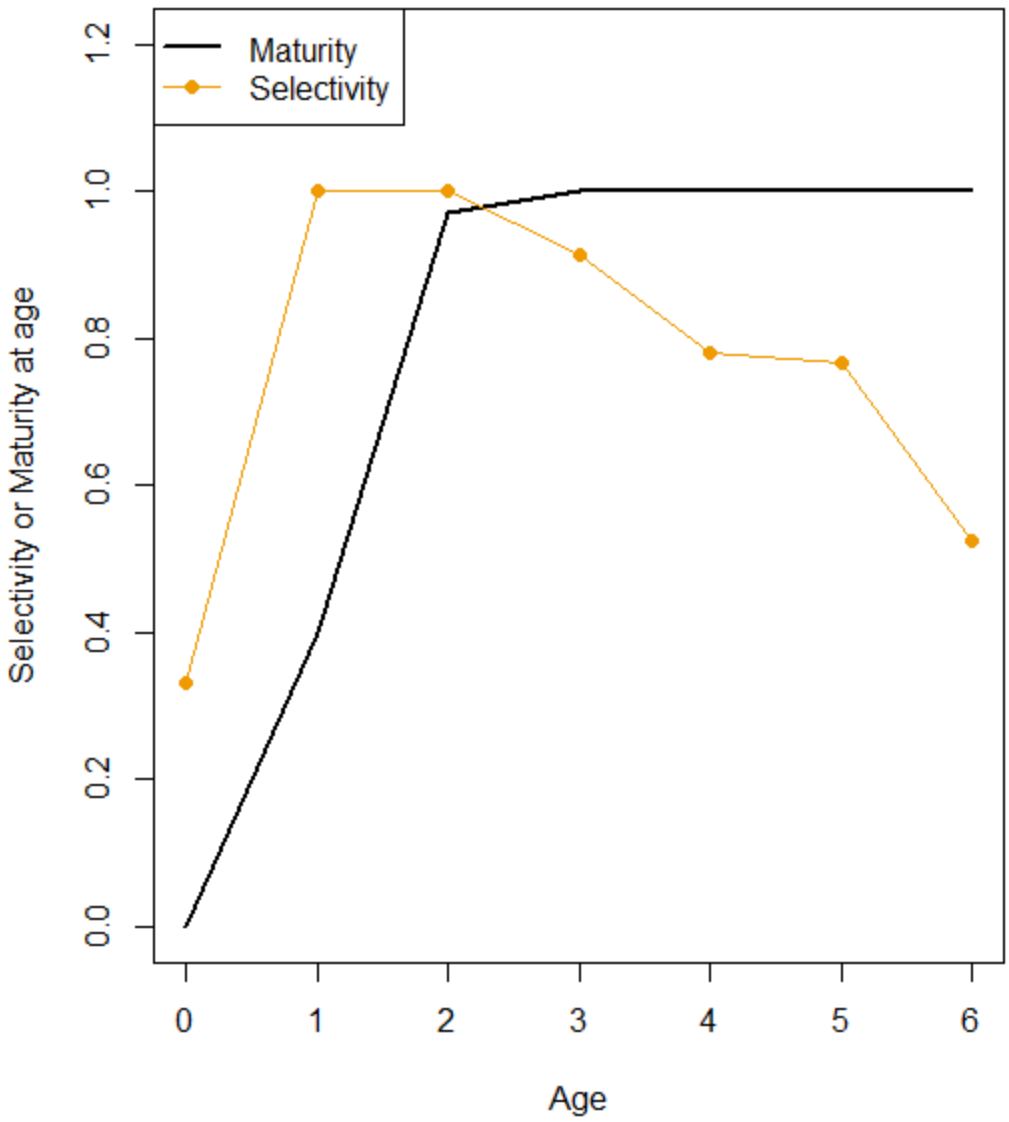

Figure B8.2. Maturity ogive and composite selectivity pattern used to estimate bluefish reference points.

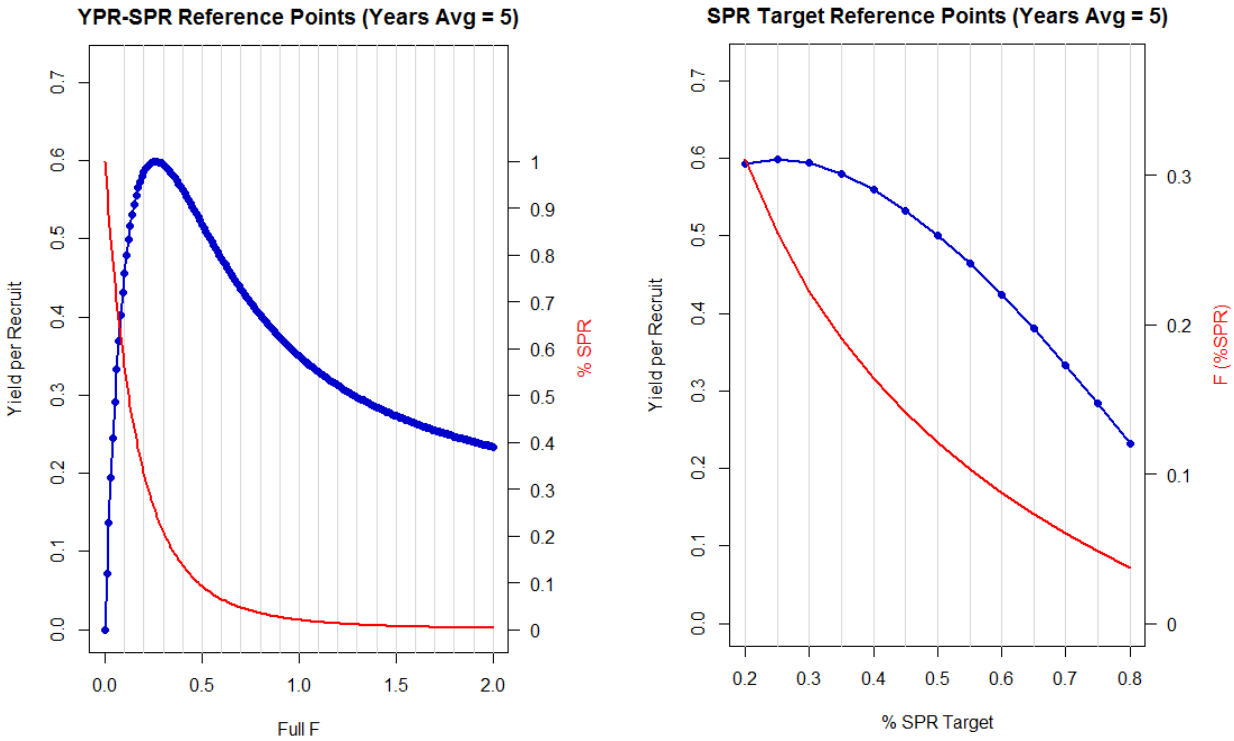

Figure B8.3. YPR and SPR curves for bluefish.

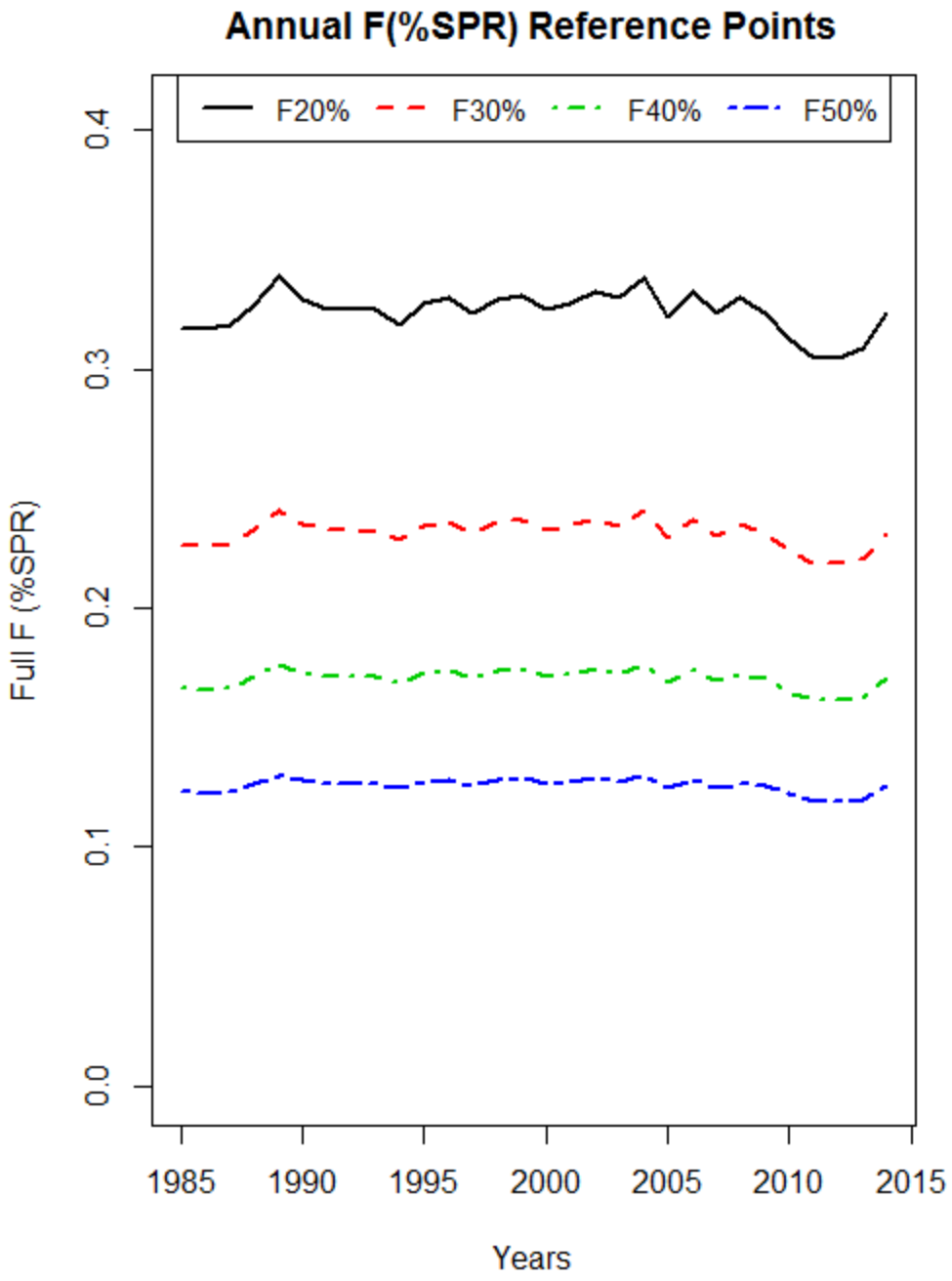

Figure B8.4. Annual estimates of F %SPR reference points.

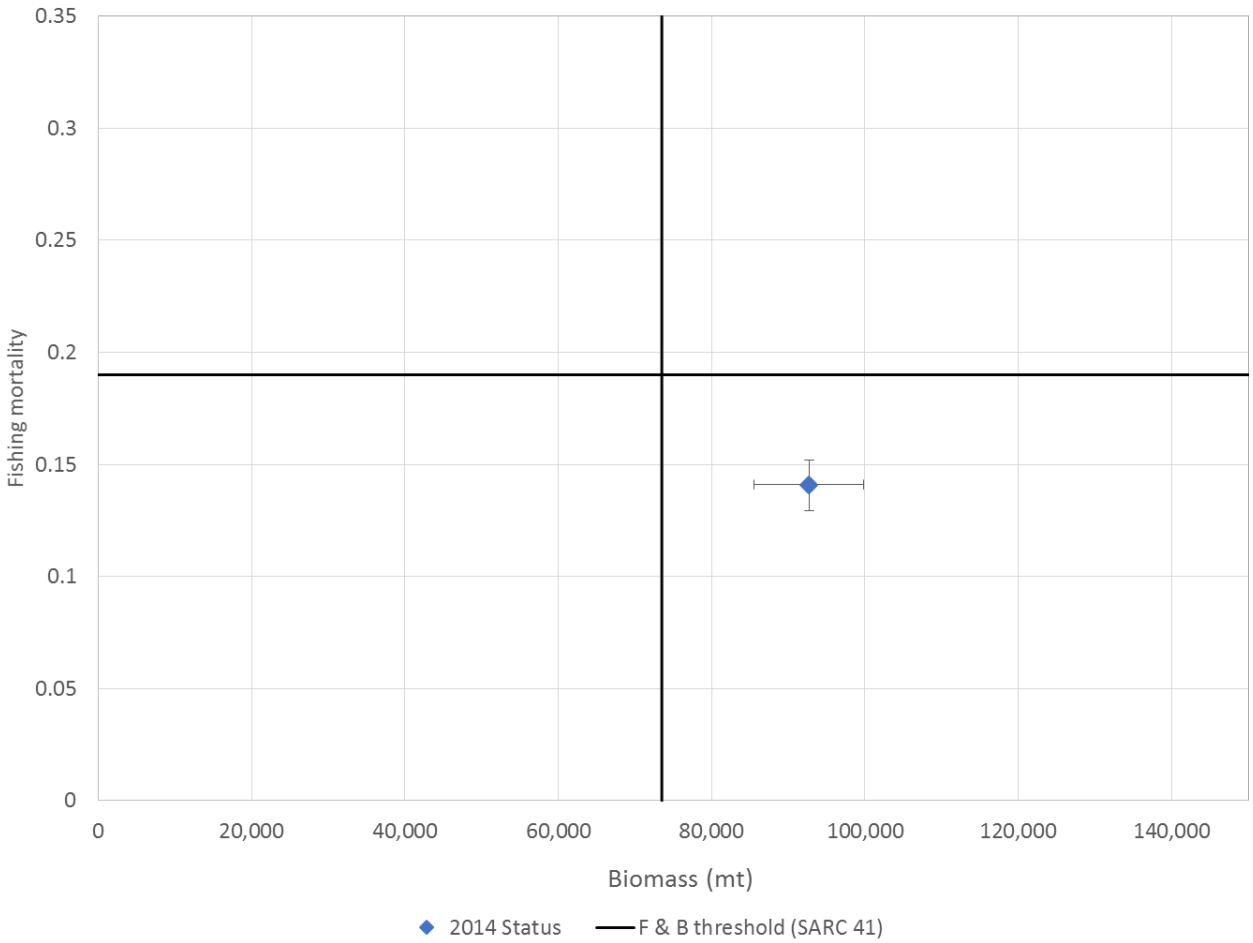

Figure B9.1. Stock status in 2014 (diamond) from the continuity run plotted with the F and biomass thresholds from the previous benchmark assessment (solid lines).
Error bars on the status estimated indicate 95% confidence intervals.

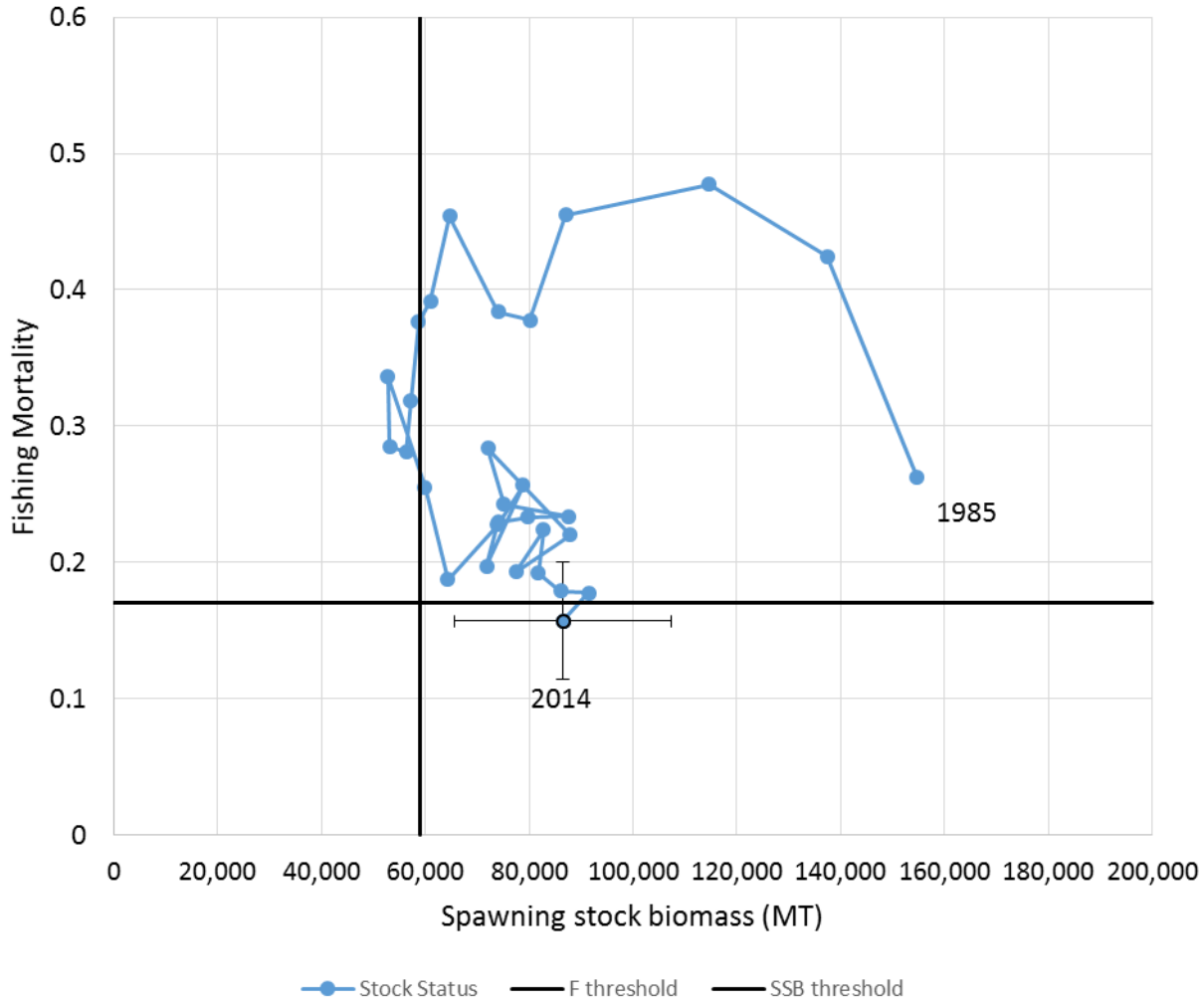

Figure B9.2. Annual stock status estimates from the final revised model run plotted with the F and biomass thresholds for this assessment (solid lines). Error bars on the status estimated indicate 95% confidence intervals.

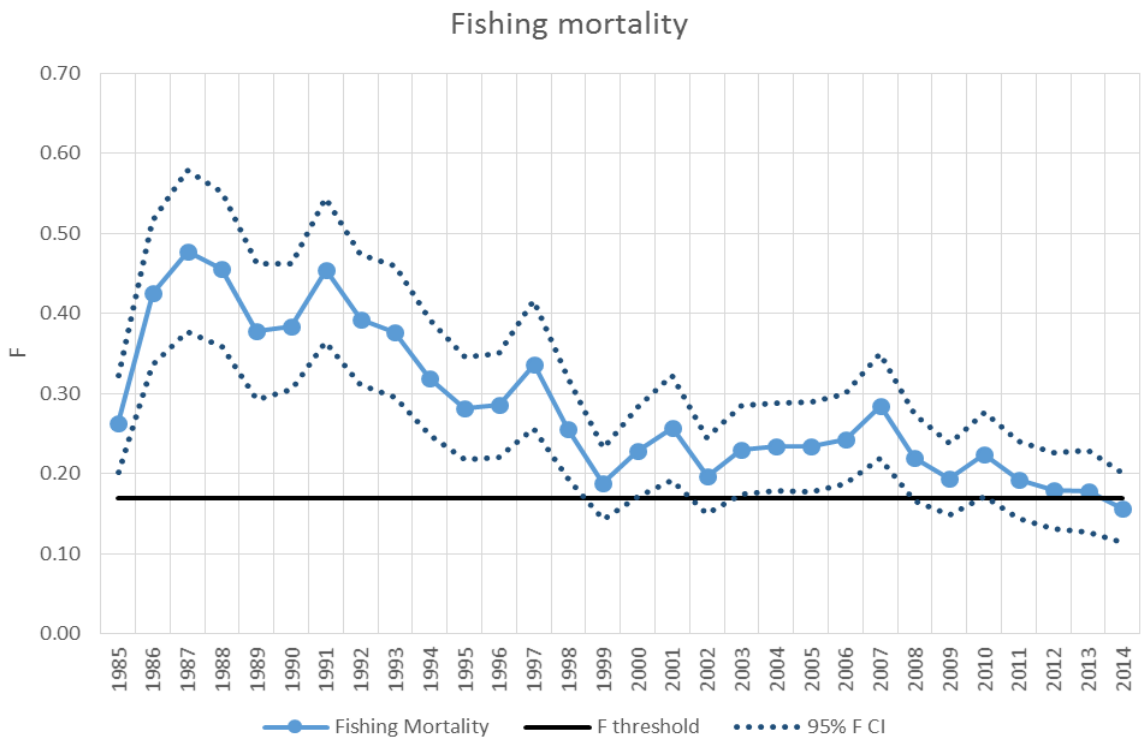

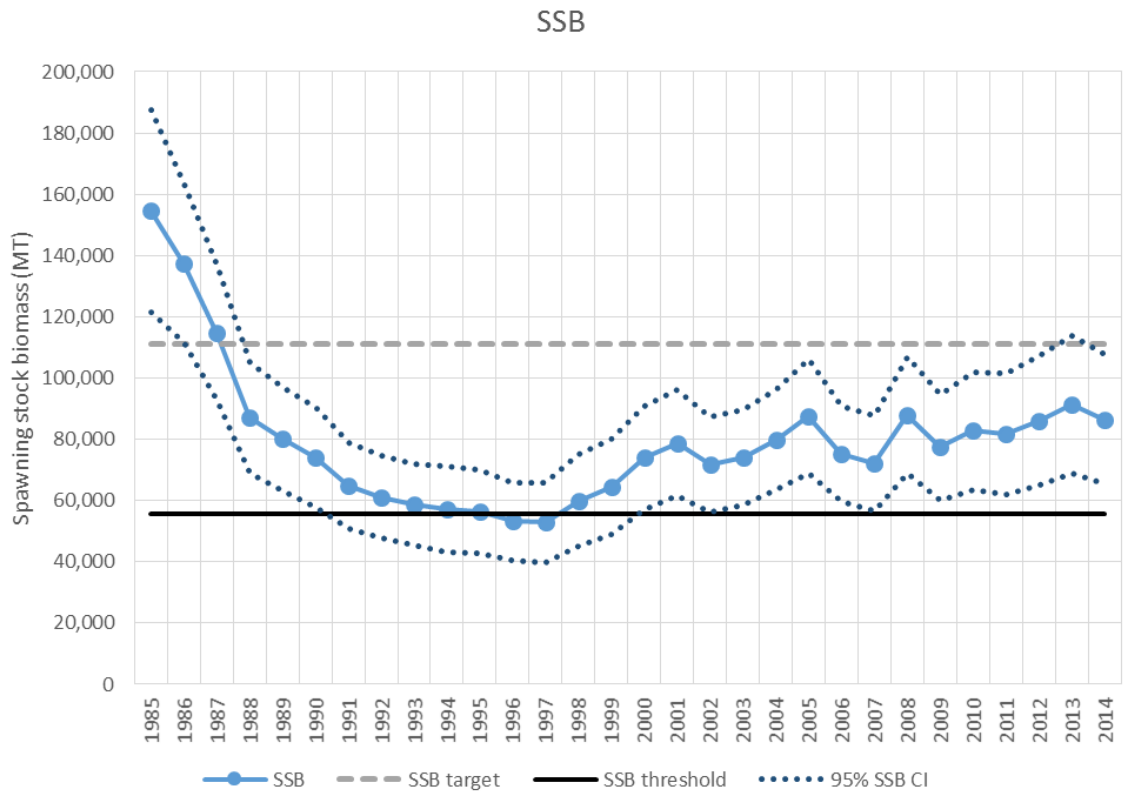

Figure B9.3. Fully selected F (top) and spawning stock biomass (bottom) from the final revised model run plotted with their respective overfishing and overfished thresholds and 95% confidence intervals.

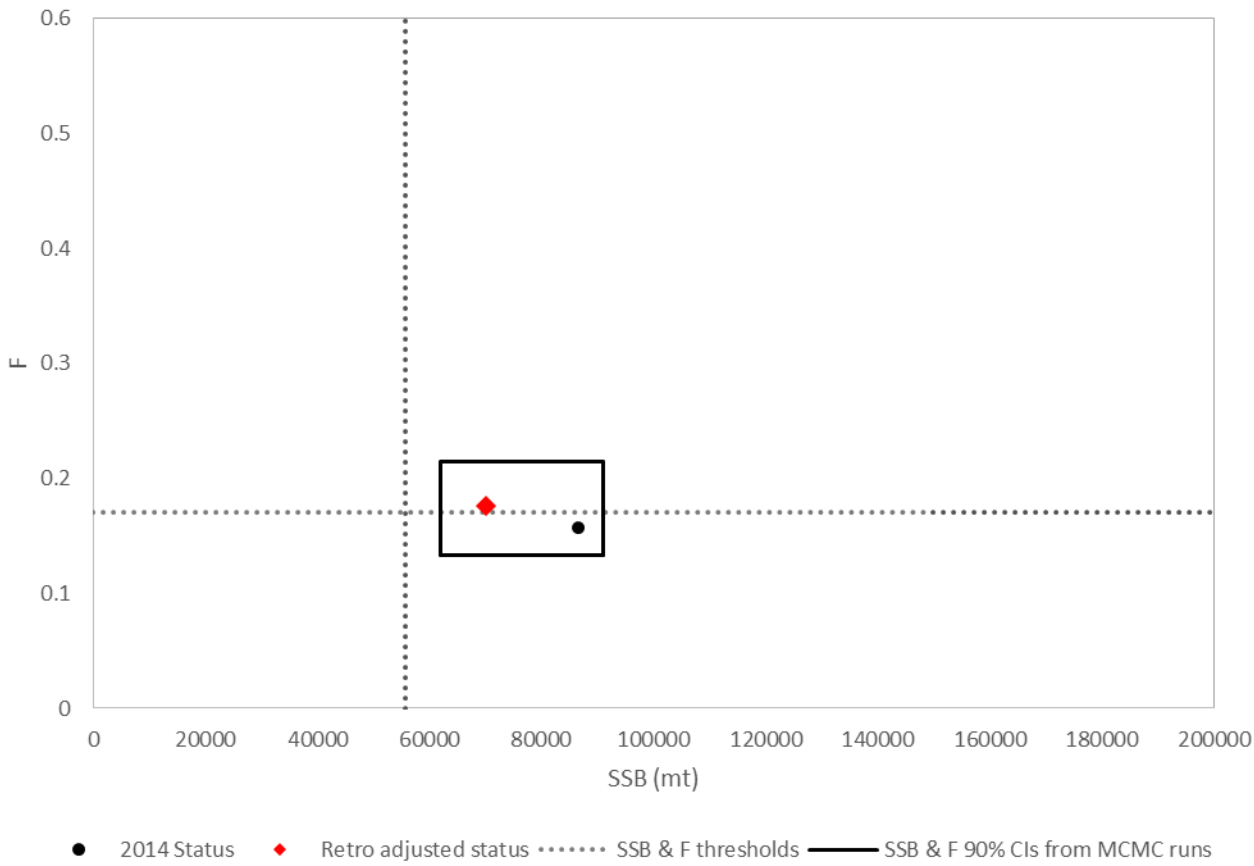

Figure B10.1. 2014 Stock status of bluefish with and without adjustment for retrospective bias, compared to the 90% confidence bounds of the MCMC model runs.

Figure B10.2. **Projected landings (top) and spawning stock biomass (bottom) under various F scenarios. Shaded bands indicated the 5th and 95th percentiles of the F_{MSY} bootstrap runs. The solid red line indicates the overfished biomass threshold.**

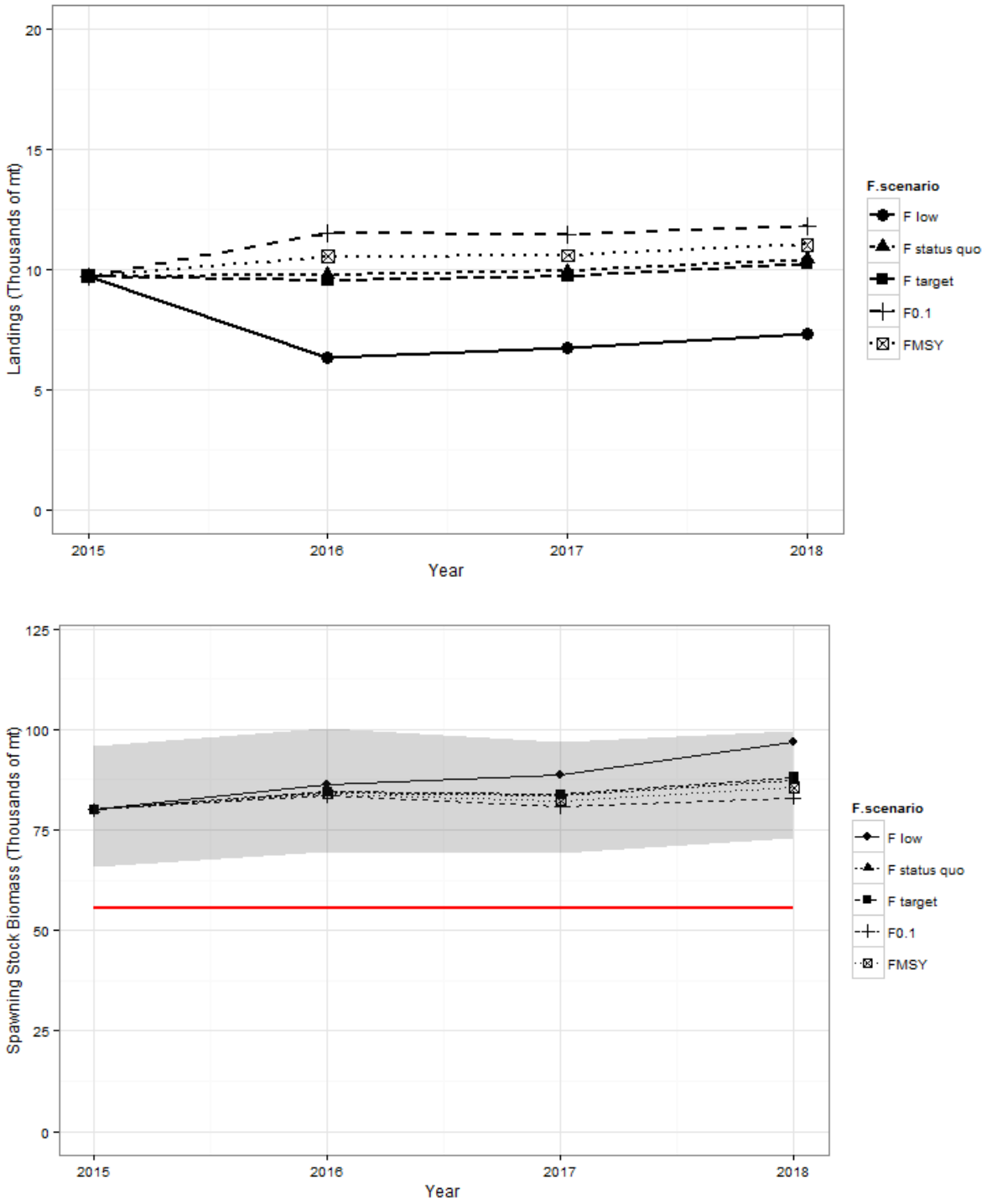

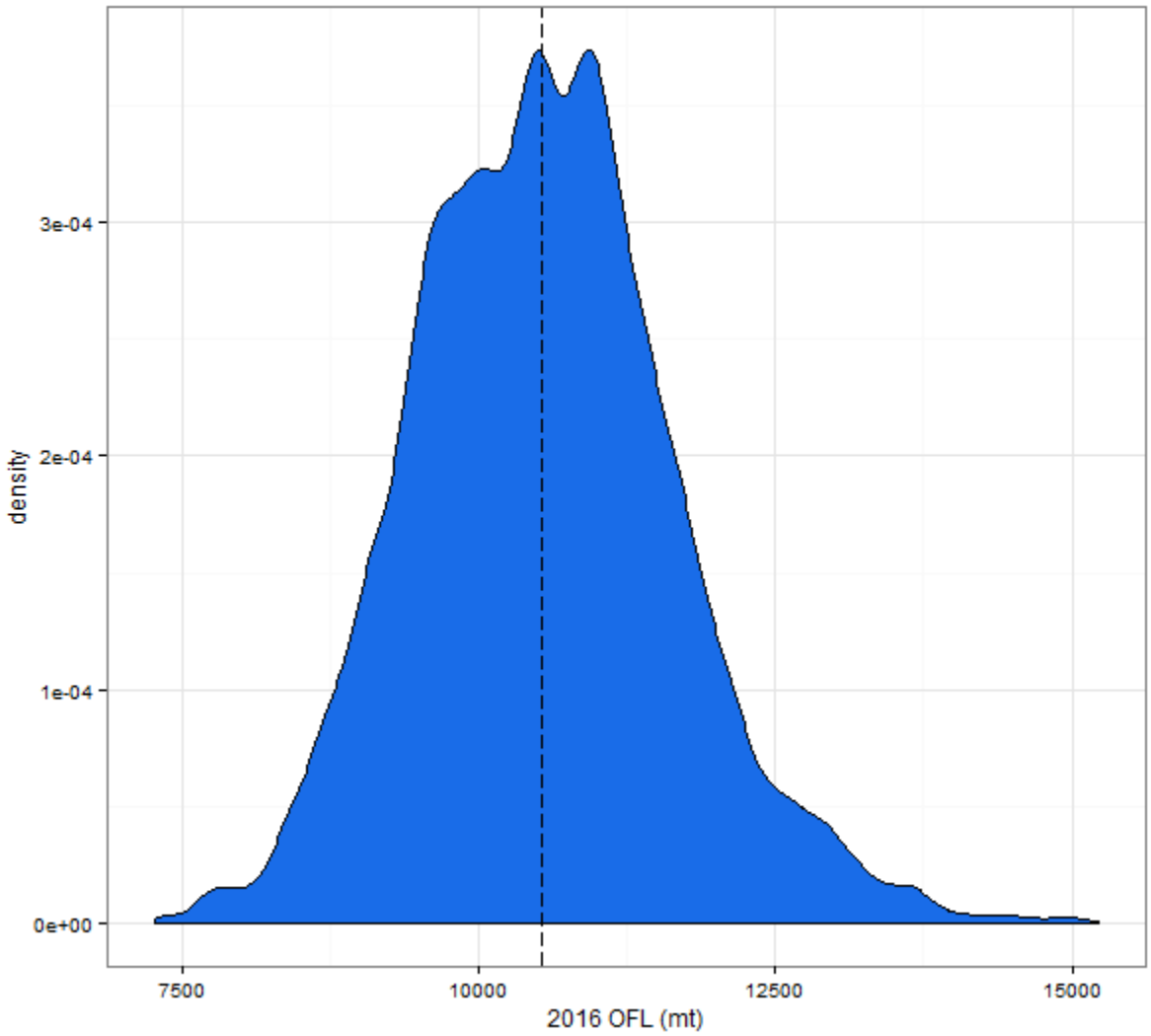

Figure B10.3. Distribution of 2016 OFL estimate from revised final model projections. The dashed vertical line indicates the median estimate.

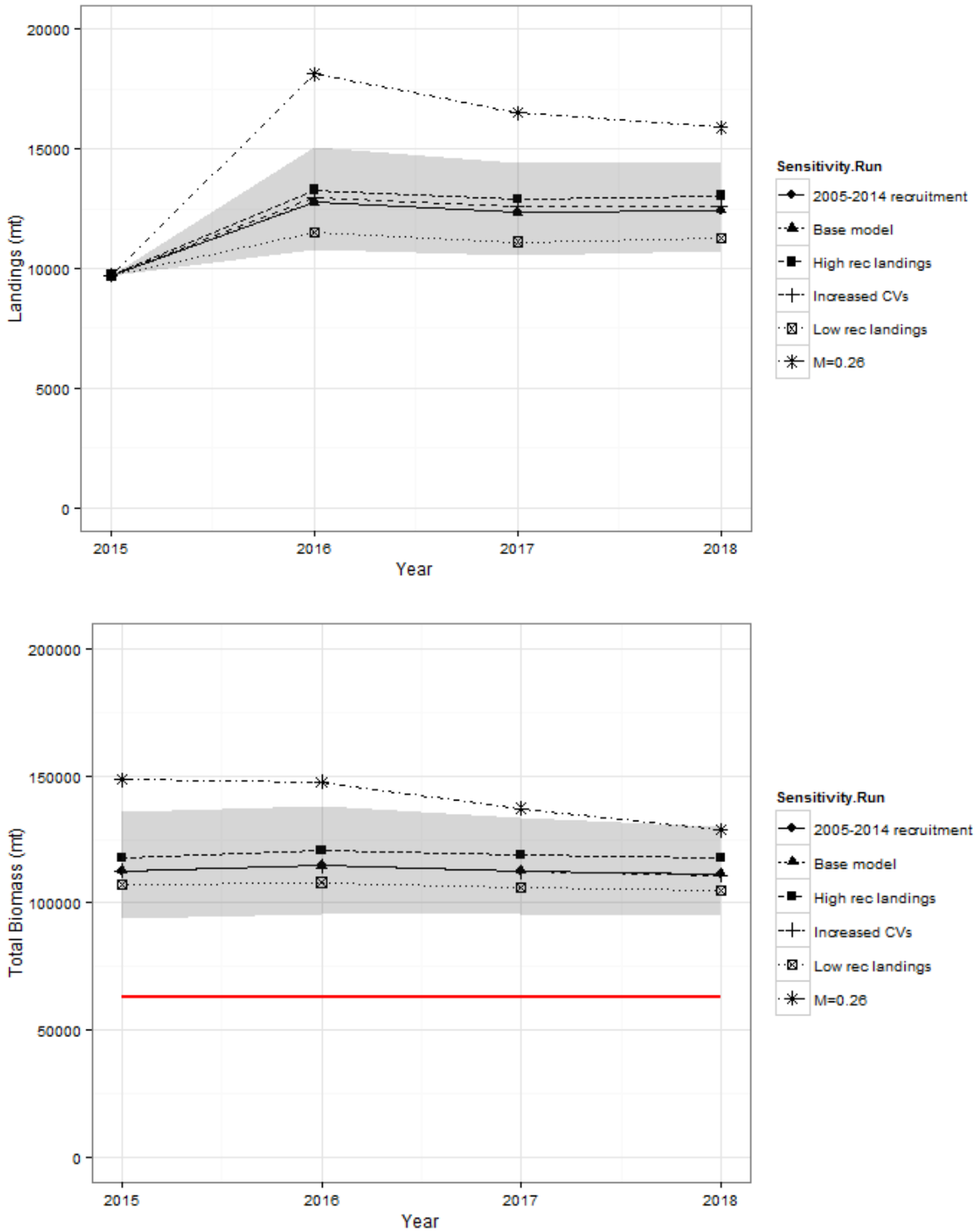

Figure B10.4. Sensitivity runs of projected landings (top) and biomass (bottom) under F_{MSY}. Shaded bands indicated the 5th and 95th percentiles of the preferred base model bootstrap runs. The solid red line indicates the overfished biomass threshold.

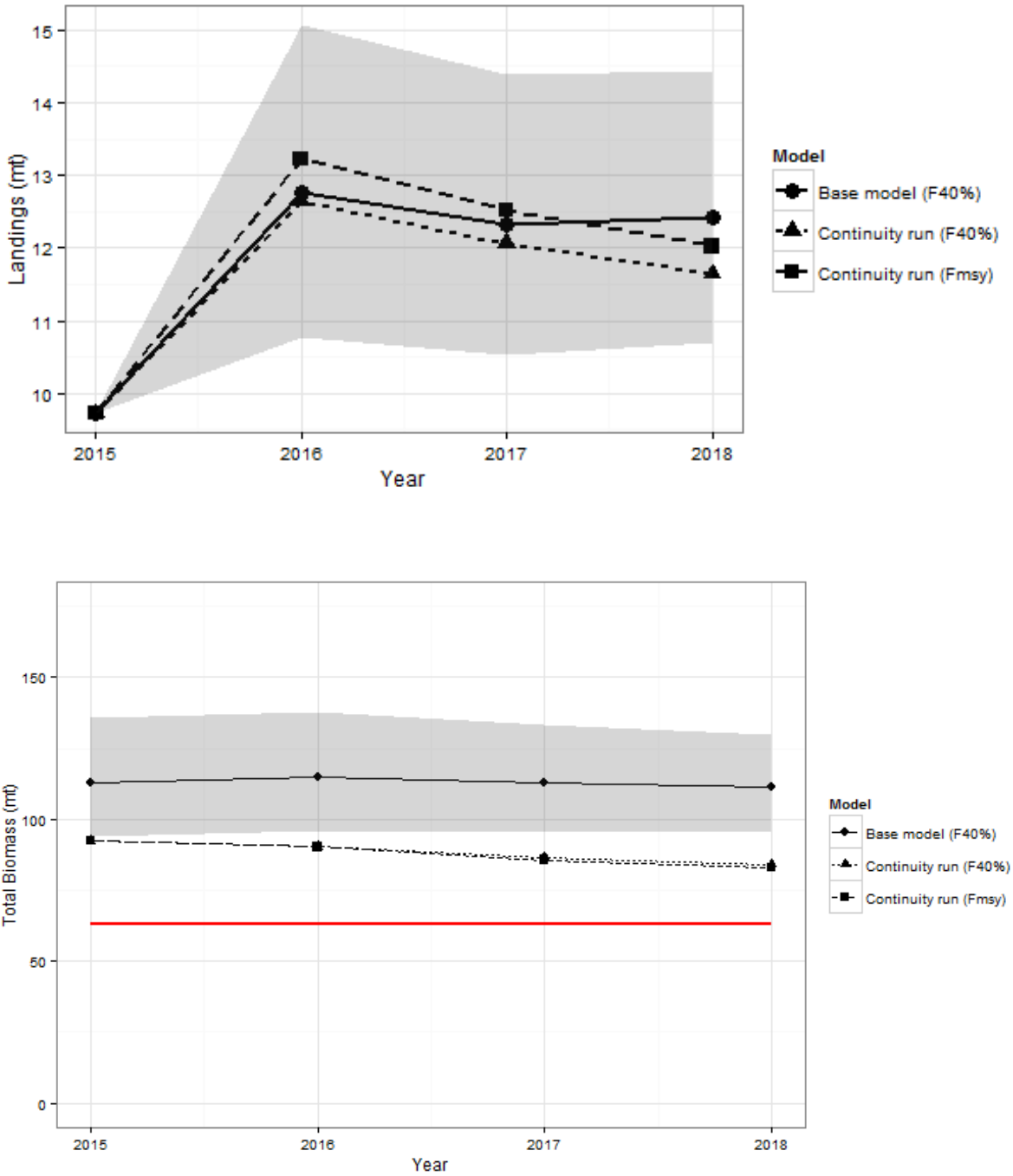

Figure B10.5. Projected landings (top) and biomass (bottom) for the continuity run model and the final revised model from this assessment. Shaded bands indicated the 5th and 95th percentiles of the preferred base model bootstrap runs. The solid red line indicates the overfished biomass threshold from the final revised model.